Enzymatisch generiertes Nanopartikelwachstum
für Biochipsysteme in der Vor-Ort-Analytik

Dissertation

zur Erlangung des akademischen Grades doctor rerum naturalium
(Dr. rer. nat.)

vorgelegt dem Rat der Chemisch-Geowissenschaftlichen Fakultät der
Friedrich-Schiller-Universität Jena

von Diplom-Ingenieur (FH) Thomas Schüler
geboren am 30.01.1979 in Sondershausen

Gutachter:

1. Prof. Dr. Jürgen Popp

Friedrich-Schiller-Universität Jena

Institut für physikalische Chemie

Helmholtzweg 4, 07743 Jena

2. PD Dr. Wolfgang Fritzsche

Institut für Photonische Technologien

Albert-Einstein-Straße 9, 07745 Jena

3. PD Dr. Till Bachmann

University of Edinburgh Medical School

Division of Pathway Medicine

49 Little France Crescent, Edinburgh

Tag der öffentlichen Verteidigung: 28.10.2009

Inhaltsverzeichnis

Kapitel 1

Zusammenfassung

1.1 Motivation und Stand der Forschung

Die heutige Bioanalytik steht vor einer grundlegenden Veränderung ihrer standardanalytischen Nachweisverfahren. Ein Schwerpunkt ist der Wandel des gegenwärtigen zentralisierten Standards zu einer innovativen dezentralisierten Analytik. Der wachsende Bedarf nach schnellen und unkomplizierten Analysesystemen für bioanalytische Anwendungen stellt sowohl eine Herausforderung an die wissenschaftliche als auch die technische Konzeptentwicklung und deren Umsetzung dar. Vor allem die steigende Nachfrage nach kostengünstigen und robusten Vor-Ort einsetzbaren Analysesystemen kann mit den momentan genutzten standardisierten Verfahren nicht mehr erfüllt werden. Daher besteht eine Notwendigkeit in der Entwicklung moderner bioanalytischer Verfahren. Die Dezentralisierung der bioanalytischen Diagnostik für einen Einsatz außerhalb spezialisierter Laboratorien stellt hierbei ein Grundmotiv dar. Durch eine einfache und verständliche Bedienbarkeit sollen diese neuartigen Systeme auch dem geschulten Laien die Benutzung erlauben. Als generelle Bezeichnung dieser zukunftsorientierten Systeme hat sich der Begriff *Point-of-care* etabliert [1]. *Point-of-care*-Systeme bezeichnen transportable, einfache Strategien, welche schnelle Analysen mit hohen Sensitivitäten und Spezifitäten für eine Vor-Ort einsetzbare Analytik verbinden [2-7]. Ein zusätzlicher Anspruch ist die erforderliche Robustheit der mobilen, transportablen Analysegeräte. Im Vergleich zu den konventionellen Verfahren liefert die *Point-of-care*-Analytik eine schnelle, transparente Diagnostik mit einfachen und preiswerten Tests, welche eine anschließende sofortige Behandlung Vor-Ort ermöglichen. Daher sind für *Point-of-care*-Anwendungen komplexe, kompliziert zu bedienende und störanfällige Geräte ungeeignet. Neben der Minimierung des manuellen

Aufwands sollten bei solchen Systemen die Ergebnisse direkt vorliegen und einfach zu verstehen sein. Die Eignung dieser stabilen Schnelltests für einen Einsatz Vor-Ort führt zu einer Verkürzung der Analysezeit, wodurch in der modernen Diagnostik und Analytik immer häufiger Untersuchungen außerhalb spezialisierter Labore favorisiert werden. Typische Beispiele für *Point-of-care*-Systeme sind derzeit Diabetes-, Schwangerschafts- oder Alkoholtests.

Aufgrund der Vielfalt der organischen Verbindungen steht die Bioanalytik zusätzlich vor der Herausforderung einzelne Analyte selektiv in komplexen Matrices zu bestimmen, oder auch alle in einer Probe enthaltenen Komponenten. Dies ist insbesondere wichtig bei biologischen Proben und relevant in der klinischen Analytik, in der Proteomik und in der Systembiologie. Die analytischen Verfahren basieren auf den spezifischen physikalischen und chemischen Eigenschaften der Biomoleküle wie beispielsweise deren Form, Ladung, Polarisierbarkeit oder die Affinität zu anderen Molekülen. Beispielsweise nutzen diese Systeme die natürlichen charakteristischen Wechselwirkungen unterschiedlicher Biomoleküle, unter anderem zwischen DNA-DNA, DNA-RNA, Protein-Protein oder Protein-DNA für analytische Anwendungen aus. Dieses so genannte Schlüssel-Schloss-Prinzip erlaubt hierbei den hochspezifischen Nachweis von Proteinen, DNA, RNA, Zellen oder Geweben [8]. Dadurch kann auch eine Trennung komplexer biologischer Proben und der Nachweis einer bestimmten darin enthaltenen Komponente ermöglicht werden.

Der Einsatz spezieller Mess- und Regeltechnik schafft anschließend die Vorraussetzung für eine qualitative und quantitative Auswertung der analytisch relevanten Informationen. Weitere Anforderungen an ein bioanalytisches Nachweisverfahren sind wichtige Faktoren wie Miniaturisierung, Parallelisierung, Automatisierung, Hochdurchsatz und Kosteneinsparung.

In diesem Zusammenhang haben vor allem die Biochipsysteme in den letzten Jahren das Potenzial bewiesen, um eine automatisierte Vor-Ort-Analytik mit den geforderten Parametern zu realisieren [9]. Sie bilden eine kleine, kompakte Plattform, mit deren Hilfe verschiedene analytische Untersuchungen durchgeführt werden können. Dieses Verfahren wird sehr vielfältig eingesetzt, beispielsweise in der Umweltanalytik, Lebensmitteltechnologie, Biochemie, molekularen Genetik und Diagnostik, Medizin und der Pharmakologie [10, 11]. Die Vorteile von Biochips sind ihre Parallelität, Miniaturisierung, der hohe Probendurchsatz und die Möglichkeit zur Automatisierung [12, 13]. Biochips erlauben den Nachweis einer großen Anzahl von Zielmolekülen in einem einzigen Durchlauf. Dadurch werden die Kosten für eine Analyse durch einen verringerten Einsatz der Reagenzien reduziert. Des Weiteren können Biochips mit neuartigen Herstellungsverfahren günstig produziert und eingesetzt

werden [14]. Eine Automatisierung aller Prozessschritte eines Biochips ermöglicht die Konstruktion von laborunabhängigen Analysesystemen für den Vor-Ort-Einsatz [15]. Die verringerten Kosten von Biochips, die Platz sparenden Aspekte der Miniaturisierung und der hohe Durchsatz den die Automatisierung ermöglicht, verleiht klare Vorteile gegenüber nicht chipbasierten Technologien. Die genannten Vorteile sind die Hauptursachen für die stetige Weiterentwicklung dieser Methode. Mittlerweile gibt es eine Vielzahl kommerzieller Biochipsysteme für die Analyse spezieller Biomoleküle: *Affymetrix* (Affymetrix Inc., Santa Clara, USA), *ParoCheck* (Symbio Vaccin GmbH, Herborn, Deutschland), *Nanogene* (Nanogene Inc., San Diego, USA), *ArrayIt* (MicroSpotting Solution Plus, Telechem International, Sunnyvale, USA), *Eppendorf* (Eppendorf Biochip Systems, Hamburg, Deutschland). Trotz der momentanen Forschung und Entwicklung kann mit diesen kommerziellen Systemen gegenwärtig, aufgrund mangelnder Robustheit und geringen Sensitivitäten, keine Vor-Ort-Analytik realisiert werden.

Um eine chipbasierte Bioanalytik in der Vor-Ort-Diagnostik zu verwenden ist die erfolgreiche Immobilisierung der so genannten Fängermoleküle auf den Chipoberflächen die grundlegende Vorraussetzung. Die Fängermoleküle sind in einem geordneten Raster in mikroskopisch kleinen Spots auf planaren Oberflächen immobilisiert [16]. Diese immobilisierten Moleküle müssen dann spezifische Reaktionen mit ihren komplementären Partnern eingehen können. Zusätzlich ist auch die Stabilität der Bindung zwischen den Fängermolekülen und den Chipoberflächen von großer Bedeutung. Biomoleküle können entweder durch kovalente oder elektrostatische Wechselwirkungen auf dem Chip gebunden werden. Dabei wird eine stabile kovalente Bindung bevorzugt. Durch ein Ablösen der Fängermoleküle von der Chipoberfläche im Verlauf des Analyseprozesses können instabile Bindungen zu einer Verringerung der Sensitivität führen. Aus diesem Grund wurden verschiedene Oberflächen und deren Modifikationen auf ihre Eignung als Trägeroberflächen für Biochips untersucht [17-20]. Als Trägermaterialien für Biochips dienen vorwiegend Glas oder Silizium, es ist aber auch ein Einsatz von Polymeren möglich [21, 22]. Glas oder Siliziumoberflächen werden üblicherweise mit einer Monolage, welche aktive organische funktionelle Gruppen enthält, modifiziert. Mit der Funktionalisierung der Trägeroberfläche wird die Bindungseffizienz des Chips für Biomoleküle erhöht. Beispielsweise werden Thiol- [23], Amino- [24], Aldehyd- [25] oder Epoxymodifizierungen [26] eingesetzt. Es konnte auch gezeigt werden, dass eine Mischung verschiedener Funktionalitäten eine Erhöhung der Anbindung von Biomolekülen zur Folge hat [27]. Die funktionellen Gruppen werden auf den Chipoberflächen durch kovalente Bindungen zwischen verschiedenen Siloxanen und Oberflächensilanolen etabliert

[28]. Modifizierte Oberflächen besitzen den Vorteil der direkten Reaktion mit funktionalisierten Biomolekülen. Dazu werden Biomoleküle beispielsweise mit Thiol- oder Amino-Funktionen versehen. Die resultierende Ausbildung von Disulfiden [29] oder amidartigen Verbindungen [26, 30] zwischen Oberflächen gebundenen Aldehyden [31], Epoxiden [20] oder Aminen führt zu der gewünschten stabilen Immobilisierung. Aufgrund dieses Vorteils sind modifizierte Glas- bzw. Siliziumoberflächen für Biochipanwendungen weit verbreitet. Allerdings führt die chemische Behandlung der Oberflächen zu einem erhöhten Kosten- und Zeitaufwand.

Polymere benötigen zum Teil keine Modifizierung, da die Möglichkeit besteht die funktionellen Gruppen direkt in das Grundgerüst der Polymere einzubetten [22]. Sie stellen somit eine kostengünstige Alternative zu den konventionellen Materialien dar. Des Weiteren sind sie aufgrund ihres Potenzials 3D-Strukturen zu realisieren aussichtsreiche Trägeroberflächen für Biochips. Dadurch kann eine deutliche höhere Anzahl an Fängermolekülen im Vergleich zu 2D-Oberflächen immobilisiert werden. Jedoch werden Polymere in klassischen fluoreszenzbasierten Systemen aufgrund von störender Hintergrundfluoreszenz nur vereinzelt eingesetzt. Bei der Wahl des Materials ist zusätzlich darauf zu achten, dass die Trägeroberfläche nicht durch unspezifische Anbindungen von Biomolekülen zu einem Hintergrundsignal führt.

Die anschließende Reaktion der nachzuweisenden Zielmoleküle mit den gebundenen Fängermolekülen führt zur Ausbildung eines Hybrids beider Moleküle auf der Biochipoberfläche. Für den Nachweis der spezifischen Interaktionen von Biomolekülen auf einem Biochip ist meist ein zusätzlicher Marker notwendig. Zur Markierung der Zielmoleküle gibt es eine Vielzahl an Möglichkeiten: Fluoreszenzfarbstoffe, radioaktive Marker, Chemilumineszenz, metallische Nanopartikel, redoxaktive Moleküle oder der Einsatz von Enzymen [32-35]. Die Detektion kann anschließend abhängig von dem gewählten Marker über verschiedene Methoden durchgeführt werden: optisch, spektroskopisch, gravimetrisch, elektrochemisch oder elektrisch.

Das etablierte Nachweisverfahren stellt dabei die Markierung mit Fluoreszenzfarbstoffen dar [36]. Diese Methode ermöglicht einen hochsensitiven Nachweis und kann durch die Verwendung unterschiedlicher Farbstoffe auch zum *Multilabeling* herangezogen werden. Nachteilig sind jedoch Effekte wie *Bleaching* (Ausbleichen der Farbstoffe) und *Quenching* (Reduzierung des Signals durch die Umgebung) [37]. Eine mögliche Lösung bieten die so genannten *Quantum Dots* [38, 39]. Diese nanoskaligen Strukturen aus Halbleitermaterial verfügen über stabile Signale und können durch Variation ihrer Form und Größe in ihren

optischen und elektronischen Eigenschaften beeinflusst werden. Jedoch speziell in Bezug auf die Entwicklung von tragbaren Systemen für die Vor-Ort-Analytik stellen die benötigte Auswertetechnik und die anfallenden Kosten Probleme dar. Erste Entwürfe tragbarer Fluoreszenzreader zeigen zudem eine geringe Sensitivität und mangelnde Robustheit [40, 41]. Aus diesem Grund werden metallische Nanopartikel [32, 42, 43] und auch Enzyme [44-46] als aussichtsreiche Alternativen zur Markierung mit Fluoreszenzfarbstoffen verwendet.

Enzyme werden in bioanalytischen Tests und in der Biosensorik seit langem erfolgreich als Markierungen zum Nachweis von Biomolekülen eingesetzt. Standardverfahren wie der ELISA (*enzyme linked immunosorbend assay*) [47] und der Westerblot [48, 49] werden seit den 70er Jahren in biomolekularen, immunologischen und bioanalytischen Laboren eingesetzt. Durch den Einsatz relevanter Enzyme konnten so verschiedene Nachweise für klinisch relevante Analyten entworfen werden. Die Verwendung von Enzymen für bioanalytische Nachweissysteme nutzt die hohe Spezifität und die hohen Umsatzraten enzymatischer Reaktion aus, um maßgeschneiderte sensitive und spezifische Verfahren für die Analyse unterschiedlichster Substrate zu realisieren [50, 51]. Ein weiterer Beweggrund für die Verwendung von Enzymen als Marker für biomolekulare Interaktionen ist das breite Wissen über ihren Aufbau, die Struktur sowie ihre Reaktionen und Funktionen [52-54]. Durch ihre katalytischen Eigenschaften und das Vorkommen in lebenden Organismen werden diese Moleküle zumeist als Biokatalysatoren bezeichnet [55]. Eines ihrer wichtigsten Merkmale ist ihre hohe Substratspezifität. Enzyme gehören aufgrund ihres Aufbaus aus Aminosäuren zu den Proteinen [56]. Ihre Aktivität kann durch Umgebungsparameter wie die Temperatur oder den pH-Wert beeinflusst werden. Eine Hemmung der enzymatischen Reaktion erfolgt durch entsprechende Inhibitormoleküle, die mit dem Enzym in Wechselwirkung treten. Heutzutage werden viele Enzyme rekombinant hergestellt [57]. Der Vorteil dieses Verfahrens ist die Herstellung von Enzymen im Produktionsmaßstab, wodurch die Kosten reduziert werden und große Mengen dieser Biomoleküle hergestellt werden können. Außerdem war es dadurch auch möglich ihre Aktivität zu verbessern und die Thermostabilität zu erhöhen oder die pH-Toleranz und kinetischen Eigenschaften zu verbessern. Dazu finden sich in der Literatur unterschiedlichste Beispiele [58, 59].

Durch den Einsatz enzymatischer Reaktionen auf Chipoberflächen wird das analytische Potenzial von Enzymen mit den bereits beschriebenen Vorteilen von Biochips kombiniert. Ein schneller, spezifischer, einfacher und ökonomischer Nachweis sind die hauptsächlichen Einsatzgründe. Grundsätzlich können Enzyme direkt auf der Chipoberfläche immobilisiert sein, um einen Nachweis von bestimmten Substrat- oder auch Inhibitormolekülen zu

erreichen. Des Weiteren ist es auch möglich Enzyme mit Biomolekülen zu konjugieren, um einen indirekten Nachweis von biomolekularen Wechselwirkungen durch eine anschließende enzyminduzierte Reaktion nachzuweisen. In beiden Fällen sind die Enzyme an den Oberflächen assoziiert, so dass sie während des Nachweises nicht in Lösung diffundieren und verdünnt werden. Dadurch sind die Enzyme in ihrer Wirkung lokal auf einen bestimmten räumlichen Bereich eingeschränkt. Jedoch führt eine Immobilisierung zu einem zusätzlichen Schritt in der Kinetik der Gesamtreaktion. Das Substrat muss in diesen Fall zu Beginn an das gebundene Enzym transportiert werden. In den meisten Fällen geschieht dieses passiv durch Diffusion. Daher kann man die Kinetik eines immobilisierten Enzyms als zwei-Schritt Prozess betrachten, bestehend aus dem Transport des Substrates zum Enzym und der eigentlichen enzymatischen Reaktion. Da der Substrattransport der limitierende Faktor ist, wird ein aktiver Transport der Substrate bevorzugt [60, 61]. Aus diesem Grund kann eine Enzymimmobilisierung den dynamischen Messbereich eines bioanalytischen Nachweises beeinflussen, indem die Sensitivität des Enzyms verringert wird. Die Anbindung der Enzyme auf Chipoberflächen stellt an die Trägeroberfläche spezifische Anforderungen, deren technische Anwendungen erfordern zusätzlich bestimmte andere Qualitäten (chemisch, morphologisch, mechanisch). Die chemischen Wechselwirkungen mit dem Protein müssen so angepasst werden, dass keine unerwünschten Nebeneffekte, wie zum Beispiel eine Inaktivierung des Enzyms, erfolgen. Gebräuchliche Trägermaterialien sind dabei die schon bereits für Biochips beschriebenen Oberflächen: Polysaccharide (Cellulose, Dextran), synthetische Polymere (Polystyrol, Acrylamid) und anorganische Träger (z. Bsp. Silizium, Glas, Aluminiumoxid). Außerdem ist auch der Abstand des Enzyms zur Oberfläche für dessen Aktivität von Bedeutung, diese kann über entsprechende *Spacer* (z. Bsp. Alkylgruppen) definiert eingestellt werden [62]. Letztendlich ist der Nachweis der enzymatischen Reaktion auf den Chipoberflächen für eine Analyse ausschlaggebend. Dieser kann durch verschiedene Methoden erbracht werden. Hauptsächlich werden Amperometrie [63, 64] oder Fluoreszenz genutzt [65]. Auch der enzymatische Umsatz von chromogenen Substraten kann auf Biochips genutzt werden [66]. Jedoch besteht in allen Fällen das Problem der Signalinstabilität, da die enzymatischen Reaktionen zumeist lösliche Produkte hervorbringen. Aus diesem Grund werden neben Enzymen auch metallische Nanopartikel als Marker für bioanalytische Zwecke verwendet. Durch den Einsatz von Metallnanopartikeln auf Biochips werden stabile Signale erreicht.

Kolloidale Lösungen von Metallnanopartikeln sind seit langem bekannt. Quantitative Erklärungsversuche für ihre Farberscheinungen wurden seit Mitte des 19. Jahrhunderts unternommen. Die Erkenntnisse wurden erstmalig von Faraday und Mie beschrieben, welche sich mit den optischen Eigenschaften und deren theoretischen Berechnung beschäftigten [67, 68]. Für die Aufklärung der heterogenen Natur kolloidaler Lösungen sowie für die dabei angewandten Methoden erhielt Zsigmondy 1925 den Nobelpreis für Chemie [69, 70].

Vielfältige optische Eigenschaften, wie resonant überhöhte Lichtstreuung und -absorption sowie nichtlineare Signalverstärkung machen Metallnanopartikel für eine Vielzahl physikalischer, chemischer und biophysikalischer Anwendungen interessant. Größtenteils nutzen diese Anwendungen aus, dass in Metallnanopartikeln Plasmonen, Kollektivoszillationen der Leitungselektronen, angeregt werden können, die zum Auftreten ausgeprägter Resonanzen in den optischen Spektren führen [71, 72]. Die optischen Eigenschaften von Nanopartikeln hängen dabei stark von ihrer Größe, Form, Zusammensetzung und der Umgebung ab [73].

Die technologischen Fortschritte hinsichtlich der Synthese und der exakten Charakterisierung haben in den letzten beiden Jahrzehnten in mehreren wissenschaftlichen Disziplinen ein großes Interesse vor allem an Gold- und Silbernanopartikeln ausgelöst. So lässt sich durch Laserbestrahlung von Goldnanopartikeln gezielt Wärme in der lokalen Umgebung der Partikel deponieren, was zum Beispiel zur selektiven photothermischen Molekülschädigung in medizinischen Anwendungen vorgeschlagen wurde [74]. Es konnte gezeigt werden, dass die Lichtstreuung dieser Partikel um bis zu fünf Größenordnungen intensiver als das Fluoreszenzsignal von üblicherweise in der Biologie zu Markierungszwecken eingesetzten Fluorophoren ist [75]. Das Lichtstreusignal einzelner Gold- oder Silberpartikel lässt sich mit einem handelsüblichen Lichtmikroskop betrachten und wird stark von der lokalen dielektrischen und chemischen Umgebung der Partikel beeinflusst. Die starke Lichtstreuung ist außerdem begleitet von einer hohen elektrischen Feldverstärkung in der Umgebung der Partikel, die für nicht lineare Lichterzeugung und für die oberflächenverstärkte Raman-Spektroskopie ausgenutzt wird [76]. Aufgrund ihrer hohen Extinktionskoeffizienten mit bis zu 10^{11} M^{-1} cm^{-1} können metallische Nanopartikel ebenfalls für einen Nachweis durch Messung der Extinktion verwendet werden [77]. Diese einzigartigen Eigenschaften weckten das Interesse für den Einsatz von Metallnanopartikeln für eine biochipbasierte Analytik und ermöglichten die Entwicklung von verschiedensten bioanalytischen Nachweisverfahren [32]. Zur Biofunktionalisierung der Nanopartikel kann beispielsweise thiolmodifizierte DNA genutzt werden [42, 78, 79]. Gleiche Ergebnisse konnten durch die Verwendung von Biotin-

modifizierter DNA und Streptavidin konjugierten Goldnanopartikeln erreicht werden [80]. Ihre besonderen optischen Eigenschaften werden in der Entwicklung von Verfahren zur Messung von Absorption oder Streuung ausgenutzt [81-84]. Beispielsweise wurden einfache colorimetrische DNA-Nachweise auf Basis von Goldnanopartikeln entwickelt [85]. Durch Änderung der Abstände von Metallnanopartikeln untereinander kann die Plasmonenresonanz beeinflusst werden. Mirkin und Mitarbeiter modifizierten verschiedene Ansätze von Goldnanopartikeln mit unterschiedlichen DNA-Sequenzen. Durch die Mischung der Lösungen und die Zugabe von einzelsträngigen komplementären Zielmolekülen bildeten die Nanopartikel DNA-vermittelte Aggregate, mit genau definierten Partikelabständen. Dabei konnte eine Verfärbung der Lösung von Rot nach Blau beobachtet werden. Die Ursache für diesen Farbumschlag lag in der Wechselwirkung zwischen den komplementären DNA-Strängen und der daraus resultierenden Distanz zwischen den Goldnanopartikeln. Ein Erwärmen der Mixtur auf die entsprechende Schmelztemperatur führte zum Denaturieren des DNA-Hybrids, wodurch sich die Lösung wieder Rot färbte.

Besonders interessant für den Bereich der Bioanalytik ist die Möglichkeit Metallnanopartikel durch eine anschließende autometallographische reduktive Metallabscheidung zu vergrößern [86, 87]. Dabei werden die ursprünglichen Nanopartikel als Reaktionskeim genutzt, wobei so genannte *Core-Shell*-Strukturen entstehen [88]. Das induzierte Wachstum der Partikel führt zu einer Verstärkung des Signals, wodurch die Sensitivität und die Nachweisgrenze eines bioanalytischen Nachweises verbessert werden können. In ersten Versuchen war es möglich die Bindungsereignisse von Nanopartikel-markierten Biomolekülen an Oberflächen gebundene Fängermoleküle mit Hilfe der Rasterkraftmikroskopie (*atomic force microscopy*, AFM) nachzuweisen [89]. Durch die Verwendung von transparenten Oberflächen konnte eine optische Detektion von Nanopartikel-markierten DNA-Molekülen aufgrund von reflektiertem und transmittiertem Licht erfolgen [90]. Dieser Ansatz wurde genutzt, um spezifische Wechselwirkungen zwischen DNA-Molekülen auf Biochips nachzuweisen. Die Verwendung der gebundenen Nanopartikel als Reaktionskeim für eine anschließende reduktive Silberabscheidung führte zu einer Erhöhung der Sensitivität bis in den femtomolaren Bereich. Die Auswertung konnte sogar mit einem handelsüblichen Flachbettscanner erfolgen [91].

Dieses einfache Detektionsverfahren war die Grundlage für die Entwicklung von verschiedenen portablen Analysegeräten, die auf der Markierung mit Goldnanopartikeln und anschließender Silberabscheidung basieren: *Nanosphere* (Nanosphere Inc., Northbrook, USA), *Eppendorf* (Eppendorf Biochip Systems GmbH, Hamburg, Deutschland), *Clondiag* (CLONDIAG chip technologies GmbH, Jena, Deutschland).

Zusätzlich zu den großen Extinktionskoeffizienten haben viele Metallnanopartikel auch sehr große Streukoeffizienten. Dies erlaubt eine sensitive und quantitative Bioanalyse durch das gestreute Licht von Nanopartikel-markierten Biomolekülen [92].

Das Spektrum des gestreuten Lichts hängt wiederum stark von den Partikelbeschaffenheiten ab (Größe, Material, Form). Dadurch war es möglich mit unterschiedlichen Partikeln auf einem Biochip ein *Multilabeling* durchzuführen [93]. Im Vergleich zu den auf Absorption beruhenden Verfahren konnte die Nachweisgrenze durch Messung des gestreuten Lichts der Partikel um bis zu vier Größenordnungen verringert werden, da hierbei bereits ein einzelner Partikel für ein messbares Signal ausreichend ist. Dadurch war es möglich DNA-Proben im zeptomolaren Bereich nachzuweisen [94].

Des Weiteren kann von metallischen Nanopartikeln gestreutes Licht elektromagnetische Felder verstärken. Dieser Effekt wird in der oberflächenverstärkten Raman-Spektroskopie ausgenutzt (*surface enhanced Raman spectroscopy*, SERS). Es ist bekannt, dass Metallnanopartikel Raman-gestreutes Licht bis zu einen Faktor von 10^{14}-10^{15} verstärken können [95]. Das Prinzip von SERS Messungen wurde für den Nachweis von Nanopartikel-markierter DNA und RNA auf Chipoberflächen 2002 von Cao gezeigt [96]. Diese Methode verbindet die hohe Sensitivität von SERS mit dem spezifischen *Fingerprint* der Raman-Spektroskopie. Verschiedene Entwicklungen zu SERS in der klinischen Diagnostik und für biologische Anwendungen sind bereits beschrieben [97, 98].

Neben der Vielfalt an Methoden, die die optischen Eigenschaften von Metallnanopartikeln ausnutzen, existieren nicht optische Verfahren, welche auf Messungen der elektrischen Leitfähigkeit, dem Redoxpotenzial oder der Partikelmasse beruhen.

Die spezifische Masse von Nanopartikeln wird in elektromechanischen oder gravimetrischen Konzepten verwendet, um hochsensitive Nachweise durchzuführen. Das Prinzip wurde sowohl für Quarzmikrowaagen (*quarz crystal microbalance,* QCM) und oszillierende Mikrokantilever gezeigt [99]. Zwar kann diese Methode auch labelfrei eingesetzt werden, jedoch erhöht der Gebrauch von Nanopartikeln die Sensitivität dieser Systeme deutlich. Für gravimetrische Verfahren konnten durch die zusätzliche Verwendung von Goldnanopartikeln und anschließender Silberabscheidung Nachweisgrenzen im picomolaren Bereich erreicht werden [100].

Zusätzlich kann die elektrische Leitfähigkeit von metallischen Nanopartikeln ausgenutzt werden, um die Interaktion von Biomolekülen auf der Chipoberfläche nachzuweisen [101]. Die Immobilisierung von Metallnanopartikeln in einem Elektrodenspalt kann die Elektroden durch einen leitfähigen, metallischen Film verbinden [101]. Die Änderung der Leitfähigkeit

über den Elektrodenspalt kann durch eine einfache Gleichstrommessung realisiert werden. Mit diesem einfachen Verfahren können biomolekulare Wechselwirkungen, zum Nachweis von Mikroorganismen, unter Verwendung von Nanopartikel-markierten Biomolekülen auf einen Biochip durchgeführt werden [102]. Geringe Konzentrationen an Biomolekülen führen zu geringen Partikeldichten, welche keine leitfähige Schicht im Elektrodenspalt generieren. Eine nachträgliche Silberabscheidung kann auch in diesen Fall die Sensitivität verbessern [101, 103]. Durch die Nanopartikel beziehungsweise Analytkonzentration und die verwendete Silberabscheidungszeit kann ein direkter quantitativer Bezug zur Konzentration der nachzuweisenden Biomoleküle hergestellt werden. Die Konstruktion eines mobilen und robusten Auslesegerätes für elektrisch auswertbare Biochips war der grundlegende Schritt in Richtung eines laborunabhängigen Systems [104]. Eine parallele Kontrolle des elektrischen Signals während des reduktiven Silberabscheidungsprozesses ermöglicht eine direkte Überprüfung des Signalverlaufs und des entstehenden Hintergrundes. Die Online-Kontrolle der autometallographischen Reaktion wurde bereits von Diessel 2004 beschrieben [105].

Die kapazitive Messung bietet eine weitere Möglichkeit der chipbasierten Untersuchung von Biomolekül-Interaktionen [106]. Diese Methode bedarf keiner vollständig leitfähigen Strukturen, um die Bindung von Biomolekülen und Metallnanopartikeln zu detektieren. Allerdings benötigt dieser Ansatz aufwendige, teuere Technologien und anspruchsvollere Elektrodenstrukturen, wodurch er weniger interessant für eine kostengünstige, tragbare Vor-Ort-Analytik ist.

Elektrochemische Verfahren beruhen auf dem indirekten Nachweis metallischer Nanopartikel durch Redoxprozesse. Durch einen oxidativen Schritt können anschließend die resultierenden Metallionen der Partikel elektrochemisch nachgewiesen werden. Für Goldnanopartikel-markierte DNA konnte das bereits durch *Anodic Stripping Voltametry* oder *Potentiometric Stripping* gezeigt werden [107, 108]. Die Signalintensität ist abhängig von der Art des Metalls und dessen Konzentration.

Nachteilig bei den beschriebenen Nanopartikelmarkierungen sind die oft unspezifischen Partikelanlagerungen und zusätzlich unspezifischen Metallabscheidungen. Eine Alternative bieten neuartige enzymatische Prozesse zur Metallabscheidung. Die hohe Spezifität einer enzymatischen Reaktion soll die Probleme der Nanopartikelmarkierungen beseitigen. Dazu wird an die Zielmoleküle anstatt eines Metallnanopartikels ein Enzym gebunden, welches dann in einer spezifischen Reaktion auf der Oberfläche Metallnanopartikel erzeugt.

In den letzten Jahren wurden Bestrebungen unternommen, um Enzyme als Katalysatoren für die Generierung von metallischen Nanopartikeln zu nutzen [109]. Diese Kombination hatte

das Ziel die schnelle und hochspezifische Reaktion der Enzyme mit den einzigartigen Eigenschaften von Metallnanopartikeln zu verbinden. Dadurch erweiterte sich das Anwendungsgebiet von Enzymen in der Bioanalytik, da die bisher katalysierten Nachweisreaktionen nur instabile, zumeist wasserlösliche Produkte erzeugten. Ein enzyminduziertes Wachstum von Metallnanopartikeln führt zu stabilen Signalen die nicht ausbleichen oder verblassen. Erstmalig wurde der Prozess des enzyminduzierten Wachstums metallischer Nanopartikel als Anwendung in der Immunhistologie und *In-situ*-Hybridisierung beschrieben [110, 111]. In diesen beiden Feldern bestand das Problem, dass die bisher enzymatisch umgesetzten Moleküle nach der Reaktion schnell zu diffundieren begannen, was zu einer Verringerung der Sensitivität und der räumlichen Auflösung des Signals führte. Die Vorteile eines enzyminduzierten Wachstums von Metallnanopartikeln, wie die effiziente Reaktion, die Stabilität und Reproduzierbarkeit führten zur Testung unterschiedlicher Enzyme auf ihre Fähigkeit Metallnanopartikel oder unlösliche Produkte zu generieren. Die elektrochemische Detektion von Silbernanopartikeln, abgeschieden durch alkalische Phosphatase, ist eine der ersten beschriebenen Reaktion für eine chipbasierte Bioanalytik [112-114]. Durch alkalische Phosphate induziertes Wachstum von Silbernanopartikeln wurde ebenfalls für die *Dip-Pen-Nanolithography* genutzt [115]. Dabei wurde eine AFM (*atomic force microscopy*)-Spitze in eine Enzymlösung getaucht und anschließend im permanenten Kontakt über eine Oberfläche geführt. Durch die anschließende enzymatische Reaktion entstanden so metallische Leiterbahnen im Nanometermaßstab. Weitere in molekularbiologischen Tests häufig eingesetzte Enzyme, wie Glukoseoxidase und Acteylcholinesterase wurden als mögliche Initiatoren zum Wachstum von metallischen Nanopartikeln beschrieben [109, 116].

Die vorliegende Arbeit beschäftigt sich mit Meerrettichperoxidase (*horseradish peroxidase, HRP*) induziertem Nanopartikelwachstum und der Anwendung dieses Prinzips in der Biochipanalytik. Meerrettichperoxidase gehört zur Gruppe der Oxidoreduktasen und enthält als Hämenzym einen Eisen(III) Komplex. Das Enzym besitzt eine hohe Substratspezifiät zu Wasserstoffperoxid. In dessen Gegenwart ist HRP in der Lage eine Vielzahl von phenolischen und aromatischen Aminoverbindungen zu oxidieren [117]. Des Weiteren ist bekannt, dass zu hohe Konzentrationen an Wasserstoffperoxid zur Denaturierung und folglich der Inaktivierung des Enzyms führen [118]. Allerdings kann die enzymatische Reaktion nicht mit einem Metallion als Substrat durchgeführt werden. Da das Metallion nicht direkt mit dem Enzym interagieren kann. Das enzyminduzierte Wachstum von Silbernanopartikeln ist demnach nicht ohne ein sekundäres Reagenz möglich, welches anschließend des Metallion reduziert. Durch Verwendung eines speziellen Reaktionskits ist das Enzym in der Lage

Silbernanopartikel zu generieren [119, 120]. Die bekannten Reaktionsabläufe bestimmter Enzyme und ihre Eignung metallische Nanopartikel zu erzeugen, führte zu Bestrebungen diese Biomoleküle zur Markierung auf Biochips zu nutzen. Dadurch sollten die abgeschiedenen Nanopartikel für eine Bioanalytik zugänglich gemacht werden.

Um einen Aktivitätsverlust und Instabilität der Enzyme auf den Biochipoberflächen durch Trocknungseffekte oder nicht optimale Umgebungsparameter zu vermeiden, sind grundlegende Kenntnisse über die verwendeten Enzyme notwendig, um eine bestmögliche Leistungsfähigkeit der Chipplattform zu gewährleisten. Somit ist die Biochiptechnologie auf eine Automatisierung, sowie eine genaue Steuerung und Regelung (z. Bsp. Temperatur) angewiesen, um nachteilige Reaktionen, wie eine Deaktivierung der Enzyme durch falsche Reaktionsbedingungen, zu verhindern. In den letzten Jahren wurden viele Anstrengungen unternommen die Biochiptechnologie weiterzuentwickeln und zu automatisieren. Die grundsätzlichen Vorteile einer Automatisierung sind die verringerten Analysezeiten, der geringe manuelle Aufwand, die Verringerung von Fehlern bei der Versuchsdurchführung und die Kostenreduzierung für eine komplette Analyse.

Biochips wurden in verschiedene Technologien integriert, um einen bestimmten Grad an Automatisierung zu erreichen [121, 122]. Dabei kamen beispielsweise Piezoelemente [123], Zentrifugen [124], Rotatoren [125] oder elektrische Felder zum Einsatz [126]. Diese Methoden erlauben eine induzierte Bewegung der nachzuweisenden Moleküle, wodurch eine Verkürzung der Diffusionswege erreicht wird. Zusätzlich wurde auch die Möglichkeit der Verbindung mit mikrofluidischen Systemen untersucht [1]. Mit Hilfe der Mikrofluidik lassen sich neuartige miniaturisierte Analysesysteme für chemische und biologische Anwendungen realisieren [127]. Damit stellt die Mikrofluidik eine viel versprechende Ergänzung zu der Biochiptechnologie dar. Vorzüge wie Miniaturisierung, geringer Probenverbrauch, verringerte Analysezeit, Hochdurchsatz und Automatisierung können mit mikrofluidischen Systemen erreicht werden [128]. Besonders bei der Verwendung von sensitiven Biomolekülen, wie Enzymen, kann die Kombination mit der Mikrofluidik die Stabilität dieser Moleküle sicherstellen. Beispielsweise können so Austrocknung oder Inaktivierung durch Einstellung bestimmter Pufferbedingungen (pH-Wert, Salzgehalt) vermieden werden.

In herkömmlichen Biochipsystemen ist die spezifische Bindung zwischen Fänger- und Zielmolekülen hauptsächlich diffusionslimitiert. Der passive Stofftransport als Geschwindigkeits-bestimmender Schritt ist auch die Begründung für die langen Inkubations- bzw. Anbindungszeiten konventioneller Chipsysteme. Bei festgelegtem Druck und konstanter Temperatur ist, analog zur Thermodynamik, der chemische Gradient die treibende Kraft für

die Diffusion. Jedoch gerade im Hinblick auf eine Vor-Ort-Diagnostik sind kurze Analysezeiten erwünscht. Daher wird ein aktiver Transport der Zielmoleküle bevorzugt. Auch hier bietet die Mikrofluidik eine gute Möglichkeit Flüssigkeiten während der Prozessschritte zu bewegen, um die Analysezeit zu verkürzen. Eine Bewegung der Flüssigkeiten führt zur Aufhebung der Diffusionslimitierung der Prozessschritte, wodurch die Reaktionszeiten drastisch reduziert werden können.

Neben der Entwicklung miniaturisierter optischer Techniken wird insbesondere eine elektrische Detektion für chipbasierte Biomolekülnachweise favorisiert. Die erleichterte Interpretation der Daten erscheint neben dem einfachen und robusten Nachweis als eine gute Basis für eine Automatisierung der Technologie. In dieser Arbeit wurde das enzyminduzierte Wachstum von Silbernanopartikeln für einen chipbasierten elektrischen Nachweis von Biomolekülen in ein mikrofluidisches System integriert [129]. Das Verfahren wurde aufgrund seiner Robustheit, Einfachheit und dem Potenzial zur Entwicklung eines mobilen, austauschbaren und kostengünstigen Gerätes für die Vor-Ort-Diagnostik ausgewählt. Der elektrisch auslesbare DNA-Chip wurde dazu in eine speziell angefertigte Durchflusskammer integriert. Bei der Entwicklung von *Point-of-care*-fähigen Geräten stehen flexible, zuverlässige Geräte mit simpler Handhabung im Vordergrund. Ein einfacher Austausch von wichtigen Bestandteilen der Durchflusskammer soll Kontaminationen verhindern und einen verlässlichen Betrieb gewährleisten. Die Ergebnisse dieser Arbeit legen die Basis für die Entwicklung eines komplett automatisierten Systems mit dem Ziel einer mobilen transportablen Bioanalytik für den chipbasierten elektrischen Biomolekül-Nachweis.

1.2 Eigene Forschungsergebnisse

1.2.1 Trägeroberflächen und Herstellung von Biochips

Bei der Verwendung eines Biochips ist die verlässliche, reproduzierbare Immobilisierung von Biomolekülen der Schlüsselschritt für einen sensitiven und spezifischen bioanalytischen Nachweis. Im Rahmen dieser Arbeit wurde ein Verfahren zur kovalenten Anbindung der Fängermoleküle auf epoxyfunktionalisierten Chipoberflächen genutzt. Dazu wurden die Fängermoleküle an ihrem 5´-Ende mit einer zusätzlich eingebrachten Aminofunktionalisierung modifiziert. Die anschließende Anbindung auf der epoxy-funktionalisierten Chipoberfläche benötigt nach Standardverfahren, Inkubationszeiten von mehreren Stunden bis zu einem Tag. Eine Verkürzung der Anbindungszeit konnte durch ein UV-*cross-linking* der Fänger-DNA mit den Chipoberflächen erreicht werden. Hierzu wurden die Chips nach dem Aufbringen der aminomodifizierten einzelsträngigen Fängermoleküle für kurze Zeit mit UV-Licht bestrahlt. Das Einbringen von Energie führt dazu, dass sich die Epoxyringe öffnen, wodurch die Anbindung der Aminofunktion der Fänger-DNA erleichtert wird.

Es wurden unterschiedliche Trägeroberflächen sowohl mit, als auch ohne Oberflächenmodifizierung, auf ihre Eignung für den Einsatz eines UV-*cross-linkings* untersucht. Es konnte gezeigt werden, dass die modifizierten Oberflächen verglichen mit unmodifizierten Oberflächen stärkere und homogenere Signale aufwiesen. Jedoch können auch unmodifizierte Glasoberflächen zur Immobilisierung von Fängermolekülen durch ein UV-*cross-linking* genutzt werden. Zusätzlich wurde auch der Einfluss der Modifizierung der Fängermoleküle untersucht. In den durchgeführten Versuchen konnte nachgewiesen werden, dass bei bestehender Oberflächenmodifizierung eine zusätzliche Modifizierung der Fängermoleküle nicht notwendig ist, um eine Immobilisierung zu erreichen. Da die Modifizierung der Fänger-DNA mit funktionellen Gruppen ein aufwendiges und teures Verfahren darstellt, konnten durch das UV-*cross-linking* neben dem bereits erwähnten Zeitfaktor auch die Preise für die Fängermoleküle reduziert werden.

Es ist bekannt, dass DNA durch die Bestrahlung mit UV-Licht geschädigt werden kann [130]. Es können Effekte wie beispielsweise die Thymindimerisierung auftreten. Dabei werden benachbarte Thymidine im DNA-Strang verkettet, wodurch die Erbinformation anschließend nicht korrekt abgelesen werden kann. Eine Schädigung der DNA konnte in den durchgeführten Versuchen nicht festgestellt werden. Nach dem UV-*cross-linking* der

Fängermoleküle mit den epoxyfunktionalisierten Oberflächen waren diese einer anschließenden Hybridisierung vollständig zugänglich. Es konnte eine klare Diskriminierung zwischen der komplementären Sequenz und den *Mismatch*-Proben (DNA Proben, die Basenfehlpaarungen in ihrer Sequenz enthalten) erzielt werden. Auch die Kontrollen bestätigten in allen Tests die erhaltenen Ergebnisse.

Die optimalen Bedingungen waren fünf Minuten Bestrahlung bei 254 nm mit einer Leistungsdichte von 23,96 mW/cm^2. Das UV-*cross-linking* eignete sich sowohl für die konventionellen Chipmaterialien wie Glas und Silizium, als auch für verschiedene Polymere (PEN und PBEMA). Es konnten die gleichen Sensitivitäten und Spezifitäten, verglichen mit dem Verfahren ohne UV-*cross-linking*, erreicht werden.

Der grundlegende Funktionsnachweis für den chipbasierten elektrischen Nachweis von DNA wurde für verschiedene Stämme der Gattung *Kitasatospora* (Gram-positive Bakterien der Familie Streptomycetacea) anhand von PCR (*polymerase chain reaction*) Produkten der 16s-23s rDNA-ITS (*internal transcribed spacer*)-Region durchgeführt. Dabei konnten Konzentrationen in einem Bereich von 1 ng/ml bis 1 µg/ml Biotin-markiertem PCR Produkt nachgewiesen und korrekt identifiziert werden. Die Ergebnisse führten zu einer exakten taxonomischen Einordnung der untersuchten Spezies von *Kitasatospora*. Diese Arbeit zeigte das analytische Potenzial des chipbasierten elektrischen Nachweises von Biomolekülen und war die Basis für alle folgenden Untersuchungen. Die taxonomische Identifikation von Bakterien auf dem DNA-Chip mit elektrischer Detektion läuft nach dem in Abbildung 1 dargestellten Prinzip ab. Zu Beginn wird auf der epoxymodifizierten Biochipoberfläche einzelsträngige Fänger-DNA in einen Spalt zwischen zwei Elektroden immobilisiert. Im Anschluss erfolgt die Hybridisierung der Biotin-markierten PCR-Produkte. Die PCR-Produkte der 16s-23s rDNA-ITS-Region, erlauben die Verwendung eines einzigen Primerpaars für alle untersuchten Stämme von *Kitasatospora*. Da dieser Bereich der rDNA sowohl über hoch konservierte als auch sehr variable Bereiche, die zur Speziesunterscheidung genutzt werden können, verfügt. Durch die Biotinmarkierung wird die Anbindung von einem Streptavidin-Meerrettichperoxidase-Konjugat ermöglicht. Im letzten Schritt führt das enzyminduzierte Wachstum von Silbernanopartikeln zum Überbrücken des Elektrodenspaltes und somit zu einem messbaren Anstieg der elektrischen Leitfähigkeit. Dieses Ereignis kann im Anschluss durch eine einfache Gleichstrommessung erfasst und ausgewertet werden [104]. Das Prinzip des elektrischen chipbasierten Nachweises von DNA ist zusätzlich in den folgenden Abbildungen verdeutlicht (2.1 Abb. 1, 2.2 Abb. 2 und 2.3 Abb. 4).

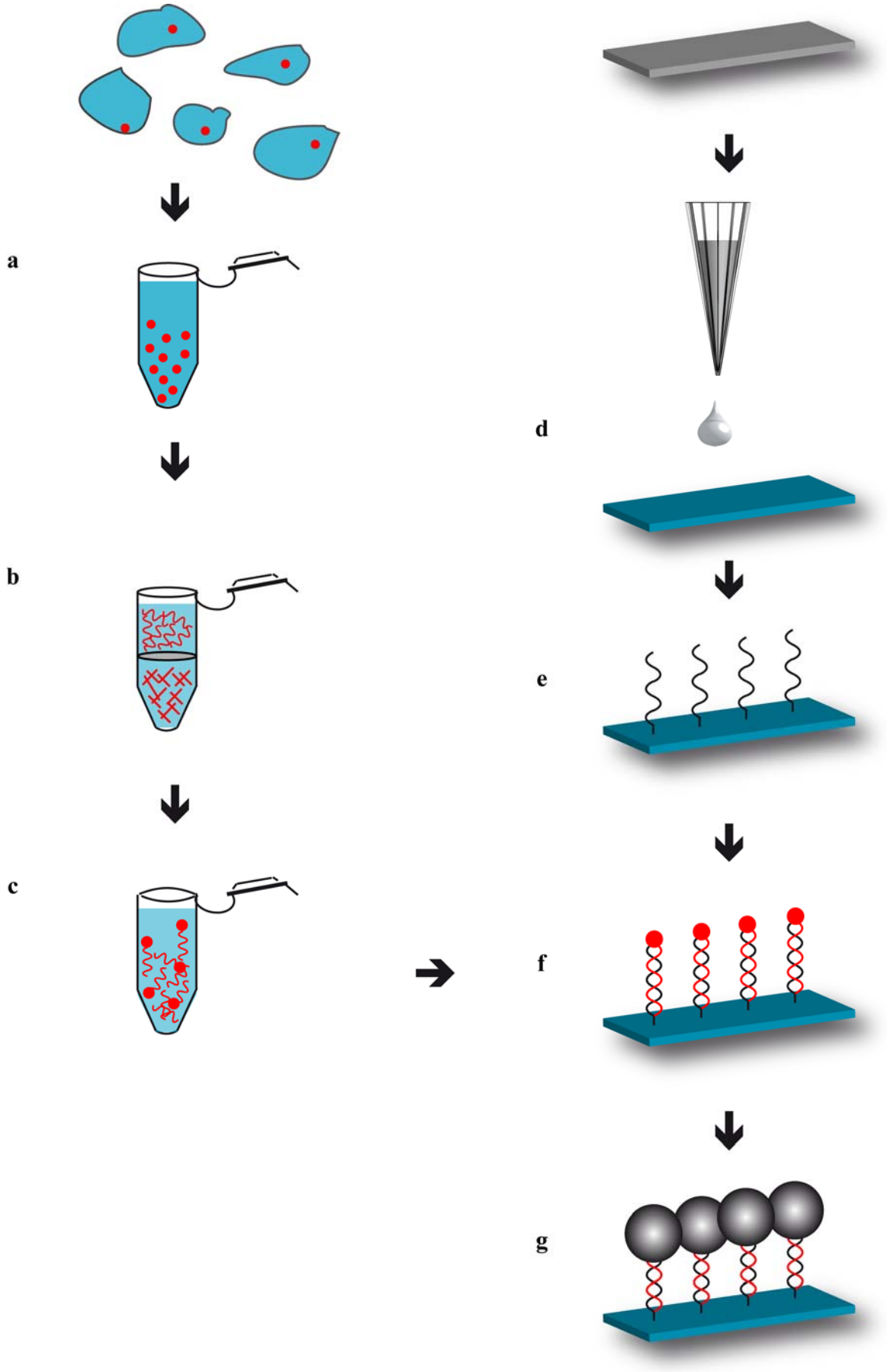
a
b
c
d
e
f
g

Abbildung 1 Prozessablauf zum speziesspezifischen Nachweis von *Kitasatospora*, mit Hilfe Biotin-markierter PCR Produkte, auf einem Biochip.
Nach Zellaufschluss (a) und Filtration (b) der Zellbestandteile erfolgte im Anschluss eine PCR (c), unter Verwendung von Biotin-markierten Primern, der 16s-23s rDNA-ITS-Region. Die Immobilisierung einzelsträngiger Fängermoleküle auf der epoxyfunktionalisierten Biochipoberfläche (d, e) ermöglichte die anschließende Hybridisierung der Biotin-markierten PCR-Produkte (f). Die Anbindung von Streptavidin konjugierter Meerrettichperoxidase erlaubte ein enzyminduziertes Wachstum von Silbernanopartikeln (g), welche über eine elektrische Messung nachgewiesen werden konnten.

Die enzyminduzierte metallographische Reaktion verhindert eine Wiederverwendbarkeit des Biochips. Ein Entfernen des abgeschiedenen Metalls würde zu einer Beschädigung der für die elektrische Signalerfassung notwendigen mikrostrukturierten Leiterbahnen führen. Für den Nachweis von *Kitasatospora* wurden die metallischen Leiterbahnen auf einer Siliziumoberfläche durch aufwendige photolithographische Prozesse aufgebracht. Für ein Einwegprodukt waren dadurch die Herstellungskosten bei geringen Stückzahlen deutlich zu hoch. Aus diesem Grund wurde nach alternativen Herstellungsverfahren für die Strukturierung der metallischen Leiterbahnen gesucht. Das Siebdruckverfahren bietet, auch für kleinere Stückzahlen, eine kostengünstige Möglichkeit, Plattformen für eine chipbasierte Analyse von Biomolekülen zu etablieren. Besonders für aufwendige und teure Elektrodenlayouts und Strukturen stellt dieses Herstellungsverfahren eine interessante Alternative dar. Bei der Untersuchung der Siebdruckelektroden fiel zu Beginn ihre raue und unregelmäßige Struktur auf (2.2 Abb. 1). Es wurden zwei Metalle zum Drucken der Elektrodenbahnen getestet, Gold und Platin. Durch seine stabileren Elektroden und die einfachere Handhabung während des Druckprozesses wurden im Anschluss die Goldelektroden bevorzugt verwendet. Die Auflösungsgrenze des Siebdruckverfahrens liegt im Bereich von 50 µm. Somit ist die Breite des Elektrodenspaltes ungefähr fünfmal größer im Vergleich zu den photolithographischen Strukturen (10 µm Spaltbreite).
Die Nachweisgrenze lag für die enzyminduzierte metallographische Reaktion bei 50 pM der nachzuweisenden DNA. Durch Verwendung von Glas als Trägeroberfläche konnte ein zusätzlicher optischer Nachweis als Kontrolle des elektrischen Signals eingeführt werden. Dazu wurden die Silberspots durch Lichtmikroskopie in Transmission analysiert. Die resultierenden Grauwerte ergaben eine Nachweisgrenze von 5 pM. Da für die optische Detektion der enzymatisch generierten Silbernanopartikel keine durchgehende leitfähige

Schicht notwendig ist, kann mit dieser Methode eine höhere Sensitivität erreicht werden. Auch ein nicht geschlossener Partikelfilm führt in diesem Fall zu einer Änderung der Transmission.

Durch die Verwendung der enzymatisch gewachsenen Partikel als Reaktionskeim für eine anschließende autometallographische reduktive Silberabscheidung konnte die Sensitivität für die elektrische Messung auf 500 fM erhöht werden (2.2 Abb. 5). Weitere Metallabscheidungen führten zu einem messbaren Anstieg des Hintergrundsignals, so dass die Nachweisgrenze für die elektrische Detektion, auf den Siebdruckelektrodenchips, mit 500 fM bestimmt wurde. Der Vorteil der elektrischen Messung gegenüber der optischen Detektion liegt in den großen dynamischen Messbereich, der neben der qualitativen Auswertung prinzipiell auch eine quantitative Bestimmung des Signals ermöglicht. In den durchgeführten Versuchen erlaubte die zusätzliche optische Kontrolle die Überprüfung der Ergebnisse der elektrischen Detektion. Dadurch konnte die Richtigkeit der elektrisch gewonnenen Daten bestätigt werden.

Durch die Verwendung von *Mismatch*-Proben wurde die Spezifität des Nachweises überprüft. Eine hohe Spezifität der Ergebnisse ist für biologische Anwendungen von großer Bedeutung, beispielsweise für eine korrekte speziesspezifische Unterscheidung. Es war sogar möglich die komplementäre Sequenz (vollständige Übereinstimmung der Basenabfolge) von einer Sequenz mit einem *Mismatch* (eine Basenfehlpaarung) zu unterscheiden.

Der Vorteil der Siebdruckstrukturen liegt in den deutlich reduzierten Herstellungskosten verglichen mit standardphotolithographischen Methoden. Die gedruckten Strukturen weisen eine hohe Stabilität auf. Das, auf den photolithographisch hergestellten Chips, etablierte Standardprotokoll konnte ohne Änderungen auf die Siebdruckchips übertragen werden. In den durchgeführten Versuchen konnten mit den Siebdruckelektroden die gleichen Sensitivitäten und Spezifitäten im Vergleich zu photolithographisch hergestellten Elektrodenstrukturen erreicht werden. Ein Einfluss des größeren Elektrodenspaltes und der unregelmäßigen Elektrodenstrukturen konnte hierbei nicht festgestellt werden.

Weitere Kostenersparnisse sollten durch die Verwendung von Polymeren anstelle von Glas oder Silizium als Trägermaterial für die elektrisch auslesbaren Biochips erreicht werden. Dazu wurden Polyethylen-Naphthalat (PEN)-Folien getestet. Die PEN-Folien besaßen keine eingebettete Funktionalisierung in ihrer Struktur, so dass zur Anbindung der Fängermoleküle eine Oberflächenmodifizierung der Folien notwendig war. Ein weiteres Problem waren die fehlenden Elektrodenstrukturen, welche für einen elektrischen Nachweis erforderlich sind. Die Verwendung der PEN-Folien bietet den Vorteil, dass über einen *Roll-to-Roll*-Prozess die

Elektrodenstrukturen auf die Folienoberflächen gedruckt werden können. Damit besteht die Möglichkeit einer schnellen Produktion von einer großen Stückzahl an flexiblen Biochipoberflächen für den elektrischen Nachweis von Biomolekülen. In den Versuchen wurden PEN-Folien mit unterschiedlichen Stärken untersucht. Des Weiteren wurden zwei Herstellungsverfahren zur Aufbringung der Elektrodenstrukturen auf den Foliensubstraten getestet. Zum einen die direkte Metallbeschichtung und zum anderen ein üblicher *Lift-off* (Abhebetechnik oder Haftmaskentechnik)-Prozess. Beide Methoden zeigten eine gute Auflösung (2.3 Abb. 2,3). Die Stabilität und Qualität der Elektroden war nicht abhängig von der Stärke der PEN-Folien. Die Biochips auf PEN-Basis konnten erfolgreich für einen Nachweis von DNA eingesetzt werden. Das Nachweisprinzip war analog zu den Biochips auf Silizium oder Glas. Die einzelsträngigen Fängermoleküle konnten erfolgreich im Spalt zwischen den jeweiligen Elektroden immobilisiert werden. Die Biotin-markierte nachzuweisende DNA konnte aus Lösung an die immobilisierten Fängermoleküle hybridisiert werden. Das abschließende enzymatisch induzierte Partikelwachstum zeigt eine deutliche Silberabscheidung auf den PEN-Folien, im Bereich der einzelnen Elektrodenspalte (2.3 Abb. 5,6). Die damit verbundene Erzeugung einer leitfähigen Brücke konnte wiederum durch eine einfache Gleichstrommessung nachgewiesen werden. Die elektrischen Messungen zeigten auch, dass die beiden verwendeten Herstellungsverfahren keinen Einfluss auf die Leistungsfähigkeit des Nachweisprinzips haben. Auch die getesteten *Mismatch*-Proben (analog zu den Versuchen auf den Siebdruckelektrodenchips) zeigten die erwarteten Signalunterschiede im Vergleich zu der komplementären Sequenz (2.3 Abb. 5,6). Die erhaltenen Ergebnisse waren im Hinblick auf die Sensitivität und Spezifität vergleichbar zu den Silizium oder Glasoberflächen. Wie auch auf den Siebdruckchips, mit Glas als Trägermaterial, konnte auch auf den transparenten PEN-Folien eine zusätzliche optische Kontrolle mitgeführt werden. Die optischen Signale bestätigten auch hier die Ergebnisse der elektrischen Messungen. Es ist daher geplant in anschließenden Arbeiten einen Nachweis mit zwei voneinander unabhängigen Messmethoden zu etablieren, um eine zeitlich permanente Signalüberprüfung auf diesen Biochips zu gewährleisten. Der dabei entstehende höhere Aufwand kann mit der gegenseitigen Kontrolle beider Messmethoden, der Verhinderung von falsch positiven bzw. falsch negativen und einem höheren dynamischen Messbereich begründet werden.

Die PEN-Folien konnten mit dem gleichen Standardprotokoll behandelt werden ohne das eine Beschädigung der Elektroden oder ein Verlust der Funktionalität beobachtet werden konnte.

Alle drei verwendeten Oberflächen (Silizium, Glas und PEN-Folien) haben für einen bioanalytischen Nachweis die Notwendigkeit einer Oberflächenmodifizierung gemein. Das heißt, die Trägeroberflächen müssen für die kovalente Anbindung der einzelsträngigen Fängermoleküle funktionalisiert werden. Die eingesetzte Oberflächenchemie führt auf den Chipsubstraten eine reaktive Epoxyfunktionalisierung über ein Organosilan ein. An den Epoxygruppen können in einem weiteren Schritt endständig aminofunktionalisierte Oligonukleotide durch Ausbildung eines sekundären Amids anbinden. Prozessablauf und Aufwendungen sind für alle drei verwendeten Oberflächen gleich und bedeuten erhöhte Kosten und Zeitaufwand.

Aus diesem Grund bestand das Interesse an der Entwicklung einer Chipplattform, die keine Oberflächenmodifizierung benötigt, um Biomoleküle kovalent auf ihrer Oberfläche zu binden. Deshalb wurde ein Konzept zur Realisierung eines vielseitigen *Ready-to-Spot*-Einwegpolymers für einen Nanopartikel als auch einen labelfreien Nachweis von Biomolekülen, basierend auf optischen und massenspektroskopischen Verfahren, entworfen. Im Unterschied zu herkömmlichen Biochips aus Silizium oder Glas benötigt dieses neuartige Polymer keinerlei Modifikationen oder zusätzliche Aktivierungsschritte, um Biomoleküle auf der Oberfläche zu immobilisieren. Die Bindungsfunktionalität wird während des Herstellungsprozesses direkt in das Polymergrundgerüst integriert. Dadurch war es möglich auf der Polymerplattform unmittelbar nach der Herstellung, ohne weitere Zwischenschritte, Biomoleküle zu immobilisieren. Der Zeit- und Kostenaufwand konnte mit diesem Polymer deutlich verringert werden.

Die Stoffchemie des Polymerchips wurde ausgiebig untersucht. Da sich die Epoxyfunktionalisierung für die Immobilisierung von DNA auf Glas und Silizium als sehr geeignet erwiesen hat, wurde diese Funktionalisierung auch für die Polymerchips verwendet. Der Polymerchip wurde durch eine Copolymerisation auf Basis von Methacrylaten hergestellt. Die erforderlichen Epoxygruppen wurden über das Monomer Glycidyl-Methacrylat in das Polymer eingebettet. Für das Polymerrückgrat wurden unterschiedliche Methacrylate getestet: Methyl-Methacrylat (schwach hydrophob), Butyl-Methacrylat (stark hydrophob) oder Methyl-Methacrylat-[2-(methacryloyloxy)-ethyl]dimethyl-(3-sulfopropyl)-ammonium (zwitterionisch). Durch die unterschiedlichen Monomere konnten die Oberflächeneigenschaften des Polymers beeinflusst und auf die gewünschten Parameter eingestellt werden (2.4 Abb. 2). Somit war es möglich neben der Hydrophobizität auch die Affinität der Oberfläche für die Adsorption verschiedener Biomoleküle zu steuern.

Die Qualität und Stabilität der Immobilisierung von Biomolekülen auf der Polymeroberfläche wurde mit MALDI/TOF-MS, AFM und Fluoreszenzmessungen untersucht. Außerdem wurden unspezifische Absorption von DNA und Proteinen sowie der Einfluss von Salzen und verschiedenen Puffern auf die Leistungsfähigkeit des Polymers getestet. Dazu wurde auch die Beeinträchtigung der DNA-Hybridisierung in verschiedenen Reaktionsmilieus analysiert. Die nachzuweisende Ziel-DNA wurde hierbei sowohl in humaner Plazenta-DNA als auch *E.coli*-Zelllysat verdünnt, um einen realen Nachweis in einer biologischen Probe zu simulieren. Durch die zusätzlich eingetragenen Komponenten wie nicht komplementäre DNA, Proteine, Lipide und Salze sollte die Stabilität und Spezifität von DNA-DNA Wechselwirkungen auf dem Polymer erprobt werden. Die Ergebnisse wiesen nur geringe Unterschiede zwischen den Signalen auf. Die Sensitivität und Spezifität des Chips konnte auch in komplexen Medien (*E.coli*-Zelllysat und humane Plazenta-DNA) bestätigt werden (2.4 Abb. 4b).

Basierend auf den Messdaten der MALDI/TOF-MS-Analyse, der Lichtmikroskopie (Transmission nach enzyminduziertem Wachstum von Silbernanopartikeln) und der Fluoreszenz wurde das Copolymer aus Glycidyl-Methacrylat und Butyl-Methacrylat als optimale Oberfläche für weitere Biochipanalysen ausgewählt (PBEMA). Davor war es jedoch wichtig eine homogene Verteilung, sowie eine optimale Dichte, der Epoxygruppen für die Fängermolekülanbindung auf der Polymeroberfläche sicherzustellen. Aus diesem Grund wurden Polymere mit unterschiedlichen Verhältnissen und Glycidyl-Methacrylat und Butyl-Methacrylat hergestellt. Die molaren Verhältnisse wurden auf 1:13,3; 1:26,6 und 1:39,9 PBEMA eingestellt. Ein Verhältnis von 1:13,3 zeigte die höchste Signalstärke verbunden mit einer sehr homogenen Oberflächenbeladung an Fängermolekülen.

Ein weiterer Vorteil des Polymerchips ist die Möglichkeit verschiedene aktuell verwendete bioanalytische Nachweisverfahren auf der gleichen Oberfläche unter den gleichen Bedingungen zu testen. Diese Arbeit zeigte erstmalig die Kombination und Integration von momentan genutzten Detektionssystemen (MALDI/TOF-MS, Fluoreszenz, AFM, Translumineszenz) auf einer kostengünstigen *Ready-to-Spot*-Polymerplattform. Ein Vergleich der Sensitivitäten der Verfahren ist in 2.4 Abb. 4a gezeigt. Die Nachweisgrenze für MALDI/TOF-MS lag im nanomolaren Bereich. Mit einer Sensitivität im picomolaren Bereich war die Nachweismethode über einen Fluoreszenzfarbstoff deutlich empfindlicher. Die Sensitivität des enzyminduzierten Wachstums von Silbernanopartikeln ist abhängig von der Reaktionszeit (es wurden 1, 3, und 5 min getestet). Bei maximaler Reaktionszeit von fünf Minuten lag die Nachweisgrenze im femtomolaren Bereich. Längere Reaktionszeiten des enzymatischen Prozesses führten zu einem Anstieg des Hintergrundsignals und wurden

deshalb nicht in die Betrachtungen mit einbezogen. Der Vorteil von MALDI/TOF liegt allerdings in der zusätzlichen Information über die Beschaffenheit der DNA. Es war möglich einen Unterschied zwischen verschieden langen DNA-Sequenzen festzustellen. Dazu wurden Sequenzen mit 20, 30 und 40 Basenpaar Länge verwendet. Eine vergleichbare Aussage ist mit herkömmlichen Hybridisierungsassays über Fluoreszenz- oder Nanopartikelmarkierungen nicht möglich.

Die aktiven Epoxygruppen des Polymers sind für mehrere Monate stabil, was eine Lagerung der Chips vor ihren bioanalytischen Einsatz ermöglicht. Zusätzlich besteht die Möglichkeit den Polymerchip in unterschiedlichsten Geometrien und Strukturierungen herzustellen, um ihn für verschiedene Auswertesysteme nutzbar zu machen. Das Herstellungsverfahren kann sehr einfach modifiziert werden, um Medium- oder Hochdichtearrays auf der Chipoberfläche zu realisieren. Durch Änderungen der Zusammensetzung des Copolymers (Variation der Verhältnisse der Monomere oder Verwendung anderer Monomere) können maßgeschneiderte Oberflächen für die Analytik verschiedener Biomoleküle entworfen werden. Des Weiteren können so Oberflächen hergestellt werden, die eine erhöhte Affinität zu Proteinen besitzen oder Proteine daran hindern an der Oberfläche zu adsorbieren. Wenn unspezifische Bindungen von Proteinen auf einer Oberfläche ausgeschlossen werden können, ist die Untersuchung von spezifischen DNA-Protein-Wechselwirkungen realisierbar.

Ein Nachteil des Polymers sind derzeit die fehlenden Elektrodenstrukturen. In den durchgeführten Versuchen konnten ausschließlich optische oder spektroskopische Verfahren getestet werden. Eine Möglichkeit leitfähige Elektrodenbahnen auf das Polymer aufzubringen, könnte das *Inkjet-Printing*-Verfahren bieten. Hierbei werden über einen handelsüblichen Tintenstrahldrucker kolloidale Lösungen von Metallnanopartikeln auf die Polymeroberfläche gedruckt. Die Kompatibilität dieser Methode mit der Polymeroberfläche muss noch geprüft werden.

1.2.2 Metallische Nanopartikel für einen chipbasierten elektrischen Nachweis von Biomolekülen

Für die Verwendung von metallischen Nanopartikeln als bioanalytische Marker ist die Biofunktionalisierung, das heißt die Anbindung von Biomolekülen (DNA oder Proteine) auf der Oberfläche der Partikel, von großer Bedeutung. Die Entwicklung von stabilen und einfachen Methoden zur Biofunktionalisierung der Partikel ist daher ein wichtiger Punkt in der Entwicklung von bioanalytischen Verfahren, welche auf einen Nachweis von metallischen Nanopartikeln beruhen. Eine momentan häufig eingesetzte Methode ist die Modifizierung mit Streptavidin, um die Partikel an ein Biotin-modifiziertes Molekül zu binden.

Die interessanten Eigenschaften metallischer Nanopartikel erlauben dabei eine große Bandbreite an Nachweisverfahren, die auch neue optische und elektrische Methoden beinhaltet. Dabei haben vor allem elektrische Methoden das Potenzial für eine Vor-Ort-Analytik, durch stabile Signale und kostengünstige, robuste Nachweissysteme gezeigt. Des Weiteren kann die Sensitivität von Nanopartikel-basierten Systemen durch zusätzliche spezifische Metallabscheidungen erhöht werden.

Genaue Kenntnisse von diesen Abscheidungsprozessen erlauben Rückschlüsse über die Geschwindigkeit der Reaktion und die entstehende Partikelgröße. Für einen elektrischen Nachweis von Biomolekülen kann so durch die Nanopartikel beziehungsweise Analytkonzentration und die verwendete Metallabscheidungszeit ein direkter quantitativer Bezug zur Konzentration der nachzuweisenden Biomoleküle hergestellt werden. Dazu wurde die Nanopartikel-basierte Generierung von leitfähigen Schichten in einem Elektrodenspalt mithilfe von AFM und Gleichstrommessungen charakterisiert und quantifiziert. Dabei konnte die Bedeckungsdichte der Chips mit Nanopartikeln (nach Metallabscheidung) genau ermittelt werden, ab der eine leitfähige Brücke zwischen den Elektroden etabliert wurde. Des Weiteren verhilft das Verständnis über Metallabscheidungsprozesse an Nanopartikeln zum Design von idealen Elektrodenlayouts. Ein wichtiger Punkt ist dabei die Größe des Elektrodenspaltes. Grundsätzlich konnte kein erheblicher Einfluss der Spaltbreite auf die Entstehung einer leitfähigen Schicht beobachtet werden. Das ist hauptsächlich dadurch zu erklären, dass die durchschnittliche Entfernung der einzelnen Partikel bei einer homogenen Verteilung nicht abhängig von der Größe des Elektrodenspaltes ist. Solang die mit Fängermolekülen bedeckte Fläche deutlich größer ist als der Elektrodenspalt, können nur geringe Abweichungen zwischen unterschiedlich großen Elektrodenspalten festgestellt werden. Vor allem bei einer inhomogenen Verteilung der Nanopartikel kann es durch die verringerte Wahrscheinlichkeit

für die Entstehung einer leitfähigen Brücke mit steigender Spaltbreite zu abweichenden Resultaten kommen. Daher ist ein optimales Ergebnis bei annährend vergleichbaren Größen von Spaltbreite und Spotdurchmesser zu erwarten. Auf Basis dieser Arbeiten könnten so einfache und schnelle quantitative Rückschlüsse für eine Vor-Ort-Analytik gezogen werden. Allerdings hat sich gezeigt, dass die unspezifische Anlagerung von Nanopartikeln auf Chipoberflächen, verbunden mit den notwendigen langen Verstärkungszeiten zu einem erhöhten Hintergrundniveau führt. Daher wurde nach einem alternativen System zur Herstellung von metallischen Nanopartikeln gesucht.

Das enzyminduzierte Wachstum von Silbernanopartikeln zeichnet sich vor allem durch die hohe Spezifität und die Geschwindigkeit der Reaktion aus. Die durchgeführten Arbeiten sollten Aufschluss über die Reaktionsgeschwindigkeit, die entstehende Partikelform, Limitierungen der Reaktion und die Beeinflussung des Hintergrundniveaus geben. Das Meerrettichperoxidase induzierte Partikelwachstum wurde auf Einzelpartikelniveau mit Hilfe standardmikroskopischer Techniken untersucht. Es wurden sowohl die Form, als auch die Dimensionen der individuellen Strukturen analysiert. In diesen Untersuchungen wurde eine Wüstenrosen-ähnliche Form der generierten Silberpartikel festgestellt.

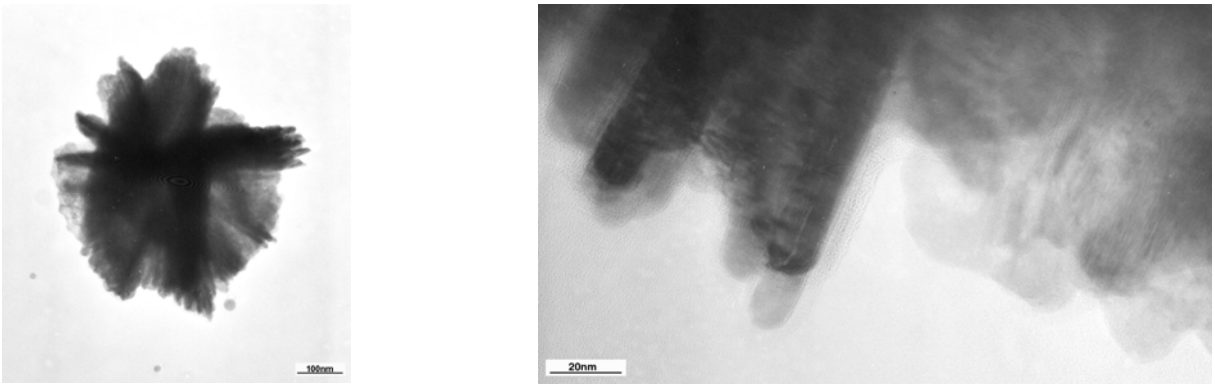

Abbildung 2 TEM-Aufnahmen eines enzymatisch gewachsenen Silberpartikels mit Wüstenrosen-ähnlicher Struktur. Im rechten Bild ist die Feinstruktur aus Silberstäbchen deutlich zu erkennen.

Durch hochauflösende TEM (*transmission electron microscopy*)-Aufnahmen (Abbildung 2) konnte gezeigt werden, dass die Feinstruktur der Partikel aus kristallinen Stäbchen besteht, welche ineinander wachsen und so die charakteristischen Partikelformen erzeugen. Untersuchungen zur Partikelhöhe und Partikelvolumen zeigten ein Abbrechen der schnellen enzymatischen Reaktion nach fünf Minuten (2.7 Abb. 4,5). Dieser Effekt kann durch die

Inaktivierung des Enzyms erklärt werden. Mit längeren Verstärkungszeiten umgibt sich das Enzym mit einer Silberhülle. Das führt dazu, dass das Enzym kein weiteres Substrat umsetzen kann und die Reaktion abstoppt. Die Erklärung für das langsame weitere Wachstum der Partikel nach fünf Minuten ist eine zweite Reaktion parallel zu der enzymatischen Reaktion. Diese Reaktion ist in ihrem Verlauf vergleichbar mit konventionellen autometallographischen reduktiven Metallabscheidungen auf Nanopartikeln. Mit höheren Enzymkonzentrationen oder längeren Verstärkungszeiten wachsen die enzymatisch hergestellten Silberpartikel ineinander und erzeugen somit deutlich größere, komplexere Strukturen. Die Effizienz der Reaktion kann durch die Variation der eingesetzten Menge an Enzym beeinflusst werden. Durch die Bindung mehrerer Enzyme in einem Komplex kann dadurch sehr schnell eine große Anzahl an Nanopartikeln erzeugt werden. Das ist vor allem für einen hochsensitiven Nachweis auf den elektrisch auslesbaren Biochip von Interesse. Allerdings sind die erhaltenen Wachstumskinetiken durch die Diffusion limitiert. Durch eine aktive Bewegung der Flüssigkeiten während der Reaktion könnte das Partikelwachstum weiter beschleunigt werden. Die gewonnenen Erkenntnisse sind wiederum für die Interpretation der Messdaten auf dem elektrischen Biochip wichtig und können für eine spätere Quantifizierung eingesetzt werden.

Die besondere und einzigartige Form der enzymatisch gewachsenen Silberpartikel ermöglicht, neben der Ausnutzung ihrer elektrischen Leitfähigkeit, auch einen Einsatz für spektroskopische Anwendungen. Das breite Absorptionsprofil der Partikel erlaubt die Verwendung als SERS (*surface enhanced Raman spectroscopy*) Substrat bei unterschiedlichen Anregungswellenlängen. Die Wüstenrosen-ähnliche Struktur mit den stäbchenförmigen Einzelkristallen ist grundlegend für die nachgewiesen hohe SERS-Aktivität der Partikel. In dieser Arbeit wurde eine Beziehung zwischen der SERS-Aktivität und der elektrischen Leitfähigkeit der Silberpartikel gefunden. Üblicherweise nimmt die SERS-Aktivität von Nanopartikeln rapide ab, sobald die Partikel nahe genug zueinander angeordnet sind, um eine leitfähige Brücke zu erschaffen. Das ist durch eine laterale Ausbreitung der lokalen Oberflächenplasmonen innerhalb der gebildeten leitfähigen Partikelschicht zu erklären. Aufgrund der Form der enzymatisch gewachsenen Silberpartikel tritt dieser Effekt selbst bei sehr dichten, leitfähigen, Partikelstrukturen nicht auf. Daher war es möglich durch das enzyminduzierte Wachstum von Silbernanopartikeln eine Relation zwischen der Leitfähigkeit und der entsprechenden SERS-Aktivität herzustellen. Durch eine einfache und schnelle Messung der elektrischen Leitfähigkeit konnte eine direkte Aussage über das SERS-Verstärkungs- Potenzial der Partikel getroffen werden. Mit einer 60%igen Bedeckungsdichte

im Elektrodenspalt wurde der Schwellenwert der Leitfähigkeit erreicht. Dieser Wert ist sowohl vergleichbar mit den vorherigen Ergebnissen für Metallnanopartikel und einer anschließenden Silberabscheidung als auch für das enzymatische Wachstum von Silbernanopartikeln. Eine Beladung mit Silberpartikeln im Elektrodenspalt von 50 – 70% war ausreichend, um einen elektrischen Kontakt zwischen den Elektroden herzustellen. In diesem Bereich wurde auch das Maximum der SERS-Aktivität erreicht. Somit ist keine weitere aufwendige Charakterisierung unter Verwendung von Standardmolekülen zur Testung der Oberflächen notwendig. Weiterhin sind die SERS-Substrate auf Basis von enzymatischen Silberpartikeln kostengünstig, einfach und auch in großen Stückzahlen herzustellen. Ihre Anwendbarkeit konnte durch die Analyse von biologisch relevanten Molekülen demonstriert werden.

1.2.3 Automatisierung für *Point-of-care*-Anwendungen

Um den chipbasierten elektrischen Nachweis von Biomolekülen für eine Vor-Ort-Analytik zugänglich zu machen, war eine Automatisierung der gesamten Prozessschritte notwendig. Die damit verbundene, erleichterte Bedienbarkeit führt zur Vermeidung von Fehlern in der Handhabung, wodurch diese Technologie auch dem geschulten Laien zur Verfügung steht. Die grundsätzlichen Anforderungen an ein laborunabhängiges bioanalytisches System sind dabei Mobilität, Robustheit, Flexibilität und natürlich eine schnelle Analyse der zu untersuchenden Probe. Im Rahmen dieser Arbeit konnte der einfache, robuste und ökonomische chipbasierte Ansatz mit elektrischer Detektion in ein mikrofluidisches System integriert werden, mit dem Ziel ein benutzerfreundliches Gerät für die Vor-Ort-Analytik zu entwickeln. Die entworfene Durchflusskammer ist die Basis für die Automatisierung der chipbasierten elektrischen Detektion von Biomolekülen als Anwendung in den Lebenswissenschaften (2.8 Abb.3).

Um Flüssigkeiten über den Chip zu transportieren und während der einzelnen Reaktionen eine Bewegung der Flüssigkeit zu induzieren, wurde eine Schlauchpumpe verwendet. Die aktive Bewegung führte zu einer erhöhten Bindungseffizienz der nachzuweisenden Biomoleküle mit den immobilisierten Fängermolekülen. Durch die Aufhebung der Diffusionslimitierung konnte der Analyseprozess beschleunigt werden. Die daraus folgende schnelle Reaktion aller Prozessschritte führte zu einer drastischen Verkürzung der Gesamtzeit für einen Nachweis (von über vier Stunden auf drei Minuten für 5 nM an nachzuweisender DNA, 2.8 Abb. 6).

Durch die Verwendung einer austauschbaren Silikondichtung mit mäanderförmigen Strukturen konnte der elektrisch auslesbare Biochip in ein mikrofluidisches System ohne Verlust von Funktionalität, Sensitivität und Spezifität integriert werden. Ein entsprechendes Temperatur- und Mikrofluidikmanagement erlaubte die Einstellung der optimalen Reaktionsparameter. Durch die verwendeten Technologien wurde ein einfacher Ansatz für die Herstellung eines *Point-of-care*-Gerätes entwickelt, welcher problemlos auf unterschiedliche Anwendungen angepasst werden kann. Aufgrund seiner Robustheit ist das Verfahren als tragbares Analysesystem für bioanalytische Prozesse einsetzbar. Die Nachweisgrenze für einen Versuch außerhalb der Durchflusskammer lag, ohne zusätzliche Metallabscheidung, bei 50 pM. Die gleiche Konzentration konnte mit dem mikrofluidischen System nachgewiesen werden. Jedoch betrug die Analysezeit nur ein Viertel der bisher benötigten Nachweisdauer. Die Nachweisgrenze ist vergleichbar mit anderen in der Literatur beschriebenen Verfahren, die ebenfalls eine aktive Bewegung der Flüssigkeiten einsetzen [131-133].

Die Nachweisgrenze könnte durch eine Verlängerung der enzymatischen Silberabscheidung weiter verringert werden. Der Einfluss der Reaktionszeit konnte bereits für die Verwendung auf den Polymeroberflächen gezeigt werden (2.4 Abb. 4a). Allerdings führten längere Reaktionszeiten in dem mikrofluidischen System zu einem schnellen Anstieg des Hintergrundniveaus. Das wurde vor allem an den Bauteilen der Durchflusskammer, wie den Schlauchverbindungen und der Silikondichtung sichtbar. Aus diesem Grund wurde eine Reaktionszeit von drei Minuten als Standard verwendet. Die erhaltenen Signale wurden sowohl elektrisch als auch optisch in Transmisssion ausgewertet. In einer späteren Anwendung spielt der optische Nachweis allerdings keine Rolle. Hier wurden die elektrischen Messdaten zusätzlich überprüft, um ihre Exaktheit zu kontrollieren. In allen Versuchen bestätigten die optischen Daten die Werte der elektrischen Messungen.

Bei höheren Konzentrationen der nachzuweisenden Moleküle kann die Analysezeit weiter reduziert werden. So betrug die Nachweisdauer für nanomolare Konzentrationen nur noch zehn Minuten. Natürlich sind diese Konzentrationen für eine Routinediagnostik nicht realistisch. Aus diesem Grund wird aktuell an der Verbindung des Biochips mit einer vorgeschalteten PCR gearbeitet.

Aufgrund seiner Unkompliziertheit können die Teile der Durchflusskammer und ihre Funktionen leicht auf andere Anwendungen angepasst werden. Beispielsweise können das Chiplayout (Anzahl der Messpunkte, Anordnung der Elektrodenstrukturen) oder die Strukturen in der Silikondichtung (für den mikrofluidischen Kanal) einfach geändert werden.

Diese Arbeit bildete die Grundlage für die Entwicklung eines bioanalytischen Werkzeugs für die Vor-Ort-Analytik. Spätere Arbeiten werden alle notwendigen Komponenten (Pumpe, Auslesegerät, Durchflusskammer) in ein Gerät integrieren, um ein System zu verwirklichen, das auch von ungeschultem Personal außerhalb von spezialisierten Laboren verwendet werden kann. Dazu ist die Installation von Ventilen geplant. Die Verwendung einer speziellen Software erleichtert die Interpretation der Messdaten durch die Umwandlung in einen einfach zu verstehenden Farbcode. Dafür kann das Auslesegerät über eine *Bluetooth*-Schnittstelle mit einem PDA (*personal digital assistant*) oder einem mobilen Telefon verbunden werden. Die Unabhängigkeit des Systems kann durch den Einbau von aufladbaren Batterien weiter erhöht werden. Untersuchungen zur Online-Detektion des elektrischen Signals, zeitgleich zu der enzymatischen Reaktion, sollen die Möglichkeit zur Quantifizierung des Signals demonstrieren.

1.2.4 Schlussfolgerungen

Insgesamt wurde in dieser Arbeit die Leistungsfähigkeit eines chipbasierten elektrischen Nachweises von Biomolekülen unter Verwendung von enzymatisch gewachsenen Silbernanopartikeln demonstriert (2.1, 2.9). Durch die Testung und Verwendung von unterschiedlichen Chipplattformen konnte die Technologie weiter verbessert werden (2.3, 2.4). Gerade der Einsatz von Polymeren als Trägeroberfläche stellt aufgrund von verbesserten Bindungseigenschaften für Biomoleküle eine viel versprechende Verbesserung zu den ursprünglich verwendeten Glas- und Siliziumoberflächen dar. In Verbindung mit dem Siebdruckverfahren zur Herstellung der benötigten Leiterbahnen konnte ein kostengünstiger, sensitiver und spezifischer Nachweis von Biomolekülen erreicht werden (2.2). Die enzymatische Reaktion zur Generierung von Silberpartikeln ist durch ihre hohe Spezifität und Geschwindigkeit eine ausgezeichnete Alternative als Marker zu metallischen Nanopartikeln und zusätzlichen reduktiven Metallabscheidungsprozessen (2.5, 2.6, 2.7). Aufgrund der besonderen Wüstenrosen-ähnlichen Form können die enzymatisch generierten Nanopartikel auch für spektroskopische Betrachtungen herangezogen werden. Die gefundene Beziehung zwischen der elektrischen Leitfähigkeit und der SERS-Aktivität der Partikel ermöglicht hierbei eine einfache Charakterisierung der Partikel und die Vorhersage ihrer SERS-Aktivität. Durch die Integration der vorgestellten Technologie in ein mikrofluidisches System konnte die Basis für eine vollständige Automatisierung der chipbasierten elektrischen Detektion von

Biomolekülen gelegt werden (2.8). Durch die Erfüllung der Grundanforderungen an ein *Point-of-care*-Gerät wie beispielsweise die Robustheit, Einfachheit, Schnelligkeit und Sensitivität ist das entwickelte Verfahren für einen Einsatz außerhalb spezialisierter Labore geeignet.

Mit den Beiträgen dieser Arbeit konnte das Potenzial der Kombination einer neuartigen enzymatischen Reaktion zur Herstellung metallischer Nanopartikel mit einer chipbasierten Bioanalytik für *Point-of-care*-Applikationen erfolgreich demonstriert werden.

Literaturverzeichnis

1. Sorger, P.K., *Microfluidics closes in on point-of-care assays*,Nature (2008) **26,** 1345-1346.

2. Marsh, P. and Cardy, D.L., *Molecular diagnostics: future probe-based strategies*,Methods Mol Biol (2004) **266,** 167-89.

3. Huckle, D., *Point-of-care diagnostics: will the hurdles be overcome this time?* ,Expert Rev Med Devices (2006) **3,** 421-6.

4. Weile, J. and Knabbe, C., *Current applications and future trends of molecular diagnostics in clinical bacteriology*,Anal Bioanal Chem (2009) **394,** 731-42.

5. Huckle, D., *Point-of-care diagnostics: an advancing sector with nontechnical issues*,Expert Rev Mol Diagn (2008) **8,** 679-88.

6. Holland, C.A. and Kiechle, F.L., *Point-of-care molecular diagnostic systems--past, present and future*,Curr Opin Microbiol (2005) **8,** 504-9.

7. Daw, R., *Lab on a chip*,Nature (2006) **442,** 367.

8. Southern, E., Mir, K. and Shchepinov, M., *Molecular interactions on microarrays*,Nat Genet (1999) **21,** 5-9.

9. Persidis, A., *Biochips*,Nature Biotechnology (1998) **16,** 981-983.

10. Heilmann, J., *Moderne Bioassay Methoden*, in *Pharmakognosie-Phytopharmazie*. 2006, Springer Verlag.

11. Rusnak, M.G., *Biotechnology of Diagnostics: Emerging Oppertunities*,Nature (1995) **13,** 1056-58.

12. Venkatasubbarao, S., *Microarrays--status and prospects*,Trends Biotechnol (2004) **22,** 630-7.

13. Wang, J., *From DNA biosensors to gene chips*,Nucleic Acids Res (2000) **28,** 3011-3016.

14. Schüler, T., Asmus, T., Fritzsche, W. and Möller, R., *Screen printing as cost-efficient fabrication method for DNA-chips with electrical read-out*,Biosensors Bioelectronics (2009) **24,** 2077-84.

15. Heller, M.J., *DNA microarray technology: devices, systems, and applications*,Annu Rev Biomed Eng (2002) **4,** 129-53.

16. Schena, M., *Microarray analysis*. 2003, Hoboken, New Jersey.: Wiley-Liss Verlag.

17. Dufva, M., *Fabrication of high quality microarrays*,Biomol Eng (2005) **22,** 173-84.

18. Diehl, F., Grahlmann, S., Beier, M. and Hoheisel, J.D., *Manufacturing DNA microarrays of high spot homogeneity and reduced background signal*,Nucleic Acids Res (2001) **29,** e38.

19. Seurynck-Servoss, S.L., Baird, C.L., Rodland, K.D. and Zangar, R.C., *Surface chemistries for antibody microarrays*,Front Biosci (2007) **12,** 3956-64.

20. Taylor, S., Smith, S., Windle, B. and Guiseppi-Elie, A., *Impact of surface chemistry and blocking strategies on DNA microarrays*,Nucleic Acids Res (2003) **31,** e87.

21. Peter, M., Schüler, T., Furthner, F., Rensing, P.A., van Heck, G.T., Schoo, H.F., Möller, R., Fritzsche, W., van Breemen, A.J., and Meinders, E.R., *Flexible biochips for detection of biomolecules*,Langmuir (2009) **25,** 5384-90.

22. Ibanez, A.J., Schüler, T., Möller, R., Fritzsche, W., Saluz, H.P., and Svatos, A., *DNA detection using a triple readout optical/AFM/MALDI planar microwell plastic chip*,Anal Chem (2008) **80,** 5892-8.

23. Rogers, Y.H., Baucom, P.J., Huang, Z.J. et al., *Immobilization of oilgonucleotides onto a glass support via disulfide bonds: a method for preparation of DNA microarrays*,Anal. Biochem. (1999) **266,** 23-30.

24. Li, J., Wang, H., Zhao, Y., Cheng, L., He, N., and Lu, Z., *Assembly method fabrication linkers for covalently bonding DNA on glass surfaces*,Sensors (2001) **1,** 53-59.

25. Schena, M., Shalon, D., Heller, R., Chai, A., Brown, P.O., and Davis, R.W., *Parallel human genome analysis: microarray-based expression monitoring of 1000 genes*,Proc Natl Acad Sci U S A (1996) **93,** 10614-9.

26. Lamture, J.B., Beattie, K.L., Burke, B.E., Eggers, M.D., Ehrlich, D.J., Fowler, R., Hollis, M.A., Kosicki, B.B., Reich, R.K., Smith, S.R., Varma, R.S., and Hogan, M.E., *Direct detection of nucleic acid hybridization on the surface of a charge coupled device*,Nucleic Acids Res (1994) **22,** 2121-5.

27. Chiu, S.K., Hsu, M., Ku, W.C., Tu, C.Y., Tseng, Y.T., Lau, W.K., Yan, R.Y., Ma, J.T., and Tzeng, C.M., *Synergistic effects of epoxy- and amine-silanes on microarray DNA immobilization and hybridization*,Biochem J (2003) **374,** 625-32.

28. Oh, S.J., Hong, B.J., Choi, K.Y. and Park, J.W., *Surface modification for DNA and protein microarrays*,Omics (2006) **10,** 327-43.

29. Chrisey, L.A., Lee, G.U. and O'Ferrall, C.E., *Covalent attachment of synthetic DNA to self-assembled monolayer films*,Nucleic Acids Res (1996) **24,** 3031-3039.

30. Wong, A.K. and Krull, U.J., *Surface characterization of 3-glycidoxypropyltrimethoxysilane films on silicon-based substrates*,Anal Bioanal Chem (2005) **383,** 187-200.

31. Zammatteo, N., Jeanmart, L., Hamels, S., Courtois, S., Louette, P., Hevesi, L., and Remacle, J., *Comparison between different strategies of covalent attachment of DNA to glass surfaces to build DNA microarrays*,Anal Biochem (2000) **280,** 143-50.

32. Festag, G., Schüler, T., Steinbrück, A., Csáki, A., Möller, R., and Fritzsche, W., *Chip-based molecular diagnostics using metal nanoparticles*,Expert Opinion on Medical Diagnostics (2008) **2,** 813-828.

33. Enders, G., *Gene profiling--chances and challenges*,Acta Neurochir Suppl (2004) **89,** 9-13.

34. Rajeevan, M.S., Dimulescu, I.M., Unger, E.R. and Vernon, S.D., *Chemiluminescent analysis of gene expression on high-density filter arrays*,J Histochem Cytochem (1999) **47,** 337-42.

35. Cheung, V.G., Morley, M., Aguilar, F., Massimi, A., Kucherlapati, R., and Childs, G., *Making and reading microarrays*,Nat Genet (1999) **21,** 15-9.

36. Schena, M., Shalon, D., Davis, R.W. and Brown, P.O., *Quantitative monitoring of gene expression patterns with a complementary DNA microarray*,Science (1995) **270,** 467-70.

37. Festag, G., Steinbrück, A., Wolff, A., Csaki, A., Moller, R., and Fritzsche, W., *Optimization of gold nanoparticle-based DNA detection for microarrays*,J Fluoresc (2005) **15,** 161-70.

38. Alivisatos, A.P., *Semiconductor clusters, nanocrystals, and quantum dots*,Science (1996) **271,** 933-937.

39. Han, M., Gao, X., Su, J.Z. and Nie, S., *Quantum-dot-tagged microbeads for multiplexed optical coding of biomolecules*,Nature Biotechnology (2001) **19,** 631-635.

40. Kang, C.C., Chang, C.C., Chang, T.C., Liao, L.J., Lou, P.J., Xied, W., and Yeungd, E.S., *A handheld device for potential point-of-care screening of cancer*,The Analyst (2007) **132,** 745-749.

41. Myers, F.B. and Lee, L.P., *Innovations in optical microfluidic technologies for point-of-care diagnostics*,Lab on a Chip (2008) **8,** 2015-2031.

42. Mirkin, C.A., Letsinger, R.L., Mucic, R.C. and Storhoff, J.J., *A DNA-based method for rationally assembling nanoparticles into macroscopic materials*,Nature (1996) **382,** 607-9.

43. Csaki, A., Möller, R. and Fritzsche, W., *Gold nanoparticles as novel label for DNA diagnostics*,Expert Rev. Mol. Diagn. (2002) **2,** 187-193.

44. Wang, J., *On-chip enzymatic assays*,Electrophoresis (2002) **23,** 713-8.

45. Sun, H., Chattopadhaya, S., Wang, J., Yao, S.Q., *Recent developments in microarray-based enzyme assay: from functional annotation to substrate/inhibitor fingerprinting*,Anal. Bioanal. Chem. (2006) **386,** 416-426.

46. Diaz-Mochon, J.J., Tourniaire, G. and Bradley, M., *Microarray platforms for enzymatic and cell-based assays*,Chem Soc Rev (2007) **36,** 449-57.

47. Engvall, E. and Perlmann, P., *Enzyme-linked immunosorbent assay (ELISA). Quantitative assay of immunoglobulin G*,Immunochemistry (1971) **8,** 871-4.

48. Renart, J., Reiser, J. and Stark, G.R., *Transfer of proteins from gels to diazobenzyloxymethyl-paper and detection with antisera: a method for studying antibody specificity and antigen structure*,Proc Natl Acad Sci U S A (1979) **76,** 3116-20.

49. Towbin, H., Staehelin, T. and Gordon, J., *Electrophoretic transfer of proteins from polyacrylamide gels to nitrocellulose sheets: procedure and some applications*,Proc Natl Acad Sci U S A (1979) **76,** 4350-4.

50. Katz, E., Heleg-Shabtai, V., Willner, B., Willner, I. and Bückmann, A.F., *Electrical contact of redox enzymes with electrodes: novel approaches for amperometric biosensors*,Bioelectrochemistry and Bioenergetics (1997) **42,** 95-104.

51. Wang, J., *Glucose Biosensors: 40 years of advances and challenges*,Electroanalysis (2001) **13,** 983-988.

52. Fischer, E., *Einfluss der Konfiguration auf die Wirkung der Enzyme*,Bericht der deutschen Chemischen Gesellschaft (1894) **27,** 2985-2993.

53. Michaelis, L. and Menten, M., *Die Kinetik der Invertinwirkung*,Biochem. Zeitschrift (1913) **49,** 333-369.

54. Bisswanger, H., *Enzymkinetik (Theorie und Methoden)*. Vol. 3. Auflage. 2000: Wiley VCH.

55. Buchholz, K., *Biokatalysatoren und Enzymtechnologie*. 1996: Wiley VCH.

56. Gey, M.H., *Instrumentelle Analytik und Bioanalytik*. Vol. 2. Auflage. 2007: Springer Verlag.

57. Kopetzki, E., Lehnert, K. and Buckel, P., *Enzymes in diagnostics: achievements and possibilities of recombinant DNA technology*,Clin Chem (1994) **40,** 688-704.

58. Helianti, I., Morita, Y., Yamaura, Y., Murakami, K., Yokoyama, K., and Tamiya, E., *Characterization of native glutamate dehydrogenase from an aerobic hyperthermophilic archaeon Aeropyrum pernix*,Applied Microbioloy and Biotechnology (2001) **56,** 388-394.

59. Sode, K., Ootera, T., Shirahane, M., Witarto, A.B., Igarashi, S., and Yoshida, H., *Increasing the thermal stability of the water soluble pyrroloquinoline quinine glucose dehydrogenase by single amino acid replacement*,Enzyme and Microbial Technology (2000) **26,** 491-496.

60. Castner, J.F. and Wingard, L.B., Jr., *Mass transport and reaction kinetic parameters determined electrochemically for immobilized glucose oxidase*,Biochemistry (1984) **23,** 2203-10.

61. Limoges, B., Saveant, J.M. and Yazidi, D., *Quantitative analysis of catalysis and inhibition at horseradish peroxidase monolayers immobilized on an electrode surface*,J Am Chem Soc (2003) **125,** 9192-203.

62. Afanassiev, V., Hanemann, V. and Wölfl, S., *Preparation of DNA and protein microarrays on glass slides coated with an agarose film*,Nucleic Acid Research (2000) **28,** 66-70.

63. Albers, J., Grunwald, T., Nebling, E., Piechotta, G. and Hintsche, R., *Electrical biochip technology--a tool for microarrays and continuous monitoring*,Anal Bioanal Chem (2003) **377,** 521-7.

64. Wang, J., Chatrathi, M.P. and Ibanez, A., *Glucose biochip: dual analyte response in connection to two pre-column enzymatic reactions*,Analyst (2001) **126,** 1203-6.

65. Hadd, A.G., Raymond, D.E., Halliwell, J.W., Jacobson, S.C. and Ramsey, J.M., *Microchip device for performing enzyme assays*,Anal Chem (1997) **69,** 3407-12.

66. Müller, R., Ditzen, A., Hille, K., Stichling, M., Ehricht, R., Illmer, T., Ehninger, G., and Rohayem, J., *Detection of herpesvirus and adenovirus co-infections with diagnostic DNA-microarrays*,Journal of Virological Methods (2009) **155,** 161-166.

67. Mie, G., *Beiträge zur Optik trüber Medien speziell kolloidaler Metallösungen*,Annalen der Physik (1908) **25,** 377-445.

68. Faraday, M., *Experimental relations of gold (and other metals) to light*,Philos Trans R Soc Lond (1857) **147,** 145-181.

69. Zsigmondy, R., *Über kolloidale Lösungen*,Zeitschrift für Elektrochemie (1902) **36,** 684-687.

70. Zsigmondy, R.A., *Zur Erkenntnis der Kolloide*. 2nd edition, 1919 ed. 1905, Jena: G. Fischer.

71. Haes, A.J., Stuart, D.A., Nie, S. and Van Duyne, R.P., *Using solution-phase nanoparticles, surface-confined nanoparticle arrays and single nanoparticles as biological sensing platforms*,J Fluoresc (2004) **14,** 355-67.

72. Aslan, K., Lakowicz, J.R. and Geddes, C.D., *Plasmon light scattering in biology and medicine: new sensing approaches, visions and perspectives*,Curr Opin Chem Biol (2005) **9,** 538-44.

73. Kelly, K.L., Coronado, E., Zhao, L.L. and Schatz, G.C., *The Optical Properties of Metal Nanoparticles: The Influence of Size, Shape, and Dielectric Environment*,J Phys Chem B (2003) **107,** 668-677.

74. Csaki, A., Garwe, F., Steinbruck, A., Maubach, G., Festag, G., Weise, A., Riemann, I., Konig, K., and Fritzsche, W., *A Parallel Approach for Subwavelength Molecular Surgery Using Gene-Specific Positioned Metal Nanoparticles as Laser Light Antennas*,Nano Lett (2007)

75. Schultz, S., Smith, D.R., Mock, J.J. and Schultz, D.A., *Single-target molecule detection with nonbleaching multicolor optical immunolabels*,Proc Natl Acad Sci U S A (2000) **97,** 996-1001.

76. Freeman, R.G., Grabar, K.C., Allison, K.J., Bright, R.M., Jackson, M.A., Smith, P.C., Walter, D.G., and Natan, M.J., *Self-Assembled Metal Colloid Monolayers: An Approach to SERS Substrates*,Science (1995) **267,** 1629-1632.

77. Yguerabide, J. and Yguerabide, E.E., *Light-scattering submicroscopic particles as highly fluorescent analogs and their use as tracer labels in clinical and biological applications. I. Theory*,Analytical Biochemistry (1998) **262,** 137-156.

78. Letsinger, R.L., Elghanian, R., Viswanadham, G. and Mirkin, C.A., *Use of a steroid cyclic disulfide anchor in constructing gold nanoparticle-oligonucleotide conjugates*,Bioconjug Chem (2000) **11,** 289-91.

79. Brust, M., Walker, M., Bethell, D., Schiffrin, D.J. and Whyman, R., *Synthesis of thiol-derivatized gold nanoparticles in a two-phase liquid-liquid system*,Journal of the Chemical Society, Chemical Communications (1994) 801-802.

80. Alexandre, I., Hamels, S., Dufour, S., Collet, J., Zammatteo, N., De Longueville, F., Gala, J.L., and Remacle, J., *Colorimetric silver detection of DNA microarrays*,Anal Biochem (2001) **295,** 1-8.

81. Yguerabide, J. and Yguerabide, E.E., *Light-scattering submicroscopic particles as highly fluorescent analogs and their use as tracer labels in clinical and biological applications. II. Experimental Characterization*,Analytical Biochemistry (1998) **262,** 157-176.

82. Yguerabide, J. and Yguerabide, E.E., *Resonance light scattering particles as ultrasensitive labels for detection of analytes in a wide range of applications*,J Cell Biochem Suppl (2001) **Suppl 37,** 71-81.

83. Kreibig, U. and Vollmer, M., *Optical Properties of Metal Clusters*. Series in Materials Science, ed. Springer. Vol. 25. 1995, Berlin.

84. Li, J., Xu, C., Zhang, Z., Wang, Y., Peng, H., Lu, Z., and Chan, M., *A DNA-detection platform with integrated photodiodes on a silicon chip*,Sensors and Actuators B (2005) **106,** 378-382.

85. Storhoff, J.J., Elghanian, R., Mucic, R.C., Mirkin, C.A. and Letsinger, R.L., *One Pot Colorimetric Differentiation of Polynucleotides with Single Base Imperfections Using Gold Nanoparticle Probes*,J. Am. Chem. Soc. (1998) **120,** 1959-1964.

86. Hacker, G.W., Grimelius, L., Danscher, G., Bernatzky, G., Muss, W., Adam, H., and Thurner, J., *Silver acetate autometallography: an alternative enhancement technique for immunogold-silver staining (IGSS) and silver amplification of gold, silver, mercury and zinc in tissues*,J Histotechnol (1988) **11,** 213-221.

87. Festag, G., Steinbrück, A., Csaki, A. and Fritzsche, W., *Single particle studies of the autocatalytic metal deposition onto surface-bound gold nanoparticles reveal a linear growth*,Nanotechnology (2007) **17,** 1-10.

88. Steinbrück, A., Csaki, A., Festag, G. and Fritzsche, W., *Preparation and Optical Characterization of Core-Shell Bimetal Nanoparticles*,Plasmonics (2006) **1,** 79-85.

89. Csaki, A., Möller, R., Straube, W., Köhler, J.M. and Fritzsche, W., *DNA monolayer on gold substrates characterized by nanoparticle labeling and scanning force microscopy*,Nucleic Acids Res (2001) **29,** e81.

90. Reichert, J., Csaki, A., Köhler, J.M. and Fritzsche, W., *Chip-based optical detection of DNA hybridization by means of Nanobead Labeling*,Anal. Chem. (2000) **72,** 6025-6029.

91. Taton, T.A., Mirkin, C.A. and Letsinger, R.L., *Scanometric DNA array detection with nanoparticle probes*,Science (2000) **289,** 1757-1760.

92. Fritzsche, W. and Taton, T.A., *Metal nanoparticles as labels for heterogeneous, chip-based DNA detection*,Nanotechnology (2003) **14,** R63-R73.

93. Taton, T.A., Lu, G. and Mirkin, C.A., *Two-color labeling of oligonucleotide arrays via size-selective scattering of nanoparticle probes*,J Am Chem Soc (2001) **123,** 5164-5.

94. Elghanian, R., Storhoff, J.J., Mucic, R.C., Letsinger, R.L. and Mirkin, C.A., *Selective colorimetric detection of polynucleotides based on the distance-dependent optical properties of gold nanoparticles*,Science (1997) **277,** 1078-81.

95. Nie, S. and Emory, S.R., *Probing Single Molecules and Single Nanoparticles by Surface-Enhanced Raman Scattering*,Science (1997) **275,** 1102-6.

96. Cao, Y.W., Jin, R. and Mirkin, C.A., *Nanoparticles with Raman spectroscopic fingerprints for DNA and RNA detection*,Science (2002) **297,** 1536-1540.

97. Vo-Dinh, T., Yan, F. and Wabuyele, M.B., *Surface-enhanced Raman scattering for medical diagnostics and biological imaging*,J Raman Spectroscopy (2005) **36,** 640-647.

98. Hering, K., Cialla, D., Ackermann, K., Dorfer, T., Moller, R., Schneidewind, H., Mattheis, R., Fritzsche, W., Rosch, P., and Popp, J., *SERS: a versatile tool in chemical and biochemical diagnostics*,Anal Bioanal Chem (2008) **390,** 113-24.

99. Okahata, Y., Kitamura, Y., Hagiwara, N. and Furusawa, H., *Quantitative detection of binding of PCNA protein to DNA strands on a 27 MHz quartz-crystal microbalance*,Nucleic Acids Symp Ser (2000) **44,** 243-244.

100. Su, M., Li, S. and Dravid, V.P., *Microcantilever resonance-based DNA detection with nanoparticle probes*,Applied Physics Letter (2003) **82,** 3562-3564.

101. Möller, R., Csaki, A., Köhler, J.M. and Fritzsche, W., *Electrical classification of the concentration of bioconjugated metal colloids after surface adsorption and silver enhancement*,Langmuir (2001) **17,** 5426-5430.

102. Möller, R., Schüler, T., Günther, S., Carlsohn, M.R., Munder, T., and Fritzsche, W., *Electrical DNA-chip-based identification of different species of the genus Kitasatospora*,Appl Microbiol Biotechnol (2008) **77,** 1181-8.

103. Csaki, A., Kaplanek, P., Möller, R. and Fritzsche, W., *The optical detection of individual DNA-conjugated gold nanoparticle labels after metal enhancement*,Nanotechnology (2003) **14,** 1262-1268.

104. Urban, M., Möller, R. and Fritzsche, W., *A paralleled readout system for an electrical DNA-hybridization assay based on a microstructured electrode array.*,Review of Scientific Instruments (2003) **74,** 1077-1081.

105. Diessel, E., Grothe, K., Siebert, H.M., Warner, B.D. and Burmeister, J., *Online resistance monitoring during autometallographic enhancement of colloidal Au labels for DNA analysis*,Biosens Bioelectron (2004) **19,** 1229-35.

106. Nacke, T., Barthel, A., Friedrich, J., Helbig, M., Sachs, J., Schäfer, M., Peyerl, P., and Pliquett, U., *A new hard and software concept for impedance spectroscopy analysers for broadband process measurements*,IFMBE Proceedings (2007) **17,** 194–197.

107. Dequaire, M., Degrand, C. and Limoges, B., *An electrochemical metalloimmunoassay based on a colloidal gold label*,Anal Chem (2000) **72,** 5521-8.

108. Wang, J., Xu, D., Kawde, A.N. and Polsky, R., *Metal nanoparticle-based electrochemical stripping potentiometric detection of DNA hybridization*,Anal Chem (2001) **73,** 5576-81.

109. Willner, I., Baron, R. and Willner, B., *Growing Metal Nanoparticles by Enzymes*,Advanced Materials (2006) 1109-1120.

110. Hainfeld, J.F., Eisen, R.N., Tubbs, R.R. and Powell, R.D., *Enzymatic Metallography: A simple new staining method*, in *Proceedings of Microscopy and Microanalysis 2002*, Voekl, E., Piston, D., Gauvin, R., Lockley, A.J., Bailey, G.W., and McKernan, S., Editors. 2002, Cambridge University Press: New York. p. 916CD.

111. Mayer, G., Leone, R.D., Hainfeld, J.F. and Bendayan, M., *Introduction of a novel HRP substrate-Nanogold probe for signal amplification in immunocytochemistry*,Journal of Histochemistry and Cytochemistry (2000) **48,** 461-469.

112. Hwang, S., Kim, E., Kwak, J., *Electrochemical Detection of DNA Hybridization Using Biometallization*,Anal. Chem. (2005) **77,** 579-584.

113. Fanjul-Bolado, P., Hernandez-Santos, D., Gonzalez-Garcia, M.B. and Costa-Garcia, A., *Alkaline phosphatase-catalyzed silver deposition for electrochemical detection*,Anal Chem (2007) **79,** 5272-7.

114. Zhang, P., Chu, X., Xu, X., Shen, G. and Yu, R., *Electrochemical detection of point mutation based on surface ligation reaction and biometallization*,Biosens Bioelectron (2008) **23,** 1435-41.

115. Basnar, B., Willner, I. and Willner, B., *Synthesis of Nanowires Usinf Dip-Pen Nanolithography and Biocatalytic Inks*,Advanced Materials (2006) 713-718.

116. Willner, I., Basnar, B., Willner, B., *Nanoparticle-enzyme hybrid systems for nanobiotechnology*,FEBS Journal (2007) **274,** 302-309.

117. Silaghi-Dumitrescu, R.L., *HRP: A summary of its structure, mechanism and substrate diversity*,LABPV—Peroxidase Biotechnology and Application 1–17 (2006)

118. Hernandez-Ruiz, J., Arnao, M.B., Hiner, A.N.P., Garcia-Canovas, F. and Acosta, M., *Catalase-like activity of horseradish peroxidase : relationship to enzyme inactivation by H2O2*,Biochem. J. (2001) **354,** 107-114.

119. Schüler, T., Steinbrück, A., Festag, G., Möller, R. and Fritzsche, W., *Enzyme-induced growth of silver nanoparticles studied on single particle level*,Journal of Nanoparticle Research (2008) **11,** 939-946.

120. Festag, G., Schüler, T., Möller, R., Csáki, A. and Fritzsche, W., *Growth and percolation of metal nanostructures in electrode gaps leading to conductive paths for electrical DNA analysis*,Nanotechnology (2008) **19,** 125303 (9pp).

121. Dittrich, P.S., Tachikawa, K. and Manz, A., *Micro total analysis systems. Latest advancements and trends*,Anal Chem (2006) **78,** 3887-908.

122. Morais, S., Carrascosa, J., Mira, D., Puchades, R. and Maquieira, A., *Microimmunoanalysis on standard compact discs to determine low abundant compounds*,Anal Chem (2007) **79,** 7628-35.

123. Toegl, A., Kirchner, R., Gauer, C. and Wixforth, A., *Enhancing results of microarray hybridizations through microagitation*,J Biomol Tech (2003) **14,** 197-204.

124. Peytavi, R., Raymond, F.R., Gagne, D., Picard, F.J., Jia, G., Zoval, J., Madou, M., Boissinot, K., Boissinot, M., Bissonnette, L., Ouellette, M., and Bergeron, M.G., *Microfluidic device for rapid (<15 min) automated microarray hybridization*,Clin Chem (2005) **51,** 1836-44.

125. Pappaert, K., Vanderhoeven, J., Van Hummelen, P., Dutta, B., Clicq, D., Baron, G.V., and Desmet, G., *Enhancement of DNA micro-array analysis using a shear-driven micro-channel flow system*,J Chromatogr A (2003) **1014,** 1-9.

126. Edman, C.F., Raymond, D.E., Wu, D.J., Tu, E., Sosnowski, R.G., Butler, W.F., Nerenberg, M., and Heller, M.J., *Electric field directed nucleic acid hybridization on microchips*,Nucleic Acids Res (1997) **25,** 4907-14.

127. Haeberle, S. and Zengerle, R., *Microfluidic platforms for lab-on-a-chip applications*,Lab Chip (2007) **7,** 1094-110.

128. Abgrall, P. and Gu´e, A.M., *Lab-on-chip technologies: making a microfluidic network and coupling it into a complete microsystem—a review*,J. Micromech. Microeng. (2007) **17,** 15-49.

129. Schüler, T., Kretschmer, R., Jessing, S., Urban, M., Fritzsche, W., Möller, R., and Popp, J., *A disposable and cost efficient microfluidic device for the rapid chip-based electrical detection of DNA*,Biosens Bioelectron (2009)

130. Sinha, R.P. and Häder, D.P., *UV-induced DNA damage and repair: a review*,Photochem. Photobiol. Sci. (2002) **1,** 225-236.

131. Erickson, D., Liu, X., Krull, U. and Li, D., *Electrokinetically Controlled DNA Hybridization Microfluidic Chip Enabling Rapid Target Analysis*,Anal Chem (2004) **76,** 7269-7277.

132. Noerholm, M., Bruus, H., Jakobsen, M.H., Telleman, P. and Ramsing, N.B., *Polymer microfluidic chip for online monitoring of microarray hybridizations*,Lab Chip (2004) **4,** 28-37.

133. Benoit, V., Steel, A., Torres, M., Yu, Y.Y., Yang, H., and Cooper, J., *Evaluation of three-dimensional microchannel glass biochips for multiplexed nucleic acid fluorescence hybridization assays*,Anal Chem (2001) **73,** 2412-20.

Kapitel 2

Veröffentlichungen

Auf den nachfolgenden Seiten sind die Nachdrucke der im Rahmen dieser Dissertation erschienenen Publikationen aufgeführt. Die Urheberrechte sind jeweils auf dem Deckblatt angegeben.

2.1 Electrical DNA-chip-based identification of different species of the genus *Kitasatospora*

Robert Möller, Thomas Schüler, Sebastian Günther, Marc René Carlsohn, Thomas Munder, and Wolfgang Fritzsche

Appl. Microbiol. Biotechnol. (**2008**) 77:1181–1188

Appl Microbiol Biotechnol (2008) 77:1181–1188
DOI 10.1007/s00253-007-1241-0

METHODS

Electrical DNA-chip-based identification of different species of the genus *Kitasatospora*

Robert Möller · Thomas Schüler · Sebastian Günther · Marc René Carlsohn · Thomas Munder · Wolfgang Fritzsche

Received: 24 July 2007 / Revised: 3 October 2007 / Accepted: 5 October 2007 / Published online: 10 November 2007

Abstract The identification of different *Kitasatospora* strains has been shown with a DNA-chip based on an electrical readout scheme. The 16S-23S rDNA internal transcribed spacer region of these *Actinomycetes* was used for identification. Two different capture probes per strain were immobilized on the chip. The capture probes were spotted on a DNA-chip with electrode structures for an electrical DNA detection. A biotinylated PCR product of the 16S-23S rDNA region was incubated on the chips and bound to its complementary capture sequences. Followed by a gold nanoparticle or enzyme labeling and a deposition of silver, the binding of the PCR product was detected by an increase of the measured conductivity on the chip. To show the applicability of this detection system, four strains of *Kitasatospora* were chosen for an identification using the DNA-chip with electrical detection. Each strain was clearly identified using the system. Concentrations of the polymerase chain reaction (PCR) products within the range of 1 ng/ml to 1 μg/ml were detected and identified. These tests are the first application of this novel electrical detection scheme for the identification and classification of microorganisms. The presented results show that the DNA-chip with electrical detection can be used for a robust and cost-efficient DNA analysis.

Keywords DNA-chip · Electrical readout · *Kitasatospora* · Gold nanoparticles · 16S-23S rDNA

W. Fritzsche
Institute of Photonic Technology,
P.O. Box 100239, 07702 Jena, Germany

S. Günther · M. R. Carlsohn · T. Munder
Leibniz-Institute for Natural Product Research and Infection Biology e.V.–Hans-Knöll-Institute,
Beutenbergstr. 11a,
07743 Jena, Germany

Present address:
R. Möller (✉) · T. Schüler
Institute for Physical Chemistry, Friedrich-Schiller-University,
Helmholtzweg 4,
07743 Jena, Germany
e-mail: robert.moeller@ipht-jena.de

Present address:
S. Günther
Department of Veterinary Medicine, Freie Universität Berlin,
Oertzenweg 19b,
14163 Berlin, Germany

Present address:
T. Munder
CLONDIAG Chip Technologies,
Löbstedter Str. 103–105,
07749 Jena, Germany

Introduction

In screening experiments for novel microbial producers of bioactive substances, the reliable characterization of the isolates is the most time-consuming part of work. Frequently, much work is invested in isolates that later turn out to belong to known species. Additionally, phenotypic studies often do not allow a definite differentiation between closely related taxa. The short but turbulent taxonomic history of *Kitasatospora* nicely exemplifies the difficulties in determining correct taxonomic positions of isolates. The genus was first proposed by Omura et al. (1982) in 1982 and includes 18 valid species to date. However, based on

16S rDNA data, Wellington et al. (1992) proposed in 1992 that *Kitasatospora* should be reduced to synonym with *Streptomyces*. Ochi and Hiranuma (1994) later supported this proposal. This reclassification was undone in 1997 by Zhang et al. (1997). The authors showed that *Streptomyces* and *Kitasatospora* formed two stable monophyletic branches, when analyzing sequence data of the 16S-23S internal transcribed spacer (ITS). However, a phenotypic differentiation between both genera is still hard to achieve.

These difficulties illustrate the need for a fast and reliable system for the identification of microrganisms (Günther et al. 2006). Therefore, the application of DNA-chips for these purposes is a tempting promise. The DNA-chip technology combines the accuracy of sequence analysis with the speed of arrays. A second important point is the possibility of detecting various strains in a single experiment. The detection of binding events on a DNA-chip is normally achieved by labeling target DNA with fluorescent dyes. Fluorescence labeling also allows for multicolor labeling and multiplexed detection of different DNA targets hybridized to the same DNA-chip or micro-array (Cheung et al. 1999; Schena et al. 1996). Nevertheless, fluorescent dyes also have some disadvantages: The dyes are expensive, they photobleach, and the equipment needed to image fluorescent-labeled DNA-chips is expensive and bound to specialized laboratories (Fare et al. 2003; Fritzsche and Taton 2003). Because of those disadvantages, there is a need for new inexpensive labeling and detection schemes for DNA-chips that also allow for the miniaturization of the equipment and the realization of devices for on-site use that are no longer bound to a use in specialized laboratories. Systems with electrical read-out are especially promising for such applications (Drummond et al. 2003). One of these new approaches for chip-based DNA detection is the conductivity-based readout (Möller et al. 2001; Park et al. 2002). Here, a gap between two electrodes is bridged with conductive material (silver) after the binding of target DNA, leading to a massive rise in the measured conductivity over the gap (Fig. 1). Because this detection scheme does not require the use of any optical equipment, the realization of inexpensive and robust equipment for the readout of the chips becomes possible.

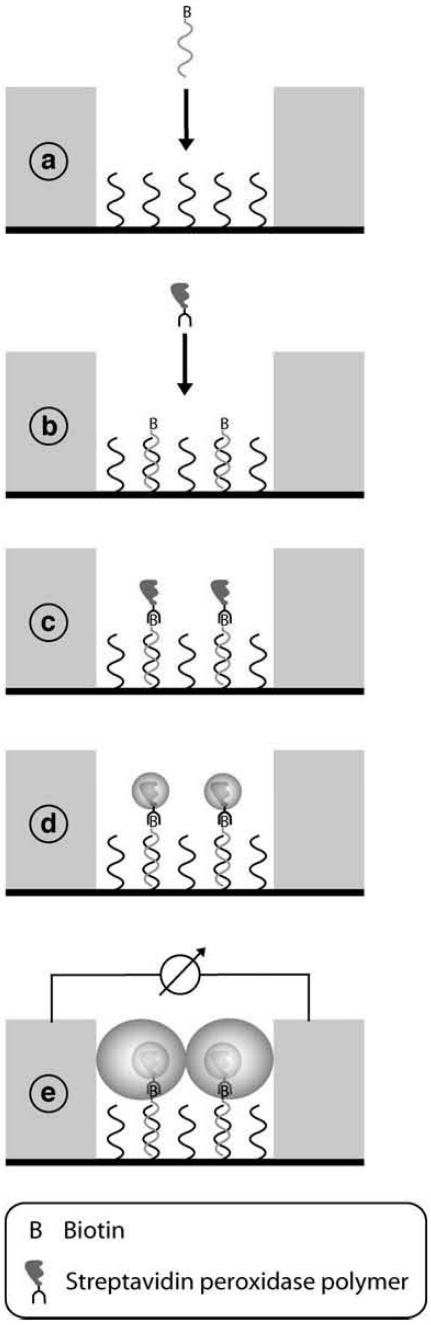

Fig. 1 Scheme of the chip-based electrical detection. Capture DNA is immobilized in the gap between two electrodes and the chip is incubated with biotinylated PCR product (**a**). Afterwards, the streptavidin peroxidase polymer is bound to the biotin modification of the PCR product (**b**, **c**), followed by the enzymatic deposition of silver (**d**). For a signal enhancement, an autometallographic silver enhancement can be applied, leading to a further growth of the silver particles formed by the enzymatic silver deposition (**e**). Streptavidin gold nanoparticle conjugates can also be used as "seeds" for the deposition of silver, then only autometallographic silver enhancement is used for the metal deposition

In this study, we report on a robust and inexpensive detection scheme for a chip-based DNA detection using an electrical readout. This was applied to reliably discriminate different strains of the *Actinomycetes* genus *Kitasatospora* by using the 16S-23S intergenic spacer as the target region.

Materials and methods

Chip preparation

The centerpiece of the electrical readout of a DNA chip is a microstructured chip with 42 electrode gaps, each 10 μm wide. All structures on the chip surface were manufactured by standard photolithographic procedures. As substrate for the DNA chips, 4″ silicon wafers with a 100-nm layer of silicon dioxide were used. To protect the chip surface and to minimize the effects of the unspecific background, a microstructured 200-nm thick layer of silicon nitride was deposited on the chip surface. This protective layer covered the entire chip except for the contact pads for the readout of the chip and windows of 250×250 μm over each of the 42 electrode gaps. These windows allowed the surface modification of the silicon dioxide surface and the immobilization of the capture DNA.

For the binding of the amino-modified capture DNA, the chip surface was modified with (3-glycidyloxypropyl) trimethoxysilane as described elsewhere (Möller et al. 2000). To deposit small volumes of the capture DNA solution, a pin spotter (SpotBot; TeleChem International, Sunnyvale, CA, USA) was used. After incubation for several hours in a humidified chamber at 37°C, the chips were thoroughly washed to remove all unbound capture DNA. To block all remaining reactive groups, incubation for 15 min in a 50 mM ethanolamine solution in 0.1 M Tris with 0.1% sodium dodecyl sulfate (SDS) pH 9.0 was used. Finally, the chips were washed with distilled water and dried under a stream of nitrogen. The substrates were then ready for the hybridization of the 5′biotin-labeled polymerase chain reaction (PCR) amplification products.

Hybridization

Before the hybridization, the 5′-biotin-labeled PCR amplification products were mixed with the hybridization buffer and heated for 5 min at 95°C and finally put on ice for 2 min. For the hybridization, 6× SSPE buffer was used. Droplets of 100 μl of the denatured PCR product were given on the chip and incubated for 1 h at 65°C in a humidity chamber. Afterwards, the substrates were washed for 5 min each in 2× saline-sodium citrate (SSC) and 0.2% SDS, 2× SSC and 0.2× SSC. Finally, the chips were dried under a stream of nitrogen.

Silver deposition

As seeds for the deposition of silver to the chip surface, streptavidin conjugates with gold nanoparticles (5 nm gold particles; British Biocell) or a streptavidin peroxidase polymer (Sigma-Aldrich) were used. The exact labeling procedure and the protocol for the autometallographic silver deposition and the enzymatic silver deposition with the EnzMet™ reagent (Nanoprobes, Yaphank, NY, USA) is described elsewhere (Möller et al. 2005).

Conductivity measurement

For the measurement of the conductivity, a custom-built measurement device was used (Urban et al. 2003). Briefly, the reader device is constructed around a special socket that holds and contacts the chip. The reader is controlled by an embedded PC that also controls a multiplexed ohmmeter for a semi-parallel measurement of all 42 measurement spots. The processing of the data is also done by the embedded PC, and the results are shown on a display. The results can be stored in the reader and also can be transferred to standard PCs for further data analysis.

Bacterial strains and culture conditions

The *Kitasatospora* species were obtained from the Hans-Knöll-Institute culture collection and from the German Collection of Microorganisms and Cell Cultures GmbH (DSMZ). Strains were cultivated at 28°C for 3 days in shake flasks containing organic medium 79 (Prauser et al. 1987).

Isolation of genomic DNA from *Kitasatospora* species and PCR amplification

Cells were harvested by centrifugation at 3,000 rpm for 3 min. The isolation of genomic DNA from 20 μl of cell pellet was performed with the DNeasy-tissue kit (Qiagen, Düsseldorf, Germany). The success of the DNA isolation was analyzed on 2% agarose gels, and the DNA was stored at −20°C before PCR. Amplification of the 16S-23S rDNA ITS region was achieved with the primers SGK1 (5′-GGTTGGATCCACCTCCTT-3′) and SGK2 (5′-TGCCAAGGCATCCAC-3′) using 2 U of Taq DNA polymerase in a total reaction volume of 50 μl according to (Günther et al. 2006). PCR products were finally purified by isopropanol precipitation.

Results

Previous experiments showed that a DNA-chip with an electrical detection based on a resistance measurement can be used for the detection of short synthetic DNA molecules (Li et al. 2003; Möller et al. 2001; Park et al. 2002). Gold nanoparticles were used as labels in those experiments. An autometallographic silver enhancement of the surface-bound gold nanoparticles was needed to achieve a detectable drop in the measured resistance. The principle

of this readout scheme is illustrated in Fig. 1. To bind the DNA to the nanoparticles, a thiol-modification of the DNA was used (Storhoff et al. 1998). In another approach, the modification of DNA with biotin was used to bind DNA to conjugates of streptavidin and gold nanoparticles (He et al. 2000). It was also shown that there was a correlation between the measured resistance, the concentration of the target DNA, and the time for the silver deposition (Möller et al. 2001). This allows a quantification of the measurements. An increase in the sensitivity and a reduction of the non-specific background was achieved by using a streptavidin peroxidase conjugate instead of gold nanoparticles for a highly specific deposition of silver on the chip surface (Möller et al. 2005). In our experiments, we used gold nanoparticles and the streptavidin peroxidase complex for the deposition of silver (for the analysis of our measured values we plotted the measured conductivity over the enhancement time).

Construction of the DNA-chip

To prove that the electrical chip-based DNA detection is suited for the rapid and reliable identification of bacterial strains and isolates, four strains of *Kitatsatopora* (*K. chochleata*, *K. kifunense*, *K. phosalacinea*, and *K. setae*) were chosen. Two specific capture probes for each *Kitatsatopora* strain were immobilized on the chip (Table 1). Four electrode gaps were modified with one specific capture DNA sequence each. Two universal (uni1; uni3) capture sequences were also immobilized (Table 1). These sequences hybridize with all *Kitasatospora* PCR products and present a positive control. Two electrode gaps would remain unmodified and serve as negative controls in the experiments. All the above-mentioned capture sequences had been evaluated on another microarray format (Array Tube®; Clondiag, Jena, Germany). The selection process, the design, and the evaluation of the capture probes is described elsewhere (Günther et al. 2006). In brief, the internal transcribed spacer (ITS) between the 16S and 23 S rRNA genes was selected for the classification of *Kitasatospora*. This region is well suited as a genetic marker for molecular taxonomy on the species level because it is known to be more variable than the rRNA genes themselves (Gurtler and Stanisich 1996; Zhang et al. 1997). A primer pair (SGK1 and SGK2; Table 1) was designed for the amplification of the ITS sequences, and biotin was integrated in the PCR products by using 5′-biotin-labeled primers.

Table 1 Sequences of the capture DNA molecules that were immobilized on the DNA-chip with the electrical readout and the used primers

	Sequence 5-3′	Taxonomic classification
coch 1	ggtcaccagcttggtgtgtcgggcac	*K. chochleata*
coch 2	attcggcacactcggtagggatcactag	*K. chochleata*
kif 1	gaaagcgtttcttgagtctggtgtgt	*K. kifunense*
kif 2	attcggcacactgggtgatggttcgtg	*K. kifunense*
phos 1	agacagggaccgcttggtgtgtcggg	*K. phosalacinea*
phos 2	attcggcacacacggttgggatctgc	*K. phosalacinea*
set 1	gaaagcgcttcgtctggtcgtcgggt	*K. setae*
set 2	attcggcacgatgaacgagacgagcggt	*K. setae*
uni 1	gctcatgggtggaacgttgactattcg	*Kitasatospora*
uni 3	gcacgttgttgggtcctgagggaa	*Kitasatospora*
SGK1	Biotin ggttggatccacctcctt	
SGK2	tgccaaggcatccac	

Optimization of signal strength and selectivity

Several experiments were performed to optimize the signal strength and the specificity. The effects of the hybridization temperature were studied by altering the temperature ranging from 54–70°C in 2°C intervals. Raising the temperature led to a decrease in signal strength but an increase in specificity (data not shown). At 70°C, the signal was highly specific but hardly detectable. For optimal results, a hybridization temperature of 65°C was chosen, leading to highly specific signals on the chips with a minimum of cross hybridization.

For the silver signal enhancement, the chips were either marked with streptavidin gold nanoparticles or the streptavidin peroxidase conjugate. A comparison of the results of the two labeling methods confirmed the previously achieved results. With the enzyme-based silver deposition on the chip, the background level was lower and the sensitivity was at least two orders of magnitude higher (Möller et al. 2005). Therefore, only the enzymatic silver deposition was used for further testing. Before the enzymatic silver deposition, the conductivity values of all chips were measured to avoid false positives due contaminations on the chip. Without any silver deposition, the measured conductivity was lower than 10^{-7} S. If a higher conductivity value was detected on any electrode gap, those gaps were not used for further analysis. After an initial enzymatic silver deposition of 5 min, the conductivity values for each gap on the chip were measured in the reader. If the target DNA concentration was lower than 1 μg/ml, the signal was too low for detection and additional steps of autometallographic silver enhancement were needed (Hacker et al. 1993). Therefore, the detection process involved several steps and measurements, which are also depicted in the figures: an initial control with no silver deposition (0), a measurement after the enzymatic silver deposition (Enzyme), and measurements after each autometallographic silver deposition step of 2 min for further signal enhancement (Fig. 2). More than two enhancement steps of 2 min each normally lead to a strong

Appl Microbiol Biotechnol (2008) 77:1181–1188

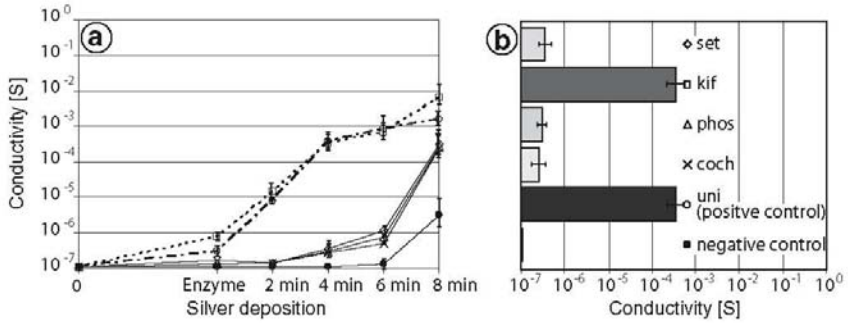

Fig. 2 Typical measurement with the DNA-chip with electrical detection. The chip was incubated with 0.1 μg/ml biotinylated PCR product of *K. kifunense*, followed by an enzymatic silver deposition for 5 min and further silver depositions in steps of 2 min each. With the measured conductivity values, one can clearly distinguish between the positive signals for *Kitasatospora* DNA (uni as positive control) and the specific signal for *K. kifunense* (*kif*). After more than two additional enhancement steps of 2 min, a significant raise in the signals of the other capture probes can be observed caused by an unspecific background. The values at 4-min enhancement were used due to the optimal signal-to-background ratio (**a**). After an enzymatic silver enhancement and two autometallographic silver enhancement steps, the best signal-to-background ratio is achieved (**b**)

increase of the background signal, making further measurements impractical.

In all experiments, the measured conductivity values for the complementary probe DNA and the positive control were always at least two orders of magnitude higher than the measured values from the noncomplementary spots and the unmodified electrode gaps (negative control). A reliable detection of DNA and the classification of *Kitasatospora* strains with the above described protocol were possible with DNA concentrations in the range between 1 ng/ml to 1 μg/ml (Fig. 3).

When a biotin-labeled PCR product of one of the four chosen *Kitasatospora* species was hybridized under the above-mentioned conditions, a clear identification of all four species was achieved. Control experiments with PCR product of other *Kitasatospora* species (*K. griseola* and *K. mediocidica*) showed no detectable result. Only the universal control sequences (uni1, uni3) showed that

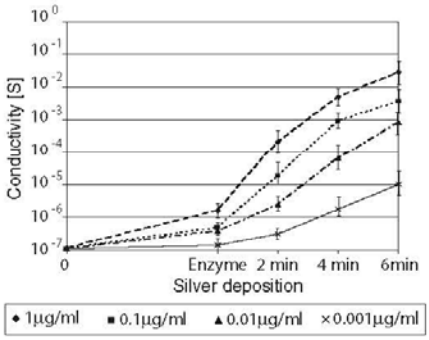

Fig. 3 Concentration dependency of the measured electrical signal. Measured conductivity values for *K. phosalacinea* with different concentration of PCR product in the range of 1 μg/ml to 1 ng/ml, similar results were achieved for all four chosen strains

Kitasatospora DNA had been hybridized to the chip. These results demonstrate that cultures of microorganisms can be successfully and rapidly identified with a DNA-chip with electrical detection (Fig. 4).

In all experiments, the universal control sequence (uni1) showed a very low or no signal. Only uni3 gave a dependable signal for the detection of *Kitasatospora*, so only the values of uni3 were used in the tests. These findings were consistent with results from the Array Tube® microarray system as described by Günther et al. (2006). All other capture sequences exhibited constant signals when incubated at the same conditions. The two capture sequences per species showed very similar results throughout the experiments. For analysis, the average conductivity over all eight measurement spots for one species was taken. This procedure allowed a quick interpretation of the results from the chip. For the universal capture sequences, only the measurements with the uni3 sequence were used because of the above described problem.

Analysis of mixed samples

To determine if the parallel detection of DNA from different *Kitasatospora* strains was possible with our detection scheme, the chips were incubated with a mixture of different PCR products at the same time. The incubation with multiple PCR products revealed that all strains were exactly identified. When incubated with equal amounts of DNA from each strain, it was noticed that the signals for each strain differed slightly (Fig. 4). This is probably due to minor differences in the binding kinetics of the capture probes. These results are also consistent with the results achieved when the chips were incubated with the DNA from just one strain, and the signals from different chips

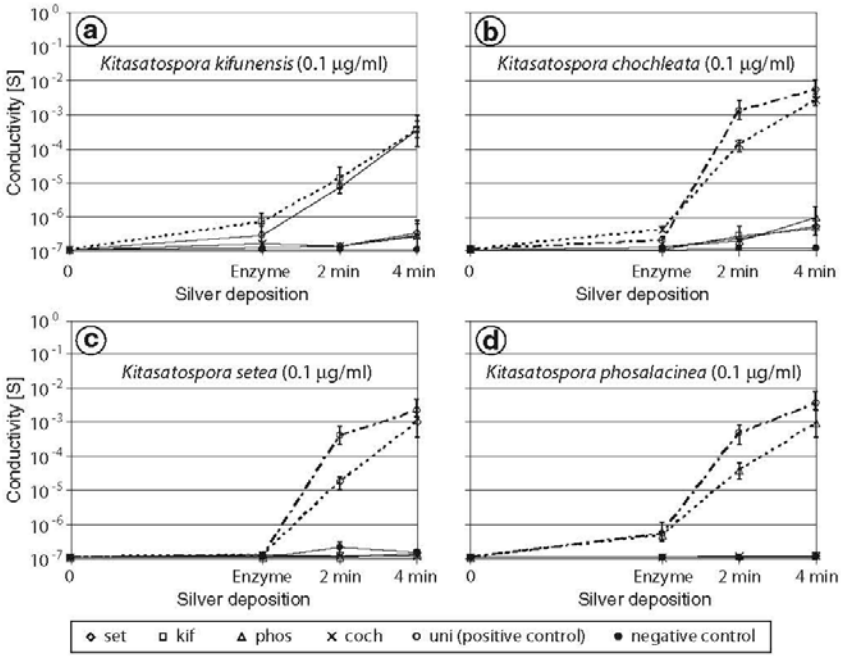

Fig. 4 Identification of the four chosen *Kitasatospora* strains using the DNA-chip with electrical detection. Different chips were incubated with 0.1 µg/ml biotinylated PCR product from one of the four chosen *Kitasatospora* strains each. With the measured conductivity values, one could easily differentiate the different strains. Each chip showed only a raise in the conductivity values for the specific DNA it was incubated with and in the positive control for *Kitasatospora* DNA (uni). Shown are the results of four different chips incubated with **a** *K. kifunense*, **b** *K. chochleata*, **c** *K. setae*, and **d** *K. phosalacinea* biotinylated DNA

incubated with different DNA were compared afterwards. Normally, the *K. chochleata* probes showed a faster increase in signal strength especially after the first 2 min of autometallography silver enhancement. In contrast, the *K. kifunense* probes showed the slowest response. These differing binding kinetics complicate the possible quantification of the DNA concentration based on the measured conductivity values.

To show that a differentiation between different concentrations of target DNA is also possible, the chips were incubated with a mixture of different DNA in various concentrations. The results showed that a clear differentiation of the different PCR products was achieved (Fig. 5). However, a standard that allows the exact determination of the concentration of DNA, which was incubated on the chip, has not been established yet. It is only possible to have a roughly estimate of the dimension of concentration and a ratios of the different DNAs. In Fig. 5, the results of two experiments are shown. Repeated experiments with different mixtures of PCR products consistently revealed the true composition of the DNA mixture.

In further experiments the validity of the method was extended to mixed culture samples of *Kitasatospora* and to spiked environmental samples. After DNA isolation,

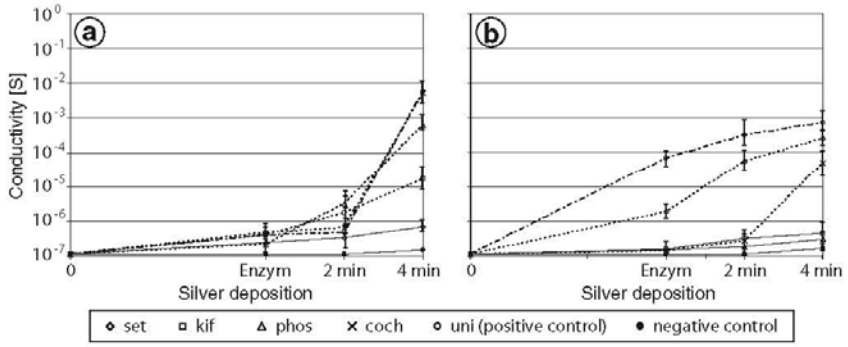

Fig. 5 Toward quantification of different *Kitasatospora* strains in a mixture. Two chips were incubated with a mixture of different biotinylated *Kitasatospora* PCR products. **a** This chip was incubated with PCR products from *K. chochleata* (1 µg/ml), *K. phosalacinea* (0.1 µg/ml),and *K. kifunense* (0.05 µg/ml). **b** Incubation with *K. setae* (1 µg/ml) and *K. chochleata* (0.05 µg/ml) DNA. Only a semi-quantification of the DNA concentration is possible because no standard has yet been established

purification and PCR all used *Kitasatopara* strains were clearly detected and identified.

Discussion

To characterize populations of microorganisms, microscopic, biochemical, physiological methods, and selective culture plantings are used. Recently, these methods had become supported by molecular biological techniques. These techniques are especially interesting for the initial characterization of microorganisms because of their speed and reliability and also because they allow the analysis of non-cultivable strains.

The data from the current study shows that a classification of bacteria belonging to the genus *Kitasatospora* is possible with an electrical DNA-chip detection scheme. Using species-specific oligonucleotides derived from the ITS region of *Kitasatospora*, a clear classification of the four chosen strains from pure cultures was achieved. The application of an electrical detection allows for a faster screening of samples for bacterial strains of this genus with a robust detection scheme, which is well suited for miniaturization. This could lead to the development of a transportable device for use outside of specialized laboratories.

The signals detected from the chip were very strong, clearly distinguishable, and could be used for a classification of *Kitasatospora* strains from pure culture without any ambiguity. However, different binding kinetics for the individual *Kitasatospora* strains and their immobilized capture probes were found. Because of these different binding kinetics, an exact quantification of the DNA concentration is not yet possible when the chip was incubated with a mixture of DNA molecules from different *Kitasatospora* strains. To overcome these problems, capture molecules have to be designed with comparable binding kinetics. Another solution would be the studying of the binding kinetics of each capture molecule to allow a correct determination of the DNA concentration with the measured conductivity values.

There is no clear explanation why the universal capture probe uni1 gave hardly any signals in all tests performed on the chip surface. All capture sequences had been corrected for possible hairpin structures and dimer formation (Günther et al. 2006). One reason might be some unpredictable secondary structures. In future tests, this capture probe will be replaced.

The newly developed chip allows the effective detection of microorganisms within 4 h. Despite of the necessary equipment, currently available sequencing technologies need much more time to get reliable results, are more expensive, and not practicable for point-of-care detection.

To take complete advantage of a classification of microorganisms with a DNA-chip, more capture DNAs have to be immobilized on a chip surface, enabling the user to scan for a broad variety of microorganisms. Therefore, more measurement spots have to be included on one chip, which could be achieved to some extent (about 120 spots per chip) by just changing the design of the chip. Future chips should also incorporate universal capture probes for other *Actinomycetes* to allow a correct classification. One could also imagine a hierarchical system of chips that would start with the genus classification and work from there to classify the microorganisms in a given sample.

The further development of the electrical chip-based DNA detection should also include the development of an exact quantification, which would allow the user to determine the number of microorganisms in a given sample. Although the potential for quantification has been demonstrated in this study and in other tests, it was only possible to roughly estimate the DNA concentration by the measured conductivity. Standard procedures have to be developed to allow the precise quantification of DNA concentrations with a chip-based electrical detection system. Such quantification would be very useful in application like water quality control or food safety. For "real life" applications, an increased sensitivity of the system would also be useful. This could be achieved by a more specific additional autometallography silver enhancement and so enabling longer enhancement times without an increasing background signal. An active mixing during hybridization would also boost the sensitivity of the system, as it has been shown on other chip-based detection systems (Schaupp et al. 2005).

The electrical DNA detection has the potential to be further developed in a transportable detection system for on-site use. To do so, the sample preparation and especially the incubation have to be automated. This would reduce possible errors due to mishandling and would enable less skilled personal to use such a detection device.

This work describes the classification of different *Kitasatospora* strains using a chip-based detection method. Although a DNA-chip is used for the classification, there is no need for any complicated or expensive optical equipment for the readout of our chip. Rather, a detection scheme based on conductivity measurements is used based on the deposition of silver through an enzymatic reaction. This robust and cost-efficient detection scheme enables the development of transportable detection device for on-site testing.

The classification of different strains of microorganisms can be achieved using this detection method. The microarray technology used might not be suited to detect new species within a sample, but known species can be sorted out and interesting samples can be processed according to the species or genus present when screening soil samples,

isolates, or pure cultures. The microarray technology will also greatly accelerate the screening process for cultures of microorganisms. The technology described has the potential for miniaturized and robust DNA detection, which can be done outside of specialized laboratories, opening new applications for DNA-chip technology.

Acknowledgements We would like to thank R.D. Powell and J.F. Hainfeld from Nanoprobes (Yaphank, NY, USA) for their constant help in establishing the enzymatic silver deposition on the DNA-chips with electrical detection and for providing the EnzMet™ reagents supported by NIH SBIR grant 2R44 GM064257-02. Funding by the DFG (Fr 1348/5–2) is acknowledged.

References

Cheung VG, Morley M, Aguilar F, Massimi A, Kucherlapati R, Childs G (1999) Making and reading microarrays. Nat Genet 21 (1 Suppl):15–19

Drummond TG, Hill MG, Barton JK (2003) Electrochemical DNA sensors. Nat Biotechnol 21(10):1192–1199

Fare TL, Coffey EM, Dai H, He YD, Kessler DA, Kilian KA, Koch JE, LeProust E, Marton MJ, Meyer MR, Stoughton RB, Tokiwa GY, Wang Y (2003) Effects of atmospheric ozone on microarray data quality. Anal Chem 75(17):4672–4675

Fritzsche W, Taton TA (2003) Metal Nanoparticles as Labels for Heterogeneous, Chip-Based DNA Detection. Nanotechnology 14: R63–R73

Günther S, Groth I, Grabley S, Munder T (2006) Design and evaluation of an oligonucleotide-microarray for the detection of different species of the genus *Kitasatospora*. J Microbiol Methods 65:226–236

Gurtler V, Stanisich VA (1996) New approaches to typing and identification of bacteria using the 16S-23S rDNA spacer region. Microbiology 142(Pt 1):3–16

Hacker GW, Graf AH, Hauser-Kronberger C, Wirnsberger G, Schiechl A, Bernatzky G, Wittauer U, Su HC, Adam H, Thurner J et al (1993) Application of silver acetate autometallography and gold-silver staining methods for in situ DNA hybridization. Chin Med J (Engl) 106(2):83–92

He L, Musick MD, Nicewarner SR, Salinas FG, Nekovic SJ, Natan MJ, Keating CD (2000) Colloidal Au-enhanced surface plasmon resonance for ultrasensitive detection of DNA hybridization. J Am Chem Soc 122:9071–9077

Li J, Xue M, Lu Z, Zhang Z, Feng L, Chan M (2003) A high-density conduction-based micro-DNA identification array fabricated with a CMOS compatible process. IEEE Trans Electron Devices 50(10):2165–2170

Möller R, Csaki A, Köhler JM, Fritzsche W (2000) DNA probes on chip surfaces studied by scanning force microscopy using specific binding of colloidal gold. Nucleic Acids Res 28:e91

Möller R, Csaki A, Köhler JM, Fritzsche W (2001) Electrical classification of the concentration of bioconjugated metal colloids after surface adsorption and silver enhancement. Langmuir 17:5426–5430

Möller R, Powell RD, Hainfeld JF, Fritzsche W (2005) Enzymatic control of metal deposition as key step for a low-background electrical detection for DNA chips. Nano Lett 5(7):1475–1482

Ochi K, Hiranuma H (1994) A taxonomic review of the genera *Kitasatosporia* and *Streptoverticillium* by analysis of ribosomal protein AT-L30. Int J Syst Bacteriol 44(2):285–292

Omura S, Takahashi Y, Iwai Y, Tanaka H (1982) *Kitasatosporia*, a new genus of the order Actinomycetales. J Antibiot (Tokyo) 35(8): 1013–1019

Park SJ, Taton TA, Mirkin CA (2002) Array-based electrical detection of DNA with nanoparticle probes. Science 295(5559):1503–1506

Prauser H, Schütze B, Martin K (1987) IMET (National collection of microorganisms) catalogue of strains ZIMET, Jena

Schaupp CJ, Jiang G, Myers TG, Wilson MA (2005) Active mixing during hybridization improves the accuracy and reproducibility of microarray results. Biotechniques 38(1):117–119

Schena M, Shalon D, Heller R, Chai A, Brown PO, Davis RW (1996) Parallel human genome analysis: Microarray-based expression monitoring of 1000 genes. Proc Natl Acad Sci U S A 93:10614–10619

Storhoff JJ, Elghanian R, Mucic RC, Mirkin CA, Letsinger RL (1998) One-pot colorimetric differentiation of polynucleotides with single base imperfections using gold nanoparticle probes. J Am Chem Soc 120:1959–1964

Urban M, Möller R, Fritzsche W (2003) A paralleled readout system for an electrical DNA-hybridization assay based on a micro-structured electrode array. Rev Sci Instr 74:1077–1081

Wellington EM, Stackebrandt E, Sanders D, Wolstrup J, Jorgensen NO (1992) Taxonomic status of *Kitasatosporia*, and proposed unification with Streptomyces on the basis of phenotypic and 16S rRNA analysis and emendation of *Streptomyces* Waksman and Henrici 1943, 339AL. Int J Syst Bacteriol 42(1):156–160

Zhang Z, Wang Y, Ruan J (1997) A proposal to revive the genus *Kitasatospora* (Omura, Takahashi, Iwai, and Tanaka 1982). Int J Syst Bacteriol 47(4):1048–1054

2.2 Screen printing as cost-efficient fabrication method for DNA-chips with electrical readout for the detection of viral DNA

Thomas Schüler, Tim Asmus,Wolfgang Fritzsche, and Robert Möller

Biosensors Bioelectronics (**2009**) 24(7): 2077-84

G Model
BIOS-3034; No. of Pages 8
ARTICLE IN PRESS

Biosensors and Bioelectronics xxx (2008) xxx–xxx

Contents lists available at ScienceDirect

Biosensors and Bioelectronics

journal homepage: www.elsevier.com/locate/bios

Screen printing as cost-efficient fabrication method for DNA-chips with electrical readout for detection of viral DNA

Thomas Schüler[a,*], Tim Asmus[b], Wolfgang Fritzsche[c], Robert Möller[a]

[a] JBCI, Institute of Physical Chemistry, Friedrich-Schiller University Jena, Helmholtzweg 4, 07743 Jena, Germany
[b] Heraeus Sensor Technology GmbH, Reinhard-Heraeus-Ring 23, 63801 Kleinostheim, Germany
[c] Institute of Photonic Technology, Albert-Einstein-Straße 9, 07745 Jena, Germany

ARTICLE INFO

Article history:
Received 25 August 2008
Received in revised form 23 October 2008
Accepted 24 October 2008
Available online xxx

Keywords:
Electrical DNA-chip
Horseradish peroxidase
Enzyme induced silver deposition
Screen printed electrodes

ABSTRACT

The fast development in the field of DNA analytics is driven by the need for cost-effective and high-throughput methods for the detection of biomolecules. The detection of DNA using metal nanoparticles as labels is an interesting alternative to the standard fluorescence technique. Fluorescence is highly sensitive and broadly established, but shows limitations, for example instability of the signal and the requirement for sophisticated and high-cost equipment. A recently developed approach realizes a method for the electrical detection of DNA, based on the induction of silver nanoparticles growth in microelectrode gaps on the surface of a DNA-chip. This breakthrough towards robust and cost-effective detection was still hampered by the need for microstructured (and therefore expensive) substrates. We demonstrate that it is possible to utilize screen printed electrode structures for a chip-based electrical DNA detection. The electrode structures were produced on a glass substrate which made an additional optical readout possible. The screen printed structures show the required precision and are compatible with the applied biochemical protocols. A comparison with chip substrates produced by standard photolithography showed the same sensitivity and specificity for the screen printed chips. Screen printing of electrode structures for DNA-chip with electrical detection offers an interesting and cost-efficient possibility to produce DNA-chips with microstructured electrodes.

1. Introduction

The identification and analysis of biomolecules is an important task especially in fields of life science, food technology, forensic and environmental research (Schena et al., 1998). During the last decade DNA-chips could show the potential as analytical tool in these areas. First of all the requirements for high-throughput, specific reactions and high sensitivity could be fulfilled by microarray technology (Wang, 2000; Schena, 2003). Nowadays various microarray-based approaches are used to detect binding events of biomolecules on surfaces of so-called biochips (Choi et al., 2007; Marquette et al., 2008; Warsinke, 2008). Thereby, simple detection methods that require only simple instrumentation and readout techniques are of growing interest (Cheung et al., 1999; Heller, 2002). Furthermore, nanoparticles demonstrated their potential as alternative labels to the standard labelling of oligonucleotides by fluorescent dyes (Mirkin et al., 1996; Csaki et al., 2002). Nanoparticles allow for a variety of detection schemes for bioanalytical investigations, such as optical, electrical, or electrochemical approaches (Gonzalez-Garcia et al., 2000; Wang et al., 2001; Albers et al., 2003; Drummond et al., 2003; Fritzsche and Taton, 2003). They promise to overcome the cost-related problems of fluorescence detection, which requires rather complicate and thereby expensive instrumentation, which is not easily adaptable for point-of-care applications with decentralized (and cost-effective) equipment needs (Fritzsche, 2001). Approaches using the conductive properties of metal nanoparticles offer simple and cost-effective detection units (Park et al., 2000, 2002). Despite their analytical performances these systems are still at the stage of proof-of-concept and further developments are needed for real life diagnostic applications (Marquette et al., 2006). Especially the requirement for electrode gap structures with micrometer precision makes the production of the chip expensive (Avramescu et al., 2002; Marquette et al., 2006). The precision is mainly determined by the process of capture-DNA immobilization, which happens usually by spotting methods with final spot sizes of 100–200 μm and a positioning precision of about 10 μm. The gaps themselves are usually in the lower micrometer range of 1–50 μm.

* Corresponding author. Tel.: +49 3641 206 309; fax: +49 3641 206 399.
E-mail address: thomas.schueler@ipht-jena.de (T. Schüler).

0956-5663/$ – see front matter © 2008 Elsevier B.V. All rights reserved.
doi:10.1016/j.bios.2008.10.028

Please cite this article in press as: Schüler, T., et al., Biosens. Bioelectron. (2008), doi:10.1016/j.bios.2008.10.028

G Model
BIOS-3034; No. of Pages 8
ARTICLE IN PRESS

Screen printing technique, possibly one of the oldest forms of graphic art reproduction, is distinguished mainly to other methods of microstructuring by the way of film (material) deposition. The technique has a typical resolution of about 50–150 μm.

Screen printing technology is widely used for large-scale fabrication of disposable biosensors with several advantages including low cost, versatility, and miniaturization. Thereby modern sensors can be integrated in portable systems, an important requirement of analytical methods for on-site testing (Tudorache and Bala, 2007). The design and fabrication of screen printed electrodes, including microelectrodes and chemically modified electrodes expand the possibility of direct implementation of laboratory-developed screen printed electrodes in real life applications. One prominent example is the personal glucose biosensor used by diabetics (Matthews et al., 1987; Nagata et al., 1995). A thick-film biosensor can be produced on different substrates such as alumina, ceramics, PVC, gold, iron, etc., with printed conducting electrode structures consisting of carbon ink/paste, or platinum, or other metal paste (Dequaire and Heller, 2002; Susmel et al., 2003; Liao and Chou, 2006; Luo et al., 2006; de Albuquerque and Ferreira, 2007).

Thereby it is in principle compatible with any detection scheme that needs microstructured electrodes. In the following, the principles of the electrical detection as well as possible applications are described.

For the electrical readout chips with 42 electrode gaps were manufactured by screen printing. The screen printed electrodes consist of gold or platinum. Each electrode gap on the chip is a measurement point for biomolecular interactions on the chip. Each gap is modified with a specific capture sequence. In a second step biotin-labelled target-DNA hybridizes to the complementary capture-molecules on the chip surface. Due to a streptavidin modification the enzyme horseradish peroxidase (HRP) can subsequently bind between the electrodes (Möller et al., 2005). A specific deposition of silver nanoparticles driven by the enzymatic activity leads to a bridging of the electrode gap by a conductive metallic layer (Mayer et al., 2000; Willner et al., 2007). The increase of the conductivity over the electrode gap is measured afterwards by a custom-made readout device.

In this work the applicability, sensitivity, and specificity of screen printed electrodes is compared to electrodes produced by standard photolithography. To demonstrate the potential of this system cytomegalovirus (CVM) DNA is detected on the chip. The CMV belongs to the family of human herpesvirus and has one of the largest known viral genomes (Chambers et al., 1999). Especially immuno-debilitated individuals and pregnant women (e.g. 10% of infected newborns with CMV exhibit permanent mental retardation and auditory damage) are affected (Ibanez et al., 2008). During the past decades microarrays showed great potential for the analysis of viral DNA. Due to the developments in the field of miniaturization, multiplexing, and automation of chip-based detection of biomolecules, microarray technology is starting to replace traditional determination methods such as virus isolation and serological diagnosis (Zheng et al., 2008). By using viral cultures from infected patients DNA microarrays can even monitor viral load of CMV. In the presented work a short biotin-labelled fragment of CMV DNA was used for the detection. The chips were readout electrically as well as optically after the silver deposition. DNA concentrations as low as 500 fM were detectable on the electrical DNA-chip.

The presented results demonstrate the application of screen printing as a cost efficient (and potentially large scale) production method for the realization of microstructured chips for the electrical DNA detection based on nanoparticle labelling and subsequent site-specific silver deposition.

2. Experimental

2.1. Materials and reagents

DNA-oligonucleotides (both capture and target probes) were obtained from Operon (Operon Biotechnologies GmbH, Cologne, Germany). For our investigations we used a positive (already biotin labelled) control (5′-NH_2-C6-CAT AGA ATC AAG GAG CAC ATG CTG AAA AAA-biotin-3′), a complementary capture sequence (5′-NH_2-C6-TTT TTT CAG CAT GTG CTC CTT GAT TCT ATG-3′), a sequence containing 1 mismatch (5′-NH_2-C6-TTT TTT CAG CAT G**G**G CTC CTT GAT TCT ATG-3′), a sequence containing 3 mismatches (5′-NH_2-C6-TTT TTT CAG CAT **TAT** CTC CTT GAT TCT ATG-3′), and a negative control (5′-ACT GAC TGA CTG ACT GAC TGA CTG GGC GGC GAC CT-NH_2-C7-3′). The biotin-labelled target-DNA (5′-biotin-CAT AGA ATC AAG GAG CAC ATG CTG AAA AAA-3′) had only a biotin modification. The streptavidin conjugated horseradish peroxidase was purchased from Sigma (Streptavidin-Peroxidase Polymer, Ultrasensitive, Sigma–Aldrich, Taufkirchen, Germany). Silver enhancement kit for enzyme induced silver deposition was supplied by Nanoprobes (EnzMet® kit, Nanoprobes Inc., Yaphank, NY, USA). Microarray printing buffer was obtained from ArrayIt (Micro Spotting Solution Plus, TeleChem International, Sunnyvale, USA). Chemicals for phosphate buffer solution (PBS pH 7,4), saline sodium citrate (SSC pH 7), and sodium dodecyl sulphate (SDS) were ordered by Merck (Merck KGaA, Darmstadt, Germany). Tween20, hydroquinone and silver acetate were also ordered by Sigma. The organo silane (3-glycidyloxypropyl)-trimethoxysilane used for the surface modification of the DNA-chips was purchased from ABCR (ABCR GmbH, Karlsruhe, Germany).

2.2. Preparation of the electrode structures

The metallic microelectrode structures of the biochips, a square at 0.5 in. size, were printed on 50 mm × 50 mm glass samples (Fig. 1). For the analysis of different probes each chip contains 42 measurement points (electrode gaps) on the surface. Due to the resolution of the fabrication method the electrode gaps on the chips have a width of about 50 μm. Glass substrates were washed and tempered prior to screen printing. Electrode and conducting path structures were realized using low firing Au and Pt (W.C. Heraeus GmbH, Hanau, Germany). Depending on the composition of the electrode structures a gold or platinum paste was used for screen printing. The platinum resinate paste consists of an organic platinum compound with a low content of noble metal. By a burn-in process the organic compound starts to decompose. Thereby, a thin platinum layer remains. For the gold electrodes a low burn-in gold paste was used. The control biochips were made by standard photolithography on silicon wafer.

2.3. Chip-based electrical detection of DNA

Screen printed substrates were chemically modified with (3-glycidyloxypropyl)-trimethoxysilane (GOPS) for the binding of amino-modified single stranded (ss) capture-DNA molecules (Wong and Krull, 2005). The screen printed chips were cleaned by sonication for 5 min each with acetone, ethanol, and water. After a drying step by nitrogen the entire chip surface was epoxy modified, by immersing the chips in a 10 mM GOPS solution in dry toluene for 7 h at 70 °C. In the end they were washed 2× 5 min each with toluene, ethanol, and water.

The deposited capture DNA was modified with a C6-Aminolink on the 5ĩ or 3ĩ end. These modified molecules were attached to the epoxy (introduced by GOPS) modified surface. The attachment occurs by a secondary amine formation between the epoxysilane

Please cite this article in press as: Schüler, T., et al., Biosens. Bioelectron. (2008), doi:10.1016/j.bios.2008.10.028

G Model
BIOS-3034; No. of Pages 8
ARTICLE IN PRESS

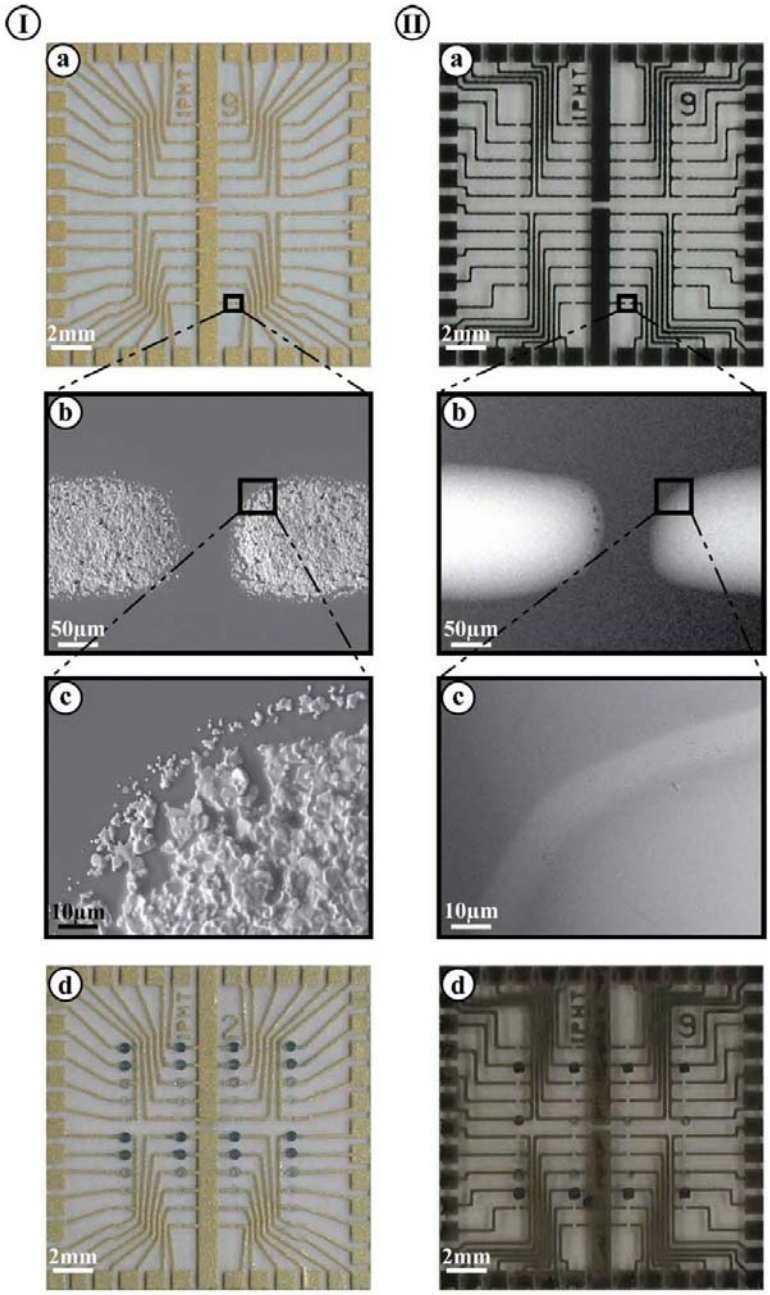

Fig. 1. Screen printed chips with gold (Ia) and platinum (IIa) electrode structures. The black spots (Id and IId) represent the signals observed on chips after enzyme induced silver deposition. SEM images show the ultrastructure of gold (I b,c) and platinum (II b,c) electrodes.

monolayer and the 5ĭ or 3ĭ-amino modification of the DNA. To detected CMV-DNA on the screen printed chips different 30 bp long ss capture sequences were spotted by a non-contact Nanoplotter from GeSIM (Gesellschaft fuer Silizium-Mikrosysteme mbH, Großerkmannsdorf, Germany). Beside a positive (already biotin-labelled) and a negative control, we immobilized a complementary sequence, a sequence containing 1 mismatch, and a sequence containing 3 mismatches. The concentration of the spotted capture DNA in the microarray printing buffer was 10 µM. For the binding of amino-modified oligonucleotides to an epoxy surface the used buffer should have a pH between 8.5 and 9.0. The biotin-labelled target-DNA was diluted stepwise from 500 nM to 5 fM. Fig. 2 gives a short overview about the principle of the chip-based electrical detection of DNA. Conditions for the surface modifica-

Please cite this article in press as: Schüler, T., et al., Biosens. Bioelectron. (2008), doi:10.1016/j.bios.2008.10.028

G Model
BIOS-3034; No. of Pages 8
ARTICLE IN PRESS

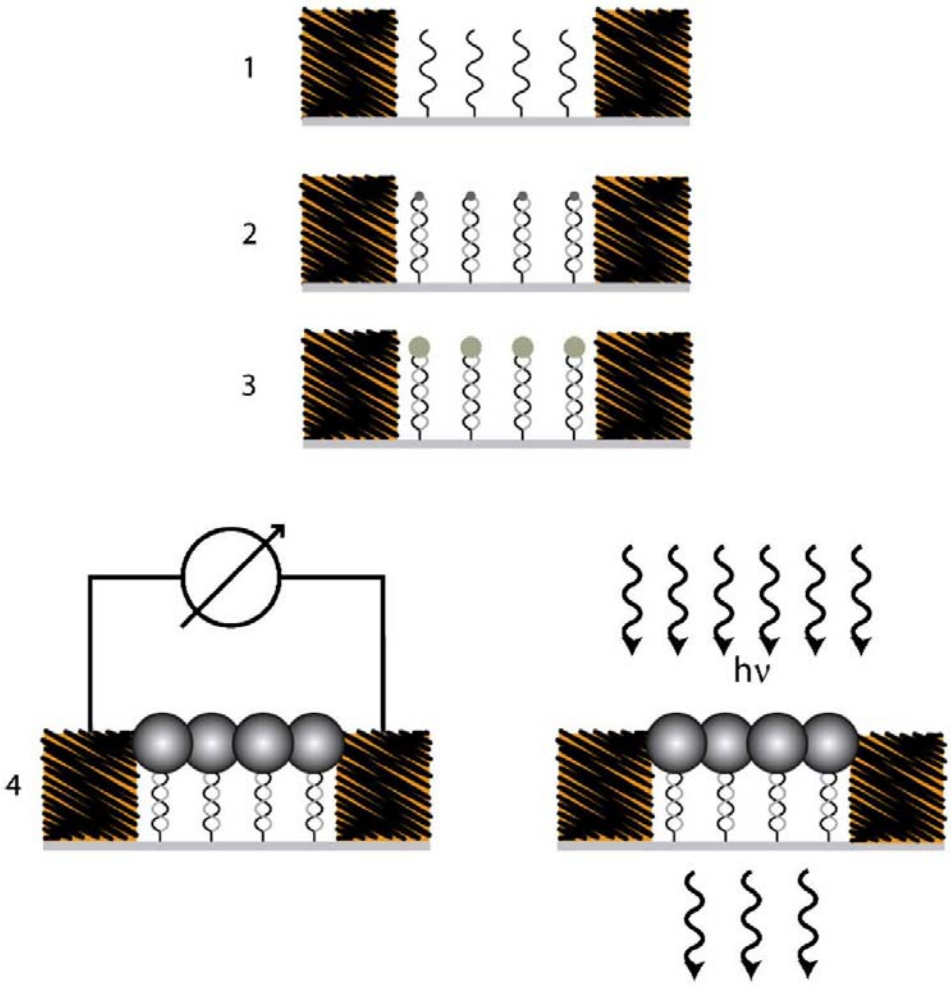

Fig. 2. Principle of chip-based electrical detection of DNA. After spotting single stranded (ss) capture molecules between two microelectrodes (1) the biotin-labelled target-DNA hybridizes at the specific partner immobilized on the chip surface (2). The biotin serves as binding molecule for streptavidin-horseradish peroxidase-polymer (3). A final enzyme induced silver deposition leads to a metallic layer between the electrodes. The readout could be performed by electrical measurement (conductivity of the gap filled by interconnected silver nanoparticles) or by optical transmission measurements (light absorption of the deposited silver) (4).

tion, immobilization, hybridization, and binding of the horseradish peroxidase like temperature, incubation time, buffers and washing steps were described in detail elsewhere (Möller et al., 2005). Briefly, the biotin-labelled target-DNA was diluted in 5× SSC buffer and 0.1% SDS. Target-DNA sequences were taken from 150 bp PCR products of human CMV DNA. A following washing step in 2× SSC and 0.1% SDS removed unbound DNA to avoid false positive signals. The streptavidin-horseradish peroxidase-polymer was diluted 1:1000 in PBS buffer and 0.05% Tween20. This buffer was also used in the washing step after a 1 h incubation. After binding of the streptavidin-enzyme conjugate, the three solutions (A, B, and C) of silver enhancement kit (EnzMet®) from Nanoprobes were applied in small droplets on the chip surface in ratio 1:1:1. The enzyme horseradish peroxidase (HRP) catalyzes the conversion of hydrogen peroxide to water and oxygen. After adding the special EnzMet® enhancement kit made by Nanoprobes, silver nanoparticles will be immediately formed by the enzymatic activity. A sufficient density of silver nanoparticles leads to a conductive layer that connects both electrodes. In general the height of the deposited silver layer is around 200–300 nm. The advantage of using an enzyme to deposit silver nanoparticles is the combination of the fast and highly specific reaction of the enzyme with the unique properties of metallic nanoparticles (e.g. specific mass, conductivity, optical properties). The silver spots do not fade or bleach, and we only could obtain a minimal background (unspecific silver deposition). The reaction was stopped after 5 min to avoid unspecific silver deposition. The main difference between the enzyme induced silver deposition and the non-specific silver deposition, induced by autocatalytic processes in the enhancement kit, is the reaction time. The enzyme catalyzed reaction is very fast and the specificity as well as the efficiency is very high. Depending of the concentration of DNA a signal will be detectable after a few minutes of enzymatic reaction (1–5 min).

In contrast to the non-specific reaction, this will need much longer deposition time to influence the signals on the chip (10–15 min). For this reason we stopped the enzyme induced silver

Please cite this article in press as: Schüler, T., et al., Biosens. Bioelectron. (2008), doi:10.1016/j.bios.2008.10.028

G Model
BIOS-3034; No. of Pages 8
ARTICLE IN PRESS

deposition after 5 min to avoid an interference of the unspecific silver deposition. After the initial enzymatic silver deposition no false positive signals were detectable.

To improve the signal intensity already enzymatically deposited silver nanoparticles could be used as reaction seed for additional nanoparticles induced silver deposition (Festag et al., 2006). For that purpose 200 mg hydroquinone was dissolved in 40 ml citrate buffer. To provide silver ions for the reaction, 80 mg silver acetate was dissolved in 40 ml double deionised water. Both solutions were mixed 1:1 on the DNA-chip (Zhang et al., 2004). Due to the additional enhancement steps using chemical reducing agents unspecific silver deposition began to rise. A further stepwise reaction longer than 10 min (5 × 2 min) led to a high percentage of false positive signals on the chips, approximately 50% of all chips used in this work. For this reason measured results after 6 min (3 × 2 min) nanoparticle induced silver deposition were not used for data evaluation.

The silver deposition leads to bridging the electrode gap by a conductive layer of silver nanoparticles. A measured increase of the conductivity over the electrode gap serves as signal in the DNA-chip reader (Urban et al., 2003). With glass as surface material an additional transmissive optical detection of the signal to control the electrical measurement was possible (Fritzsche et al., 2002). Therefore, the grey values of the silver spots were evaluated by image analysis software Image J (Barrett, 2008), after imaging by a standard slide film-scanner.

2.4. Electrical measurement

After the enzymatic reaction the signals on the screen printed chip were detected by a specially developed readout device. This DNA-chip reader and its technical aspects where described elsewhere (Urban et al., 2003). By the use of DC-measurement we could build a cost-effective, mobile, and robust device with a simple detection system.

For the electrical readout of the chip, the DNA-chip reader has an integrated PLCC-test-and-burn-in-socket with 48 contacts. The reader itself is controlled by an embedded PC, which is based on a SC400 microcontroller from AMD. Measured data will be directly shown on the liquid crystal display. To save the measured data the reader contains a flash-memory. By a multiplexer the 42 electrode gaps will be read out by an ohm-meter. Due to a RS232-serial interface the reader can be easily connected to a PC for control and data transfer.

3. Results and discussion

3.1. Characterization of chip fabrication methods

The potential of the novel detection approach was already demonstrated in former work (Möller et al., 2008) but utilized then silicon chips. The electrode structures on the surface were produced by sophisticated photolithography methods. This method offers a highly reproducible chip production and gap sizes smaller than 50 μm, but is limiting future applications by the high costs for microstructure fabrication based on clean room technology. An alternative production method for chips with electrode structures is screen printing. The screen printed chips were produced with a price of about 10 times less than chips produced by standard photolithography. The main reasons for this cost difference are the expensive clean room technology for photolithography, the equipment that is needed and the size of the chips. If the size of the chips becomes very small, photolithography will be automatically become more economic. However, this will necessarily lead to a high quantity of chips. Alternatively larger wafers may reduce costs too, but require bigger machines and instrumentation and an even higher quantity of chips to keep the whole process economical. The size of the chips is defined by the number of measurement points, the size of the electrode gap, and the distance between the conductor paths, the contacting areas for the electrical readout as well as the practical handling of the chip. This makes the further reduction of the chip size complicated. So, screen printing offers a cost efficient alternative for the production of chips with electrode structures as needed for an electrical chip-based DNA detection. Microstructured chips were used as standard in order to compare the novel screen printing electrodes with more established solutions. Both chip types were compared with respect to the geometry of the electrodes, the conductivity of the metallic structures as well as stability (Table 1).

Photolithographically fabricated chips exhibit highly homogenous and reproducible structures. In contrast, screen printed electrodes are rougher, less defined and of larger height. The layout of the printed chip design is equal to the photolithographic layout. In order to be compatible with the readout contacts as well as the spotting protocols (regarding spot positions), no change in the chip layout was possible. The larger height (up to one magnitude) does not result in higher conductivity in the case of the gold screen printed structures. The platinum electrodes appeared to be more homogenous, but showed a lower conductivity when the untreated electrode structures were tested. A microscopic (light and SEM) investigation showed that the platinum structures exhibited microcracks within the structures (Fig. 3). These microcracks apparently interrupt the paths of the screen printed platinum electrodes resulting in less conductive structures. Therefore the following experiments on screen printed chips were performed with gold electrodes.

3.2. Optical and electrical measurement

After the enzymatic reaction the signals were detected by electrical (DNA-chip reader) and optical (flatbed scanner and subsequent image processing) readout (Fig. 4). For the optical detection we could detect CMV concentration of 5 pM. The small rise at 50 fM is caused by a false positive signal (unspecific silver deposition). Furthermore the reaction is highly specific. There is a clear distinction between 1 mismatch and the complementary sequence. The limit of detection (50 pM) of the electrical readout system is an order of magnitude higher than the limit of detection (5 pM) of the

Table 1
Characterization of the chips realized by various fabrication methods, photolithography (a) and screen printed gold electrodes (b) as well as screen printed platinum electrodes (c) in terms of conductivity of the conductor paths, roughness and thickness.

	Characteristics				
	Thickness (μm)	Roughness (μm)	Conductivity (S/m)		Gap width (μm)
			Min	Max	
(a) Photolithography	0.1	±0.001	2	1	10
(b) Gold	12	±3	1	0.417	~50
(c) Screen printing platinum	0.22	±0.02	0.0125	0.006	~50

Please cite this article in press as: Schüler, T., et al., Biosens. Bioelectron. (2008), doi:10.1016/j.bios.2008.10.028

G Model
BIOS-3034; No. of Pages 8
ARTICLE IN PRESS

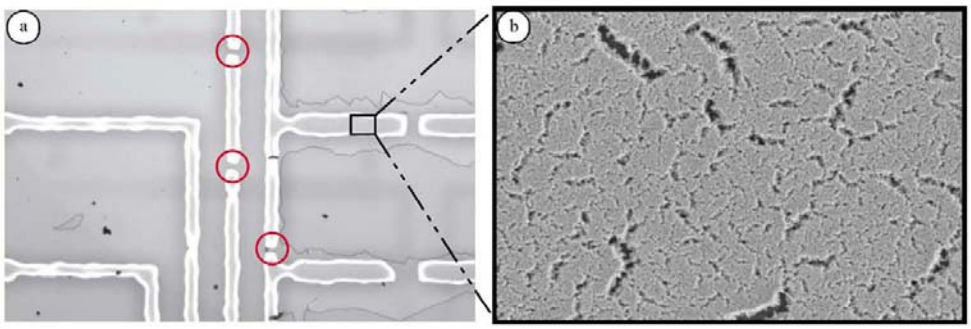

Fig. 3. Light microscopic image of screen printed platinum structures on a DNA-chip (a); the red circles mark breaks in the conductor paths. The SEM image (b) is an enlarged section of a platinum electrode.

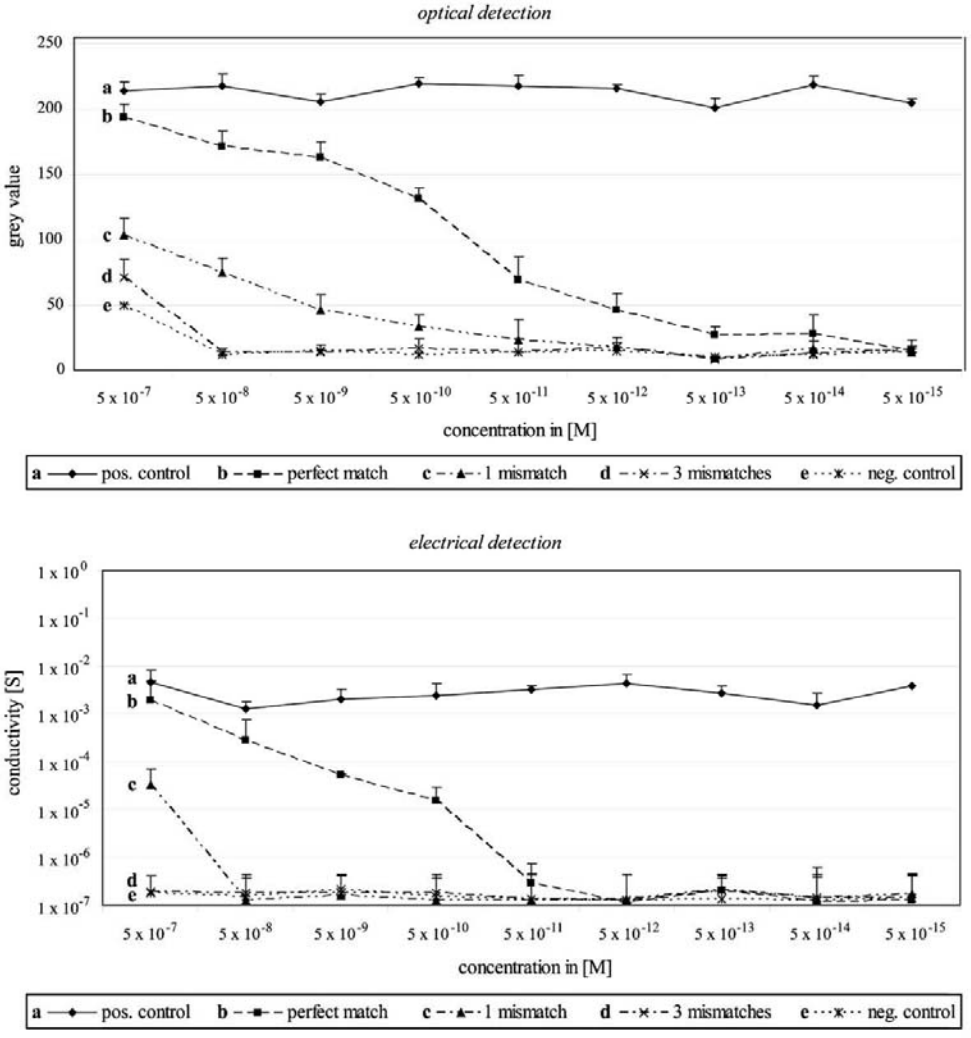

Fig. 4. Comparison between optical and electrical readout. The concentration-dependent signal intensity is displayed in both diagrams for different capture-DNA sequences (complementary DNA, sequenced containing 1 mismatch, sequence containing 3 mismatches, and a negative control). With the optical detection concentrations of 5 pM could be detected, the electrical method allows detection of target-DNA down to 50 pM.

Please cite this article in press as: Schüler, T., et al., Biosens. Bioelectron. (2008), doi:10.1016/j.bios.2008.10.028

G Model
BIOS-3034; No. of Pages 8
ARTICLE IN PRESS

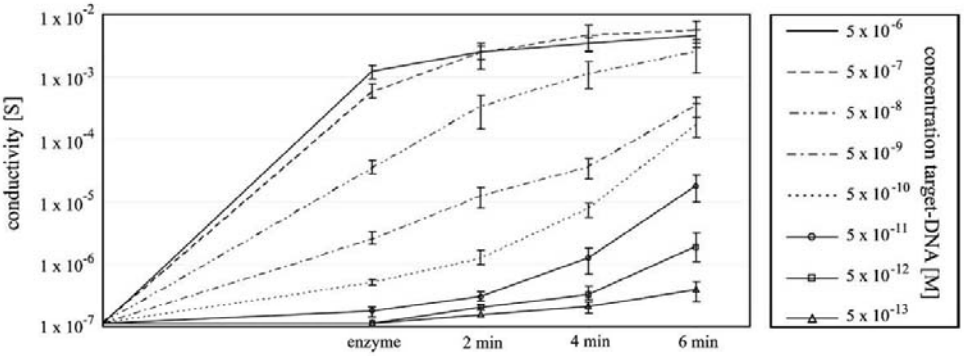

Fig. 5. By further silver enhancement steps using enzymatic generated silver nanoparticles as reaction seed, the detection limit could be reduced to a target-DNA concentration of 500 fM.

optical system. Nevertheless the specificity of both detection systems is comparable. We were able to clearly distinguish between the mismatch sequences and the perfect match with the optical and electrical detection system.

Due to the maladjustment of single nucleotides the binding process, between capture-DNA and the biotin-labelled target sequence, is restricted. Thereby, a higher amount of mismatches in the DNA strand leads to lower hybridization efficiency. By immobilization of different capture sequences the specificity of a bioanalytical tool can be determined. Later on the signal intensity (enzyme induced silver deposition detected by optical as well as electrical methods) gives a statement about the binding process.

For the experiments, every capture-DNA sequence was immobilized on eight different measurement points on the chip surface, and two untreated electrode gaps on every chip served as absolute negative control to avoid false positive signals. Once, a signal was detected on one of the untreated control electrode gaps, caused by unspecific silver deposition, the chips were not used for further data evaluation.

To analyze the results, the mean values over all eight measurement points on one chip (containing the same capture DNA) were calculated. Afterwards the mean values of the conductivity for the different capture-DNA sequences (complementary, 1 mismatch, 3 mismatches, and negative control) were compared. The electrical detection allows signal detection over a large measurement scale (from 0.1 μS to 1 S). If the difference of the mean values of the conductivity was less than one order of magnitude between the measurement points containing complementary DNA and the mean values for any other measurement points no specific differentiation of the DNA sequence was possible.

3.3. Sensitivity

As shown in previous work the sensitivity of the electrical readout can be improved by additional enhancement steps following the initial particle formation (Festag et al., 2007). Therefore the enzymatically deposited particles were used as reaction seed. Further silver enhancement steps induce the growth of the silver nanoparticles in the gap between the electrodes, which leads via interparticle bridging to a short-cut of the electrode gap even at low concentrations of CMV-DNA. We used a stepwise (3 × 2 min) nanoparticle induced silver deposition to reduce the limit of detection to 500 fM (Fig. 5). Longer enhancement times respectively more enhancement steps would not increase the signal, because of false positive signals (induced by the increasing background). The additional silver deposition on the screen printing chips leads to a similar sensitivity as already demonstrated for the microfabricated chips. With both chip types CMV-DNA at a concentration of 500 fM was detected. However, the chips produced by photolithography showed a higher conductivity as the chip produced by screen printing. This difference in the conductivity is probably caused by the flat and homogenous structures of the conducting electrodes of the chips produced by photolithography. Since, the photolithographic chips were produced on silicon an optical comparison between both types of chips using a transmission measurement was not possible. All experiments were repeated with the same parameters and showed the same results as the previous tests. Every chip contained measurement points for positive and negative controls. To avoid an overloading of the diagram (Fig. 5) the control values are not shown. Nevertheless all controls on every chip showed the expected data (no signal on the negative control and clear detectable signal on the positive control).

4. Conclusion

Screen printing technology offers a cost-effective opportunity to establish platforms for the chip-based analysis of biomolecules. This fabrication method represents an interesting alternative, especially for systems with sophisticated electrode layouts and structures. In our experiments the screen printed substrates showed the same sensitivity and specificity compared to DNA-chips produced by standard photolithography on silicon. Furthermore the electrode structures exhibit a high stability. The additional optical readout helps to control the electrical system. Further work will be aimed at the integration of the screen printed chip in a microfluidic system to automate the electrical chip-based detection of DNA. The integration in a flow cell improves the electrical DNA-chip technology in order to allow the use outside of specialized laboratories for on-site testing. An additional online detection of the enzyme induced silver deposition should help to avoid false positive signals. Furthermore a parallel control of the signal will elude the need for additional enhancement steps. Simultaneously we will extend our studies to analyze also proteins and RNA on the screen printed chips.

Acknowledgements

Funding of research project "Jenaer Biochip Initiative" (JBCI) within the framework "Unternehmen Region – Inno Profile" from the Federal Ministry of Education and Research, Germany (BMBF) is gratefully acknowledged. The authors thank Sven Jessing for the support in the laboratory.

Please cite this article in press as: Schüler, T., et al., Biosens. Bioelectron. (2008), doi:10.1016/j.bios.2008.10.028

G Model
BIOS-3034; No. of Pages 8
ARTICLE IN PRESS

We thank Nanoprobes for the kind support with EnzMet® enhancement kit, Daniell Malsch for the help with evaluation of the optical readout as well as Franka Jahn for SEM imaging and Matthias Urban for development and construction of the DNA-chip reader.

References

Albers, J., Grunwald, T., Nebling, E., Piechotta, G., Hintsche, R., 2003. Anal. Bioanal. Chem. 377 (3), 521–527.
Avramescu, A., Andreescu, S., Noguer, T., Bala, C., Andreescu, D., Marty, J.L., 2002. Anal. Bioanal. Chem. 374 (1), 25–32.
Barrett, S., 2008. Image SXM v1.85. From http://www.liv.ac.uk/~sdb/ImageSXM/.
Chambers, J., Angulo, A., Amaratunga, D., Guo, H., Jiang, Y., Wan, J.S., Bittner, A., Frueh, K., Jackson, M.R., Peterson, P.A., Erlander, M.G., Ghazal, P., 1999. J. Virol. 73 (7), 5757–5766.
Cheung, V.G., Morley, M., Aguilar, F., Massimi, A., Kucherlapati, R., Childs, G., 1999. Nat. Genet. 21 (1 Suppl.), 15–19.
Choi, J.W., Oh, B.K., Kim, Y.K., Min, J., 2007. J. Microbiol. Biotechnol. 17 (1), 5–14.
Csaki, A., Moller, R., Fritzsche, W., 2002. Expert Rev. Mol. Diagn. 2 (2), 187–193.
de Albuquerque, Y.D., Ferreira, L.F., 2007. Anal. Chim. Acta 596 (2), 210–221.
Dequaire, M., Heller, A., 2002. Anal. Chem. 74 (17), 4370–4377.
Drummond, T.G., Hill, M.G., Barton, J.K., 2003. Nat. Biotechnol. 21 (10), 1192–1199.
Festag, G., Schüler, T., Steinbrück, A., Csaki, A., Fritzsche, W., 2006. Scanning Probe Microscopy in Life Sciences. JPK, Berlin.
Festag, G., Steinbrück, A., Csaki, A., Fritzsche, W., 2007. Nanotechnology 17, 1–10.
Fritzsche, W., 2001. J. Biotechnol. 82 (1), 37–46.
Fritzsche, W., Csaki, A., Möller, R., 2002. SPIE 4626, 17–22.
Fritzsche, W., Taton, T.A., 2003. Nanotechnology 14, R63–R73.
Gonzalez-Garcia, M.B., Fernandez-Sanchez, C., Costa-Garcia, A., 2000. Biosens. Bioelectron. 15 (5–6), 315–321.
Heller, M.J., 2002. Annu. Rev. Biomed. Eng. 4, 129–153.
Ibanez, A.J., Schüler, T., Möller, R., Fritzsche, W., Saluz, H.P., Svatos, A., 2008. Anal. Chem. 80 (15), 5892–5898.
Liao, W.Y., Chou, T.C., 2006. Anal. Chem. 78 (12), 4219–4223.
Luo, Y.C., Do, J.S., Liu, C.C., 2006. Biosens. Bioelectron. 22 (4), 482–488.
Marquette, C.A., Corgier, B.P., Heyries, K.A., Blum, L.J., 2008. Front. Biosci. 13, 382–400.
Marquette, C.A., Lawrence, M.F., Blum, L.J., 2006. Anal. Chem. 78 (3), 959–964.
Matthews, D.R., Watson, E.B.A., Holman, R.R., Steemson, J., Hughes, S., Scott, D., 1987. Lancet 329 (8536), 778–779.
Mayer, G., Leone, R.D., Hainfeld, J.F., Bendayan, M., 2000. J. Histochem. Cytochem. 48 (4), 461–469.
Mirkin, C.A., Letsinger, R.L., Mucic, R.C., Storhoff, J.J., 1996. Nature 382 (6592), 607–609.
Möller, R., Powell, R.D., Hainfeld, J.F., Fritzsche, W., 2005. Nano Lett. 5 (7), 1475–1482.
Möller, R., Schüler, T., Günther, S., Carlsohn, M.R., Munder, T., Fritzsche, W., 2008. Appl. Microbiol. Biotechnol. 77 (5), 1181–1188.
Nagata, R., Yokoyama, K., Clark, S.A., Karube, I., 1995. Biosens. Bioelectron. 10 (3–4), 261–267.
Park, S.J., Lazarides, A.A., Mirkin, C.A., Brazis, P.W., Kannewurf, C.R., Letsinger, R.L., 2000. Angew. Chem. 112 (21), 4003–4006.
Park, S.J., Taton, T.A., Mirkin, C.A., 2002. Science 295 (5559), 1503–1506.
Schena, M., 2003. Microarray Analysis. Wiley-Liss Verlag, Hoboken, New Jersey.
Schena, M., Heller, R.A., Theriault, T.P., Konrad, K., Lachenmeier, E., Davis, R.W., 1998. Trends Biotechnol. 16 (7), 301–306.
Susmel, S., Guilbault, G.G., O'Sullivan, C.K., 2003. Biosens. Bioelectron. 18 (7), 881–889.
Tudorache, M., Bala, C., 2007. Anal. Bioanal. Chem. 388 (3), 565–578.
Urban, M., Möller, R., Fritzsche, W., 2003. Rev. Sci. Instrum. 74, 1077–1081.
Wang, J., 2000. Nucleic Acids Res. 28 (16), 3011–3016.
Wang, J., Xu, D., Kawde, A.N., Polsky, R., 2001. Anal. Chem. 73 (22), 5576–5581.
Warsinke, A., 2008. Adv. Biochem. Eng. Biotechnol. 109, 155–193.
Willner, I., Basnar, B., Willner, B., 2007. FEBS J. 274, 302–309.
Wong, A.K., Krull, U.J., 2005. Anal. Bioanal. Chem. 383 (2), 187–200.
Zhang, G.-J., Möller, R., Kretschmer, R., Csaki, A., Fritzsche, W., 2004. J. Fluoresc. 14 (4), 369–375.
Zheng, Z.B., Wu, Y.D., Yu, X.L., Shang, S.Q., 2008. J. Med. Virol. 80 (6), 1042–1050.

Please cite this article in press as: Schüler, T., et al., Biosens. Bioelectron. (2008), doi:10.1016/j.bios.2008.10.028

2.3 Flexible biochips for detection of biomolecules

Mária Péter, Thomas Schüler, Francois Furthner, Peter A. Rensing, Gert T. van Heck, Herman F. M. Schoo, Robert Möller, Wolfgang Fritzsche, Albert J. J. M. van Breemen, and Erwin R. Meinders

Langmuir (**2009**) 25(9): 5384-90

Langmuir

Subscriber access provided by FRIEDRICH SCHILLER UNIV JENA

Article

Flexible Biochips for Detection of Biomolecules

Ma#ria Pe#ter, Thomas Schu#ler, Franc#ois Furthner, Peter A. Rensing, Gert T. van Heck, Herman F. M. Schoo, Robert Mo#ller, Wolfgang Fritzsche, Albert J. J. M. van Breemen, and Erwin R. Meinders

Langmuir, **Article ASAP** • DOI: 10.1021/la8037457 • Publication Date (Web): 30 March 2009

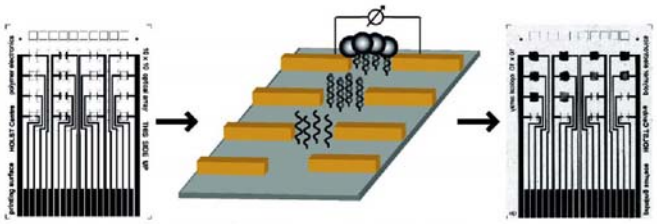

PEN foil based DNA chip

More About This Article

Additional resources and features associated with this article are available within the HTML version:

- Supporting Information
- Access to high resolution figures
- Links to articles and content related to this article
- Copyright permission to reproduce figures and/or text from this article

View the Full Text HTML

Langmuir
Article
pubs.acs.org/Langmuir

Flexible Biochips for Detection of Biomolecules

Mária Péter,*[,†] Thomas Schüler,*[,‡] François Furthner,[†] Peter A. Rensing,[†] Gert T. van Heck,[†] Herman F. M. Schoo,[†] Robert Möller,[‡] Wolfgang Fritzsche,[§] Albert J. J. M. van Breemen,[†] and Erwin R. Meinders[†]

[†]*Holst Centre/Netherlands Institute for Applied Scientific Research (TNO), High Tech Campus 31, Postbus 8550, 5605 KN Eindhoven, The Netherlands,* [‡]*JBCI, Institute for Physical Chemistry, Friedrich-Schiller-University, Helmholtzweg 4, Jena, Germany and* [§]*Institute of Photonic Technology, Albert-Einstein-Strasse 9, Jena, Germany*

Received November 11, 2008. Revised Manuscript Received February 16, 2009

Miniaturization of biosensors is envisaged by the development of biochips consisting of parallel microarray patterns of binding sites on rigid substrates, such as glass or silicon. Thin plastic substrates are promising flexible alternatives because of the possibility for large-area roll-to-roll manufacturing of disposable chips at lower costs. Mature optical lithography technology faces many challenges when used to pattern flexible foils as a result of the substrate instabilities, especially at higher temperatures. In this work, flexible biochips with gold electrode patterns were fabricated on thin polyethylene naphthalate (PEN) foils using photolithography. The gold electrode structures of the chips were manufactured by direct metal patterning and by lift-off processing. Both methodologies resulted in well-defined electrode patterns as concluded from optical microscopy and scanning electron microscopy (SEM) characterization and resistance measurements. The biochips were successfully employed for the electrical and optical detection of DNA molecules. The DNA detection was based on the immobilization of capture DNA between electrode gaps, hybridization with biotin-labeled target DNA, and enzymatic silver enhancement.

Introduction

The development of miniaturized biochips for the detection of DNA or other biological molecules or complexes is evolving rapidly. It is expected that this development will result in rapid, reliable, and reproducible point-of-care test protocols for the detection of small sample quantities at relatively low cost.[1,2] Biochips usually consist of patterned microarrays of binding sites that are capable of capturing and binding molecules of interest, such as DNA, from solution.[3] The captured molecules can be detected on the basis of markers.[4,5] Fluorescent labeling of DNA molecules is one of the most commonly used marking method for optical detection.[6] This method is quite selective and specific but also has some shortcomings. Fluorescent labels can bleach or quench, which may hamper the analysis of results and/or makes it labor-intensive.[7] Nanoparticle labeling was proposed as a very attractive alternative approach, broadening the detection scheme beyond optical toward electrical detection.[8] When using sandwich-type assays, the detection becomes even easier.[9] In this approach, the complementary capture DNA is immobilized by spotting or printing in the electrode gaps of a specially designed electrode microarray of a biochip and subsequently hybridized with the target DNA. In the following step, a nanoparticle-labeled second molecule is specifically bound to the target. An additional metal enhancement process is used to enlarge the nanoparticles, eventually resulting in the formation of a conductive bridge over the electrode gap causing a detectable resistance drop.[10−12] If the electrodes are not protected, then the use of nanoparticles for the electrical detection of DNA in combination with the metal enhancement step can cause nonspecific metal growth on the electrodes as well, thus lowering the sensitivity of the assay. To overcome this drawback, an enzymatic metal enhancement was proposed that enables highly specific metal deposition only at the enzyme sites.[13] The method assures both high sensitivity and high specificity.[14−16]

The most commonly used substrates for biochip manufacturing are rigid glass or oxidized silicon on which the electrode microarrays are defined by conventional photolithography.[17,18] These substrates are brittle and can easily break during handling. Moreover, these biochips are for single use

*Corresponding authors. E-mail: maria.peter@tno.nl; thomas.schueler@ipht-jena.de.

(1) Heller, M. J. *Annu. Rev. Biomed. Eng.* **2002**, *4*, 129 153.
(2) Venkatasubbarao, S. *Trends Biotechnol.* **2004**, *22*, 630 637.
(3) Schena, M.; Heller, R. A.; Theriault, T. P.; Konrad, K.; Lachenmeier, E.; Davis, R. W. *Trends Biotechnol.* **1998**, *16*, 301 306.
(4) Wang, J. *Nucleic Acids Res.* **2000**, *28*, 3011 3016.
(5) Festag, G.; Schüler, T.; Steinbrück, A.; Csáki, A.; Möller, R.; Fritzsche, W. *Expert Opin. Med. Diagn.* **2008**, *2*, 813 828.
(6) Schena, M.; Shalon, D.; Davis, R. W.; Brown, P. O. *Science* **1995**, *270*, 467 470.
(7) Csaki, A.; Moller, R.; Fritzsche, W. *Expert Rev. Mol. Diagn.* **2002**, *2*, 187 193.
(8) Mirkin, C. A.; Letsinger, R. L.; Mucic, R. C.; Storhoff, J. J. *Nature* **1996**, *382*, 607 609.
(9) Southern, E. M. *Trends Genet.* **1996**, *12*, 110 115.
(10) Festag, G.; Schüler, T.; Möller, R.; Csáki, A.; Fritzsche, W. *Nanotechnology* **2008**, *19*, 125303.
(11) Möller, R.; Csaki, A.; Köhler, J. M.; Fritzsche, W. *Langmuir* **2001**, *17*, 5426 5430.
(12) Park, S. J.; Taton, T. A.; Mirkin, C. A. *Science* **2002**, *295*, 1503 1506.
(13) Möller, R.; Powell, R. D.; Hainfeld, J. F.; Fritzsche, W. *Nano Lett.* **2005**, *5*, 1475 1482.
(14) Schüler, T.; Steinbrück, A.; Festag, G.; Möller, R.; Fritzsche, W. *J. Nanopart. Res.* **2008**, online first.
(15) Hwang, S.; Kim, E.; Kwak, J. *Anal. Chem.* **2005**, *77*, 579 584.
(16) Willner, I.; Basnar, B.; Willner, B. *FEBS J.* **2007**, *274*, 302 309.
(17) Southern, E. M.; Case-Green, S. C.; Elder, J. K.; Johnson, M.; Mir, K. U.; Wang, L.; Williams, J. C. *Nucleic Acids Res.* **1994**, *22*, 1368 1373.
(18) Schena, M. *Microarray Analysis*; Wiley-Liss Verlag: Hoboken, NJ, 2003.

 DOI: 10.1021/la8037457

only, hence cost-efficient substrates would considerably contribute to cost reductions and thereby broaden the applicability.[19] Thin polymer foils can be considered to be potential low-cost alternatives to glass and silicon oxide, paving the way for the roll-to-roll large-area fabrication of biochip arrays.[20,21] It also allows high-level integration, for instance, of microchannels and electrode arrays.

In this article, we discuss the development of plastic biochips used for the detection of DNA molecules. Optical lithography was used to pattern metal electrodes on thin polyethylene naphthalate (PEN) foils.[22] Optical lithography on flexible plastic foils is challenging because of the dimensional instability of the foils when subjected to higher temperatures and different processing conditions. Two manufacturing approaches were investigated and compared to pattern gold electrodes on PEN foils: direct metal patterning and lift-off processing. The quality of the electrodes was verified with optical microscopy and scanning electron microscopy (SEM). A second challenge in the development of a biosensor chip was the binding of capture DNA to the patterned PEN foils. The immobilization of capture DNA was successfully achieved. The processed biosensor chip was used to detect oligonucleotide DNA via enzyme labeling and silver enhancement. Flatbed scanning and resistivity measurements between the electrodes were employed to detect Ag deposition and thus the detection of target DNA.

Experimental Section

Biochip Fabrication and Characterization. The biochips were made on heat-stabilized polyethylene naphthalate (PEN) foils (Dupont Teijin Films) of different film thicknesses: 25, 50, and 75 μm PEN foils (DTF, Kaladex), and 100 and 200 μm PEN foils (DTF, TeonexQ65). The foils were temporarily laminated to a rigid support to enable the patterning of metal electrodes via optical lithography. The Si wafer/glue/foil assembly will be referred to as a foil-on-carrier (FOC), on which the foil surface is always subjected to processing. The FOC system was subjected to a heat step of 150 °C for 300 s to stabilize the assembly for higher-temperature lithography processing. Surface flatness below 3 μm was measured for the FOC assemblies using a Taylor-Hobson Talysurf (Leicester, U.K.) instrument.

Fabrication by Direct Metal Patterning. The FOC surface was coated with 100 nm Au (using a 10 nm Ti adhesion layer) by sputter deposition. The adhesion of Au to the foil was qualitatively verified by the Scotch tape test (Scotch tape manufactured by 3M, width 1.8 cm).[23] Two types of positive photoresists were explored to pattern gold on the PEN foil: HPR504 (Arch Chemicals) and AZ 1518 (Shipley, U.K.).

HPR504 was spin-coated onto the FOC and subsequently prebaked at 90 °C for 240 s. The HPR504 layer was exposed through a mask for 1 s at an energy of 44.3 mW/cm^2 and a wavelength range of 350−450 nm on a Karl Suss MA8 mask aligner. A postbaking step was followed at 120 °C for 120 s. The resist was developed using PLSI developer (OCG Microelectronics Materials). The Au was etched in the areas not protected by the photoresist for 40 s using a commercial etchant (TFA from Transene, based on KI/I_2 in water; 1:1 TFA/H_2O). Ti was etched for 30 s using a solution of HF and HNO_3 in water (1:65:150 HF/HNO_3/H_2O). The remaining resist was stripped in acetone.

AZ1518 positive resist (Shipley, U.K.) was spin-coated onto the FOC and baked at 90 °C for 240 s. The samples were exposed for 7 s at an energy of 8.6 mW/cm^2 and a wavelength range of 350−450 nm also on a Karl Suss MA-8 mask aligner. After exposure, the resist was hard-baked at 120 °C for 120 s and developed for 45 s in AZ developer (Clariant GmbH). Au and Ti were etched as described before. The remaining resist was dissolved in acetone.

Patterning by Lift-Off Processing. Futurrex NR1-3000PY negative resist was spin-coated onto the FOC (2500 rpm, 30 s). The resist was baked at 150 °C for 180 s and then cooled to room temperature. The resist layer was exposed through a mask for 40 s at an energy of 8.6 mW/cm^2 and a wavelength range of 350−450 nm on a Karl Suss MA8 mask aligner. The post-exposure bake was done at 100 °C for 120 s. The resist was developed for 30 s using Futurrex RD6 developer. Au (100 nm) was sputtered onto the surface after a short oxygen plasma treatment and adhesion layer (10 nm of Ti) deposition. The lift-off process was performed by sonication in acetone for 30 min, followed by soaking the samples for 30 min in an acetone bath. Qualitative metal adhesion was verified by the Scotch tape test.[23]

After biochip fabrication (either by direct metal patterning or lift-off processing), the PEN foils were removed from the Si carrier and characterized by optical microscopy and scanning electron microscopy. All further steps, including surface modification and detection, were performed on the free-standing, flexible biochips.

Surface Modification. After the fabrication of the metal structures, the PEN foils were chemically modified with 3-(glycidyloxypropyl)-trimethoxysilane (GOPS) for the binding of amino-modified single-stranded (ss) capture DNA molecules.[24] Before surface modification, the PEN foils were sonicated for 600 s in acetone, methanol, and finally water. Afterwards, the foil substrates were immersed in a 10 mM solution of GOPS in dry toluene for 6 h at 70 °C. Finally, the foils were washed twice with toluene, ethanol, and water for 300 s each and dried under a stream of nitrogen. The experimental details of the surface-modification process are described in the literature.[24,25]

Immobilization of Capture DNA. To detect DNA oligonucleotides on the PEN surface, different 30-base-pair (bp)-long ss capture sequences were spotted using a custom-designed PDMS (polydimethylsiloxane) mask. The capture sequences were diluted in microarray printing buffer from ArrayIt (Micro Spotting Solution Plus, TeleChem International, Sunnyvale, CA). After applying the mask to the foil surface droplets, 3 μL of the capture DNA was applied to the small cavities of the PDMS mask. The single cavities had a size of 1.9 mm × 1.9 mm and a depth of 1 mm. Next to a positive (already biotin-labeled) and a negative control array, we immobilized three single-stranded (ss) complementary sequences: a perfect match, a sequence containing one mismatch, and a sequence containing three mismatches. The DNA oligonucleotides were immobilized on the GOPS surface via a 5′-amino linker (Table 1).

Hybridization. The biotin-labeled target DNA was diluted in the hybridization buffer to adjust for different concentrations ranging from 5 μM to 5 fM. The hybridization was performed by applying droplets of the target DNA solution to the substrates, followed by incubation in a humidity chamber for 1 h at 40 °C. The substrates were washed afterwards to remove any unbound DNA. Detailed conditions of the hybridization are described elsewhere.[1] Briefly, the biotin-labeled target DNA was diluted in 5× SSC buffer containing 0.1% SDS. Target DNA sequences

(19) Marquette, C. A.; Lawrence, M. F.; Blum, L. *J. Anal. Chem.* **2006**, *78*, 959–964.
(20) Feng, C. L.; Zhang, Z.; Forch, R.; Knoll, W.; Vancso, G. J.; Schonherr, H. *Biomacromolecules* **2005**, *6*, 3243–3251.
(21) Li, Y.; Wang, Z.; Ou, L. M.; Yu, H. Z. *Anal. Chem.* **2007**, *79*, 426–433.
(22) Hu, B.; Siddiqui, A.; Ottenbrite, R. M. *Macromol. Chem. Phys.* **2002**, *203*, 1631–1635.
(23) Wei, Y.; Yeh, J.-M.; Jin, D.; Jia, X.; Wang, J.; Jang, G.-W.; Chen, C.; Gumbs, R. W. *Chem. Mater.* **1995**, *7*, 969–974.
(24) Wong, A. K.; Krull, U. *J. Anal. Bioanal. Chem.* **2005**, *383*, 187–200.
(25) Möller, R.; Csáki, A.; Köhler, J. M.; Fritzsche, W. *Nucleic Acids Res.* **2000**, *28*, e91.

Table 1. DNA Sequences Used to Demonstrate the Specific Detection of DNA on PEN Foil Substrates, Where Marked Nucleotides Represent the Mismatches Compared to the Perfect Match.

		length	sequence from 5′-3′	modification
1	positive control	30nt	CAT AGA ATC AAG GAG CAC ATG CTG AAA AAA	5′-C6aminolink, 3′-biotin
2	perfect match	30nt	TTT TTT CAG CAT GTG CTC CTT GAT TCT ATG	5′-C6aminolink
3	one mismatch	30nt	TTT TTT CAG CAT GGG CTC CTT GAT TCT ATG	5′-C6aminolink
4	three mismatches	30nt	TTT TTT CAG CAT TAT CTC CTT GAT TCT ATG	5′-C6aminolink
5	negative control	35nt	ACT GAC TGA CTG ACT GAC TGA CTG GGC GGC GAC CT	3′-C7aminolink

were taken from 150 bp PCR products of human cytomegalovirus (CMV) DNA. The following washing step using SSC and SDS removed unbound DNA to avoid false positive signals.

Binding of Horseradish Peroxidase Polymer (Enzyme Labeling). The streptavidin-horseradish peroxidase polymer (purchased from Sigma; streptavidin-peroxidase polymer, ultrasensitive, Sigma-Aldrich, Taufkirchen, Germany) was diluted in a ratio of 1:1000 in PBS buffer and 0.05% Tween20. This buffer was also used in the washing step following the incubation of 1 h at room temperature. To avoid any interference with chloride ions, the foils were shortly rinsed with distilled water before starting the enzyme-induced silver deposition.

Silver Enhancement. After the conjugate of the streptavidin enzyme was bound, the three solutions (A−C) of a silver enhancement kit (EnzMet kit, Nanoprobes Inc., Yaphank, NY) were applied in small droplets on the chip surface in a ratio of 1:1:1 following the provided protocol. The reaction was stopped after 300 s to avoid nonspecific silver deposition. To improve the signal intensity, enzymatically deposited silver nanoparticles were used as reaction seeds for additional nanoparticle-induced silver deposition. For that purpose, 200 mg of hydroquinone was dissolved in 40 mL of citrate buffer. To provide silver ions for the reaction, 80 mg of silver acetate was dissolved in 40 mL of double deionized water. Both solutions were mixed in ratios of 1:1 on the DNA chip. The reaction was stopped by rinsing the chips with water. This reaction could proceed as long as the unspecific silver deposition (background) did not appear on the foil surface. Hence, the reaction must be stopped before signals on the mismatch containing DNA sequences or the negative controls (false positive signals) were detectable.

Electrical and Optical Characterization. The silver enhancement leads to a conductive layer of silver nanoparticles that eventually can bridge the electrode gap. Thereby, a measured increase in the conductivity over the electrode gap serves as a signal. The Sourcemeter 2400 from Keithley (Keithley Instruments Inc., Cleveland, OH) was used for the electrical readout. With a minimum measurable current of 100 nA at a voltage of 1 V, the resulting detection limit of the instrument was 10 MΩ. Special custom-built microcontact units served to contact the single electrode pairs on the foil. The measured resistances were transferred later onto a PC for further data evaluation. The requirement for the detection of an electrical signal is the continuous coverage of silver nanoparticles in the electrode gap. A discontinuous silver layer leads to either very high or nonmeasurable resistance. In that case, an additional optical detection of the signal could be used as a control for the electrical signal.[26] Because of their transparency, PEN foils offer the possibility for an optical readout of the signal. To analyze the deposited silver spots by means of a transmissive optical readout, PEN foils were imaged by a common flatbed scanner, and the resulting images were converted into 8 bit monochrome pictures. Afterwards, the single gray values of the silver spots were evaluated by image analysis software Image J.[27]

Results and Discussions

Photolithography is a mature technology used to pattern rigid substrates, such as silicon or glass. The use of thin, flexible substrates in combination with lithographic processing encounters some challenges imposed by the dimensional instability and the flexibility of the foils used. Polymer substrates can easily deform when subjected to higher temperatures and solvents (both organic and inorganic). The polyethylene naphthalate (PEN) foils considered in our study have unique properties. PEN is a semicrystalline biaxially oriented polyester film with a glass-transition temperature (T_g) of 120 °C. Because of the semicrystallinity, PEN foils have superior mechanical properties as compared to amorphous polymers. The elastic modulus is about 5.5−6.0 GPa, and the tensile strength is about 250−270 MPa. Heat-stabilized foils, used in our study, can be processed at up to 180−200 °C without considerable thermal shrinkage. Because of the ester groups in the polymer, PEN foils have a high propensity to absorb water in humid environments or when immersed in water (e.g., the water permeability is 1.2 g/m^2/24 h for the 125 μm foils, data supplied by DTF).[28] However, there are special advantages associated with the presence of these functional groups. The surface can easily be functionalized (e.g., silanized without any pretreatment to facilitate the immobilization of biological molecules). The static water contact angle of a pristine PEN foil is about 65°, which assures good wetting of the foil surface by most of the commercial photoresists without the need for surface pretreatment. PEN foils have good resistance in organic solvents (toluene, acetone, etc.) and also in inorganic acids (HF, HNO_3, etc.). The described characteristics of heat-stabilized PEN allowed patterning of the foils by optical lithography and wet processing.

Handling of the foils during processing was done by temporarily fixing them to a rigid carrier as described in the Experimental Section. The method provided flat FOC surfaces (flatness below 3.0 μm). After being processed, the foils could easily be released from the Si wafer/glue interface at room temperature without causing damage to the fabricated electrode structures.

The design of the biochip is shown in Figure 1. The biochip consists of 4 rows of 4 measurements in each site (16 measurement sites in total). The gap size between the electrodes is 10 μm.

Direct Metal Patterning. For the direct metal patterning approach, the surface of the FOCs was first coated with gold. The adhesion was verified by performing a Scotch tape test.[23] Initial experiments have showed that Au adhesion to PEN is mediocre when it is deposited by sputter deposition because traces of metal were found on the Scotch tape after peel off.

(26) Fritzsche, W.; Taton, T. A. *Nanotechnology* **2003**, *14*, R63–R73.
(27) Barrett, S. In *Image SXM v1.85;* http://www.liv.ac.uk/~sdb/ImageSXM/ **2008**.
(28) MacDonald, W. A. In *Organic Electronics: Materials, Manufacturing and Applications;* Klauk, H., Ed.; Wiley-VCH: Weinheim, Germany, **2006**; Chapter 7, p 446.

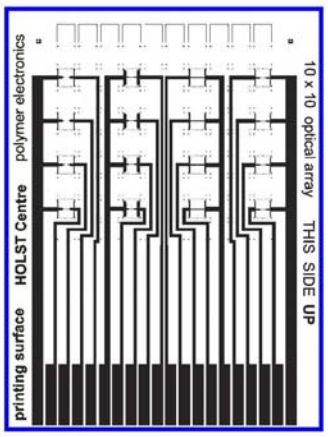

Figure 1. Biochip design with 16 measurement sites.

To promote the adhesion of the metal, the foil surface was subjected to a short oxygen plasma treatment followed by the deposition of a 10 nm Ti adhesion layer. During the Scotch tape test, no metal was removed from the foil surface, indicating better adhesion properties.[29]

Two types of positive photoresists, HPR504 and AZ1518, were considered for patterning in order to verify the influence of the resist on the pattern quality. The exposure process was optimized by using different exposure times. In the case of HPR504, 1.0 s of exposure time at higher energy (energy 44.3 mW/cm^2, wavelength 350−450 nm) was found to be the best process window to achieve the designed feature sizes. In the case of the AZ1518 resist, the best exposure time was 7 s at an energy of 8.6 mW/cm^2 in the wavelength range of 350−450 nm. Higher exposure times resulted in overexposure and a decrease in the pattern width or the total disappearance of the electrode structures after etching. Figure 2a shows a lower-magnification optical micrograph of a detection site with an electrode gap of 10 μm fabricated by direct metal patterning. After proper process optimization (adequate exposure time at a given illumination energy) and etching, the patterns obtained had good resolution with well-defined sharp edges. The quality of the patterns was not influenced by the resist used. The edge roughness of the electrodes prepared by direct patterning was inspected by SEM (Figure 3a). Gold etching occurred at the boundaries between adjacent Au grains resulting in rougher electrode edges. This edge roughening had no influence on the detection performance of the biochips. Figure 3a also shows that even after process optimization the obtained gap size is about 13 μm instead of 10 μm, indicating an under-etch of about 1.5 μm on both sides. This effect can be minimized by improving the adhesion of the resist to the gold-coated foil surface.

Biochip Fabrication by the Lift-Off Process. For the lift-off process, the FOCs were coated with a negative photoresist, Futurrex NR1-3000PY. As mentioned earlier, the surface properties of PEN allowed good surface wetting by the resist without the need for pretreatment. The best processing conditions were found by varying the exposure (at 8.6 mW/cm^2 energy and 350−450 nm wavelength) and developing times. The best exposure time was found to be 40 s. Shorter exposure times were not sufficient to cross-link the resist in the electrode gaps, for instance, which resulted in joined electrodes after the lift-off process. Longer exposure times resulted in an increase in the gap width as compared to the desired and designed sizes. The lift-off process provides good pattern quality if the exposed and developed resist structures have a negative slope. It has been found that a developing time of 30 s delivers walls with a negative slope. Resist development was followed by gold deposition. In initial experiments Au was deposited on the patterned structures without any pretreatment. This resulted in patterns with poor adhesion to PEN after Au lift off in acetone. The electrodes did not survive the Scotch tape test. To promote the adhesion of the metal, a short oxygen plasma treatment and a 10 nm Ti adhesion layer were used before sputtering a 100-nm-thick Au layer. This procedure resulted in strongly adhering electrodes with well-defined sharp patterns after the lift-off of gold.[29] Sonication for 30 min followed by 30 min of soaking in acetone did not induce damage in the Au patterns. Figure 2b shows a lower-magnification optical micrograph of a detection site with an electrode gap of 10 μm fabricated by lift-off processing. At this magnification, there is no observable difference between electrodes prepared by direct patterning or lift-off processing (Figure 2a,b). SEM pictures show that the edge roughness of the lift-off patterns is much smaller than in the case of direct patterning (Figure 3b). The gap size obtained is 9.6 μm, showing that by lift-off processing better pattern fidelity can be achieved; the gap size on the mask was designed to be 10 μm.

The generated silver spot on each measurement site was much larger (3.61 mm^2) than the electrode gap due to the large cavities of the PDMS mask. This helped to improve the contact area between the grown silver and the gold structures. For this reason, the electrical characterization of the foils did not show any influence of the electrode sizes or gap width. It has also been observed that the thickness of the foil had no influence on the quality of the electrode patterns in any of the fabrication approaches used or on the biodetection process.

Biochip Functionalization/DNA Detection. The schematic representation of biofunctionalization and the principles of optical and electrical detection are shown in Figure 4. After the immobilization of single-stranded capture DNA

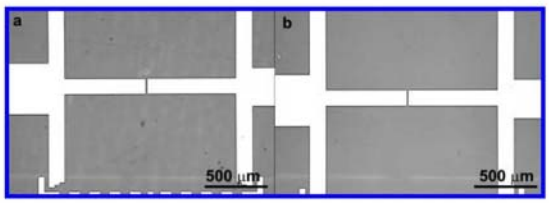

Figure 2. Optical micrographs of 10 μm electrode gaps prepared by (a) direct patterning and by (b) lift-off processing.

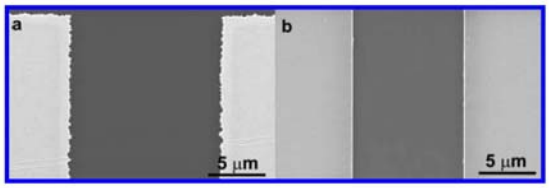

Figure 3. SEM images of 10 μm electrode gaps prepared by (a) direct patterning and by (b) lift-off processing.

(29) Péter, M.; Furthner, F.; Deen, J.; de Laat, W. J. M.; Meinders, E. M. *Thin Solid Films* **2008**, in press.

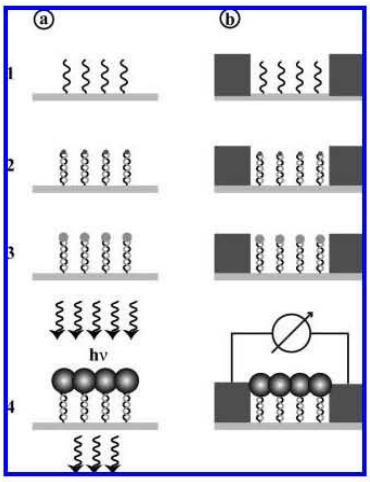

Figure 4. Methods of detection: (a) optically by transmissive microscopy and (b) electrically by measurement of the resistance. After the immobilization of single-stranded capture-DNA sequences (1), the biotin-labeled target DNA hybridizes on the specific partner on the PEN foil (2). In the following step, a streptavidin-horseradish peroxidase conjugate is bound to the biotin modification in the target DNA (3). In the end, an enzymatic reaction leads to the deposition of silver nanoparticles (4), which can be detected as described.

sequences (1), the biotin-labeled target DNA hybridizes on the specific partner on the PEN foil (2). In the following step, a streptavidin-horseradish peroxidase conjugate is bound to the biotin modification in the target DNA (3). Finally, an enzymatic reaction leads to the deposition of silver nanoparticles (4), which can be detected either optically (pathway a) or electrically (pathway b).

Because of the good stability of PEN foils in different organic solvents, they could be employed as biochip substrates using the same surface activation and modification protocols as for silicon oxide.[24,30] Even incubation in toluene at 70 °C for several hours showed no detectable impairment of the PEN foils and the microstructured electrodes. The immobilization of amino-modified ss DNA on the foil substrates was possible by first performing a surface functionalization with GOPS. The silanization leads to a self-assembled monolayer (SAM) of epoxy groups generated on the foil surface. Afterwards, the aminolink of the capture DNA can react with the epoxy modification during the formation of an amide.[31] This prefunctionalization of the surface enabled the reproducible immobilization of capture DNA and the fabrication of DNA chip arrays on foil substrates.

The successful biofunctionalization of PEN foil substrates after the surface modification was proven by the use of negative (noncomplementary sequence) and positive controls (directly biotin-labeled sequence) on the foils. The positive control should always produce clearly detectable results, contrary to nondetectable signals on the negative control. Both controls were used in all tests to ensure reliable results. In the case of false negative signals (no signal on the positive control) and false positive signals (signal on the negative control), which would indicate a problem during biofunctionalization of the foil substrate, the chips were not used for further data evaluation.

The electrical detection of DNA on PEN chips showed comparable results to those previously achieved on silicon or glass chips (500 fM).[13,32] The electrode structures on the silicon chips were also prepared by standard photolithography, whereas the electrode structure on the glass chips were produced by screen printing of a gold or platinum paste.[32] It has been found that the target DNA sequences used could be detected to concentrations of as low as 500 fM on all substrates using the electrical detection scheme.

In contrast to previously used silicon chips, PEN foils are transparent, which enables a second optical detection scheme to read out the DNA chips. The advantage of combining two detection methods is that an internal control can be established in a detection system, comparing the results from both detection methods to reveal possible false negative or false positive measurements. In this way, the reliability of the detection can be improved. Furthermore, a combination of optical and electrical detection will broaden the detection range of the system. Optical detection also provides time-resolved information about the DNA deposition process. The binding of target DNA was optically detected by measuring the intensity of transmitted light after silver enhancement. The deposited silver was analyzed by imaging the foils using a standard flatbed scanner and gray value analysis. Figure 5 shows that the optical controls confirm the electrical results. Furthermore, the optical control still gives signals at lower concentrations. This effect can be explained by the density of the deposited silver nanoparticles. The electrical detection is based on the presence of a conductive layer between the electrodes; otherwise, no signal can be detected. In the case of an optical readout, there is no need for such a dense layer of silver nanoparticles. Using light microscopy in transmission mode, even nonconnected particle clusters can serve as detection signals.

In this experiment, the low hybridization event (due to the specific interaction between capture and target) on the three mismatch probe led to a nonmeasurable electrical signal due to the lack of an electrically conductive layer. However, the optical detection of the signal was still possible. This also shows that the optical detection is more sensitive; however, the measurement range is much larger for the electrical setup (from MΩ down to a few Ω). As a consequence, for a quantitative data analysis the electrical measurement is more suited. These preliminary results need further investigations in the future.

It was also possible to differentiate between mismatch probes using either of the described detection systems. By immobilization of different mismatch sequences, we were able to investigate the specificity of the foil-based DNA detection system. The differentiation between a perfect match and a mismatch containing sequences strongly depends on the hybridization parameters (e.g., hybridization temperature and salt content of the hybridization buffer).[33,34] Because of

(30) Möller, R.; Schüler, T.; Günther, S.; Carlsohn, M. R.; Munder, T.; Fritzsche, W. *Appl. Microbiol. Biotechnol.* **2008**, *77*, 1181 1188.
(31) Lamture, J. B.; Beattie, K. L.; Burke, B. E.; Eggers, M. D.; Ehrlich, D. J.; Fowler, R.; Hollis, M. A.; Kosicki, B. B.; Reich, R. K.; Smith, S. R.; Varma, R. S.; Hogan, M. E. *Nucleic Acids Res.* **1994**, *22*, 2121 2125.
(32) Schüler, T.; Asmus, T.; Fritzsche, W.; Möller, R. *Biosens. Bioelectron.* **2008**, accepted.
(33) Han, T.; Melvin, C. D.; Shi, L.; Branham, W. S.; Moland, C. L.; Pine, P. S.; Thompson, K. L.; Fuscoe, J. C. *BMC Bioinf.* **2006**, *7*, S17.
(34) Urakawa, H.; El Fantroussi, S.; Smidt, H.; Smoot, J. C.; Tribou, E. H.; Kelly, J. J.; Noble, P. A.; Stahl, D. A. *Appl. Environ. Microbiol.* **2003**, *69*, 2848 2856.

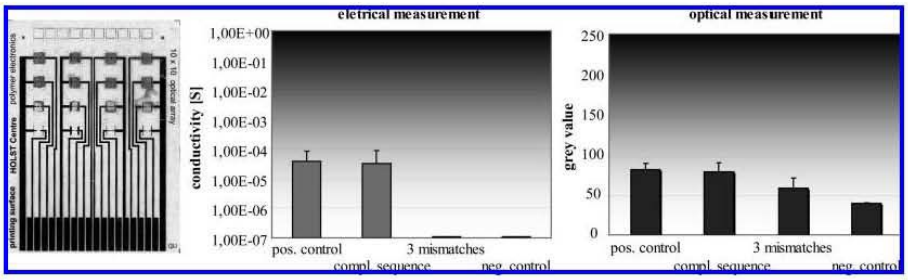

Figure 5. PEN foil with microstructured electrodes after biofunctionalization and enzyme-induced silver deposition (comparison electrical and optical readout). The PEN foil displays a typical result after enzyme-induced silver deposition. We immobilized the positive control in the first row, the complementary sequence in the second row, the complementary sequence containing three mismatches in the third row, and the negative control in the fourth row. The target DNA concentration was 5 nM.

the maladjustment of single nucleotides, the binding process between capture DNA and the biotin-labeled target sequence is restricted. Thereby, a higher number of mismatches in the DNA strand leads to lower hybridization efficiency. By immobilization of different capture sequences, the specificity of a bioanalytical tool can be determined. Later on, the signal intensity (enzyme-induced silver deposition detected by optical as well as electrical methods) gives an indication of the binding process. Depending on their positions in the capture DNA sequence, the signals on the mismatch containing sequences cannot be completely eliminated. The differentiation between the complementary sequence and the complementary sequence containing one mismatch becomes difficult if the mismatch is located at the terminal end of the DNA. With the described hybridization parameters, we could demonstrate on PEN foils a single mismatch differentiation for sequences taken from 150 bp PCR products of human cytomegalovirus (CMV) DNA. Figure 6 displays the sensitivity and specificity that are achievable on the PEN foil substrates. For all concentrations used here, the sequence-specific detection of target DNA leads to a clear discrimination between both sequences, which is represented by the optical as well as by the electrical results in Figure 6. The optimal concentration in this set of experiments is 5 nM. The differentiation between a perfect match and mismatch probes becomes more difficult at higher concentrations (5 μM), which is a typical effect in microarray technology. At lower concentrations (5 pM, 5 fM), the signal intensity of both the perfect match and the mismatch probes decreases. Therefore, the intensity ratio between the perfect match and mismatch probes changes again.

We were able to distinguish even between the complementary sequence and the complementary sequence containing one mismatch. In principle, both methods can be used for signal analysis. Additionally, the combination of both measurement methods allows control over each other to avoid false positive and false negative measurements. The data of the electrical signals show the same behavior as the optical readout. The advantage of the electrical method is the higher dynamic range of measurements. Because of the extended dynamic measurement range (from 10 MΩ down to a few Ω), the electrical measurement exhibits the potential to differentiate accurately between the signals on each measurement point and to detect even low variances. Therefore, it seems to be beneficial to develop the electrical detection method further to be used later for quantitative analysis of the measured signals (e.g., by an internal standard) on the foil chips. The optical readout allows only a qualitative estimation of the biomolecule interactions on the foil surface. To support this approach, more tests need to be performed.

Conclusions

Flexible biochips have been fabricated on polyethylene naphthalate (PEN) foils with different thicknesses by optical lithography. Two electrode-patterning methodologies were compared: direct metal patterning and a lift-off process. Gold patterns with good resolution were obtained by both methods. The quality of the patterns was not influenced by the thickness of the foils used. The electrode structures were stable; they survived the Scotch tape peeling test and the biofunctionalization process. The electrode edges of the patterns prepared by the two different approaches were different: during direct patterning, the metal etched along the grain boundaries resulted in an increased edge roughness, whereas the structures made by the lift-off process were much sharper. The biochips made with both patterning methods were successfully employed in DNA detection. The capture DNA was successfully immobilized on the functionalized PEN surface between the electrode gaps by spotting through a PDMS mask. The biotin-labeled target DNA was captured from solution, followed by a silver enhancement procedure that led to the formation of a conductive bridge between the electrodes in the gaps. The resistance drop between the electrodes was detected during the electrical characterization. Electrical measurements also showed that the two electrode-patterning methodologies had no influence on the sensing performance of the electrodes. Images of the biochips recorded after the detection process was completed showed that strong silver enhancement occurred only in the gaps in which there was no mismatch between the immobilized capture DNA and target DNA.

The same functionalization protocols established for silicon and glass surfaces were also used in the case of biochips made on PEN. This resulted in comparable sensitivities to those of the classical microarray surfaces (500 fM). Further experiments will verify the sensitivity of these new platforms for the analysis of biomolecules. Besides the future possibility of biochip manufacturing in roll-to-roll processes, another advantage of using PEN foils is that no surface-activation steps, such as plasma treatment or wet etching, are required before silanization. Furthermore, optical and electrical detection principles can be combined into a single analysis platform. Future work will focus on the integration of polymeric chips into microfluidic devices for the total automation of the detection of biomolecules. This will help to improve the specificity as well as the sensitivity of the system by thermal management and active hybridization.

F **DOI:** 10.1021/la8037457 *Langmuir* **XXXX,** *XXX(XX),* 000–000

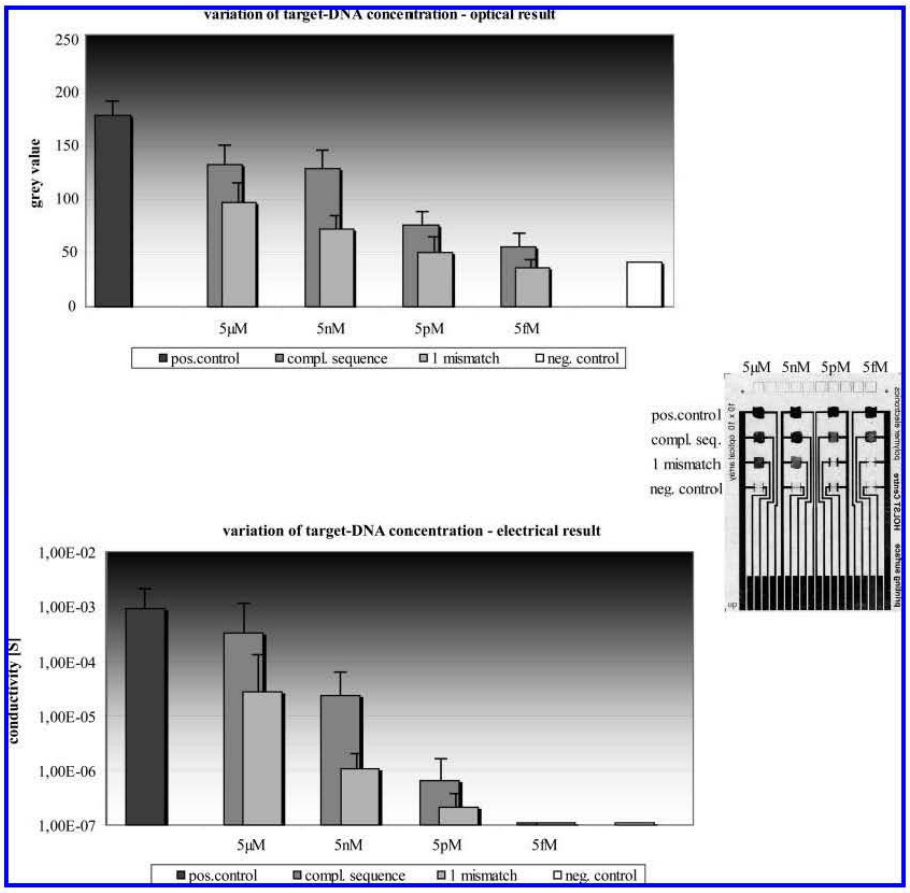

Figure 6. Dynamic range and differentiation of a single mismatch on PEN foils using an optical as well as an electrical readout.

Acknowledgment. The research work was performed as a joined development project in the framework of the Holst Centre-TNO (The Netherlands) in collaboration with the Institute for Physical Chemistry (University Jena) and the Institute of Photonic Technology (IPHT) located in Jena, Germany. We gratefully acknowledge the contributions of the Holst Centre partners Philips, ASML, Polymer Vision, and Singulus Mastering to the work described in this article. Funding of research project "Jenaer Biochip Initiative" (JBCI) within the framework "Unternehmen Region – Inno Profile" from the Federal Ministry of Education and Research, Germany (BMBF) is gratefully acknowledged. Nanoprobes is acknowledged for providing the EnzMet kit for the enzymatic silver deposition.

2.4 DNA detection using a triple readout optical/AFM/MALDI planar microwell plastic chip

Alfredo J. Ibanez[#], Thomas Schüler[#], Robert Möller, Wolfgang Fritzsche, Hans-Peter Saluz, and Ales Svatos

Anal. Chem. (**2008**) 80(15): 5892-8

Anal. Chem. **XXXX**, *xxx*, 000–000

DNA Detection Using a Triple Readout Optical/ AFM/MALDI Planar Microwell Plastic Chip

Alfredo J. Ibáñez,[†,‡] Thomas Schüler,[§] Robert Möller,[§] Wolfgang Fritzsche,[∥] Hans-Peter Saluz,[⊥] and Aleš Svatoš*,[†]

Mass Spectrometry Research Group, Max Planck Institute for Chemical Ecology, Hans-Knoell-Strasse 8, 07745, Jena, Germany, Jenaer Biochip Initiative, Institute for Physical Chemistry, Friedrich Schiller University, Helmholtzweg 4, 07743 Jena, Germany, Institute of Photonic Technology, Albert-Einstein-Strasse 9, 07745, Jena, Germany, and Leibniz Institute for Natural Product Research and Infection Biology, Hans Knöll Institute, Beutenbergstrasse 11a, 07745, Jena, Germany

A ready-to-spot disposable DNA chip for specific and sensitive detection of DNA was developed. Plastic copolymeric substrate chemistry was optimized to selectively couple the target DNA with the active chip surface. At the same time, the developed substrate limits the unspecific adsorption of probe DNA molecules or additional polar contaminants in the test samples to the chip surface. The combination of glycidyl and *n*-butyl methacrylates was found to best fit the requirements of the assay. The fabricated DNA microarrays have mechanical properties similar to those of the glass or silicon substrates and, at the same time, provide chemically reactive surfaces that do not require lengthy chemical modification. An additional advantage of the plastic microchip is its compatibility with different analytical readout techniques, such as mass spectrometry (MALDI-TOF/MS), optical detection (fluorescence and enzyme-induced metal deposition), and imaging techniques (atomic force microscopy). These multiple readout techniques have given us the ability to compare the sensitivity, selectivity, and robustness of current state-of-the-art bioanalytical methods on the same platform exemplified by successful DNA-based detection of human cytomegalovirus. The obtained sensitivity for enzymatically enhanced silver deposition (10^{-15} M) surpasses that of conventional fluorescence readouts. In addition, the assay's dynamic range (10^{-6}–10^{-15} M), reproducibility, and reliability of the DNA probe detection speaks for the silver deposition method. At compromised sensitivity (10^{-9} M), the length of the DNA probes could be checked and, alternatively, DNA single point polymorphisms could be analyzed.

The use of microarray-based technology is growing rapidly and has had considerable impact on genomic and proteomic research.[1,2] Crucial factors in microarray technology are the surface chemistry of the substrate enabling the defined immobilization of the capture molecules[3,4] and the sensitivity/selectivity of the readout associated with the instrument.[5]

Previously, glass, silicon, and quartz have been the primary DNA microarray substrates due to their low background signals during fluorescence readout.[6–8] Nevertheless, the chemical groups on the surface of the glass, silicon, and quartz solid structures are not suitable for directly immobilizing biomolecules; hence, recent chemical modification protocols as well as thin-layer coatings have been applied to the surface of glass, silicon, and quartz to bind DNA, RNA, proteins, etc. In addition, new platforms are constantly being developed to improve the ability of molecules to bind to the surface.[9]

Furthermore, the progress in the field of DNA microarray can be described in terms of (a) throughput and (b) sensitivity. The first category refers to the huge leaps that have been made in the fabrication process concerning spot densities on silicon substrates, either in situ[10] or ex situ.[11,12] Nevertheless, as mentioned above, scientists are still interested in exploring flexible and cost-effective substrate materials with which to fabricate high-throughput and reproducible DNA microarrays;[3,13] the ideal substrate is one whose material provides inherent coupling functionality.

Recently introduced materials and technologies have increased the sensitivity and reproducibility of DNA detection. New labeling methods based on enzymatic silver deposition (i.e., enzyme metallography) can overcome the deficiencies of fluorescence labels, in particular their short lifetimes.[9] To diagnose genetic

* To whom correspondence should be addressed. E-mail: svatos@ice.mpg.de. Fax: +49-3641-571701.
† Max Planck Institute for Chemical Ecology.
‡ Present address: Scienion AG, Otto-Hahn Str. 15, 44227, Dortmund, Germany.
§ Friedrich Schiller University.
∥ Institute of Photonic Technology.
⊥ Hans Knöll Institute.

(1) Brown, P. O.; Botstein, D. *Nat. Genet.* **1999**, *21*, 33–37.
(2) Pandey, A.; Mann, M. *Nature* **2000**, *405*, 837–846.
(3) Zhou, X.; Wu, L.; Zhou, J. *Langmuir* **2004**, *20*, 8877–8885.
(4) Wong, A.; Krull, U. *Anal. Bioanal. Chem.* **2005**, *383*, 187–200.
(5) Finnskog, D.; Ressine, A.; Laurell, T.; Marko-Varga, G. *J. Proteome Res.* **2004**, *3*, 988–994.
(6) Schena, M. *Microarray Analysis*; Wiley-Liss: Hoboken, NJ, 2003.
(7) Sauer, S.; Lange, B. M. H.; Gobom, J.; Nyarsik, L.; Seitz, H.; Lehrach, H. *Nat. Rev. Genet.* **2005**, *6* (6), 465–476.
(8) Wilgenbus, K. K.; Lichter, P. *J. Mol. Med.* **1999**, *77*, 761–768.
(9) Möller, R.; Powell, R. D.; Hainfeld, J. F.; Fritzsche, W. *Nano Lett.* **2005**, *5*, 1475–1482.
(10) Fodor, S. P. A. *Science* **1999**, *277*, 393–395.
(11) Schena, M.; Shalon, D.; Davis, R. W.; Brown, P. O. *Science* **1995**, *270*, 467–470.
(12) Okamoto, T.; Suzuki, T.; Yamamoto., N. *Nature* **2000**, *18*, 438–441.
(13) Wang, J. *Nucleic Acids Res.* **2000**, *28*, 3011–3016.

10.1021/ac800426v CCC: $40.75 © XXXX American Chemical Society
Published on Web 06/21/2008

diseases and detect infectious agents, labels such as metal nanoparticles,[14–17] enzymes,[9,18–20] and quantum dots[21,22] are usually preferred, due to their rapid and simple synthesis, reproducibility, and stability. In addition, the sensitivity and robustness of DNA chips have also increased due to the use of different readout detectors, for example, electrochemical approaches,[16,17,20] light-scattering,[15,23] surface plasmon resonance,[24] atomic force microscopy,[25] and label-free methods (e.g., MALDI-MS).[26–29]

The human herpes virus 5 or cytomegalovirus (CMV) has the largest genome (~235 kb) of the human herpes virus family, which includes herpes simplex (1 and 2), Epstein–Barr, and varicella-zoster virus.[30,31] Although CMV is not highly contagious, it is the most common congenital infection (80% of the world population is infected)[32] and is particularly hazardous in immunocompromised individuals[31,32] and pregnant women (e.g., 10% of infected newborns with CMV exhibit permanent mental retardation and auditory damage).[32,33]

Thanks to developments in the field of miniaturization in recent decades, biosensors, chips, and in particular microarrays have shown great capability to analyze viral DNA.[7,8,13] In the case of CMV, microarray technology is starting to replace traditional methods such as ELISA and latex agglutination, because microarrays allow multiplexed, parallel analysis. DNA microarrays can monitor the viral load of CMV-infected patients using only viral cultures from urine, throat swabs, or tissue samples.[32–36]

(14) Mirkin, C. A.; Letsinger, R. L.; Mucic, R. C.; Storhoff, J. J. *Nature* **1996**, *382*, 607–609.
(15) Xu, X.; Georganopoulou, D. G.; Hill, H. D.; Mirkin, C. A. *Anal. Chem.* **2007**, *79*, 6650–6654.
(16) Wang, J.; Xu, D.; Kawde, A.-N.; Polsky, R. *Anal. Chem.* **2001**, *73*, 5576–5581.
(17) Ambrosi, A.; Castañeda, M. T.; Killard, A. J.; Smyth, M. R.; Alegret, S.; Merkoci, A. *Anal. Chem.* **2007**, *79*, 5232–5240.
(18) Fritzsche, W.; Taton, T. A. *Nanotechnology* **2003**, *14*, R63–R73.
(19) Willner, I.; Baron, R.; Willner, B. *Adv. Mater.* **2006**, *18*, 1109–1120.
(20) Wang, J.; Kawde, A.-N.; Jan, M. R. *Biosens Bioelectron.* **2004**, *20*, 995–1000.
(21) Zhang, C. Y.; Yeh, H. C.; Kuroki, M. T.; Wang., T. H. *Nat. Mater.* **2005**, *4*, 826–831.
(22) Wang, J. *Small* **2005**, *1*, 1036–1043.
(23) Yguerabide, J.; Yguerabide, E. E. *J. Cell. Biochem. Suppl.* **2001**, *37*, 71–81.
(24) Kukanskis, K.; Elkind, J.; Melendez, J.; Murphy, T.; Miller, G.; Garner, H. *Anal. Biochem.* **1999**, *274*, 7–17.
(25) Csaki, A.; Kaplanek, P.; Möller, R.; Fritzsche, W. *Nanotechnology* **2003**, *14*, 1262–1268.
(26) Liu, Y. H.; Bai, J.; Zhu, Y.; Liang, X.; Siemieniak, D.; Venta, P. J.; Lubman, D. M. *Rapid Commun. Mass Spectrom.* **1995**, *9*, 735–743.
(27) Kirpekar, F.; Nordhoff, E.; Larsen, L. K.; Kristiansen, K.; Roepstorff, P.; Hillenkamp, F. *Nucleic Acids Res.* **1998**, *26*, 2554–2559.
(28) Kepper, P.; Reinhardt, R.; Dahl, A.; Lehrach, H.; Sauer, S. *Clin. Chem.* **2006**, *52*, 1303–1310.
(29) Schuerenberg, M.; Laubbert, C.; Eickhoff, H.; Kalkum, M.; Lehrach, H.; Nordhoff, E. *Anal. Chem.* **2000**, *72*, 3436–3442.
(30) Novotny, J.; Rigoutsos, I.; Coleman, D.; Shenk, T. *J. Mol. Biol.* **2001**, *310*, 1151–1166.
(31) Yen-Moore, A.; Straten, M. V.; Carrasco, D.; Evans, T. Y.; Tyring, S. K. *Clin. Dermatol.* **2000**, *18*, 423–432.
(32) Yang, S.; Ghanny, S.; Wang, W.; Galante, A.; Dunn, W.; Liu, F.; Soteropoulos, P.; Zhu, H. *J. Virol. Methods* **2006**, *131*, 202–208.
(33) Pagana, K. D.; Pagana T. J. *Mosby's manual of diagnostic and laboratory tests* ; Mosby: St. Louis, MO, 1992; pp 401–402.
(34) Korimbocus, J.; Scaramozzino, N.; Lacroix, B.; Crance, J. M.; Garin, D.; Vernet, G. *J. Clin. Microbiol.* **2005**, *43*, 3779–3787.
(35) Chambers, J.; Angulo, A.; Amaratunga, D.; Guo, H.; Jiang, Y.; Wan, J. S.; Bittner, A.; Frueh, K.; Jackson, M. R.; Peterson, P. A.; Erlander, M. G.; Ghazal, P. *J. Virol.* **1999**, *73*, 5757–5766.

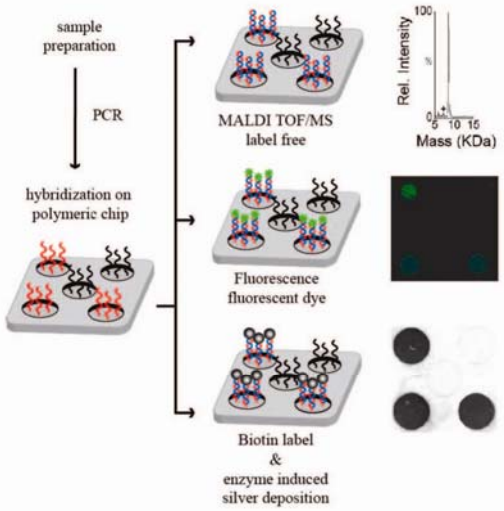

Figure 1. Schematic workflow of the multiple readouts compatible with the copolymeric planar DNA microarray chip (DNA chip). The multiple readout methods shown here are (a) MALDI-TOF/MS, (b) fluorescence, and (c) enzymatic silver enhancement.

Matrix-assisted laser desorption/ionization time-of-flight mass analyzers (MALDI-TOF/MS) have become effective tool for DNA studies,[34–36] because in contrast to fluorescence, they directly measure a physical property of the DNA (i.e., mass), thus reducing the number of false positive signals. Hence, a microarray system that couples both optical and mass spectrometry readout formats promises to be extremely sensitive and selective. Nevertheless, the use of silicon-, glass-, or quartz-based microarrays is clearly not economically optimal because of the costly material and fabrication techniques involved compared to those required by polymer microstructures that are equal quality in terms of structure resolution and planarity of the surface.[37–39]

In this paper, we describe the development of a low-cost material that can be readily reacted with biomolecules—in this case, ssDNA—to generate high-throughput microarray platforms (Figure 1). As a proof of concept, CMV DNA sequence was used to illustrate the performance of the copolymeric DNA chip. The following work extends our current research on the copolymeric plastic chips (i.e., pMALDI chips) that have so far been used for protein analysis by MALDI-MS.[40]

EXPERIMENTAL SECTION

Chemicals and DNA Sequences. Methyl methacrylate, butyl methacrylate, glycidyl methacrylate, and 2-(methacryloyloxy)ethyldimethyl(3-sulfopropyl)ammonium hydroxide (all containing hydroquinone monomethyl ether as stabilizer), Ultrasensitive Streptavidin–Peroxidase Polymer (S2438), and 3-hydroxypicolinic acid were purchased from Sigma. Benzoin methyl ether and

(36) Fujimuro, M.; Nakaso, K.; Nakashima, K.; Sadanari, H.; Hisanori, I.; Teishikata, Y.; Diane Hayward, S.; Yokosawa, H. *Exp. Mol. Pathol.* **2006**, *80*, 124–131.
(37) Marko-Varga, G.; Ekström, S.; Helldin, G.; Nilsson, J.; Laurell, T. *Electrophoresis* **2001**, *22*, 3978–3983.
(38) Ekström, S.; Nilsson, J.; Helldin, G.; Laurell, T.; Marko-Varga, G. *Electrophoresis* **2001**, *22*, 3984–3992.
(39) Berhane, B. T.; Limbach, P. A. *Anal. Chem.* **2003**, *75*, 1997–2003.
(40) Muck, A.; Svatoš, A. *Talanta* **2007**, *74*, 333–341.

Table 1. DNA Sequences of Probes and Targets Used in This Work

function	abbrev	length	sequence 5′−3′	modification
probe	0mis	30	TTT TTT CAG CAT GTG CTC CTT GAT TCT ATG	5′-aminohexyl
	NC	35	**ACT GAC TGA CTG ACT GAC TGA CTG GGC GAC CT**	5′-aminohexyl
	3mis	30	TTT TTT CAG CAT **TAT** CTC CTT GAT TCT ATG	5′-aminohexyl
	1mis	30	TTT TTT CAG CAT GGG CTC CTT GAT TCT ATG	5′-aminohexyl
probe control	B-0mis	30	TTT TTT CAG CAT GTG CTC CTT GAT TCT ATG	5′-aminohexyl, 3′-biotin
	F-0mis	30	TTT TTT CAG CAT GTG CTC CTT GAT TCT ATG	5′-aminohexyl, 3′-FITC
	B-NC	35	**ACT GAC TGA CTG ACT GAC TGA CTG GGC GAC CT**	5′-aminohexyl, 3′-biotin
	F-NC	35	**ACT GAC TGA CTG ACT GAC TGA CTG GGC GAC CT**	5′-aminohexyl, 3′-FITC
	B-3mis	30	TTT TTT CAG CAT **TAT** CTC CTT GAT TCT ATG	5′-aminohexyl, 3′-biotin
	B-1mis	30	TTT TTT CAG CAT GGG CTC CTT GAT TCT ATG	5′-aminohexyl, 3′-biotin
target	30mer	30	CAT AGA ATC AAG GAG CAC ATG CTG AAA AAA	
	B-30mer	30	CAT AGA ATC AAG GAG CAC ATG CTG AAA AAA	5′-biotin
	F-30mer	30	CAT AGA ATC AAG GAG CAC ATG CTG AAA AAA	5′-FITC
	20mer	20	CAT AGA ATC AAG GAG CAC AT	
	B-20mer	20	CAT AGA ATC AAG GAG CAC AT	5′-biotin
	40mer	40	GGG GGG GGG GCA TAG AAT CAA GGA GCA CAT GCT GAA AAA A	
	B-40mer	40	GGG GGG GGG GCA TAG AAT CAA GGA GCA CAT GCT GAA AAA A	5′-biotin

activated alumina (Grade CG20) were obtained from Polysciences (Warrington, PA). The horseradish peroxidase silver enhancement kit, EnzMet reagent kit, was purchased from Nanoprobes Inc. (Yaphank, NY). Oligonucleotides were obtained from MWG-Biotech Inc. (High Point, NC) and had the sequences reported in Table 1. Randomly sized human DNA samples extracted from female placenta cell nuclei and *Escherichia coli* protein cell lysates were from our laboratory stock.

Sample Preparation. All stock solutions (100 μM) were prepared in double-deionized MilliQ water (ddH_2O; Millipore, Bedford, MA). The phosphate buffer solution (PBS) consisted of 0.01 M potassium monobasic phosphate, 0.137 M NaCl, and 0.003 M KCl (adjusted to pH 7.4 with sodium hydroxide). A sodium chloride/sodium citrate (SSC) buffer solution was used for the hybridization and washing steps and consisted of 0.3 M sodium citrate buffer, 3 M sodium chloride, adjusted to pH 7 with HCl.

Apparatus. A MALDI Micro MX mass spectrometer (Waters/Micromass, Manchester, UK) was used in linear (positive and negative ion) mode for the DNA analysis. The instrument operated with 5 kV set on the sample plate, −12 kV on the extraction grid; pulse and detector voltage were 1.95 and 2.35 kV, respectively. A nitrogen laser (337 nm, 5 Hz, 50 μJ/pulse) was used for ionization. MassLynx v4.0 software (Waters) served for data acquisition, and each spectrum was composed of 10 laser pulses. The pMALDI chip was fixed to a standard metallic plate with adhesive tape and introduced at the source. A mixture containing 20-, 30-, and 40-base-long ssDNA fragments was used to calibrate the mass spectrometer (using the m/z values given by the quality control department of Eurofins MWG for these ssDNAs). The signal from the 30-base-long ssDNA served as an external lock-mass reference.

^{1}H NMR spectra were recorded with Bruker AVANCE DRX 500 nuclear magnetic resonance spectrometer (Bruker, Billerica, MA) at 500.13 MHz. All spectra were measured in $CDCl_3$. The proton chemical shifts in the NMR spectrum are given in δ values relative to tetramethylsilane $\delta = 0.0$. Typically, 256 scans were accumulated per spectrum.

Chip Fabrication. The rapid prototyping of the copolymeric DNA microarrays is similar to that used for copolymeric plastic MALDI (i.e., pMALDI) chips;[40−45] the dimensions of the pMALDI chip and the well are 42 × 56 × 0.2 mm, and 2.5 (diameter) × 0.03 mm (depth), respectively. The copolymerized plastic chips were fabricated using a modified atmospheric molding procedure in which three-dimensional sample zone arrays were fabricated on a silicon substrate and used to template polymeric chips. The masters were prepared from 100-mm-diameter positive doped, <100> orientation, silicon wafers using soft photolithography and wet chemical etching. The complete fabrication procedure has been described elsewhere.[41] The atmospheric molding in situ polymerization technique yields a negative copy of the silicon substrate in a thin sandwich mold. A thin aluminum spacer and a poly(tetrafluoroethylene) seal tape was used between the silicon substrate and the glass cover plate to prepare ~0.2-mm-thick chips. The decreased thickness of the chip dramatically reduced previously observed charging effects.[44] The molding and demolding process of prepared copolymeric plastic DNA chips (Figure 2) was straightforward, as was the process previously reported for other plastic MALDI chips.[41−45]

Conjugation of the DNA Probes to the Epoxide-pMALDI Chip. Prior to immobilizing the ssDNA oligonucleotide to the surface, the copolymer was cleaned, rinsed with ddH_2O, and dried under a stream of nitrogen. A piece of the copolymeric DNA microarray was cut with scissors and dissolved in $CDCl_3$. The presence of the characteristic proton signals for the epoxide group (2.38, 2.63, and 3.13 ppm) and their relative intensity when compared to the $-OCH_2-$ signal of the backbone side chain guarantee the quality of the chip even after long-term storage at room temperature in a high-humidity environment.

The probe immobilization is based on a nucleophilic ring-opening reaction (Figure 2). The ssDNA probes used for our studies were 30-base ssDNA with different complementarities, full match, 1-base mismatch, 3-bases mismatch, and a longer non-complementary ssDNA probe (0mis, 1mis, 3mis, and NC, respectively) to the target CMV DNA sequences (Table 1). Moreover, labeled control probes were used to confirm the degree of labeling of the copolymeric DNA chip surface (Table 1).

(41) Muck, A.; Nešněrová, P.; Pichová, I.; Svatoš, A. *Electrophoresis* **2005**, *26*, 2835–2842.
(42) Muck, A.; Ibáñez, A. J.; Stauber, E. J.; Mansuorova, M.; Svatoš, A. *Electrophoresis* **2006**, *27*, 4952–4959.
(43) Ibáñez, A. J.; Muck, A.; Halim, V. A.; Svatoš, A. *J. Proteome Res.* **2007**, *6*, 1183–1189.
(44) Ibáñez, A. J.; Muck, A.; Svatoš, A. *J. Mass Spectrom.* **2007**, *42*, 634–640.
(45) Ibáñez, A. J.; Muck, A.; Svatoš, A. *J. Proteome Res.* **2007**, *6*, 3842–3848.

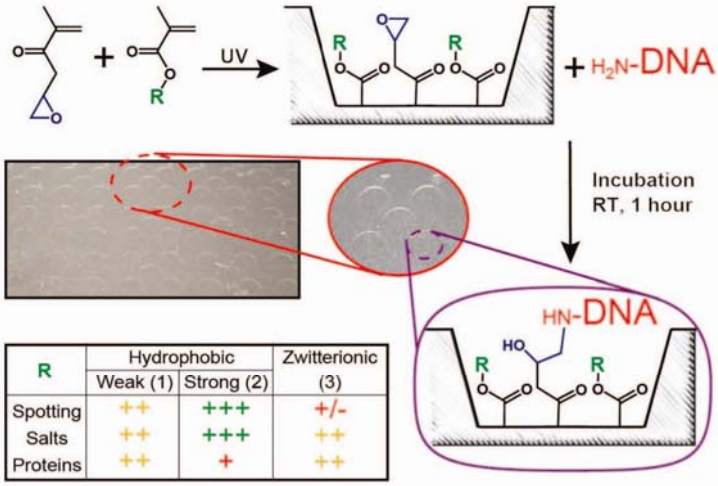

R	Hydrophobic		Zwitterionic
	Weak (1)	Strong (2)	(3)
Spotting	++	+++	+/-
Salts	++	+++	++
Proteins	++	+	++

Figure 2. Schematic representation of the copolymerization reaction formed reactive surface and the subsequent conjugation of an amino-linked DNA probe to the chip surface. The inset table shows the benefits (i.e., spot quality and tolerance to contaminants such as salts and proteins) associated with the copolymerization of different backbone monomers with glycidyl methacrylate. Quality scale: excellent (+++), very good (++), good (+), unsatisfactory (±). The R in the table represents (1) methyl, (2) butyl, and (3) 2-ethyl-2,2-dimethyl-(3-sulfopropyl)ammonium hydroxide, respectively.

The probe immobilization involved the spotting, in each microwell, of 2.0 μL of 10 μM single-stranded label-free or labeled-probe DNA (Table 1) in 1× Arrayit spotting buffer (Telechem, Sunnyvale, CA). The DNA chip was incubated for either 1 h at 50 °C or 8 h at 37 °C; subsequently, the remaining probe-spotting solution was flushed away with ddH_2O and dried under nitrogen. The remaining active surface was blocked with 50 mM ethanolamine in 0.1 M Tris and 0.1% SDS, pH 9, for 15 min. Finally, the chips were flushed with ddH_2O and dried under nitrogen.

DNA Probe Array Hybridization. For the optical and AFM detection, the biotin-modified ssDNA targets of different sizes (i.e., B-20mer, B-30mer, and B-40mer, Table 1) were used. MALDI-TOF/MS measurements were done with label-free ssDNA targets of sizes equivalent to those employed for AFM and optical detection (i.e., 20mer, 30mer, and 40mer, Table 1). Regardless of the detection method used, the ssDNA target (labeled or nonlabeled) was dissolved in 1 × SSC + 0.1% SDS and incubated with the DNA chip at least for 1 h in a humidity chamber at 37 °C. This was followed by two washing steps, first in 2 × SSC for 5 min and then in 0.2 × SSC for 5 min, and a drying step under a stream of nitrogen.

Gold Nanoparticle Deposition for AFM Analysis. For the streptavidin gold nanoparticle (5-nm gold nanoparticles; British Biocell, Cardiff, UK) labeling, 100 μL of a 1:100 dilution of the original nanoparticle solution was dissolved in PBS with 0.1% BSA. Each chip was incubated with this solution for 1 h at 37 °C in a humidity chamber. Afterward, the chips were washed six times for 5 min each in PBS with 0.05% Tween 20 and then briefly rinsed with distilled water to remove any excess of chloride ions.

Silver Deposition for Optical/AFM Analysis. Based on the streptavidin−peroxidase polymer, the substrates were incubated with a 1:1000 dilution of the original solution in PBS with 0.05% Tween 20. A 100 μL portion of this solution was applied and incubated at 20 °C for 1 h on the chip. Each pMALDI chip was then washed six times for 5 min in PBS containing 0.05% Tween 20 and then for 5 min in ddH_2O to remove any excess of unbound enzyme complexes and chloride ions that could interfere with the silver deposition reaction. The enzyme-induced silver deposition was performed using the EnzMet reagent kit. The chips were incubated with the EnzMet reagent kit for 1, 2, 3, or 5 min. Longer reaction times were used to test whether they improved the strength of the signal. However, incubation times longer than 5 min led to an increase of nonspecific signals (i.e., background) and were therefore not used. To avoid the inactivation of the enzyme, the EnzMet reagents were applied immediately after the washing step. The reaction was stopped by rinsing with ddH_2O to wash away the kit solution. After the enzyme-induced silver deposition is stopped, the enzyme becomes inactive because it is trapped by the deposited silver.

MALDI-TOF/MS for Label-Free ssDNA Analysis. The pMALDI chip was washed six times for 5 min each in PBS containing 0.05% Tween 20 and then briefly in ddH_2O to remove any excess of buffer and surfactants. Although this treatment was not necessary, it was done to maintain a similar sample handling protocol for the different analytical techniques. Subsequently, the double-stranded DNA was denatured by adding 2 μL of ddH_2O to each microwell and increasing the temperature to 98 °C for 10 min. To prevent water from evaporating, the whole microarray was placed inside a humidity chamber. To avoid the reassociation of single-stranded DNA, 1.2 μL of 3-hydroxypicolinic acid (25 mg/mL), dissolved in water/acetonitrile (1:1), was immediately added by aspirating and dispensing the solution to each well, and the analyte/matrix mixture was left to crystallize at room temperature.

Safety considerations. *Alkyl methacrylates and benzoin methyl ether are toxic substances. Other used chemicals are irritants. Accidental inhalation, ingestion, or skin contact with these chemicals should be avoided. UV light may cause damage to skin and eyes; protective goggles and gloves should be used. The polymerization should be carried out in a ventilated fume hood.*

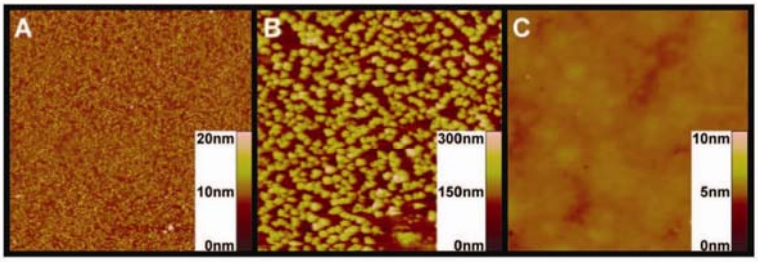

Figure 3. AFM images of the positive control measurements (10 μm $\times$ 10 μm) using (A) control probe (B-0mis) labeled with gold nanoparticles, (B) biotin-labeled control probe (B-0mis) and subsequent peroxidase-enhanced silver deposition after 5 min, and (C) peroxidase-enhanced silver deposition after 5 min on a BMA-based nonreactive DNA chip. DNA probe concentration was 10 μM. The color-coded scales of surface roughness are given in the right-hand corners of the individual images.

RESULTS AND DISCUSSION

The microarray for detecting human CMV DNA presented in this paper relies on one common ready-to-spot inexpensive substrate in combination with parallel MALDI-MS, transluminiscence/AFM, and fluorescence detection (Figure 1). To our knowledge, the present protocol represents the first example of how different state-of-the-art DNA readouts can be integrated and combined with a low-cost and ready-to-spot copolymeric microarray substrate.

Material Optimization for Copolymeric DNA Microarray Chips. The material chemistry of the plastic DNA microarray chip was extensively studied. As the epoxide group was previously found to be the most suitable linking unit for immobilizing DNA onto glass and silicon substrates,[9] the chips were prepared by copolymerizing (Figure 2) commercially available glycidyl methacrylate (i.e., epoxide-containing monomer) with a backbone monomer such as methyl methacrylate (backbone 1 in Figure 2; weakly hydrophobic), butyl methacrylate (backbone 2 in Figure 2; strongly hydrophobic), or methyl methacrylate−[2-(methacryloyloxy)ethyl]dimethyl-(3-sulfopropyl)ammonium hydroxide (backbone 3 in Figure 2; zwitterionic).

Because of the different backbone monomers employed in the fabrication of the DNA chips, different surface properties were obtained. To test the relationship between copolymer composition and the MALDI-MS, AFM, and optical transluminescence signals, the quality of the spot and its robustness, i.e., tolerance of nonspecific adsorption of common interferences present in biological studies such as salts, random DNA sequences, and proteins, were measured (inset table in Figure 2).

To evaluate the quality of the spot (i.e., wettability), the surface coverage was characterized using optical and scanning probe microscopy, and the signal intensity of the DNA ions from recorded mass spectra (MALDI-MS signals depends very much on this parameter).

Similarly, the robustness of the DNA detection was evaluated using a common sample hybridization protocol to detect CMV DNA target sequences that have dissolved in solutions of increasing complexity, such as spotting buffer (containing only salts as interference), randomly sized human placenta DNA extracts (containing salts and noncDNA as interference), and *E. coli* cell lysates (containing salts, noncDNA, lipids, and proteins as interference).

Based on MALDI-MS measurements and bright-field (optical) microscopy (i.e., which measures the light transmitted after the DNA target molecules are silver-labeled on the surface), glycidyl methacrylate/butyl methacrylate (EBMA, i.e., strongly hydrophobic, inset table in Figure 2) was selected for further use. To further optimize EBMA substrates for MALDI-MS, optical and scanning probe microscopy measurements, it was necessary to ensure a homogeneous distribution of the epoxide groups on the surface of the plastic substrates. Therefore, monomers (glycidyl methacrylate/butyl methacrylate) were copolymerized using different molar ratios: 1:13.3, 1:26.6, and 1:39.9. Furthermore, in addition to each monomer ratio, different concentrations of two different 30-base pairs capture CMV−DNA probes, a ssDNA probe, and ready labeled-probe (0mis and B-0mis, respectively), and a 35-base pair noncomplementary sequence probe (NC) were dispensed manually into each well (1.5 μL/well).

Using bright-field and scanning probe microscopy readouts (i.e., transluminescence and atomic force microscopy, respectively), we concluded that a 10 μM DNA probe immobilized on a 1:13.3 ratio pMALDI chip provided the most efficient and homogeneous distribution of active recognition sites on the polymer surface.

These results are partially illustrated in Figure 3. After the chip surface was treated with biotin-labeled probe (B-0mis, 10 μM), the probe was labeled with gold nanoparticles (Figure 3A) or silver deposition (5 min) by peroxidase-based enhancement (Figure 3B). Surface images obtained at random positions demonstrated that the sites of reaction were equally distributed across the surface. Moreover, the measurement of different heights of the formed structures in Figure 3 shows that enzymatic labeling (Figure 3B) gives bigger particles (~300 nm) than does labeling using gold nanoparticles (5 nm, Figure 3A). Figure 3C shows the control for the silver deposition labeling method, according to which a biotin-labeled probe (B-0mis) was applied to a pure butyl methacrylate surface (AFM signal not higher than 10 nm). Therefore, owing to its better signal-to-noise ratio, the horseradish peroxidase-based labeling system was preferred over the gold nanoparticle labeling system for further experiments.

Sensitivity Comparison among State-of-the-Art Techniques. A comparison based on the sensitivity between MALDI-TOF/MS and optical measurements (using FITC-labeled and enzymatically labeled targets) is shown in Figure 4A. The dynamic range of the silver enhancement kit depends on the incubation time of the peroxidase enzyme (Figure 4A shows the signal for 5-, 3-, and 1-min incubation). Moreover, while FITC labels tended to photobleach, only negligible signal decay during measurements

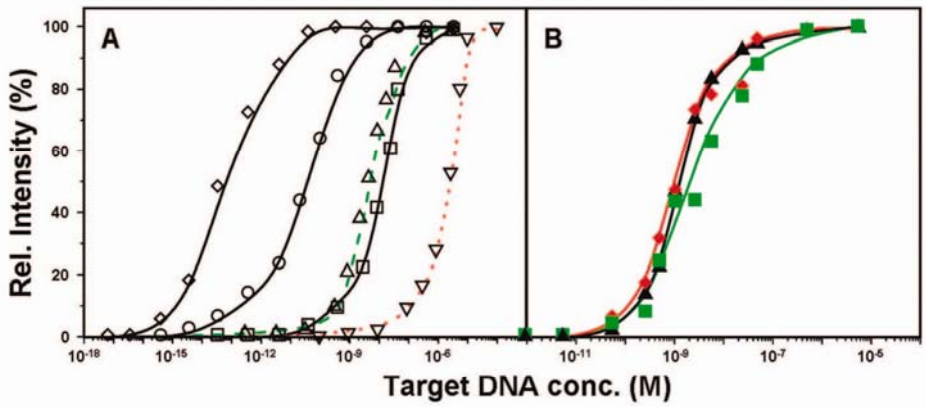

Figure 4. Comparison of calibration plots using horseradish peroxidase-based (HRP) DNA detection (i.e., transluminiscence) at different incubation times, FITC-based (i.e., fluorescence), and MALDI-TOF/MS DNA detection. Five-minute HRP incubation (◆), 3-min HRP incubation (●), 1-min HRP incubation (■), FITC (▲), and MALDI-TOF/MS (▼). (B) Reproducibility of the HRP DNA detection, using a 0mis probe and B-30mer target, in different environments: nonbackground (▲), human placenta DNA purified extract (◆), and *E. coli* cell lysates (■) using 2-min incubation time.

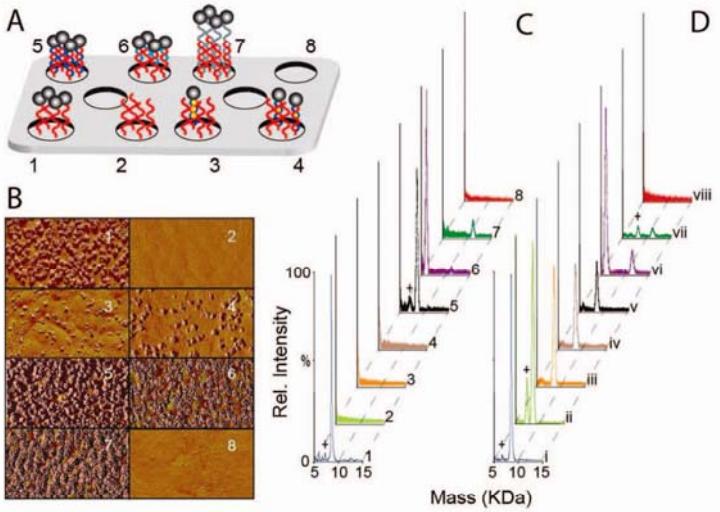

Figure 5. Reliability and validity of CMV DNA detection with two complementary readout techniques (AFM and MALDI-TOF/MS, (B) and (C), respectively). Wells 2−5 compare the hybridization efficiency of a 30-base oligomer target (30mer) to different ssDNA probe sequences: NC, and 30-base probes with 3-mismatches (3mis), 1-mismatch (1mis), and complementary sequence (0mis). Wells 6 and 7 compare the hybridization efficiency of a 30-base oligomer probe (0mis) to target ssDNA samples of different lengths with perfect complementarity to the probe: 20mers and 40mers, respectively. Well 1 contains a positive control (B-0mis for AFM and 30mer for MALDI-MS); well 8 is a blank. Roman numerals (D) represent MALDI-TOF/MS spectra of the nonbound target DNA from the respective immobilization step for the Arabic-numbered well; "+" represents $[M + H - 5A]^+$ fragment ions of the DNA.

was observed for the enzymatically deposited silver layers. Hence, the limit of detection is lower and the overall dynamic range given by horseradish peroxidase silver enhancement kit on the copolymer DNA chip is much greater (5 fM−5 μM) than that previously reported for the optical detection of CMV−DNA using either enzymatically labeled[25] and FITC-labeled targets on glass slides[46] or prestructured MALDI-MS sample supports for enhancing ssDNA detection.[29]

Robustness of the CMV Detection Based on a Plastic DNA Chip. The robustness of the optical microscopy measurements using enzymatically labeled target CMV ssDNA on the copolymerized (EBMA) is presented in Figure 4B. After 2 min of silver enhancement, consecutive calibration plots were made to detect CMV DNA on the plastic DNA chip in a spotting solution ($n = 5$, RSD = 16.7) in the presence of randomly sized human placenta DNA samples ($n = 3$, RSD = 7.1) and *E. coli* cell lysates ($n = 3$, RSD = 23.9).

Achieving Reliability in DNA Identification Using Multiple Readout Formats. Figure 5 compares the reliability and validity of the methods. For this experiment, the grid (Figure 5A) was divided in two sets: (a) Spots 3−5 contain different 30-base ssDNA probes, which were hybridized with a 30-base ssDNA target (30mer, Table 1). The nomenclature used to describe the probe in each well depends on the number of mismatches in their oligonucleotide sequence: 3 mismatches (spot 3), 1 mismatch (spot 4), or completely complementary (spot 5). The oligonucle-

otide sequence for these probes can be found in Table 1 (3-mis, 1-mis, and 0-mis, respectively). (b) Spots 6−7 contain the same completely complementary probe sequence used in spot 5 (0-mis, Table 1), but instead of hybridizing to the 30mer CMV ssDNA target sequence, as in the case of spot 5, the spots were used to study the recognition of two target ssDNA molecules that possess a complementary sequence but different lengths, i.e., a 20-base-long ssDNA target (spot 6) and 40-base-long ssDNA target (spot 7). The oligonucleotide sequence for these targets can be found in Table 1 (referred to as 20mer and 40mer, respectively).

The efficiency of the MALDI-MS, transluminescence and AFM measurements was evaluated using as references the signal from spot 5, and the positive (B-0mis in Table 1 for AFM and 30mer in Table 1 for MALDI), negative (noncomplementary probe, NC in Table 1) and blank controls, which were located in spots 1, 2, and 8, respectively.

The transluminescence and AFM readouts were able to differentiate the hybridization events in case a, providing qualitative information for the hybridization of the target to the complementary DNA (0mis, TTTTTTCAGCATGTGCTCCTTGATTCTATG), 1-mismatch (1-mis, TTTTTTCAGCATGGGCTCCTTGATTCTATG) and 3-mismatch (3-mis, TTTTTTCAGCAT**TAT**CTCCTTGATTCTATG) sequences. However, transluminescence and AFM measurements failed to differentiate the binding events in case b, since 20mer (**CATAGAATCAAGGAGCACAT**) and 40mer (GGGGGGGGGG-**CATAGAATCAAGGAGCACATGCTGAAAAAA**) target ssDNA share the same recognition sequence with the 30mer (**CATAGAATCAAGGAGCACATGCTGAAAAAA**) and hence provide similar enzymatic responses (i.e., leading to a high number of possible false positive identifications).

On the other hand, MALDI-TOF/MS instruments operating in linear mode have an accuracy of 0.2% in relation to the mass measurement. Thus, the expected mass errors, ~20 Da for typical m/z 10 000 values used here, are smaller than the addition or subtraction of the smallest nucleoside monophosphate, deoxycytidine monophosphate (289.2 Da). This makes MALDI-TOF/MS a good readout instrument for obtaining information regarding the size of the DNA sequence, which cannot be obtained in terms of matching sequence identity only. Moreover, the sensitivity for DNA MALDI-TOF/MS has been reported to be in the low-femtomole range when hydrophobic substrates are used to preconcentrate the sample DNA in a discrete spot in combination with a decreased amount of matrix.[29]

Therefore, using a readout method such as MALDI-TOF/MS, it was possible to differentiate the lengths of bound DNA (Figure 5C). Additionally, in the case of MALDI-TOF/MS analysis, the nonbound target DNA present after the hybridization step could still be analyzed (Figure 5D). For this analysis, the sample was preconcentrated either in an anion-exchange pMALDI chip (e.g., one containing a quaternary amine functionality on its surface)[42] or on a dialysis membrane and later spotted to hydrophobic (e.g., one containing *n*-butyl group) pMALDI chip[41] and subsequently measured using MALDI-TOF/MS as was the case for Figure 5D.

Unfortunately, although the plastic-based substrates used in this work enhanced the sensitivity of MALDI-MS instruments in comparison to commercial available metallic targets, our MALDI-TOF/MS instrument failed to reach the limit of detection achieved by the enzymatic-labeled transluminiscence assay (Figure 4A). Therefore, in situ DNA amplification (e.g., in situ PCR amplification) prior to MALDI-TOF/MS measurement is required.

(46) Alexandre, I.; Hamels, S.; Dufour, S.; Collet, J.; Zammatteo, N.; De Longueville, F.; Gala, J.-L.; Remacle, J. *Anal. Biochem.* **2001**, *295*, 1-8.

CONCLUSION

A versatile, ready-to-spot, disposable UV-photopolymerized plastic substrate for gold and silver nanoparticle-labeled and label-free ssDNA detection based on optical, scanning probe microscopy and mass spectrometry was developed. Unlike the conventional silicon, glass, or quartz DNA chip substrates previously used, the key advantage of this novel substrate is that the plastic material exhibits an inherent tendency to immobilize DNA, obviating the need for additional activation steps. Active functional epoxide groups are stable for months, allowing the chips to be produced before they are actually spotted with DNA probes. Moreover, the copolymerized DNA chip can be molded in different geometries, and with or without structures on the surface, to fit to different readout instruments; hence, the fabrication protocol could be easily modified to prepare medium- to high-density chips of from 10 000 to 50 000 wells with the desired shape/size patterns and surface properties; in such chips, the activity of the surface could be probed by infrared spectroscopy or by ^{1}H NMR.

Although a standard DNA sample was used to illustrate the capabilities of this novel DNA microarray substrate, the composition of the copolymeric DNA chips can be further tailored to prevent proteins from adhering to the chip (Figure 2 inset table). Eliminating the binding of nonspecific proteins to the chip surfaces will make the study of specific DNA−protein interactions feasible.

Currently, we are developing an in situ PCR amplification using a robotic pipetting device from Scienion AG to increase the analysis through-put and to extend the dynamic linear range of the MALDI-TOF/MS measurements toward lower concentrations. Furthermore, we foresee diverse applications for the fast and reliable detection of human pathogens, single nucleotide polymorphisms, and microRNA detection. Finally, this platform can be applied in areas not currently covered by commercial DNA chips, where the benefits of orthogonal readouts (sensitivity and robustness) are important, such as the study of infectious agents of toxicological or ecological relevance.

ACKNOWLEDGMENT

A.J.I. gratefully acknowledges financial support by the International Max Planck Research School "The Exploration of Ecological Interactions with Molecular and Chemical Techniques". The funding of this project by the Max Planck Society is equally acknowledged. The authors thank Emily Wheeler for editorial assistance, Steffen Harzsch for his support with the LIF measurements, and Jürgen Kroymann for helpful discussions. A.J.I. and T.S. contributed equally to the paper.

Received for review February 29, 2008. Accepted May 23, 2008.

AC800426V

2.5 Chip-based molecular diagnostics using metal nanoparticles

Grit Festag, Thomas Schüler, Andrea Steinbrück, Andrea Csáki, Robert Möller, and Wolfgang Fritzsche

Expert Opinion on Medical Diagnostics (**2008**) 2(7): 813-828

Review

Expert Opinion

Chip-based molecular diagnostics using metal nanoparticles

Grit Festag, T schüler, Andrea Steinbrück, Andrea Csáki, Robert Möller & Wolfgang Fritzsche†
Institute of Photonic Technology, POB 100239, 07702 Jena, Germany

Background: Chip-based bioanalytical methods represent a promising approach for a highly parallel and robust analysis with minimal sample volumes. Key process parameters that can be decisive for certain applications are determined by the detection scheme utilized. *Objective*: This review addresses typical requirements of chip-based detection systems, especially for the emerging field of point-of-care diagnostics that make possible field detection with less-trained personnel, robust assays as well as low instrumentation costs. *Methods*: The use of metal nanoparticles as labels represents a promising approach. They exhibit a high stability in signal and new detection schemes that would allow for robustness and low-cost readout. *Results/conclusion*: First examples of this kind have been established and are in the market, and more are in the development pipeline.

Keywords: biochip, DNA detection, gold nanoparticles, metal nanostructures, microarray, protein analysis, silver enhancement

Expert Opin. Med. Diagn. (2008) 2(7):1-16

1. Introduction

Array-based detection systems enabling the analysis of many different samples at the same time are a key development in biomolecular detection [1]. With the help of so-called DNA chips, hybridization-based expression monitoring, polymorphism detection and genotyping can be realized, as shown, for example, for DNA and protein microarray techniques in nutrition and food research or gene-expression studies in breast cancer, respectively [2,3]. **Figure 1** illustrates typical steps involved in the production of DNA chips. A typical chip-based assay in biomolecular detection probes the presence of target molecules by using capture molecules, which have a known sequence/structure and are complementary to the target. These capture molecules bind the target, and this binding is detected by labels that are either directly attached to the target (e.g., by polymerase chain reaction [PCR] or chemical modification) or added by another binding step. Beside fluorescence as a standard labeling technique, metal nanoparticles have gained more and more interest as alternative labels in clinical and biodiagnostics [4-6]. They both overcome some drawbacks of fluorescence-based methods (low stability owing to photo bleaching, elaborative readout systems) and offer interesting physical properties for new detection schemes such as optical, electrical, electrochemical and gravimetric readout. **Figure 2** shows different labeling strategies for chip-based DNA detection by metal nanostructures as labels. As gold nanoparticles are relatively easy to synthesize and biofunctionalize, they are commonly used for nanoparticle-based DNA detection and have been demonstrated in several DNA chip platforms. Although other metals (e.g., Ag, Pt, Pd) have also been used as labels, this review focuses mainly on gold nanoparticles and their use in labeling and detection of biomolecules on solid supports. The application of biofunctionalized nanoparticles to chip-based biomolecular, especially DNA, detection is described, including array fabrication, nanoparticle functionalization

informa healthcare

10.1517/17530050802218965 © 2008 Informa UK Ltd ISSN 1753-0059

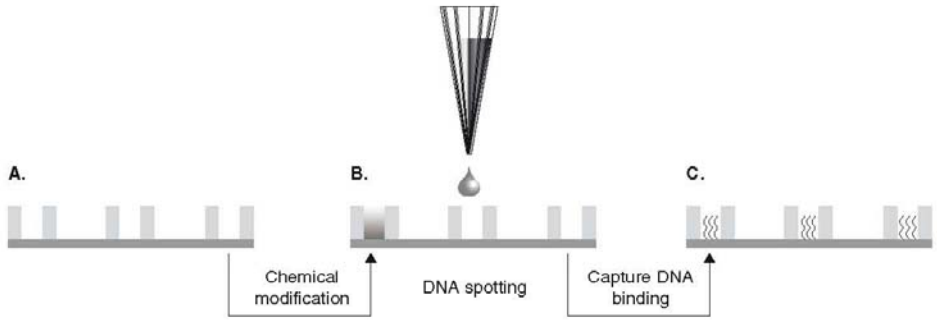

Figure 1. Scheme of DNA chip production. A. The silicon or glass chip surface (here microstructured with electrode pairs) is chemically modified (e.g., silanization) to enable DNA binding. **B.** The solution of capture molecules (oligonucleotides of a known sequence) is applied as droplets into the electrode gaps by a spotting device. **C.** The capture oligonucleotides bind covalently in the electrode gaps.

and numerous detection schemes, with special regard to rapid and cost-efficient point-of-care applications.

2. Molecular diagnostics using metal nanoparticles

2.1 Nanoparticles and biofunctionalization

To stabilize the particle labels as well as to enable the specific biorecognition reactions, the nanoparticles have to be functionalized with biomolecules, which serve as binding partners for the target molecules.

2.1.1 Nanoparticle synthesis

Metal nanoparticles are commonly used as colloids where the tiny particles as the solid dispersed phase are distributed evenly throughout the continuous liquid phase. A large variety of preparative techniques is available and nanoparticles can be produced from several metals (**Figure 3**), such as Au [7-10], Ag [11,12], Cu [13], Pd [14] and Pt [15]. Thereby, metal salts are reduced by different reductives, among which the sodium citrate reduction of gold colloids [16] is the most commonly cited method [17]. In a primary monophasic system, discrete particles are formed as a new phase (nucleation period) and grow subsequently [18]. The synthesized particles are surrounded by a layer of charged ions, which keeps the particles apart and stabilizes the colloid against aggregation. To achieve monodisperse colloids with particles of a particular size, a short period of nucleation should be followed by a period in which the particles continue to grow without forming any new particles [19]. The ratio of metal salt and reducing agent determines the size of the resulting particles: the more reducing agents, the smaller the particles [16]. As the optical properties of the nanostructures also depend strongly on their shape, a variety of shapes such as rods, prisms, cubes and even more complex-shaped nanoparticles have been created beside the spheres. In addition to these pure metal particles, bimetallic nanoparticles have gained increasing attention because of their tunable optical properties [20]. They can be classified into particles with a homogeneous distribution of two metals (alloys) and particles with a heterogeneous arrangement of the different metals (core-shell nanoparticles). Alloy nanoparticles are either synthesized in solution by simultaneous reduction of the two metals of interest [21,22] or they can be formed by laser treatment of heterogeneous nanoparticles [23]. On the other hand, core-shell nanoparticles are synthesized by the successive reduction of two metals where the nanoparticles created during the first reduction process serve as seeds for the second reduction [24-26].

To overcome some disadvantages concerning the chemical instability of the metal colloids, or to extend the biofunctionalization strategies also for metals other than gold, the particles can be coated with a dielectric shell, for example a silica shell [27], which enables the same bioconjugation strategies as for silica nanoparticles.

2.1.2 Nanoparticle biofunctionalization

The coupling of suitable ligands can both sterically stabilize the particles and provide functional groups for biorecognition reactions. Bioconjugate chemistry (e.g., summarized by [28]) has been studied most intensively for gold nanoparticles because they provide the simplest and most stable conjugation chemistry. They offer two principal strategies for their modification with nucleic acids. On the one hand, chemically modified DNA can bind directly to the Au atoms through sulfur (thiol, di-, trisulfide) or through a modification of the gold nanoparticles with succinimide or maleimide and a subsequent binding of amino-modified oligonucleotides, creating DNA–gold nanoparticle conjugates [29-34]. There is also the possibility of modifying gold nanoparticles directly with amino-modified ligands using the adsorption of the amino groups to the gold surface. However, this has not yet been demonstrated with amino-modified oligonucleotides, and the binding energies are much smaller than using thiol

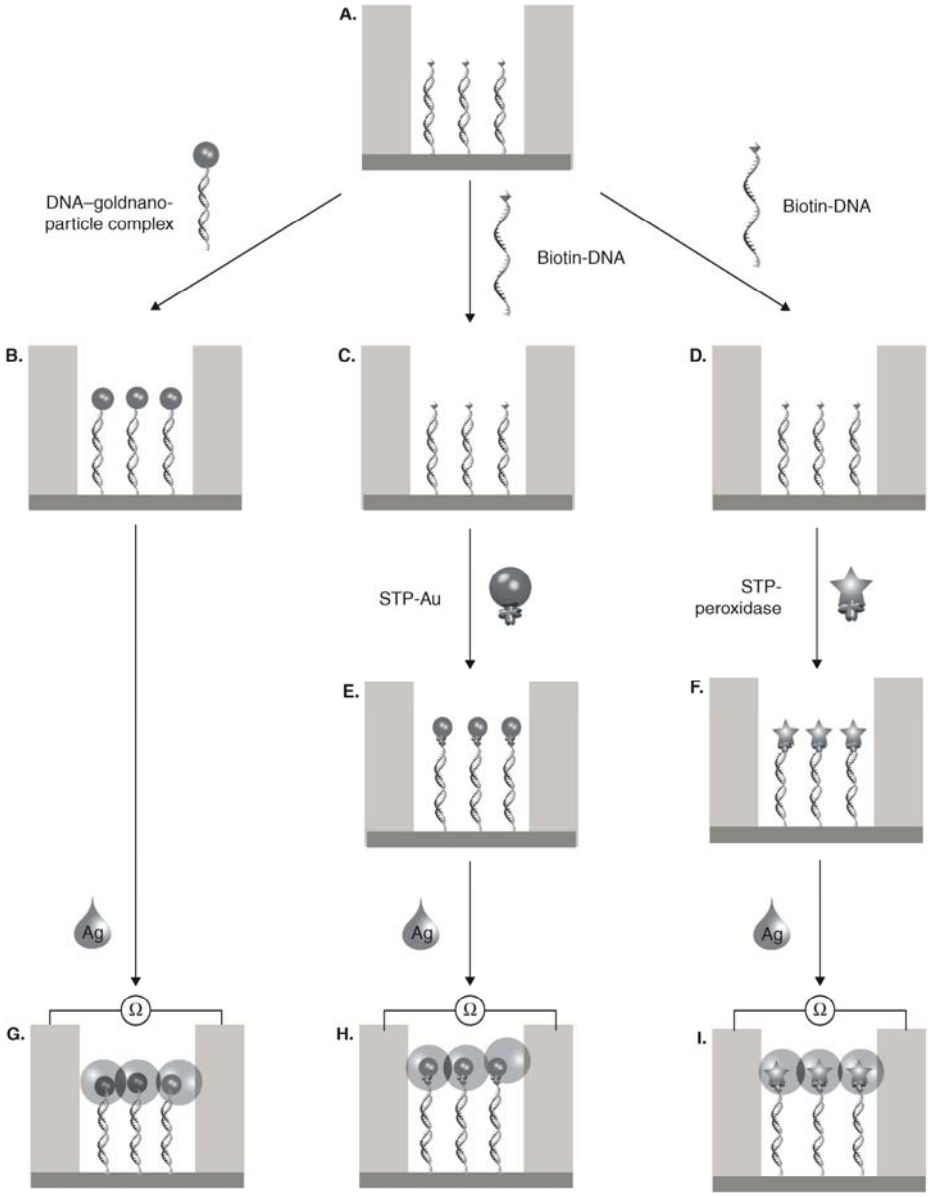

Figure 2. Hybridization and labeling for sequence-specific DNA detection by metal nanostructures. A. The immobilized capture oligonucleotides were hybridized with **B** directly gold nanoparticle-labeled target DNA or **C, D** biotin-modified target DNA. The latter ones were subsequently labeled with **E** STP-gold nanoparticles and **F** STP-peroxidase polymer. **G – I.** Final silver enhancement of the bound labels, leading to optically and electrically (conducting metal layer) readable signals.
STP: Streptavidin.

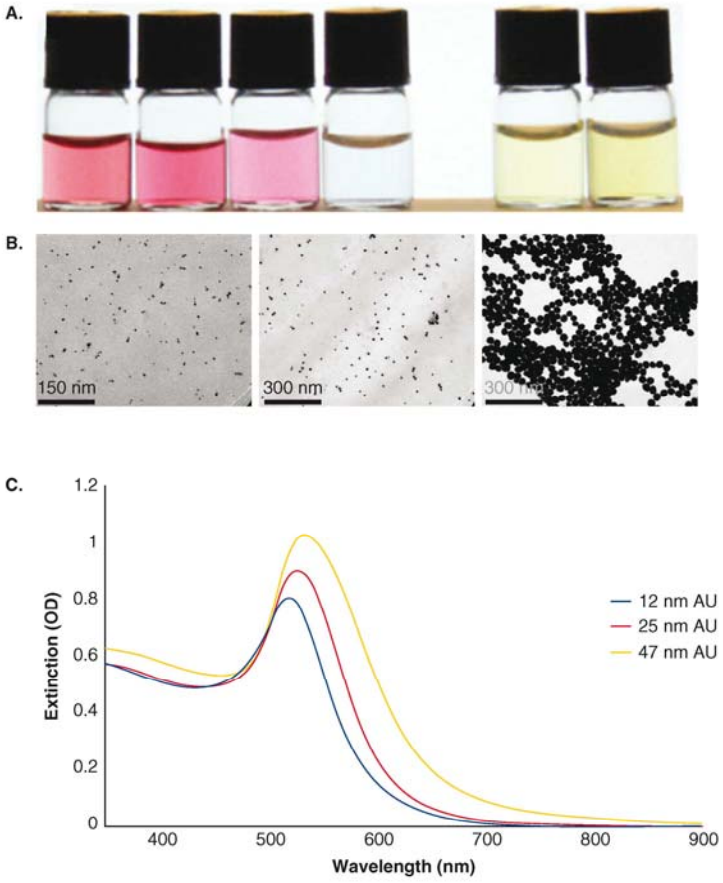

Figure 3. Surface plasmon characteristics are determined by size, shape and composition of metallic nanoparticles as shown in A for gold (left) and silver (right) particles. B. TEM investigations and ***C*** UV/VIS spectra are the standard characterization techniques.

modifications, creating DNA–gold nanoparticle conjugates that are less stable [35,36]. On the other hand, DNA bearing a biotin group can be coupled to streptavidin-modified gold nanoparticles using strategies described for the functionalization with proteins.

Proteins bind to gold surfaces for three main reasons: sulfur bonds (cysteine, methionine), charge (lysine) and hydrophobic attraction (tryptophan). Initially, protein-functionalized gold colloids were used to visualize cellular structures by electron microscopy, as described, for example, for antibodies, lectin or bovine serum albumin [37-39]. Beside the use of antibody conjugates in immunochemistry, the biotin–streptavidin system offers a large variety of extra applications where the tetravalent protein streptavidin can bind the small molecule biotin with high sensitivity and affinity [40]. Thus, biotin-modified nucleotides as well as DNA–DNA hybridization could be detected [41,42]. As streptavidin-modified gold nanoparticles are commercially available and can be applied to different biotinylated DNA – independent of their nucleotide sequence – no time-consuming nanoparticle conjugation with the DNA of interest is required.

Weaker bond energies between ligands and other metals make the modification of other metal particles more difficult but have been described for different materials [43-45]. To overcome the difficulty of modifying nanoparticles of other metals, the particles could serve as seeds for growing a gold [46,47] or a silica shell [27,48], therefore enabling coupling strategies for gold and silica surfaces, as mentioned before and summarized in [49,50].

2.1.3 *Functionalization of planar supports*

Microarrays are commonly made of silicon oxide or glass substrates, which have to be chemically modified for

biomolecule binding. In the case of DNA chips, the functionalization with capture molecules can be realized by two different strategies. During the on-chip synthesis, the capture molecules were stepwise synthesized from single nucleotides [51,52]. In the offline approach, on the other hand, presynthesized capture oligonucleotides were attached to a functionalized chip surface [53]. In principle, binding surfaces can be divided into nearly monomolecular thin films with binding sites two-dimensionally arrayed on the chip surface, and nanoporous gels, which provide a largely enhanced surface area in three dimensions. Although three-dimensional polymeric matrices have already been demonstrated in microarray applications [54,55], the thin films will be focused on, which are commonly used for chip-based molecular detection. These monomolecular binding layers have the advantage that there is no need for diffusion into pores. Capture and target molecules can access the surface unhampered, which enhances the binding rates, especially for large molecules and/or labels that would otherwise be constrained by steric hindrance. The adsorption of organic thin films is achieved mainly by the spontaneous organization of molecules into stable, well-defined structures (self-assembly). Self-assembled monolayers (SAMs) are widely used, highly ordered monomolecular films that form spontaneously on surfaces [56]. The orientated molecules bind covalently with a head group to the surface, whereas the tail groups define the binding properties of the layer to further ligands. Among the different SAM systems, organosilanes on silicon oxide surfaces are probably the most important for biological applications, especially for microarrays [57]. Once the surface offers functional groups for subsequent biomolecule binding, capture DNA (or proteins) can be covalently attached to silicon oxide surfaces by different strategies [58]. To ensure reproducible and quantitative signals, a controlled DNA immobilization procedure is required. However, substrate modification with silanes often leads to inhomogeneous surfaces and/or nonspecific binding of the labeled molecules. For that reason, silanized microarray surfaces were characterized and optimized particularly with regard to nanoparticle labeling [59].

To enable molecular interactions with other biomolecules (e.g., hybridization, antigen–antibody recognition), the immobilized capture probes should be fixed at their extremities or expose their reactive elements, respectively. Whereas this is relatively easy to achieve for capture DNA strands, which can be chemically modified at their ends, proteins are more difficult to immobilize in a productive orientation while still keeping their activity [60]. Hence, Houseman and Mrksich presented different surface-engineering strategies for protein microarrays, which ensured a highly selective and effective immobilization of ligands by preventing nonspecific adsorption of proteins [61]. Using a high-precision robot designed to manufacture DNA microarrays led to protein microarrays spotted onto chemically derivatized glass slides at extremely high spatial densities [62]. As all ligands in an array are presented at the same density in a homogeneous microenvironment, that is, having equal activities, the peptide chips are well suited for quantitative analysis of protein binding and enzymatic modifications [63].

2.2 Chip-based detection schemes

Owing to their interesting physical characteristics, metal nanoparticles can be detected by a variety of detection principles, including optical, electrochemical, electrical and gravimetric methods.

2.2.1 *Optical detection*

Colloidal solutions of metals have been known for a long time, and Michael Faraday and Gustav Mie were probably the first most famous scientists who dealt with the optical properties and theoretical calculations of colloidal solutions [64,65].

2.2.1.1 *Absorption*

Owing to their extremely high extinction coefficients, up to 10^{11} M^{-1} cm^{-1} [66], metal nanoparticles are qualified for imaging by simple optical extinction. These large coefficients and the brilliant color of many colloidal solutions are due to the collective oscillation of electrons of the conductive electron band, generating the so-called surface plasmon band in the absorption spectra [66-68]. Thereby, at a certain wavelength of light the absorption reaches a maximum level. The optical properties of nanoparticle solutions depend strongly on the particles' size, shape, composition, environment and interparticle spacing [69,70]. This was the starting point for a simple colorimetric DNA hybridization detection by means of gold nanoparticles [71,72]. The transfer of the hybridization mixture to a thin-layer chromatography plate resulted in a permanent record of the test by even enhanced color signals upon drying [71]. Later on, this solution-based detection by gold nanoparticles was applied to solid supports, where nanoparticle-labeled probes are bound to surface-immobilized capture molecules. Csaki *et al.* visualized the nanoparticle labels hybridized to monolayers of complementary capture DNA by atomic force microscopy (AFM) [73]. Thereby, individual particle labels could be detected, which enabled the characterization of (capture) DNA monolayers with a lateral resolution in the nanometer range; but this serial AFM technique is time-consuming and therefore not suitable for analyzing entire chip arrays. The use of transparent supports, however, opens the way for a chip-based optical detection by metal nanoparticles [74]. After hybridizing the capture DNA arrayed on glass chips with nanoparticle-labeled target DNA probes, the binding events could be monitored by optical means using reflected and transmitted light for the detection of the surface-bound nanoparticles (30 nm in diameter). Structures as small as 4 µm could be quantitatively read out with an ordinary microscope and digital imaging by fast absorbance measurements [75]. To enhance the sensitivity of

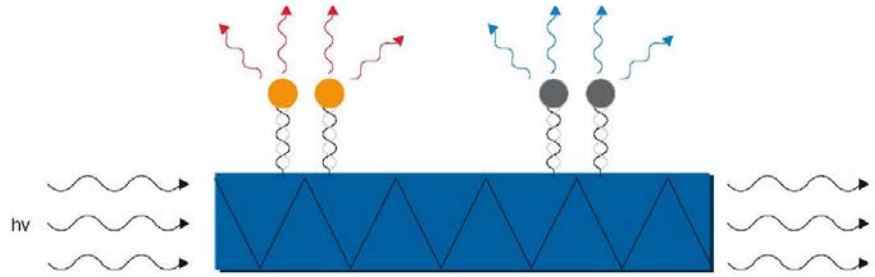

Figure 4. The significant scattering coefficients of metallic nanoparticles are used in analytical setups, such as optical waveguides. Thereby, the spectra of the scattered light depend strongly on the properties of the nanoparticle, such as material and/or size.

these techniques, based on direct imaging of the gold nanoparticles themselves, the absorbance signal can be greatly enhanced by applying a metal deposition on the surface-bound particles. This electroless silver deposition was worked out as the photographic technique and later adapted to tissue research, where the enlargement of immunogold enabled light and electron microscopic studies [76]. The surface-bound gold particles work thereby as seeds, on which silver is deposited in an autocatalytic reduction. This extra metal deposition led to particle growth and strongly enhanced their absorbance signal, leading to the term 'silver enhancement'. Thus, DNA arrays using silver enhancement of the surface-bound nanoparticle-labeled DNA probes could be detected by a conventional flatbed scanner down to a detection limit in the femtomolar range [77]. Metal enhancement enabled even the detection of individual DNA-conjugated gold nanoparticles by optical microscopy [78]. By a combination of microfabrication and DNA spotting, DNA microarrays exhibiting highly defined spot geometry and increased homogeneity in capture DNA distribution have been demonstrated, using metal nanoparticles as markers [79]. Although the described nanoparticle-based DNA detection methods used gold nanoparticles directly modified with thiolated oligonucleotides, similar results have been achieved by labeling biotinylated DNA with streptavidin-gold nanoparticles [80]. In comparison with a fluorescence-based method, the detection limit was equivalent and corresponded to 1 amol of biotinylated DNA attached on an array. As an interesting example for miniaturized point-of-care devices, Li and co-workers proposed an integrated DNA detection platform using photodiode and ordinary optical illumination [81]. Gold nanoparticle labeling and silver enhancement were used to generate opaque surfaces at areas with target DNA hybridization whose changes in light intensity were measured with integrated photodiodes. Owing to the simple detection principles allowing gold nanoparticle labeling combined with silver deposition, the development of easy-to-use and portable devices is advanced by several companies, for example Eppendorf AG (Hamburg, Germany), which uses a colorimetric detection scheme, scanning silver-enhanced gold nanoparticle labels to detect any biotinylated biomolecules.

2.2.1.2 *Scattering*

In addition to large extinction coefficients, many metal nanoparticle materials have extremely large scattering coefficients (e.g., up to 10^{-10} cm^{-2} for silver nanoparticles), which allow for extremely sensitive imaging and quantification of scattered light from nanoparticle-tagged biomolecules [82]. The spectrum of the scattered light is thereby also dependent on the surface plasmon resonance characteristics, which is determined by nanoparticles' size, shape and composition. In 1995, light scattering was first used for DNA detection on oligonucleotide arrays by using optical waveguides [83]. Particulate labels on the target DNA acted as light scattering sources when illuminated by the evanescence wave, whereas only the surface-bound labels generated a signal. With results comparable with fluorescence-based systems, real-time binding or melting events could be detected, enabling studies on dynamics of DNA hybridization and denaturation. As the scattering spectrum depends on nanoparticle size and composition, multi-label systems with nanoparticle probes are possible and have been demonstrated [84]. Thereby, oligonucleotide functionalized, 50 and 100 nm gold nanoparticle probes were hybridized to targets captured by a DNA array, using a glass slide as planar waveguide. The size-selectively scattered light was used to identify two target sequences in one solution. The demonstrated two-color labeling should be extendable to further colors using nanoparticles of different composition and size [21]. The dependence on interparticle spacing is exploited by Storhoff *et al.*, who described the changes in colorimetric scattering of gold nanoparticle probes on hybridization to complementary probes [85]. By renouncing surface-immobilized capture DNA, nucleic acid targets were recognized by DNA-modified gold probes in a homogeneous test format. The resulting color change was visualized by spotting the solutions onto an illuminated glass waveguide (**Figure 4**). In comparison with the reported absorbance-based method [71], the detection sensitivity could be

increased by over four orders of magnitude and enabled the detection of DNA targets in the zeptomolar range. A similar ultrasensitive method, the so-called bio-bar-code-based DNA detection, has been presented by Nam *et al.* [86]. The PCR-less amplification method relied on gold nanoparticle labels, which bore – besides the specific probe DNA – hundreds of copies of a bar-code DNA sequence. Thus, one binding event resulted in a multifold amount of bar-code oligonucleotide strands, which could easily be detected in a chip-based assay. This signal enhancement by bar-code molecules can also be used to detect proteins [87]. Magnetic beads loaded with primary antibodies capture the protein of interest. Thereafter, gold nanoparticles bearing hundreds of identical bar-code oligonucleotides were specifically (by means of a secondary antibody) coupled to the protein of interest. After the enrichment of the sample by applying a magnetic field, the bar-code oligonucleotides were released from the particles and could – as a highly amplified analyte – be detected in a sequence-specific DNA array.

Commercial detection systems have been developed by, for example, Genicon Sciences (now part of Invitrogen Corp., Carlsbad, CA, USA) or Nanosphere, Inc. (Northbrook, IL, USA) for DNA chip arrays based on the detection of scattered light from bound metallic nanoparticles. Among these, a microarray-based DNA hybridization assay using scattering silver nanoparticles demonstrated as well an increased sensitivity (60-fold) compared with that achieved by using fluorescent labels [88]. By detecting the scattered light of gold nanoparticle labels, Bao *et al.* were – especially at low probe concentrations – also able to detect significantly more genes compared with labeling with fluorophores, which make the resonance light scattering (RLS) particles particularly attractive for the detection and identification of low-abundance nucleic acids or for applications with a limited number of samples.

Moreover, the RLS technology can be used for ultrasensitive detection in a wide range of applications including immuno and DNA probe assays in solutions and solid phases, as well as cellular and histological, based on the gold particles' light producing power equivalent to more than 500,000 fluorescein molecules [89]. Besides the above-described DNA detection assays, Wang *et al.* showed a microarray format for the detection of proteins and protein functionality by means of resonance light scattering [90]. In particular, the highly specific and sensitive detection of enzyme activities demonstrated its potential for high-throughput screening for enzyme inhibitors, for example.

In addition to the detection of light scattered directly from metal nanoparticles, metal surfaces can enhance electromagnetic fields, which has been exploited in surface-enhanced Raman scattering (SERS). Both electrochemically roughened surfaces [91] and uniformly sized colloidal particles [11,92-94] are extremely effective at enhancing Raman scattering signals from adsorbed, Raman-active molecules. Metal nanoparticles are known to enhance Raman light scattering by factors of $10^{14} - 10^{15}$ [95]. This leads to Raman signals both more intense and stable than single-molecule fluorescence and the potential of numerous biological applications of the localized surface plasmon phenomena. Cao *et al.* introduced an array-based method for DNA and RNA detection by means of metal nanoparticles and either scanometric or Raman spectroscopic readout [96]. Au nanoparticles (13 nm in diameter) modified with both Raman-active dyes and oligonucleotides were used as probes to monitor the presence of specific target DNA strands and applied to a chip spotted with the appropriate capture DNA strands. If complementary targets were present the hybridization reaction led to nanoparticle-dye probes attached to defined spots on the microarray; but because of a lack of electromagnetic-field enhancement, no Raman scattering signal was detectable. Nevertheless, others have shown that closely spaced nanoparticles are achievable and can give SERS enhancement [70,94,97]. To overcome the problem of nanoparticle spacing that is too large for DNA detection, silver enhancing has been applied to the nanoparticle-dye probes, leading to large Raman scattering enhancement [96]. Compared with other nanoparticle-based microarray detection, this approach provides both the high sensitivity and selectivity of grayscale scanometric detection but adds a multiplexing capability because a large number of probes can be designed using the Raman tag as a narrow-band spectroscopic fingerprint. Recently, current developments and applications of SERS technology in medical diagnostics and biological imaging have been reviewed [98]. The surface-enhanced Raman DNA probes were used to detect DNA targets (e.g., gene sequences, bacteria and viral DNA) by means of hybridization to DNA sequences complementary to these probes.

In addition to the demonstrated DNA detection, approaches to detect proteins have also been shown. Among others, Xu *et al.* demonstrated an immunoassay using immunogold labels modified by Raman-active molecules and antigens, which were captured by antibody-assembled chips and analyzed by means of SERS [99]. By designing and using Raman dye-functionalized nanoparticle probes with specific protein-binding affinities, the multiplexed screening of protein interactions could be performed with SERS spectroscopy in a microarray format [100].

2.2.1.3 *Surface plasmon resonance*

In the past decade, methods based on surface plasmon resonance (SPR) have contributed significantly to the sensing and quantification of biomolecule interactions. Karlsson identified four emerging application areas: food analysis, proteomics, immunogenicity and drug discovery [101]. In a typical SPR setup, plane polarized light is totally reflected from a substrate whose opposite surface is covered by a thin gold film (± 50 nm). An evanescent electric field penetrates the gold film and molecules bound to the not illuminated

gold surface influence the refractive index and therefore the reflection angle of the beam, which is sensitively detected. This enables the analysis of biomolecule binding without using labels [102,103]. The shift in the reflection angle can be greatly enhanced by using nanoparticle labels because the bound nanoparticles have a much larger impact on the refractive index at the gold surface than unmodified biomolecules. That has been demonstrated for both an ultrasensitive detection of DNA hybridization and a sandwich immunoassay [42,104]. In addition, Stuart *et al.* summarized strategies based on localized surface plasmon resonance on nanoparticle arrays [105]. For example, Van Duyne and co-workers demonstrated a new class of nanoscale affinity biosensors based on triangular silver nanoparticles using the well-studied biotin–streptavidin system as well as an antigen–antibody sandwich assay in the detection of Alzheimer's disease [106,107].

2.2.1.4 *Photothermal imaging*

Below a certain nanoparticle size, absorption will prevail over scattering when the nanoparticles are illuminated with laser light [108]. This strong absorption causes a photothermal effect, that is, an increase in temperature around the illuminated particle. By detecting this temperature change with a sensitive interference method, gold colloids down to diameters of 2.5 nm could be detected. Although the described temperature increase might still affect attached proteins or biomolecules, an improved system may considerably reduce the label heating, which would become negligible for most biomolecules at ambient conditions, enabling biomolecule detection by photothermal effects. This has already been demonstrated for the detection and quantification of proteins arrayed on slides [109].

2.2.2 *Electrical detection*

Besides the large variety of methods relying on the optical properties of metal nanoparticles, there are also some non-optical detection strategies using their electrical conductivity, redox potential, or weight.

2.2.2.1 *Electrical*

Owing to their intrinsic electrical conductivity, metal nanoparticles lend themselves to electrical detection schemes. If positioned in a gap between two electrodes, a conducting nanoparticulate film can form and connect the electrodes, detectable by a simple DC resistance measurement. A typical approach immobilizes the capture molecules in the electrode gap, and after or during the specific biorecognition reaction the metal nanoparticle labels are introduced and bound to the biomolecule binding pairs. If nanoparticles have not bound densely enough to create a conductive layer, the bound particles can serve as seeds for an extra metal deposition, leading to particle growth and, finally, percolation of the particles. Recently, Marcon *et al.* presented the electrical detection of immunoglobulin (Ig) using a nanogap-based biosensor, where probes immobilized in electrode gaps captured IgGs from human serum [110]. The captured antigens reacted further with gold nanoparticle-labeled secondary antibodies, resulting in an increase of electrical conductance. By immobilizing oligonucleotides as capture molecules in the gap, DNA hybridization events can be detected likewise [111]. Thereby, gold nanoparticles covered with complementary target DNA led, after hybridization and silver enhancement reaction, to a significant drop in resistance. Dependent on the existing nanoparticle (i.e., analyte) concentration and the applied silver enhancement time, one can directly quantify the target concentration. Park *et al.* demonstrated a similar system, which was able to detect single-base mismatches with a selectivity factor of 10^5:1 at concentrations as low as 500 fM [112]. Further development of the electrical readout system led to a portable and robust readout device for DNA chips using DC resistance measurements [113]. The presented paralleled readout system offers the potential for a low-cost as well as highly miniaturizable method, suitable for point-of-care applications in the context of lab-on-a-chip technologies (**Figure 5**). However, as the system did not allow any online measurement during the enhancement process, the chip might be under- or overenhanced. To overcome this problem knowledge about the characteristics of nanoparticle growth as well as the features of enhancement solutions is highly desirable. By studying the autocatalytic metal deposition onto surface-bound gold nanoparticles on a single particle level, it has been found that the applied solutions differed considerably in their enhancement intensity and specificity and, moreover, that the particles grew linearly dependent on their seed size [114]. On the other hand, the stepwise process has been improved by introducing online DC resistance monitoring during the autometallographic enhancement process of gold particle-labeled analytes [115]. The application of gold nanoparticle multilayers has been described as amplifying considerably the signals from biomolecular binding events both for protein and DNA analysis [116,117].

Besides the DC approaches described, AC capacitance measurements offer a further method of detecting an electrical signal, which does not necessarily need a fully conductive structure between the electrodes. Furthermore, using interdigitated electrodes made of aluminum fingers reduced the nonspecific precipitation of silver that occurs when using noble metal electrodes [118]. This technique, however, requires much more sophisticated measurement equipment, making it less suitable for low-cost point-of-care applications.

As the nanoparticle-based labeling is often associated with nonspecific particle binding and therefore unwanted metal deposition, enzyme-based metal development offers an interesting labeling alternative, as introduced recently by [119-121]. A new approach based on enzyme-catalyzed silver deposition with horseradish peroxidase has been demonstrated for a low-background electrical detection of DNA chips [122].

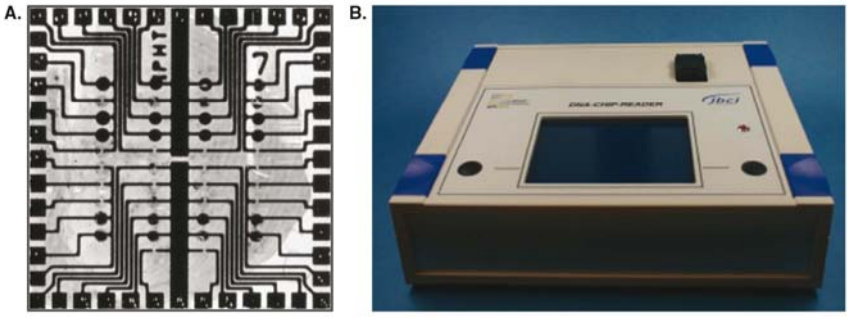

Figure 5. DNA chip detection for point-of-care analyses. A. DNA glass chip (1/2 inch) containing screen-printed platinum electrodes with 42 electrode gaps (10 µm wide) as measurement spots. The signals can be read out optically as dark spots in transmission and electrically. **B.** The portable chip reader analyzes the DNA chips in a semiparallel way by DC resistance measurement.

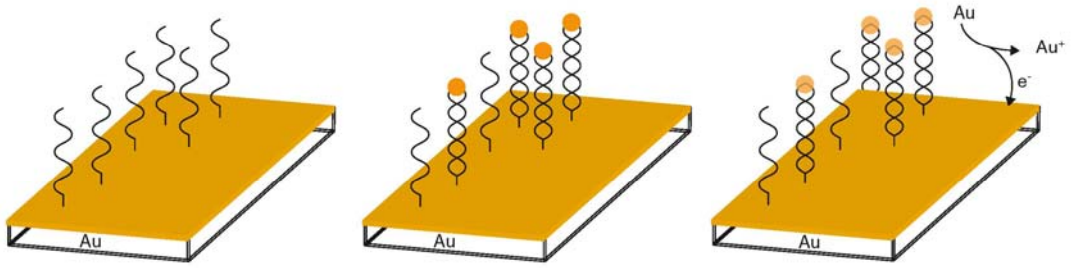

Figure 6. Electrochemical approaches use the material of particle labels such as gold for signal enhancement. After oxidative dissolving of metallic nanoparticles the resulting metal ions are detected in electrochemical setups. Thereby, the signal intensity depends on the metal and its concentration.

572 *2.2.2.2 Electrochemical* **(Figure 6)**

Besides the direct electrical detection, metal nanoparticles bound to a sensing surface can also be detected indirectly by 575 redox processes. After oxidatively dissolving the metal into an acidic solution, the resulting metal ions can be electrochemically sensed. By using gold nanoparticles as labels, this has been demonstrated for an immunoassay as well as for the detection of DNA hybridization measured by 580 anodic stripping voltammetry (ASV) or differential pulse voltammetry, respectively [123,124]. The detected signal depends thereby on the metal and its concentration. The sensitivity of the electrochemical metalloimmunoassay – comparable with colorimetric enzyme-linked immunoassays or fluorescence-585 based methods – is related to both the sensitive ASV determination of Au(III) and to the release of a large number of Au(III) ions from each gold particle anchored on the immunocomplex [123]. The use of disposable screen-printed electrodes made the approach extremely tempting for 590 low-cost and point-of-care applications [125]. Further signal amplification, and lowering of the detection limits to the picomolar range, could be achieved by precipitating more 593 metal to the colloidal gold label [126,127]. The work was extended by the use of magnetic beads bearing DNA 594 probes [128]. After the hybridization with biotinylated target DNA, streptavidin-coated gold nanoparticles were bound to the captured targets, and a catalytic silver precipitation followed. An external magnet positioned under the electrode attracted the particle–DNA assemblies. The direct electrical contact of the silver precipitates enabled solid-state 600 chronopotentiometric detection and allowed highly sensitive and selective analysis of DNA hybridization. Moreover, by using different inorganic-colloid tags, having diverse redox potentials, Wang *et al.* demonstrated a multiplexed electrochemical detection scheme [129]. Besides using metal 605 colloid tags as seeds for a subsequent silver enhancement, Fanjul-Bolado *et al.* demonstrated enzymatic genosensors with alkaline phosphatase-catalyzed silver deposition analyzed by ASV [130].

Integrating these stripping analysis schemes into an array 610 format seems to be difficult because the nanoparticle labels have to be dissolved away from the electrode surface before detection at a second electrode. An alternative could be the readout by differential pulse voltammetry (DPV), which detects the electrochemical oxidation of the metal labels 615

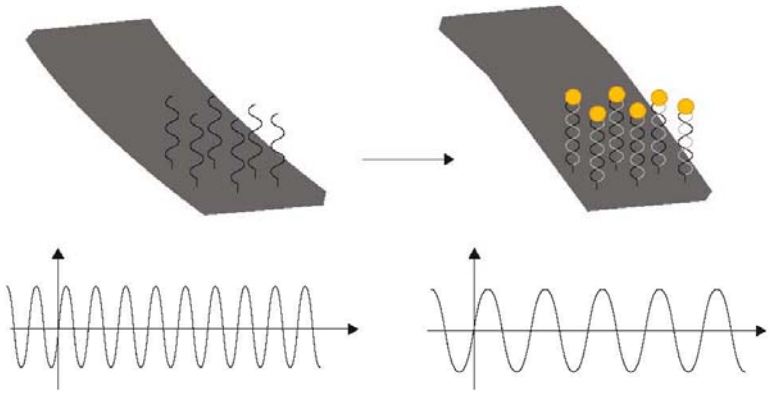

Figure 7. Mass changes of a movable microstructured cantilever induced by hybridization of a particle-labeled DNA target are detected in electromechanical methods. Therefore, the cantilever is covered with complementary capture DNA that specifically binds the particle-labeled target and thereby induces either a change in oscillation frequency (as shown in the figure) or a bending.

without the need of acidic dissolution. Ozsoz *et al.* presented a highly sensitive electrochemical genosensor, which was able to detect mutations in real PCR samples in the lower femtomolar range [33]. Although the report did not address the question of microarray formats, this method would be appropriate for biomolecule detection at arrayed microelectrodes bearing different capture molecules. Furthermore, the disposable pencil graphite electrodes made the detection system suitable for point-of-care applications.

2.2.3 *Electromechanical* (Figure 7)

As metal nanoparticles feature a very high specific mass, they can be used in detection schemes based on gravimetric principles, as has been shown for both quartz-crystal microbalances (QCMs) and oscillating microcantilevers. Even very small mass changes at the oscillating microbalance surface give rise to characteristic changes in the frequency of nanomechanical resonator detectors. The highly sensitive detection devices (capable of measuring subnanogram mass changes) allow for the detection of unlabeled biomolecules, as demonstrated for a protein binding to double-stranded DNA immobilized on a quartz-crystal microbalance [131]. However, metal nanoparticles can enhance the gravimetric detection when used as biomolecule labels because the mass of each nanoparticle is relatively large in comparison with the masses of the biomolecules themselves [132]. A further increase in sensitivity was obtained by either hybridizing a second layer of nanoparticles to the first one or extra gold deposition on the gold particle labels resulting in an amplified DNA analysis [133,134].

In comparison with the quartz crystal microbalances, microcantilevers are up to two orders of magnitude smaller than their macroscopic counterparts, and can be mass-produced as miniaturized sensor arrays [135]. Cantilever-based deflection assays are thereby also able to detect biomolecule binding without the need for external labeling. Thereby, biorecognition reactions (e.g., hybridization) on the cantilever surface functionalized with capture molecules induce a characteristic deflection of the cantilever, which is to be detected [136]. According to this study, the cantilever approach described is readily adaptable to high-throughput array formats providing distinct positive/negative signals for an easy interpretation of DNA hybridization. One step towards parallelization was demonstrated by Fritz *et al.*, who functionalized multiple cantilevers in an array with a selection of biomolecules [137]. In addition to hybridization detection, they were able to analyze antigen–antibody interactions, showing the wide-ranging applicability of this nanomechanical detection system. The use of nanoparticle labels and subsequent silver deposition on particles bound on the cantilever increased the sensitivity of the electromechanical DNA detection up to the picomolar range [135].

3. Conclusion

In this review, past work on using metal nanoparticles as labels in chip-based biomolecular detection schemes has been summarized. A crucial prerequisite is the establishment of numerous biofunctionalization strategies, which make possible the coupling of different biomolecules, in particular DNA and proteins, especially to noble metal nanoparticles. The development of stable and easy-to-handle functionalization methods remains a major challenge but can often be bypassed by commercially available particles functionalized with more general binding partners such as streptavidin.

The interesting physical nanoparticle properties provide a variety of detection schemes, including new optical and electrical readout strategies, yielding stable signals and the potential of low-cost detection systems, respectively.

Besides these advantages, nanoparticle labels, especially in connection with extra metal deposition, can be used to increase the sensitivity of existing established detection schemes, such as SERS or gravimetric methods.

Facing the choice of the optimum method, one should clearly define the requirements of the favored application. Parameters such as sensitivity, selectivity as well as the required analysis time determine considerably the detection scheme to be used. Thereby, defined point-of-care applications demand low-cost and robust readout systems, whereas the comprehensive genotyping of specialized laboratories requires highly paralleled analyses with high-throughput machines. Thus far, nanoparticles represent relatively new but promising labels in biomolecular detection. As they open the way to new application fields they will also gain growing interest from companies and suppliers developing new readout devices for nanoparticle labeling. As a consequence, chip-based detection by nanoparticle labeling will occupy more and more application areas.

4. Expert opinion

The development of new surface-based assay formats is transforming research in medicine and biological sciences as well as accelerating discoveries in pharmacy and diagnostics. Moreover, DNA microarrays or gene chips especially have gained more and more interest from non-scientific personnel who are interested in their genealogy or want to know about potential genetic risks of diseases. The success of such DNA platforms has motivated the development of peptide and protein biochips as well; but because surface-based methods rely on the immobilization of capture molecules maintaining their specific functionality, biochips have been described for DNA rather than for proteins as immobilized capture molecules. DNA features a robust structure withstanding repeated drying and heating processes usually applied to biochips, whereas proteins can lose their characteristic three-dimensional structure, that is, functionality, when leaving their native aqueous environment while being exposed to heat or other denaturing conditions. Keeping proteins as capture molecules in their native environment remains a big challenge to be solved in future, especially with regard to shelf life, which is highly desired for commercial biochips. Thereby, organic polymers provide great potential as matrix for immobilizing proteins as functional capture molecules by holding aqueous ambient conditions. Furthermore, such nanoporous gels offer higher loading capacity owing to the larger surface area.

DNA microarrays, however, which have been extensively commercialized and are now widely used for genetic analyses, should be particularly addressed in this review. In the authors' opinion, there are two main application fields for microarrays in future. On the one hand, the highly integrated analysis of entire genomes or proteomes, on the other hand, low-cost solutions for defined questions in point-of-care analyses.

The first application area is restricted to specialized laboratories that acquire orders from a vast number of subjects. These high-throughput analyses can afford sophisticated detection systems without watching every penny. For these applications, fluorescence-based labeling and readout systems will meet the demands of high specificity and sensitivity while providing multiplexing potential by the numerous available fluorescence dyes. Moreover, the standardized and highly defined conditions in the labs can tolerate the machine's susceptibility to interference. Furthermore, fluorescence labeling of biomolecules is well established and commercially available for a large variety of fluorophores. At present, it is therefore often the first choice for labeling biomolecules in research laboratories.

Contrarily, there is growing interest in biomolecular detection for so-called point-of-care applications outside specialized laboratories. For example, the food producer needs to guarantee both innocuousness and high quality of his products. That could be germfree meat as well as the lack of aroma-affecting ingredients from unwanted microorganisms. To be able to have fast analyses with minimum interference with the production, in-line or on-line monitoring systems are desirable. Another promising application area is medicine, which requires, for example, contemporary diagnostics of sepsis pathogens and their antibiotics' resistance. One can also imagine the doctor who conducts a DNA test at the medical practice in order to determine the genetic cancer risk of patients, assisting him in the choice of adequate cancer screening. In all of those cases metal nanoparticles can serve as new labels for chip-based molecular detection. Unlike fluorescence labelling, they offer the potential of stable, robust as well as low-cost signaling by providing high sensitivity and specificity. New electrical detection schemes especially can make possible easy-to-use resistance measurements, yielding yes-or-no results without the need of elaborative optical analysis and interpretation of the data.

Besides using gold nanoparticles as labels in new detection schemes, they can enhance the sensitivity of established detection systems or even increase the efficiency of molecular detection reactions. The latter has been demonstrated, for example, by adding gold nanoparticles to PCR mixture, which increased both specificity and efficiency of the reaction [138,139]. So-called bio-bar-code nanoparticles might even eliminate any preamplification by PCR before chip-based DNA analytics [140]. Thereby, the signal amplification is achieved by a couple of hundreds bar-code oligonucleotides attached to the DNA-modified gold nanoparticles. After the specific DNA–DNA hybridization reaction the nanoparticles, bearing DNA complementary to the target DNA, are accumulated. The bar-code molecules are then released from the gold nanoparticles and could subsequently be detected as highly amplified signal [141]. The bio-bar-code approach can also be used for signal amplification in the detection of other molecules [87,142]. Considering the great potential of

these new nanoscale tools, metal nanoparticles will make their way equally besides fluorescence-based methods and – in a couple of defined questions – they will even take their part.

Owing to the great potential of these new nanoscale tools, an extension of the utilization of metal nanoparticles in chip-based molecular diagnostics will be observed. Furthermore, in a couple of defined approaches they will even replace current fluorescence-based methods.

Declaration of interest

The following grants have been funding the authors' work: DGF FR 1348/5 – 2 for G Festag and W Fritzsche; Volkswagen Foundation 1/80 070 (SOBSI) for W Fritzsche; EU NUCAN (NMP-STREP 013775) for W Fritzsche and A Csaki; BMBF JBCI FK2031P513 for T Schüler and R Möller; and BMBF CBRNE-Hazards FK213N9519 for R Möller.

Bibliography

1. Stears RL, Martinsky T, Schena M. Trends in microarray analysis. Nat Med 2003;9:140-5
2. Spielbauer B, Stahl F. Impact of microarray technology in nutrition and food research. Mol Nutr Food Res 2005;49:908-17
3. Sotiriou C, Piccart MJ. Taking gene-expression profiling to the clinic: when will molecular signatures become relevant to patient care? Nat Rev Cancer 2007;7:545-53
4. Rosi NL, Mirkin CA. Nanostructures in biodiagnostics. Chem Rev 2005;105:1547-62
5. Möller R, Fritzsche W. Metal nanoparticle-based detection for DNA analysis. Curr Pharm Biotechnol 2007;8:274-85
6. Jain KK. Applications of nanobiotechnology in clinical diagnostics. Clin Chem 2007;53:2002-9
7. Zsigmondy R, Thiessen PA. Das kolloidale Gold [The colloidal gold]. Leipzig: Verlagsges, Leipzig; 1925
8. Turkevich J. Colloidal gold. Part I. Historical and preparative aspects, morphology and structure. Gold Bull 1985;18:86-91
9. Brust M, Fink J, Bethell D, et al. Synthesis and reactions of functionalized gold nanoparticles. J Chem Soc Chem Commun 1995:1655-6
10. Abid JP. Laser induced synthesis and non linear optical properties of metal nanoparticles. Lausanne: Ecole Polytechnique Federale de Lausanne; 2003
11. Lee PC, Meisel D. Adsorption and surface-enhanced Raman of dyes on silver and gold sols. J Phys Chem 1982;86:3391-5
12. Evanoff DD Jr, Chumanov G. Synthesis and optical properties of silver nanoparticles and arrays. ChemPhysChem 2005;6:1221-31
13. Mott D, Galkowski J, Wang L, et al. Synthesis of size-controlled and shaped copper nanoparticles. Langmuir 2007;23:5740-5
14. Turkevich J, Kim G. Palladium: preparation and catalytic properties of uniform size. Science (Washington, DC) 1970;169:873-9
15. Turkevich J, Miner RS, Babenkova L. Further studies on the synthesis of finely divided platinum. J Phys Chem 1986;90:4765-7
16. Frens G. Controlled nucleation for the regulation of the particle size in monodisperse gold suspensions. Nature 1973;241:20-2
17. Hayat MH. Colloidal gold: principles, methods, and applications. Academic press; 1989
18. Turkevich J, Stevenson PL, Hiller J. Nucleation and growth process in the synthesis of colloidal gold. Discuss Faraday Soc 1951;11:55-75
19. Beattie JK. Monodisperse colloids of transition metal and lanthanide compounds. Pure Appl Chem 1989;61:937-41
20. Steinbrück A, Csaki A, Festag G, et al. Preparation and optical characterization of core-shell bimetal nanoparticles. Plasmonics 2006;1:79-85
21. Link S, Wang ZL, El-Sayed MA. Alloy formation of gold-silver nanoparticles and the dependence of the plasmon absorption on their composition. J Phys Chem B 1999;103:3529-33
22. Lee I, Han SW, Kim K. Production of Au-Ag alloy nanoparticles by laser ablation of bulk alloys. Chem Commun (Camb) 2001;1782-3
23. Hartland GV, Guillaudeu S, Hodak JH. Chapter 9: laser induced alloying in metal nanoparticles – controlling spectral properties with light. In: Liebermann M, editor, Molecules as components in electronic devices. Washington, DC: American Chemical Society Publication; 2003;123(10)
24. Hodak, Henglein G, Hartland. Laser-induced inter-diffusion in AuAg core-shell nanoparticles. J Phys Chem B 2000;104:11708-18
25. Abid JP, Girault HH, Brevet PF. Selective structure changes of core–shell gold–silver nanoparticles by laser irradiation: homogeneisation vs. silver removal. Chem Commun 2001;829-30
26. Moskovits M, Srnova-Sloufova I, Vlckova B. Bimetallic Ag-Au nanoparticles: extracting meaningful optical constants from the surface-plasmon extinction spectrum. J Chem Phys 2002;116:10435-46
27. Liz-Marzán LM, Giersig M, Mulvaney P. Synthesis of nanosized gold-silica core-shell particles. Langmuir 1996;12:4329-35
28. Niemeyer CM. Nanoparticles, proteins, and nucleic acids: biotechnology meets materials science. Angew Chem Int Ed Engl 2001;40:4128-58
29. Nuzzo RG, Zegarski BR, Dubois LH. Fundamental studies of the chemisorption of organosulfur compounds on gold111. Implications for molecular self-assembly on gold surfaces. J Am Chem Soc 1987;109:733-40
30. Nuzzo RG, Allara DL. Adsoption of bifunctional organic disulfides on gold surfaces. J Am Chem Soc 1983;105:4481-3
31. Taton TA. Preparation of gold nanoparticle-DNA conjugates. Curr Protocol Nucl Acids Chem 2002;12(2):1-12
32. Reardon JE, Frey PA. Synthesis of undecagold cluster molecules as biochemical labeling reagents. 1. Monoacyl and mono[N-(succinimidooxy)succinyl] undecagold clusters. Biochemistry 1984;23:3849-56
33. Ozsoz M, Erdem A, Kerman K, et al. Electrochemical genosensor based on colloidal gold nanoparticles for the detection of Factor V Leiden mutation using disposable pencil graphite electrodes. Anal Chem 2003;75:2181-7

34. Xiao S, Liu F, Rosen AE, et al. Selfassembly of metallic nanoparticle arrays by DNA scaffolding. J Nanopart Res 2002;4:313-7
35. Leff DV, Brandt L, Heath JR. Synthesis and characterization of hydrophobic, organically-soluble gold nanocrystals functionalized with primary amines. Langmuir 1996;12:4723-30
36. Hutter E, Fendler JH, Roy D. Surface plasmon resonance studies of gold and silver nanoparticles linked to gold and silver substrates by 2-aminoethanethiol and 1,6-hexanedithiol. J Phys Chem B 2001;105:11159-68
37. Faulk WP, Taylor GM. An immunocolloid method for the electron microscope. Immunochemistry 1971;8:1081
38. Horisberger M, Rosset J, Bauer H. Colloidal gold granules as markers for cell surface receptors in the scanning electron microscope. Experientia 1975;31:1147
39. Burt JL, Gutierrez-Wing C, Miki-Yoshida M, et al. Noble-metal nanoparticles directly conjugated to globular proteins. Langmuir 2004; 20:11778-83
40. Diamandis EP, Christopoulos TK. The biotin-(strept)avidin system: principles and applications in biotechnology. Clin Chem 1991;37:625-36
41. Hiriyanna K, Varkey J, Beer M, et al. Electron microscopic visualization of sites of nascent DNA synthesis by streptavidin-gold binding to biotinylated nucleotides incorporated in vivo. J Cell Biol 1988;107:33-44
42. He L, Musick MD, Nicewarner SR, et al. Colloidal Au-enhanced surface plasmon resonance for ultrasensitive detection of DNA hybridization. J Am Chem Soc 2000;122:9071-7
43. Yamamoto M, Kashiwagi Y, Nakamoto M. Size-controlled synthesis of monodispersed silver nanoparticles capped by long-chain alkyl carboxylates from silver carboxylate and tertiary amine. Langmuir 2006;22:8581-6
44. Aslam M, Gopakumar G, Shoba TL, et al. Formation of Cu and Cu2O nanoparticles by variation of the surface ligand: preparation, structure, and insulating-to-metallic transition. J Colloid Interface Sci 2002;255:79-90
45. Meziani M, Lin Y, Sun Y-P. Conjugation of nanomaterials with proteins. In: Kumar CSSR, editor, Biofunctionalization of nanomaterials. Weinheim: WILEY-VCH; 2005. p. 183-234
46. Cao YW, Jin R, Mirkin CA. DNA-modified core-shell Ag/Au nanoparticles. J Am Chem Soc 2001;123:7961-2
47. Lyon JL, Fleming DA, Stone MB, et al. Synthesis of Fe oxide core/Au shell nanoparticles by iterative hydroxylamine seeding. Nano Lett 2004;4:719-23
48. Aslam M, Fu L, Li S, et al. Silica encapsulation and magnetic properties of FePt nanoparticles. J Colloid Interface Sci 2005;290:444-9
49. Festag G, Klenz U, Henkel T, et al. Biofunctionalization of metallic nanoparticles and microarrays for biomolecular detection. In: Kumar CSSR, editor, Biofunctionalization of nanomaterials. Weinheim: WILEY-VCH; 2005. p. 150-82
50. Drake TJ, Zhao XJ, Tan W. Bioconjugated silica nanoparticles for bioanalytical applications. In: Niemeyer CM, Mirkin CA, editors, Nanobiotechnology. Weinheim: Wiley-VCH; 2004. p. 444-57
51. Southern E, Mir K, Shchepinov M. Molecular interactions on microarrays. Nat Genet 1999;21:5-9
52. Lipshutz RJ, Fodor SP, Gingeras TR, et al. High density synthetic oligonucleotide arrays. Nat Genet 1999;21:20-4
53. O'Donnell MJ, Tang K, Köster H, et al. High density, covalent attachment of DNA to silicon wafers for analysis by MALDI-TOF mass spectrometry. Anal Chem 1997;69:2438-43
54. Bieber I, Reichert J, Klenz U, et al. Antibody arrays on micropatterned surfaces and in three-dimensional gel structures for detection of Salmonella isolates. Biotest Bull 2002;6:235-342
55. Larsson A, Du CX, Liedberg B. UV-patterned poly(ethylene glycol) matrix for mcroarray applications. Biomacromolecules 2007;8:3511-8
56. Xia Y, Whitesides GM. Soft lithography. Angew Chem Int Ed Engl 1998;37:550-75
57. Reichert J. Herstellung und Charakterisierung lateral mikrostrukturierter molekularer Monofilme auf Silicium- und Glas-Chipoberflächen für die Anwendung in Bio-Chips. [Fabrication and characterization of lateral microstrucutred molecular monolayers on silicon- and glass surfaces for biochip applications] Jena: Friedrich Schiller Universität Jena; 2003
58. Zammatteo N, Jeanmart L, Hamels S, et al. Comparison between different strategies of covalent attachment of DNA to glass surfaces to build DNA microarrays. Anal Biochem 2000;280:143-50
59. Festag G, Steinbrück A, Wolff A, et al. Optimization of gold nanoparticle-based DNA detection for microarrays. J Fluorescence 2005;15:161-70
60. Vijayendran RA, Leckband DE. A quantitative assessment of heterogeneity for surface-immobilized proteins. Anal Chem 2001;73:471-80
61. Houseman BT, Mrksich M. Towards quantitative assays with peptide chips: a surface engineering approach. Trends Biotechnol 2002;20:279-81
62. MacBeath G, Schreiber SL. Printing proteins as microarrays for high-throughput function determination. Science 2000;289:1760-3
63. Houseman BT, Huh JH, Kron SJ, et al. Peptide chips for the quantitative evaluation of protein kinase activity. Nat Biotechnol 2002;20:270-4
64. Faraday M. Experimental relations of gold (and other metals) to light. Philos Trans R Soc Lond 1857;147:145-81
65. Mie G. Beiträge zur Optik trüber Medien speziell kolloidaler Metallösungen. [Contributions to optics of hazy media of special colloidal metal solutions]. Annalen der Physik 1908;25:377-445
66. Yguerabide J, Yguerabide EE. Light-scattering submicroscopic particles as highly fluorescent analogs and their use as tracer labels in clinical and biological applications. II. Experimental characterization. Anal Biochem 1998;262:157-76
67. Kreibig U, Vollmer M. Optical properties of metal clusters. Berlin; 1995
68. Yguerabide J, Yguerabide EE. Light-scattering submicroscopic particles as highly fluorescent analogs and their use as tracer labels in clinical and biological applications. I. Theory. Anal Biochem 1998;262:137-56
69. Kelly KL, Coronado E, Zhao LL, et al. The optical properties of metal nanoparticles: the influence of size, shape, and dielectric environment. J Phys Chem B 2003;107:668-77
70. Quinten M. Local fields close to the surface of nanoparticles and aggregates of

nanoparticles. Appl Phys B 2001;73:245-55

71. Elghanian R, Storhoff JJ, Mucic RC, et al. Selective colorimetric detection of polynucleotides based on the distance-dependent optical properties of gold nanoparticles. Science 1997;277:1078-81
72. Storhoff JJ, Elghanian R, Mucic RC, et al. One oot colorimetric differentiation of polynucleotides with single base imperfections using gold nanoparticle probes. J Am Chem Soc 1998;120:1959-64
73. Csaki A, Möller R, Straube W, et al. DNA monolayer on gold substrates characterized by nanoparticle labeling and scanning force microscopy. Nucleic Acids Res 2001;29:e81
74. Reichert J, Csaki A, Köhler JM, et al. Chip-based optical detection of DNA hybridization by means of Nanobead Labeling. Anal Chem 2000;72:6025-9
75. Köhler JM, Csaki A, Reichert J, et al. Selective labeling of oligonucleotide monolayers by metallic nanobeads for fast optical readout of DNA-chips. Sens Actuators 2001;76:166-72
76. Hacker GW, Grimelius L, Danscher G, et al. Silver acetate autometallography: an alternative enhancement technique for immunogold-silver staining (IGSS) and silver amplification of gold, silver, mercury and zinc in tissues. J Histotechnol 1988;11:213-21
77. Taton TA, Mirkin CA, Letsinger RL. Scanometric DNA array detection with nanoparticle probes. Science 2000;289:1757-60
78. Csaki A, Kaplanek P, Möller R, et al. The optical detection of individual DNA-conjugated gold nanoparticle labels after metal enhancement. Nanotechnology 2003;14:1262-8
79. Zhang G-J, Möller R, Kretschmer R, et al. Microstructured arrays with pre-synthesized capture probes for DNA detection based on metal nanoparticles and silver enhancement. J Fluorescence 2004;14:369-75
80. Alexandre I, Hamels S, Dufour S, et al. Colorimetric silver detection of DNA microarrays. Anal Biochem 2001;295:1-8
81. Li J, Xu C, Zhang Z, et al. A DNA-detection platform with integrated photodiodes on a silicon chip. Sens Actuators B 2005;106:378-82
82. Fritzsche W, Taton TA. Metal nanoparticles as labels for heterogeneous, chip-based DNA detection. Nanotechnology 2003;14:R63-73
83. Stimpson DI, Hoijer JV, Hsieh WT, et al. Real-time detection of DNA hybridization and melting on oligonucleotide arrays by using optical wave guides. Proc Natl Acad Sci USA 1995;92:6379-83
84. Taton TA, Lu G, Mirkin CA. Two-color labeling of oligonucleotide arrays via size-selective scattering of nanoparticle probes. J Am Chem Soc 2001;123:5164-5
85. Storhoff JJ, Lucas AD, Garimella V, et al. Homogeneous detection of unamplified genomic DNA sequences based on colorimetric scatter of gold nanoparticle probes. Nat Biotechnol 2004;22:883-7
86. Nam JM, Park SJ, Mirkin CA. Bio-barcodes based on oligonucleotide-modified nanoparticles. J Am Chem Soc 2002;124:3820-1
87. Nam JM, Thaxton CS, Mirkin CA. Nanoparticle-based bio-bar codes for the ultrasensitive detection of proteins. Science 2003;301:1884-6
88. Oldenburg SJ, Genick CC, Clark KA, et al. Base pair mismatch recognition using plasmon resonant particle labels. Anal Biochem 2002;309:109-16
89. Yguerabide J, Yguerabide EE. Resonance light scattering particles as ultrasensitive labels for detection of analytes in a wide range of applications. J Cell Biochem Suppl 2001;(Suppl 37):71-81
90. Wang Z, Lee J, Cossins AR, et al. Microarray-based detection of protein binding and functionality by gold nanoparticle probes. Anal Chem 2005;77:5770-4
91. Burstein E, Lundquist S, Mill DL. Surface enhanced Raman scattering. In: Chang RK, Furtak TE, editors, Metal colloids. New York: Plenum; 1982. p. 67-87
92. Kerker M, Wang D-S, Chew H, et al. Surface enhanced Raman scattering. In: Chang RK, Furtak TE, editors, Metal colloids. New York: Plenum; 1982. p. 109-28
93. Creighton JA. Surface enhanced Raman scattering. In: Chang RK, Furtak TE, editors, Metal colloids. New York: Plenum; 1982. p. 315-38
94. Freeman RG, Grabar KC, Allison KJ, et al. Self-assembled metal colloid monolayers: an approach to SERS substrates. Science 1995;267:1629-32
95. Nie S, Emory SR. Probing single molecules and single nanoparticles by surface-enhanced Raman scattering. Science 1997;275:1102-6
96. Cao YW, Jin R, Mirkin CA. Nanoparticles with Raman spectroscopic fingerprints for DNA and RNA detection. Science 2002;297:1536-40
97. Musick MDK, Keefe CD, Melinda H, Natan MJ. Stepwise construction of conductive Au colloid multilayers from solution. Chem Mat 1997;9:1499-501
98. Vo-Dinh T, Yan F, Wabuyele MB. Surface-enhanced Raman scattering for medical diagnostics and biological imaging. J Raman Spectrosc 2005;36:640-7
99. Xu S, Ji X, Xu W, et al. Immunoassay using probe-labelling immunogold nanoparticles with silver staining enhancement via surface-enhanced Raman scattering. Analyst 2004;129:63-8
100. Cao YC, Jin R, Nam JM, et al. Raman dye-labeled nanoparticle probes for proteins. J Am Chem Soc 2003;125:14676-7
101. Karlsson R. SPR for molecular interaction analysis: a review of emerging application areas. J Mol Recognit 2004;17:151-61
102. Peterlinz KA, Georgiadis RM. In situ kinetics of self-assembly by surface plasmon resonance spectroscopy. Langmuir 1996;12:4731-40
103. Georgiadis RM, Peterlinz KA, Peterson AW. Quantitative measurements and modelling of kinetics in nucleic acid monolayer films using SPR spectroscopy. J Am Chem Soc 2000;122:3166-73
104. Lyon LA, Musick MD, Natan MJ. Colloidal Au-enhanced surface plasmon resonance immunosensing. Anal Chem 1998;70:5177-83
105. Stuart DA, Haes AJ, Yonzon CR, et al. Biological applications of localised surface plasmonic phenomenae. IEE Proc Nanobiotechnol 2005;152:13-32
106. Haes AJ, Chang L, Klein WL, et al. Detection of a biomarker for Alzheimer's disease from synthetic and clinical samples using a nanoscale optical biosensor. J Am Chem Soc 2005;127:2264-71
107. Haes AJ, Van Duyne RP. A nanoscale optical biosensor: sensitivity and selectivity of an approach based on the localized surface plasmon resonance spectroscopy

of triangular silver nanoparticles. J Am Chem Soc 2002;124:10596-604

108. Boyer D, Tamarat P, Maali A, et al. Photothermal imaging of nanometer-sized metal particles among scatterers. Science 2002;297:1160-3
109. Koebel M, Zimmt MB. Photothermal readout of surface-arrayed proteins: attomole detection levels with gold nanoparticle visualization. J Phys Chem B 2005;109:16736-43
110. Marcon L, Melnyk O, Stievenard D. Current based antibodies detection from human serum enhanced by secondary antibodies labelled with gold nanoparticles immobilized in a nanogap. Biosens Bioelectron 2008;23(7):1185-8
111. Möller R, Csaki A, Köhler JM, et al. Electrical classification of the concentration of bioconjugated metal colloids after surface adsorption and silver enhancement. Langmuir 2001;17:5426-30
112. Park SJ, Taton TA, Mirkin CA. Array-based electrical detection of DNA with nanoparticle probes. Science 2002;295:1503-6
113. Urban M, Möller R, Fritzsche W. A paralleled readout system for an electrical DNA-hybridization assay based on a microstructured electrode array. Rev Sci Instrum 2003;74:1077-81
114. Festag G, Steinbrück A, Csaki A, et al. Single particle studies of the autocatalytic metal deposition onto surface-bound gold nanoparticles reveal a linear growth. Nanotechnology 2007;18:015502 (10pp)
115. Diessel E, Grothe K, Siebert HM, et al. Online resistance monitoring during autometallographic enhancement of colloidal Au labels for DNA analysis. Biosens Bioelectron 2004;19:1229-35
116. Tsai C-Y, Chang T-L, Uppala R, et al. Electrical detection of protein using gold nanoparticles and nanogap electrodes. Jpn J Appl Phys Part 1 2005;44:5711-6
117. Li J, Xue M, Wang H, et al. Amplifying the electrical hybridization signals of DNA array by multilayer assembly of Au nanoparticle probes. Analyst 2003;917-23
118. Moreno-Hagelsieb LL, Pampin PE, Bourgeois R, et al. Sensitive DNA electrical detection based on interdigitated Al/Al2O3 microelectrodes. Sens Actuators B 2004;98:269-74
119. Hainfeld JF, Eisen RN, Tubbs RR, et al. Enzymatic metallography: a simple new staining method. In: Voekl E, Piston D, Gauvin R, editors, Proceedings of microscopy and microanalysis 2002. New York: Cambridge University Press; 2002. p. 916CD
120. Furuya FR, Joshi VN, Hainfeld JF, et al. Enzymatic metallography as a correlative in light and electron microscopy. In: Anderson IM, Price R, Hall E, editors, Proceedings of microscopy and microanalysis. New York: Cambridge University Press; 2004:1210CD
121. Willner I, Baron R, Willner B. Growing metal nanoparticles by enzymes. Adv Mater 2006;18:1109-20
122. Möller R, Powell RD, Hainfeld JF, et al. Enzymatic control of metal deposition as key step for a low-background electrical detection for DNA chips. Nano Lett 2005;5:1475-82
123. Dequaire M, Degrand C, Limoges B. An electrochemical metalloimmunoassay based on a colloidal gold label. Anal Chem 2000;72:5521-8
124. Castañeda MT, Merkoçi A, Pumera M, et al. Electrochemical genosensors for biomedical applications based on gold nanoparticles. Biosens Bioelectron 2007;22:1961-7
125. Authier L, Grossiord C, Brossier P. Gold nanoparticle-based quantitative electrochemical detection of amplified human cytomegalovirus DNA using disposable microband electrodes. Anal Chem 2001;73:4450-6
126. Wang J, Xu D, Kawde AN, et al. Metal nanoparticle-based electrochemical stripping potentiometric detection of DNA hybridization. Anal Chem 2001;73:5576-81
127. Cai H, Wang Y, He P, et al. Electrochemical detection of DNA hybridization based on silver-enhanced gold nanoparticle label. Anal Chim Acta 2002;469:165-72
128. Wang J, Xu D, Polsky R. Magnetically-induced solid-state electrochemical detection of DNA hybridization. J Am Chem Soc 2002;124:4208-9
129. Wang J, Liu G, Merkoci A. Electrochemical coding technology for simultaneous detection of multiple DNA targets. J Am Chem Soc 2003;125:3214-5
130. Fanjul-Bolado P, Hernandez-Santos D, Gonzalez-Garcia MB, et al. Alkaline phosphatase-catalyzed silver deposition for electrochemical detection. Anal Chem 2007;79:5272-7
131. Okahata Y, Kitamura Y, Hagiwara N, et al. Quantitative detection of binding of PCNA protein to DNA strands on a 27 MHz quartz-crystal microbalance. Nucleic Acids Symp Ser 2000;243-4
132. Zhou XC, O'Shea SJ, Li SFY. Amplified microgravimetric gene sensor using Au nanoparticle modified oligonucleotides. Chem Commun 2000;953-4
133. Patolsky F, Ranjit KT, Lichtenstein A, et al. Dendritic amplification of DNA analysis by oligonucleotide-functionalized Au-nanoparticles. Chem Commun 2000;1025-6
134. Weizmann Y, Patolsky F, Willner I. Amplified detection of DNA and analysis of single-base mismatches by the catalyzed deposition of gold on Au-nanoparticles. Analyst 2001;126:1502-4
135. Su M, Li S, Dravid VP. Microcantilever resonance-based DNA detection with nanoparticle probes. Appl Phys Lett 2003;82:3562-4
136. Hansen KM, Ji HF, Wu G, et al. Cantilever-based optical deflection assay for discrimination of DNA single-nucleotide mismatches. Anal Chem 2001;73:1567-71
137. Fritz J, Baller MK, Lang HP, et al. Translating biomolecular recognition into nanomechanics. Science 2000;288:316-8
138. Li H, Huang J, Lv J, et al. Nanoparticle PCR: nanogold-Assisted PCR with Enhanced Specificity. Angew Chem Int Ed Engl 2005;117:5230-3
139. Li M, Lin YC, Wu CC, et al. Enhancing the efficiency of a PCR using gold nanoparticles. Nucleic Acids Res 2005;33:e184
140. Nam JM, Stoeva SI, Mirkin CA. Bio-bar-code-based DNA detection with PCR-like sensitivity. J Am Chem Soc 2004;126:5932-3
141. Thaxton CS, Hill HD, Georganopoulou DG, et al. A bio-bar-code assay based upon dithiothreitol-induced oligonucleotide release. Anal Chem 2005;77:8174-8
142. Georganopoulou DG, Chang L, Nam J-M, et al. Nanoparticle-based detection in cerebral spinal fluid of a soluble pathogenic biomarker for Alzheimer's disease. Proc Natl Acad Sci USA 2005;102:2273-6

Chip-based molecular diagnostics using metal nanoparticles

Affiliation
Grit Festag, PhD student Doctoral Fellow,
T Schüler, Andrea Steinbrück PhD student,
Doctoral Fellow, Andrea Csáki PhD,
Post-doctoral Fellow, Robert Möller PhD,
Head of Jenaer Biochip Initiative,
Friedrich-Schiller-University Jena &
Wolfgang Fritzsche† PhD, Head of Nano
Biophotonics Department
†Author for correspondence
Institute of Photonic Technology,
POB 100239,
07702 Jena, Germany
Tel: +49 3641 206304; Fax: +49 3641 206344;
E-mail: fritzsche@ipht-jena.de

2.6 Growth and percolation of metal nanostructures in electrode gaps leading to conductive paths for electrical DNA analysis

Grit Festag, Thomas Schüler, Robert Möller, Andrea Csáki, and Wolfgang Fritzsche

Nanotechnology (**2008**) 19 (125303): 1-9

IOP PUBLISHING NANOTECHNOLOGY
Nanotechnology 19 (2008) 125303 (9pp) doi:10.1088/0957-4484/19/12/125303

Growth and percolation of metal nanostructures in electrode gaps leading to conductive paths for electrical DNA analysis

Grit Festag[1], Thomas Schüler[2], Robert Möller[2], Andrea Csáki[1] and Wolfgang Fritzsche[1]

[1] Nano Biophotonics, Institute of Photonic Technology, POB 100239, 07702 Jena, Germany
[2] Jenaer Biochip Initiative, Friedrich Schiller University Jena, Germany

E-mail: wolfgang.fritzsche@ipht-jena.de

Received 25 October 2007, in final form 15 January 2008
Published 20 February 2008
Online at stacks.iop.org/Nano/19/125303

Abstract

Metal nanostructures are promising novel labels for microarray-based biomolecular detection. Additional silver deposition on the surface-bound labels strongly enhances the sensitivity of the system and can lead to continuous metal areas, which enable an electrical readout especially for simple and robust point-of-care analyses. In this paper, atomic force microscopy (AFM) was used to study different routes of metal deposition on labelled DNA–DNA duplexes in electrode gaps. Besides the well-established metal-induced silver enhancement, a recently introduced enzymatic silver deposition was applied and proved highly specific. The *in situ* characterization was especially focused on the nanostructure percolation—the moment at which the nanoparticulate film becomes continuous and electrically conducting. The formation of conducting paths, continuous from one electrode to the other, was followed by complementary electrical measurements. Thereby, a percolation threshold was determined for the surface coverage with metal structures, i.e. the required metallized area to achieve conductance. Complementary graphic simulations of the growth process and graphic 'conductance measurements' were developed and proved suitable to model the metal deposition and electrical detection. This may help to design electrode arrays and identify optimum enhancement parameters (required seed concentration and shell growth) as well as draw quantitative conclusions on the existing label (i.e. analyte) concentration.

(Some figures in this article are in colour only in the electronic version)

1. Introduction

DNA microarrays are widely used for a fast and highly parallel analysis of nucleic acids [1]. Thereby, the presence of combinations of hundreds or even thousands of different analytes can be detected. A typical example of such highly integrated microarrays is expression studies, determining the difference in gene expression between healthy and, for example, cancer cells in order to identify targets for therapies. In these cases, a large number of tests combined on one substrate is required, and this justifies the rather complicated and expensive approach.

On the other hand, DNA analytics could be used for a variety of on-site applications, where the identification of DNA out of a selection of just 10 to 100 possible species but done in a simple and robust manner would open new fields of applications, for example in food processing. Here, simple techniques without the need for special personnel or complicated (and therefore expensive) readers are essential, both points where fluorescence detection fails. Here, biomolecule labelling using metal nanoparticles [2] has gained noteworthy interest because these labels have the potential to fulfil the mentioned requirements. Besides the use of their size- and distance-dependent scattering properties [3–5], an

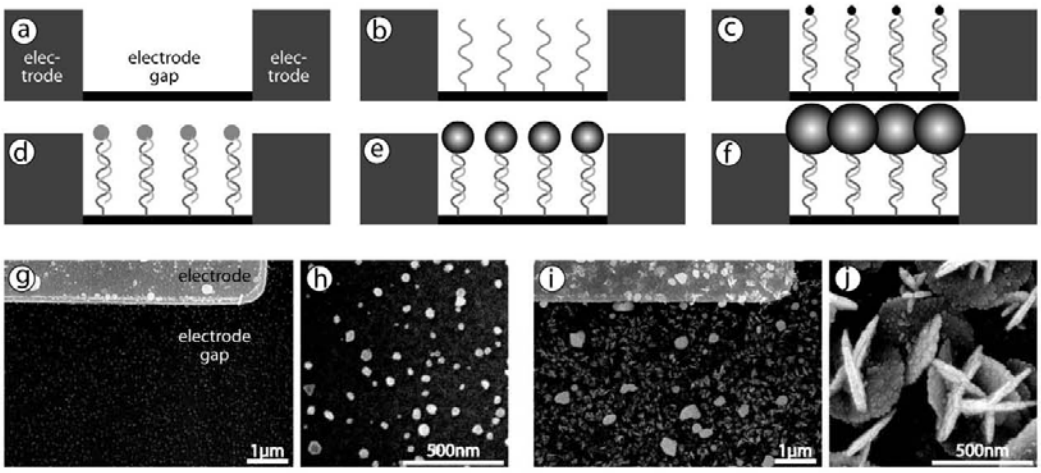

Figure 1. Scheme of the detection principle ((a)–(f)) and SEM images of metal nanostructures ((g)–(j)). To enable the electrical readout of surface-bound metal particles silicon oxide chips were micro-structured with gold electrodes (a). After the surface functionalization, different capture oligonucleotides of a known sequence were covalently immobilized (b) in the electrode gap (10 μm). The hybridization with complementary, biotin-modified target molecules led to biotinylated DNA duplexes (c), to which streptavidin-modified gold nanoparticles or an enzyme (horseradish peroxidase) could bind (d). If the subsequent silver deposition (e) (nanoparticle-induced or enzyme-catalysed with EnzMet, respectively) still did not lead to conducting paths, a further silver enhancement (f) was applied until the metal structures bridged the gap. As result of the above-mentioned detection, the SEM images show ((g), (h)) streptavidin-modified gold nanoparticles (15 nm in diameter), and ((i), (j)) enzymatically grown nanostructures (120 s EnzMet) specifically bound in an electrode gap as ((g), (i)) an overview with the partial upper electrode. ((h), (j)) The detailed views show distinctive differences in size and shape of the metal nanostructures.

additional silver deposition on immobilized particle labels offered new detection methods based on simple absorption effects [6]. The so-called autometallography was worked out as a photographic technique and has been used for decades to enhance the contrast of nanoparticle-stained samples in light and electron microscopy [7, 8]. This signal enhancement led to the term 'metal enhancement'. Besides the well-established metal-induced silver enhancement, recently introduced enzymatic metal depositions proved to be highly specific enhancement methods [9–11]. In addition to the optical detection, other approaches exploit the electrical conductivity of these metal depositions to electrically detect nanoparticle-labelled DNA molecules [12–14]. Thereby, the immobilization of capture molecules in electrode gaps was followed by a specific hybridization with complementary target probes and the introduction of gold nanoparticles as labels. Additional metal deposition on the surface-bound labels led to particle growth and percolation into a continuous layer, thereby bridging the gap between electrodes. As a result, molecular binding events could be detected by changes in electrical resistance or capacitance, respectively. A typical system is based on a half-inch chip of oxidized silicon exhibiting a micro-structured gold electrode array of 42 gaps of 10 μm width [15].

To avoid under- or over-enhancement of the samples (leading to false negative or false positive results, respectively), knowledge about the characteristics of nanoparticle growth is required. Theoretical approaches described the growth of particles on electrode surfaces as a function of experimental parameters (such as reactant concentration, time, and surface area) both for an independent growth of adjacent nanoparticles and for strong interactions [16–19]. Experimental work was done to characterize the growth of gold nanoparticles by specific metal deposition as used for signal enhancement in bioanalytics [20]. These single particle studies revealed a linear growth behaviour and a dependence of the growth rate on the seed diameter. With regard to electrical detection schemes and the formation of conducting paths, the percolation threshold is of special interest, i.e. the moment at which the nanoparticulate films become continuous to such an extent that macroscopic currents can be conducted. Optical approaches described this transition from isolated nanoparticles to an interconnected, eventually continuous metal film by a characteristic change of ellipsometric parameters [21–23] or a drop of surface-enhanced Raman scattering (SERS) enhancement when particles start to percolate [24].

However, the *in situ* (i.e. in electrode gaps) characterization of growing conductive nanostructures by metal deposition on metal seeds is of great importance for the design and optimization of test systems based on electrical detection. Moreover, a theoretical growth simulation of a given nanoparticle-surface coverage in an electrode gap is highly desirable, for example to estimate the required nanoparticle concentration or enhancement time without the need for experimental work. On the other hand, it could be possible to contrarily draw conclusions from known enhancement parameters (incubation time and growth rates) about the start concentration of metal seeds and thereby analyte molecules.

This paper describes the growth of metal nanostructures, specifically bound to DNA–DNA complexes, by electroless silver deposition regarding the formation of electrically conductive paths (figure 1). The growing particles are

characterized by AFM and scanning electron microscopy (SEM) imaging, and especially the percolation process is followed by complementary electrical measurements. The experimental results are completed by graphic simulations of the growth process and a likewise conductance check of a given nanostructure arrangement, thereby allowing us to estimate the lateral growth of the particles required to achieve conductance.

2. Materials and methods

2.1. Substrate functionalization

The characterization of the growth and percolation process was done at metal nanostructures specifically bound on a planar chip surface. To enable an electrical readout of the substrates the chips were fabricated from an oxidized silicon wafer with a 100 nm gold layer, which was micro-structured by standard photolithographic procedures resulting in an array of 42 electrode gaps, 10 μm wide [15]. Each of these measurement sites was wired to a contact pad, from which one can obtain individual readouts. The chip surface was chemically modified by (3-glycidyloxypropyl) trimethoxysilane (Sigma-Aldrich, Taufkirchen, Germany) [25, 26] to bind the amino-modified capture oligonucleotides (JenaBioscience, Jena, Germany). The DNA solutions were applied as droplets and placed directly in the electrode gaps by means of an automatic dispenser. To reveal the specificity of the DNA detection, different capture probes (20 μM in spotting solution) were immobilized in the gaps: a complementary sequence (AAGAAGAGGGATA CTTCTCTATCTCTGCA), a sequence containing a three-base pair deletion (GGTAGGAAGAAGGGAAAAGAAG... ATA CT), and a total non-complementary sequence (GCTG-CAAATACATCTCCCTCATC) as negative control. A directly biotinylated oligonucleotide worked as a positive control (TTTTTTCAGCATGTGCTCCTTGATTCTATG), leading to signals without the need for hybridization.

2.2. Hybridization and labelling

After the chip functionalization, biotin-modified target oligonucleotides (TGCAGAGATAGAGAAGTATCCTCTTCTT) were diluted in 2.5 $\times$ sodium chloride/sodium citrate (SSC) +0.1% sodium dodecyl sulfate (SDS) to 1 μM and hybridized to the capture molecules. The substrates were incubated at 62 °C for 3 h in a humidity chamber and rinsed in washing solutions of different SSC contents after standard hybridization protocols to remove not tightly bound target probes. The matching biotinylated DNA duplexes were then labelled with either 15 nm sized streptavidin-modified gold nanoparticles (STP-Au15; BBInternational, Cardiff, UK) or streptavidin-modified horseradish peroxidase–polymer complexes (STP-HRP; Sigma-Aldrich, Taufkirchen, Germany). Therefore, the stock solutions were diluted according to manufacturer's instructions and a protocol from the literature [27]: STP-Au15 1:20 (v/v) in phosphate buffered saline (PBS) pH 7.4 + 0.1% bovine serum albumin and STP-HRP 1:1000 (v/v) in PBS pH 7.4 + 0.05% Tween 20, respectively. The solution was applied on the chip as a droplet for 1 h at room temperature. After washing in PBS (3 $\times$ 5 min) or PBS + 0.05% Tween 20 (6 $\times$ 5 min), respectively, the remaining salts were removed by a short washing step in double-distilled water. Finally, the nanoparticle-labelled substrates were dried in a stream of nitrogen whereas the enzyme-labelled chips were processed immediately without allowing the enzyme to run dry.

2.3. Metal enhancement

The nanoparticle labels served as seeds for a metal-induced silver deposition by incubation with silver enhancing solution. We used either a home-made 12 mM silver acetate (AgAc)/45 mM hydroquinone solution [8, 28] or a commercial silver enhancement kit (BBI; BBInternational, Cardiff, UK). Light was avoided to prevent photo-induced unspecific silver fallout. A quasi-continuous addition of fresh solutions (every 2 min) and constant shaking should avoid localized depletion effects [20]. Tracking the enzymatic approach, the bound peroxidase complexes catalysed the silver deposition using the EnzMet ultrasensitive™ silver development kit (EnzMet; Nanoprobes Inc., Yaphank, NY). According to the manufacturer's manual, the enzyme-labelled chips were incubated for 15–300 s with the different kit components. After incubation under constant shaking the enhancement reactions were stopped by immersion in deionized water and the chips were dried in a stream of nitrogen. When there was still no conductance achieved, the chips of both labelling strategies could be further enhanced by metal-induced silver enhancement.

2.4. Characterization

2.4.1. Scanning force and electron microscopy. To study the particle growth process the chips were stepwise enhanced and analysed by atomic force microscopy (AFM). Thereby, the complete 10 μm wide electrode gap was imaged using the tapping mode in air (Dimension 3100 and NanoScope™ 5.12r2; Digital instruments, Santa Barbara, CA). Since AFM lacks the chemical/material contrast and allows mainly for height information, the samples were additionally scanned by scanning electron microscopy (SEM) to visualize especially metal nanostructures.

2.4.2. Electrical readout. The resistance measurements were carried out by a custom-built chip reader as described elsewhere in detail [15]. The signals were derived as electrical conductance from the reciprocal resistance values.

2.4.3. Image analysis and graphical simulation. AFM and SEM images were analysed by the open-source image processing and analysis program Image J 1.38, where a special plug-in enabled the import of original NanoScope™ files (12 μm $\times$ 12 μm images), keeping all height information [20]. To monitor the growth process of the metal nanostructures, the difference in particle dimensions were measured before and after the metal deposition. Since in AFM images the lateral dimensions are hampered by tip convolution, we analysed the grown particle heights. To handle the large amount of structures to be analysed in a gap (about 2000)

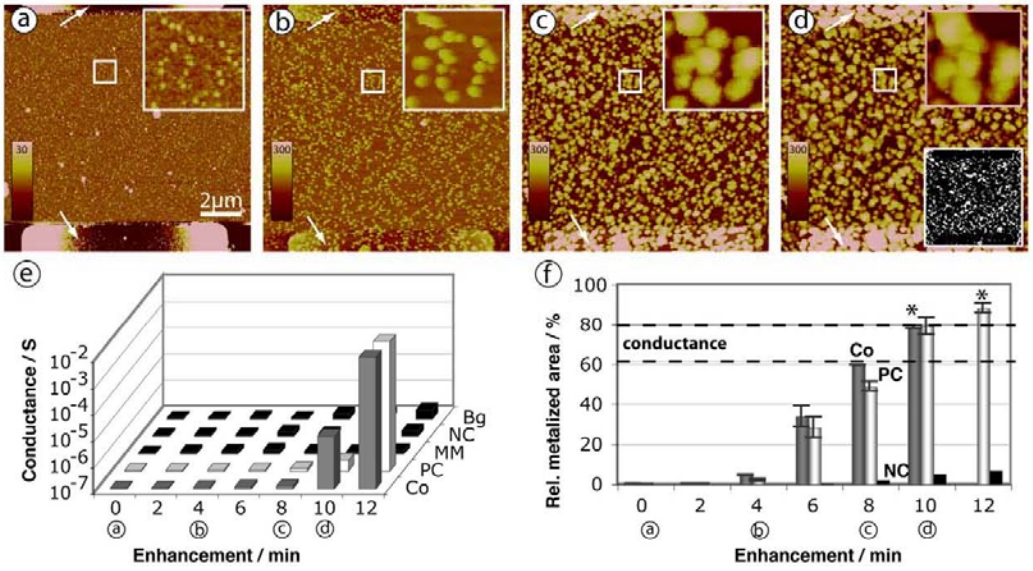

Figure 2. Metal-induced silver enhancement of gold nanoparticle labels: AFM imaging ((a)–(d); electrodes top and bottom in the picture; see arrows), corresponding measurements of electrical conductance (e) and metallized gap area (f). The capture oligonucleotides were immobilized in electrode gaps, hybridized with biotin-modified target probes and then labelled with streptavidin-gold nanoparticles (STP-Au15). The AFM revealed the growth of particle labels bound to the complementary sequence (a) without, (b) after 4 min, (c) 8 min, and (d) 10 min BBI silver enhancement™. (e) 10 or 12 min silver enhancement led to measurable conductance at the complementary sequence (Co) and the directly biotin-modified positive control (PC), respectively. (f) The relative metallized area (threshold at a height of 80 nm) was linearly dependent on the enhancement time. A metallization of about 60–80% was apparently sufficient to enable electrical conductance (∗). In contrast, the non-matching samples (mismatches MM, non-complementary negative control NC, and background Bg) revealed neither significant metal deposition nor electrical conductance. Upper right insets in (a)–(d): zoom-ins (1 μm × 1 μm as indicated in the overview) of a particle selection to show the growth and percolation of the particles. Lower right inset in (d): gap image thresholded at a height of 80 nm to point out the continuous nanoparticulate paths.

the particles were automatically identified as local maximum heights (within a noise tolerance by the *Find Maxima* function). The identified particles were either counted to determine the surface coverage with particles or served for height analysis without the need for analysing every single particle. In addition to the AFM height measurements, the grown particles were analysed in SEM images by measuring the particle area/diameter.

For a correlation between the required metallized surface area in the gap and electrical conductance we measured the surface area which was covered with metal nanostructures. The AFM files with three-dimensional particle structures were thresholded to binary images, resulting in particles as mask-like, two-dimensional structures. These black areas on a white background could be quantified easily with the image analysis program (measurement parameter 'area fraction'). Thereby, a threshold of half the mean particle height turned out to be in good agreement with SEM measurements of lateral dimensions. Moreover, the AFM images served as basis for a growth simulation to model the growth of existing nanostructures graphically with the Image J software. Thus, imaged structures were converted to particle masks by thresholding the AFM images (figures 5(a) and (b)). In the resulting binary images, the black particle areas were selected (*Create Selection* function), and subsequently each particle selection was graphically enlarged by 1 pixel (*Enlarge* function; figures 5(c) and (d)). Additionally, the visualized electrode gaps containing metal particles could be tested graphically for conductance. On the basis of the binary gap image, continuous areas connecting one electrode to the other should be identified. By using the *Flood Fill* function all connected particle areas will be coloured (e.g. in grey). Beginning with the upper electrode the colouring of the lower electrode means fully connective paths between the two electrodes (figure 5(d)).

3. Results and discussion

The electric-resistive detection is based on the formation of conductive paths between the electrodes. After hybridizing the immobilized capture DNA with complementary biotin-modified target DNA, conductive metal nanostructures could be bound to the biotin labels. Besides the well-known metal nanoparticle-based approach, metal structures could also be developed that were enzyme-catalysed. Complementary capture and target DNA should yield a sufficiently high surface density of metal labels, which are then able to percolate in the course of a subsequent metal enhancement, thereby bridging the electrode gap.

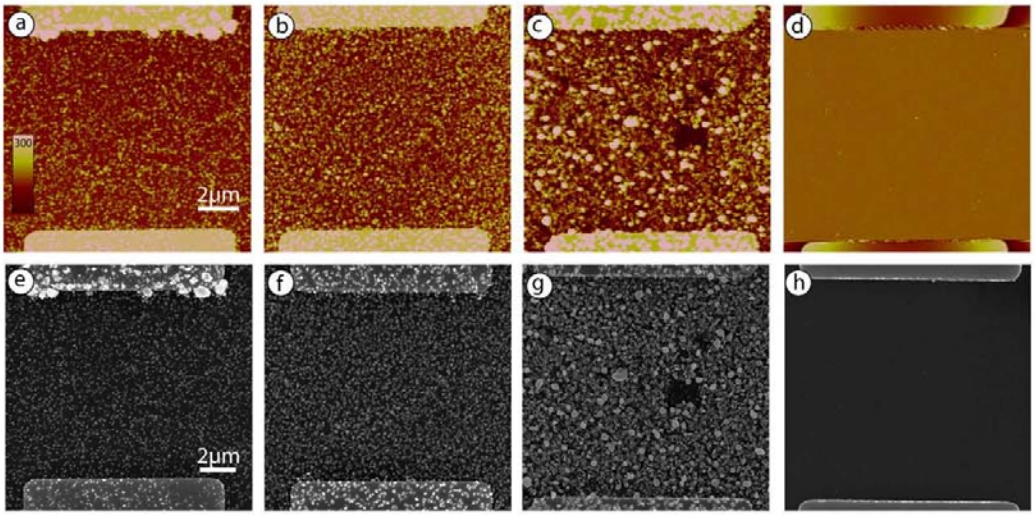

Figure 3. Enzyme-catalysed silver enhancement in AFM ((a)–(d)) and SEM ((e)–(h)). The capture oligonucleotides were immobilized in electrode gaps (electrodes top and bottom in the picture), hybridized with biotin-modified target probes and then labelled with streptavidin–horseradish peroxidase. As shown for the complementary capture sequence, the enzyme labels catalysed the silver deposition by EnzMet silver development for ((a), (e)) 15 s, ((b), (f)) 30 s, and ((c), (g)) 300 s. ((d), (h)) The partially complementary sequence showed the high specificity of the enzymatic silver deposition by the lack of significant metal deposition in the gap.

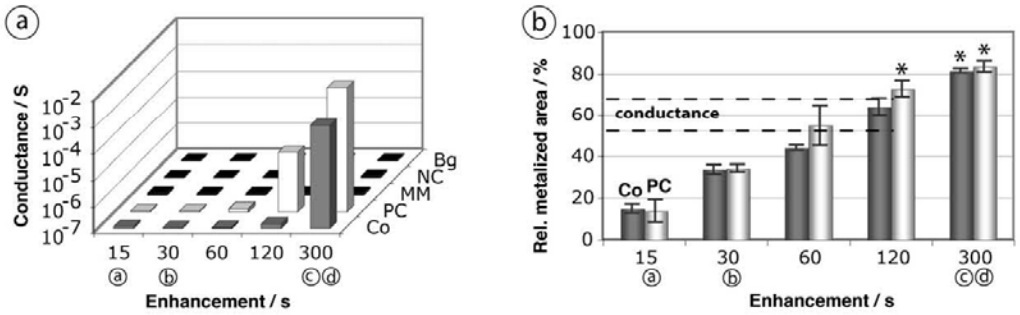

Figure 4. Enzyme-catalysed silver enhancement in electrode gaps: measurements of electrical conductance (a) and metallized gap area (b). Capture oligonucleotides were immobilized in electrode gaps, hybridized with biotin-modified target probes and then labelled with streptavidin–horseradish peroxidase. (a) The enzymatic silver deposition (EnzMet silver development) of the directly biotin-modified positive control (PC) and the complementary sequence (Co) for 120 s or 300 s, respectively, led to measurable conductance. (b) The relative metallized area (threshold at a height of 60 nm) was linearly dependent on the enhancement time. A metallization of about 50–70% was apparently sufficient to enable electrical conductance (∗). On the other hand, the non-matching probes (mismatches MM, non-complementary negative control NC, and background Bg) did not reveal any electrical conductance, pointing to the high specificity of the system.

3.1. Metal-catalysed silver deposition on gold nanoparticles

The biotinylated DNA duplexes were labelled with streptavidin-modified gold nanoparticles, 15 nm in diameter. The resulting experimental surface coverage, obtained graphically from AFM images (about 2×10^9 particles cm^{-2}), corresponded to a low coverage according to the definition by Fransaer and Penner [18]. Because no conductance had yet been achieved, the immobilized nanoparticles were subsequently enhanced with the BBI silver enhancement kit in 2 min steps. Figures 2(a)–(d) show the growing metal particles on the example of one and the same gap containing the complementary capture sequence. Both the complementary sequence (Co) and the positive control (PC) revealed numerous 15 nm sized nanoparticles, which grew dependent on the enhancement time until they filled the gap nearly completely. Correspondingly, measurable conductance was obtained after 10 or 12 min silver enhancement (Co and PC, respectively; figure 2(e)). On the other hand, the partially complementary (MM) and non-complementary (NC) sequence as well as the gaps without any capture DNA (background, Bg) lacked a significant metal deposition. Although there has been some non-specific silver deposition in the course of the enhancement process, the deposited metal structures were far from achieving measurable conductance. To reveal a probable relationship between the metallized surface area and measurable electrical conductance, the metal deposition in the

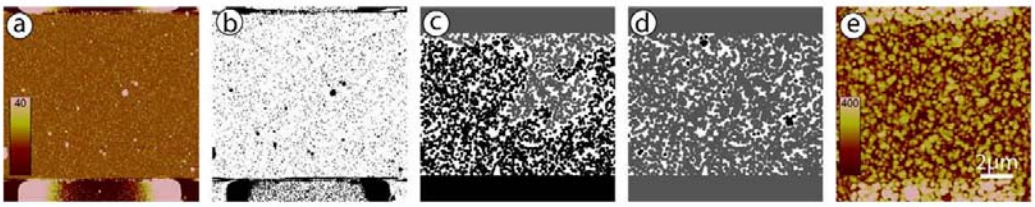

Figure 5. Simulation of nanoparticle growth and graphical conductance testing in electrode gaps (electrodes top and bottom in the picture). The capture oligonucleotides were immobilized in electrode gaps, hybridized with biotin-modified target probes and then labelled with streptavidin–gold nanoparticles (STP-Au15). At the example of the complementary probe, the (a) AFM image of the labelled but not enhanced particles was (b) thresholded (at a height of 7 nm). The obtained 'particle masks' were stepwise enlarged (1 px/24 nm per step) and ((c) and (d)) tested graphically for conductance. (c) While the enhancement of a 72 nm shell did not lead to conductance (the grey has not reached the black lower electrode), (d) a 96 nm shell enabled the bridging of the gap (lower electrode in grey). For comparison, (e) the AFM image of the correspondent conductive but experimentally enhanced sample (10 min AgAc) is shown.

gap was quantified and compared to electrical measurements. Therefore, the AFM images with bound three-dimensional particle structures were thresholded to binary images at half the mean particle height (80 nm), which has turned out to be in good agreement with SEM measurements of lateral dimensions. Thereby, all structures above the threshold height were considered, converted to two-dimensional 'particle masks' and the resulting particle areas could be quantified. First, the relative metallized area in the gap increased nearly linearly dependent on the enhancement time (figure 2(f)), pointing to an unlimited particle height growth with sufficient reagent supply. Despite some non-specific silver deposition, the extent of metal deposition of the positive DNA samples (Co, PC) exceeded that on samples without matching sequences (NC) considerably. Moreover, the obtained metallized areas were related to the electrical measurements. Thereby, a metallization of about 60–80% of the gap area seemed to enable the formation of conductive paths connective from one electrode to the other (∗). This limit could not be specified more exactly because—beside the metallized area—the distribution of the conductive structures also influences the formation of conductive paths. This could also be the reason for the fact that the complementary probe (Co) already achieved conductance whereas the positive control (PC) still lacked any drop in resistance, although both showing similar relative metallization.

3.2. Enzyme-catalysed silver deposition

Since the nanoparticle labelling is often associated with non-specific particle binding and therefore unwanted metal deposition, the enzymatic silver development offers an interesting labelling alternative. The biotinylated DNA duplexes were labelled with streptavidin-modified horseradish peroxidase polymers and subsequently incubated with EnzMet silver development for 15–300 s. Because the drying of the enzyme hampers its activity, an enzymatic re-enhancement of the sample was impossible. This is why—unlike the nanoparticle-based approach, where one and the same chip sample was stepwise enhanced—in the enzymatic approach the different incubation times of enzymatic metal deposition have been run on different supports/chips. AFM imaging (figure 3 top) of the gaps revealed distinctive metal depositions for both the complementary sequence (figures 3(a)–(c)) and the positive control, which were rising with increasing incubation time. The metal character of the structures in the gap was supported by complementary SEM imaging (figure 3 bottom). Here again, the metal deposition grew in the course of increasing enhancement time until the metal nanostructures filled the gap considerably (figures 3(e)–(g)). In contrast to the matching probes, neither the partially complementary (figures 3(d) and (h)) nor the non-complementary capture sequence showed any significant metal deposition, pointing to a highly specific hybridization, labelling and/or metal enhancement. Unlike the well-defined particle labels, the enzymatically grown metal structures were of irregular shape and size and could hardly be distinguished from each other.

Correspondent electrical measurements (figure 4(a)) revealed conductance for the positive control (PC) and the complementary sequence (Co). While after 300 s EnzMet silver development both positive capture probes led to a rise in conductance, after 120 s EnzMet incubation at least the positive control became conductive. Again, the observed discrepancy in the onset of conductance between the two positive samples is probably due to a different arrangement of the metal labels, influencing the interparticle distances and thereby the formation of conducting paths. In contrast, no conductance could be achieved for the non-matching capture sequences (MM, NC, Bg), underlining the high specificity of this detection scheme. For a correlation of the electrical conductance with the metal deposition, again, the deposited silver structures in the gap were quantified by thresholding the AFM images at half the mean particle height (60 nm; figure 4(b)).

Dependent on the enzymatic enhancement time the relative metallized gap area grew linearly for the complementary sequence and the positive control. However, about 10% relative metallization at 15 s EnzMet increased up to 80% for an incubation of 300 s. On the other hand, even for the longest incubation time the metal deposition in gaps without matching capture sequences was negligible. Furthermore, 50–70% metallized gap area seemed to enable the bridging of the electrodes. This percolation limit was comparable with percolation thresholds described in the literature. Wang and Rothberg

found that the Raman intensity dropped sharply near a percolation threshold of 50–60% because the hot spots in SERS were inactivated when conducting paths allowed plasmons to propagate [24]. As another independent analysis method, spectroscopic ellipsometry identified the onset of the electrodynamic coupling between adjacent nanoparticles to occur near the percolation threshold at a surface area coverage of 52% [22].

Additionally, we wanted to know whether the enzymatically developed samples, which were still not conductive, could be further enhanced up to conductance by metal-induced silver enhancement without objectionable non-specific metal depositions. As examples, the chips developed with EnzMet for 30 and 120 s were further treated by silver acetate/hydroquinone enhancement solutions in 2 min steps. After an acceptable enhancement interval (10 and 8 min in total, respectively) both the complementary sequence and the positive control achieved conductance, whereas the non-matching probes were still lacking a drop in resistance.

3.3. Growth simulation and graphical conductance testing

With regard to an optimization of the electrode array design, the applied size and concentration of metal labels as well as the enhancement solution (i.e. growth rate), a simulation of the enhancement process is desirable. To enable predictions about the onset of measurable conductance, the growth and percolation process of immobilized metal structures was graphically modelled (figure 5) up to the formation of conductive paths, based on AFM images of the metal-labelled but not enhanced samples. As shown for STP-Au15 labelled complementary DNA duplexes, the NanoScope™ files (figure 5(a)) were thresholded at half particle height (at 7 nm) yielding 'particle masks' as black areas in the binary image (figure 5(b)). For growth simulation the particle seeds were stepwise enlarged by 1 pixel (i.e. 24 nm for the given image resolution). Each gap image with 'enhanced' particles was then tested for conductance, graphically identified as continuous regions. Starting with the upper electrode, the connected areas were coloured in grey. Remained the lower electrode in black no conductance has been achieved, as shown for particles enlarged by a 72 nm shell (3 px) (figure 5(c)). On the other hand, a shell growth of 96 nm (4 px) led to fully conductive paths between the two electrodes, resulting in a colouring of the lower electrode as well (figure 5(d)).

For a verification of the 'graphical conductance' testing, the binary images derived from original AFM files of enhanced samples were additionally examined and compared to electrical measurements. All graphically analysed samples of both the nanoparticle samples and the enzyme-labelled samples fully corresponded to the electrical conductance measurements, proving this method a suitable alternative for graphical conductance testing especially with regard to the identification of an endpoint in graphical particle enhancement.

3.4. Height growth versus lateral growth

But how does the graphically simulated shell growth correlate with the experimental data? Because the exact shape of the nanostructures is not easily extractable from AFM images due to tip convolution, the thickness of the growing shell was analysed by measuring the growth in particle height. Different capture sequences were hybridized with biotin-modified target probes, labelled with streptavidin–gold nanoparticles (STP-Au15) and metal-induced enhanced (Co for 10 min; PC and NC for 12 min BBI silver enhancement™). The resulting mean experimental height growths in the electrode gaps were then compared to the simulated shell growth, required for electrical or graphical conductance, respectively. To estimate the non-specifically deposited silver, the mean height growth of the negative control was measured as well. Subtracting this value, the experimentally determined height differences were about twice as large as the simulated lateral growths. One possible reason for the observed discrepancy between the experimentally obtained height growth and the graphically simulated lateral growth could be that the apparent contact of adjacent particles in image analysis does not necessarily lead to a really conductive contact, thereby requiring a higher experimental shell growth. Moreover, even slight differences in the localization of contact surfaces could be crucial for the formation of conductive paths. Another interesting explanation could be a favoured growth in the z direction than in the x and y directions. This could be due to a better accessibility of the upper particle part, directly facing the enhancement solution. Furthermore, tightly neighbouring particles could compete for reagents (silver salt, reducing agent), leading to a limited growth rate if mass transport is not sufficiently warranted.

Since the lateral growth in the x and y directions was only derived from graphical simulation, the lateral dimensions should be further examined by SEM imaging. Moreover, the growth in the z direction (so far derived from the difference in local maximum heights between the samples before and after the enhancement) was further specified by measuring the height growth on a single particle level for a selected quantity of particles. To validate the size measurements with AFM (height) and SEM (diameter) first, gold nanoparticles of a defined size (20 nm in diameter with a size distribution of $\leqslant 10\%$ according to manufacturer's instructions; BBInternational, Cardiff, UK) were analysed by both methods. The measured particle height and diameter (21 ± 1 and 22 ± 2 nm by AFM and SEM, respectively) were in very good agreement with the known particle size (figure 6(a)), proving both methods as qualified for size measurements on a single particle level. Thus, the validated methods were used to compare the growth in particle height and diameter of nanoparticle labels (STP-Au15) of different capture DNA by silver deposition (Co for 10 min and PC for 12 min BBI, respectively). As assumed from the simulation results, the resulting data pointed to a stronger growth in the z direction than in the x and y directions (1.6-fold higher; figure 6(b)), suggesting a possible reagent depletion in between the particles.

4. Conclusions

In this paper, the formation of conductive parts resulting from the growth of metal nanoparticles positioned in an electrode gap was studied using both AFM and electrical measurements and was used to establish a simulation describing the process

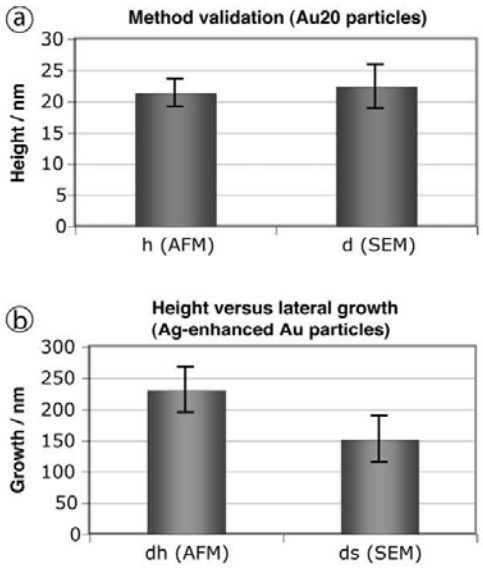

Figure 6. Comparison of height growth versus growth in the lateral direction by metal enhancement of immobilized gold nanoparticles on a single particle level. (a) 20 nm sized gold nanoparticles were analysed by AFM (particle height, (h)) and SEM (particle diameter, (d)) to validate the analysis procedures. (b) The validated measurement methods were used to determine the height and lateral shell growth of STP-Au15 particle labels of positive capture probes after silver enhancement (Co for 10 min and PC for 12 min, respectively). (a: 49; b: 121 analysed particles.)

sufficiently to predict it for a given starting set of particles. Thereby, a critical surface coverage with metal could be identified for the onset of conduction. This is a key step towards a mechanistic description of the process that is already used in the development of novel bioanalytical methods but where the understanding of the underlying mechanisms is still in its infancy. Complementary simulations of the growth process and graphic 'conductance measurements' were developed and proved suitable to model the metal deposition and electrical detection. This may help to design electrode arrays and identify optimum enhancement parameters (required seed concentration and shell growth). On the other hand, detailed knowledge about the enhancement process can enable conclusions on the present metal label, i.e. target concentration because the metal seed concentration on the surface is correlated with the onset of conductance [12]. Thinking of systematic point-of-care studies with a defined metal enhancement, simple and fast quantitative conclusions could be drawn on the basis of these investigations. The demonstrated graphic modelling does not require elaborate software, is easy to apply and therefore applicable for every interested user. Even without images from real samples one can graphically design electrode and label/seed structures to simulate the electrical detection route for individual assay layouts. An important question which could be addressed, for example, is the impact of the electrode gap size on the onset of conductance. In a first approximation, the size of the electrode gap does not significantly influence the onset of percolation, because percolation is mainly determined by the average distance of the particles for a rather homogeneous distribution. However, two points are important in this context. The electrode gap size must be smaller than the size of the capture DNA droplet that is applied using a spotting device, with a typical diameter in the 150–250 μm range. Furthermore, the percolation may be delayed with growing gap size because this decreases the possibility of a conduction path. According to our observations, this effect is less significant compared to the variations in the process (mainly due to inhomogeneous distribution of the particles) but will be addressed in future work.

Finally, the growth of gold nanoparticles by silver deposition turned out to be stronger in the z direction than in the x and y directions, which is surprising given the applied low particle seed concentration and the excess of enhancement solutions.

Acknowledgments

We thank F Jahn for SEM imaging. EnzMet™ reagents and protocols were provided by Nanoprobes Inc. This work was supported by the DFG (FR 1348/5-2) and the research project 'Jenaer Biochip Initiative' (JBCI) within the framework 'Unternehmen Region—Inno Profile' from the Federal Ministry of Education and Research, Germany (BMBF).

References

[1] Schena M, Heller R A, Theriault T P, Konrad K, Lachenmeier E and Davis R W 1998 *Trends Biotechnol.* **16** 301–6
[2] Fritzsche W and Taton T A 2003 *Nanotechnology* **14** R63–73
[3] Elghanian R, Storhoff J J, Mucic R C, Letsinger R L and Mirkin C A 1997 *Science* **277** 1078–81
[4] Storhoff J J, Elghanian R, Mucic R C, Mirkin C A and Letsinger R L 1998 *J. Am. Chem. Soc.* **120** 1959–64
[5] Taton T A, Lu G and Mirkin C A 2001 *J. Am. Chem. Soc.* **123** 5164–5
[6] Taton T A, Mirkin C A and Letsinger R L 2000 *Science* **289** 1757–60
[7] Danscher G 1984 *Histochemistry* **81** 331–5
[8] Hacker G W, Grimelius L, Danscher G, Bernatzky G, Muss W, Adam H and Thurner J 1988 *J. Histotechnol.* **11** 213–21
[9] Hainfeld J F, Eisen R N, Tubbs R R and Powell R D 2002 *Proc. Microscopy and Microanalysis 2002* ed E Voekl (New York: Cambridge University Press) p 916CD
[10] Furuya F R, Joshi V N, Hainfeld J F, Powell R D and Takavorian P M 2004 *Proc. Microscopy and Microanalysis* ed I M Anderson *et al* (New York: Cambridge University Press) p 1210CD
[11] Willner I, Baron R and Willner B 2006 *Adv. Mater.* **18** 1109–20
[12] Möller R, Csaki A, Köhler J M and Fritzsche W 2001 *Langmuir* **17** 5426–30
[13] Park S J, Taton T A and Mirkin C A 2002 *Science* **295** 1503–6
[14] Moreno-Hagelsieb L, Lobert P E, Pampin R, Bourgeois D, Remacle J and Flandre D 2004 *Sensors Actuators* B **98** 269–74
[15] Urban M, Möller R and Fritzsche W 2003 *Rev. Sci. Instrum.* **74** 1077–81
[16] Fletcher S 1983 *Faraday Trans.* 1 **79** 467–79
[17] Scharifker B 1983 *Electrochim. Acta* **28** 879–89
[18] Fransaer J L and Penner R M 1999 *J. Phys. Chem.* B **103** 7643–53

[19] Penner R M 2001 *J. Phys. Chem.* B **105** 8672–8
[20] Festag G, Steinbrück A, Csaki A and Fritzsche W 2007 *Nanotechnology* **18** 015502
[21] Oates T W H 2004 *Phys. Rev.* B **70** 195406–12
[22] Oates T W H and Mücklich A 2005 *Nanotechnology* **16** 2306–611
[23] de Vries A J, Kooij E S, Wormeester H, Mewe A A and Poelsema B 2007 *J. Appl. Phys.* **101** 1–10
[24] Wang Z and Rothberg L J 2006 *Appl. Phys.* B **84** 289–93
[25] Lamture J B *et al* 1994 *Nucl. Acids Res.* **22** 2121–5
[26] Festag G, Steinbrück A, Wolff A, Csaki A, Moller R and Fritzsche W 2005 *J Fluorescence* **15** 161–70
[27] Möller R, Powell R D, Hainfeld J F and Fritzsche W 2005 *Nano Lett.* **5** 1475–82
[28] Zhang G-J, Möller R, Kretschmer R, Csaki A and Fritzsche W 2004 *J. Fluorescence* **14** 369–75

2.7 Enzyme-induced growth of silver nanoparticles studied on single particle level

Thomas Schüler, Andrea Steinbrück, Grit Festag, Robert Möller, Wolfgang Fritzsche

Journal of Nanoparticle Research (**2008**) 11(4): 939-946

J Nanopart Res
DOI 10.1007/s11051-008-9496-7

RESEARCH PAPER

Enzyme-induced growth of silver nanoparticles studied on single particle level

Thomas Schüler · Andrea Steinbrück · Grit Festag · Robert Möller · Wolfgang Fritzsche

Received: 13 February 2008 / Accepted: 22 August 2008

Abstract Based on their interesting properties, metal nanoparticles show the potential as an analytical tool in electronic (Burmeister et al. 2004), optical (Yguerabide and Yguerabide 1998), and catalytic applications (Liu 2006). Their characteristics depend on the composition, shape, and size of the single particles. These various properties are utilized in many different approaches such as optics, magnetics (Lang et al. 2007), and laser technology (Csaki et al. 2007). We investigated an alternative method for the synthesis of nanoparticles. In this case, an enzyme, horseradish peroxidase, induces a silver deposition and replaces a metal nanoparticle as the reaction seed. Depending on the reaction time, we could obtain particles in a range of few nanometers up to more than 250 nm. For a better understanding of the enzymatic silver deposition process, the silver particles produced by this process were analyzed by SEM, TEM, and atomic force microscopy (AFM) on a single particle level after different enhancement times. The AFM images were utilized for the characterization of particle height and volume to study the enzyme kinetics, i.e., the particle growth process. Thereby, two different phases are described: a first growth phase probably induced by the enzyme-related growth, and a second, more unspecific growth based on the metal deposition onto the silver deposits. These findings may help to use the enzyme-induced silver deposition in a quantitative manner for bioanalytical applications.

Keywords Enzyme-induced silver deposition · Silver nanoparticles · Horseradish peroxidase · Volume measurement · Size enlargement

T. Schüler · R. Möller
JBCI, Institute of Physical Chemistry, Friedrich-Schiller-University Jena, Helmholtzweg 4, 07743 Jena, Germany

A. Steinbrück · G. Festag · W. Fritzsche (✉)
Institute of Photonic Technology, Albert-Einstein-Straße 9, 07745 Jena, Germany
e-mail: wolfgang.fritzsche@ipht-jena.de
URL: http://www.ipht-jena.de

Introduction

Metal nanoparticles have the potential to realize bioanalytical approaches for analysis outside dedicated laboratories, such as on-line, on-site, or point-of-care applications. Novel detection schemes with simple read-out principles are preferred due to both the stability of the assay (especially in the hand of less skilled personnel) and the lower costs of the detection equipment. First schemes to be used in principle for molecular detection were based on transmission/reflection (Reichert et al. 2000) or color changes (Storhoff et al. 2004) upon analyte binding on planar/solid supports, and has already shown the potential for simple detection by the naked eye. However, parallelization of the assays in a microarray

format usually requires stronger signals. The specific deposition of additional metal (usually silver) from the solution was found to be the enabling breakthrough for realizing paralleled assays that can be read out by simple optical (Fritzsche and Taton 2003) or electrical (Möller et al. 2001; Park et al. 2002; Urban et al. 2003) detection units. This principle, comparable to the process in silver-based photography where the seed particles are grown by specific silver/metal deposition (Hacker et al. 1988; Zhang et al. 2002), leads to a significant signal enhancement of up to several orders of magnitude, yielding considerably lower detection limits for biomolecules, in the range needed for routine diagnostic applications. Instead of using gold nanoparticles as reaction seeds for the deposition of silver, an enzymatic reaction can also be used to form metallic nanoparticles (Hainfeld et al. 2002). This enzymatic metal deposition is superior to the conventional (nanoparticle-based silver) deposition, in particular, because of its very low background signal. The enzymatic silver deposition was also introduced for an electrical DNA detection leading to an increase in absolute sensitivity, as well as in sensitivity relative to the conventional gold nanoparticle-mediated deposition (Möller et al. 2005). The enzymatic metal deposition is limited to the enzymes that are utilized as labels, thereby avoiding undesired metal deposition, e.g., on the gold microelectrodes present on electrical DNA chips. The catalytic properties of enzymes and their interactions with special substrates have been known for decades (Davis 1995). A large number of enzyme-based tests are commercially available which make use of the high specificity, sensitivity, and reaction speed of these biomolecules (Patolsky et al. 2001; Sun et al. 2006).

Currently, emerging approaches exploit enzymes, for instance horseradish peroxidase, glucose oxidase, or alkaline phosphatase, to seed metal nanoparticle growth (Hwang et al. 2005; Willner et al. 2006). The advantage of these methods is to combine the highly specific and fast enzymatic reaction and the optical, electrical, and catalytic properties of metal nanoparticles (Katz and Willner 2004; Willner et al. 2007). This approach also promises the further benefit of stability and non-reversibility of the signals (Patolsky et al. 1999; Basnar et al. 2006).

Although first reports on the use of enzymes for electrical detection were quite promising, a further extension of this work requires a better understanding of the underlying mechanisms. Optimizations of the protocols used regarding background, reagent use, and time needed are typical next steps towards a broader application, and therefore a thorough study is needed. This article addresses this goal by studying the processes not only by using conventional ensemble measurements, but also by investigating the enzymatic metal deposition on the nanoscale and single molecule level.

Materials and methods

In order to follow the growth of the enzyme-generated silver particles, the horseradish peroxidase was immobilized on silicon oxide or mica substrates prior to enhancement by stepwise reaction with the Enz-Met^{TM} reagent (Nanoprobes, Yaphank, NY) at room temperature under normal lighting conditions. For the investigation of the enzyme kinetics, a streptavidin-horseradish peroxidase-polymer (Sigma-Aldrich, Taufkirchen, Germany) was used. The planar substrates were incubated with a 1:1,000 dilution of the streptavidin-peroxidase-polymer in double distilled water. A volume of 30 µL of this solution was applied on every sample and incubated for 5 min at room temperature. Finally, the substrates were subjected to a stream of nitrogen to remove the bulk water, and a silver enhancement kit was then immediately applied to the substrates to avoid the drying of the enzyme polymer. The enzymatic reaction was stopped by a short washing step with water and dried under nitrogen. Atomic force microscopy (AFM) was used to study the silver deposition process at single particle level with nanometer resolution. After each enhancement step, the samples were measured under air using the tapping mode AFM (NanoScope version 5.12, Dimension 3100, Digital Instruments, Santa Barbara, CA). Due to drying, the enzyme became inactive and the reaction could not be started again. For this reason, every enhancement step was carried out on a new sample. In order to monitor the growth of the particles and to obtain a detailed view for single particle analysis, a scan size of 2.56 µm × 2.56 µm was chosen so that the individual enzyme structures were still visible. The particle heights were studied using the image analysis software Image SXM (Barrett 2008) based on grey tone (representing height)

analysis of ca. 400 particles from original AFM images. In order to characterize the particle growth depending on the metal growth time, different enhancement steps were investigated. As a negative control, the experiments were also conducted without horseradish peroxidase to show any background signal. Further investigations include the measurement of the particle volume using free software Gwyddion (Klapetek 2007). For confirmation, scanning and transmission electron microscopy (SEM and TEM, respectively) were utilized. In the growth curves, the resulting particle heights or volumes were plotted against enhancement time.

Results

AFM imaging allows the control of different metal enhancement methods at nanometer resolution on the single particle level. As demonstrated in the case of autocatalytic nanoparticle growth (Festag et al. 2007), a detailed knowledge of the growth characteristics and the kinetics can be obtained, and the influence of factors like enhancement time, enhancement solution, or original particle size could be revealed.

Following the enzymatic enhancement over various steps by SEM, the ongoing growth of the particles and the resulting increase in the coverage of the substrate becomes apparent (Fig. 1a–c), similar to that observed on surfaces with gold nanoparticles in the course of autocatalytic metal enhancement as shown in earlier work (Möller et al. 2001). In contrast to the autocatalytic growth of spherical particles, which retain their overall geometry but increase their diameter, in the case of enzyme-induced growth, a more complex geometry is observed. After extended enhancement times in overview images (Fig. 1c), a flake-like structure of several platelets standing on each other is readily observed in zoomed images (Fig. 1d). Often a base platelet that is usually oriented approximately parallel to the substrate plane holds several others that stand on the base and are interpenetrating, leading to a desert rose-like appearance. On comparing the three enhancement times, the increasing size of the individual structures and the resulting growing surface coverage are clearly visible. For the given parameters (starting enzyme surface concentration 1 µg/mL), a 5-min enhancement time results in a high surface coverage of metal structures connected to each other. This coverage would lead to a strong optical signal in transmission mode or electrical conductivity in the case of electrical DNA chip detection (detection would require two electrodes on the substrate). The relationship of optical properties with particle density (particle size) was demonstrated for gold nanoparticles (Reichert et al. 2000), and after for silver deposition using gold nanoparticles as reaction seed (Csaki et al. 2003) for optical transmission or reflection, respectively.

In studying the images at various enhancement times, a more and more pronounced flake-like structure is observed over time. At 1 min, the structures appear almost globular in these overview images; at 3 min, some indications for flakes standing upright can be observed; and at 5 min, these flakes perpendicular to the substrate plane are quite obvious even in the lower resolution overview images. In order to characterize the enzyme-induced silver deposition in the early stage and to reveal the morphology of the flake formation process, particles from such samples were further investigated by TEM. The images in Fig. 2 show silver particles after 10 and 30 s enhancement time. On one hand, the typical

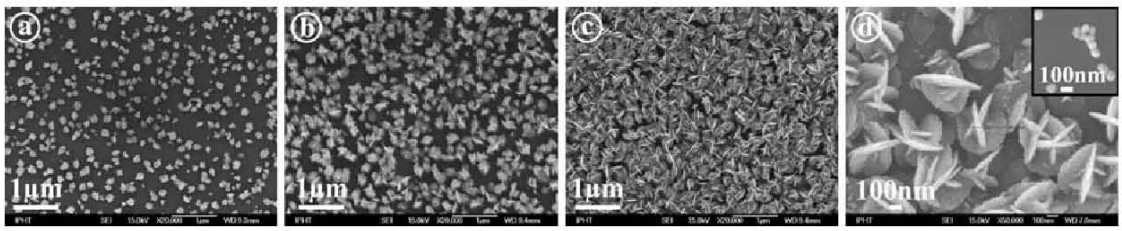

Fig. 1 SEM images showing a time series of 1 min (**a**), 3 min (**b**), and 5 min (**c**) enzymatic silver deposition. A higher magnification at 5 min is shown in (**d**) and illustrates the irregular structure of enzymatically grown silver nanoparticles after 5 min deposition. Inset (**d**): well-defined 60 nm gold nanoparticles after silver enhancement for comparison

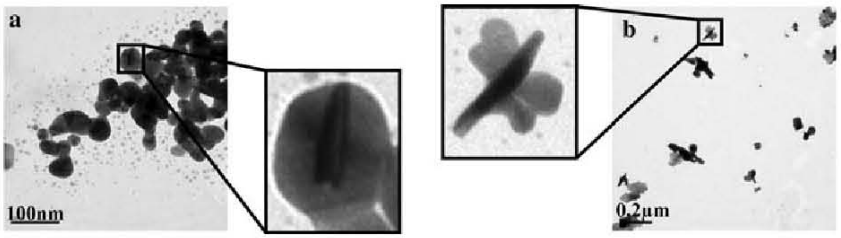

Fig. 2 TEM images of silver nanoparticles produced by enzymatic deposition after 10 (**a**, scale bar 100 nm) and 30 s (**b**, scale bar 200 nm) reaction time, respectively, illustrating the irregular particle shapes with desert rose-like structures

structures (with base plate and perpendicular plates) are already apparent and appear to originate in the early stage of particle growth (as displayed in the enlarged sections in both images), but are less pronounced, especially in the 10 s images, and therefore hardly recognizable in images with lower resolution. Darker regions in the TEM images indicate thicker (and therefore in this case) higher regions. On the other hand, a broad distribution of the particles with respect to size as well as shape is noticeable. This effect could be caused by diffusion-limited processes and/or local concentration differences. Moreover, the applied enzyme complex is a multimer with a variation in the number of enzymes per complex, so that different numbers of enzymes could lead to variations in the amount of deposited metal.

An important point for the potential application of the metal enhancement technique is the understanding of the time dependence of the metal deposition. In order to investigate its growth kinetics, the single particles were measured and characterized after every enhancement step.

Typical AFM images for each enhancement time studied are shown in Fig. 3. Due to sample tip convolution, the fine structure of the enzymatic complexes is less clearly resolved than in the case of SEM or TEM. However, the overall size presented by the maximum height is easily extracted from the images. Moreover, AFM imaging does not change the sample properties in the same manner as metal decoration or other sample preparation steps needed for SEM or TEM imaging. Therefore, studies of one and the same particle going through several modification steps are possible, as already demonstrated for metal nanoparticle-based enhancement (Festag et al. 2007). Additionally, other image processing procedures such as volume determination (see below) become possible. Because all images presented in this figure are at the same lateral and height scale, the increase in size with respect to both width (increasing diameter) and height (increasing brightness) becomes apparent. The original height of the enzyme complexes of about 2 nm (top left) before enhancement grows in the course of the experiments up to about 250 nm at 30 min. Although the convolution by the tip geometry leads to the aforementioned loss in sharpness and clarity of the structures, the basic geometry of the flakes is still resolvable. Especially in the center row, the upright flake that is typical for the structures appears as bright rod-like structure along the base plate.

About 400 particles were measured at every enhancement step, and the height values were extracted from the AFM images. Plotting the frequency of the measured height for all the enhancement steps (Fig. 4a) shows clearly the continuous increase over time for the studied period of up to 30 min enhancement. After 2 min, the peaks in Fig. 4a become wider, indicating a broadening distribution in particle height over time that is overlayed on the continuous increase due to metal deposition.

Upon examination of the mean heights as plotted in Fig. 4b, a fast and linear growth between 0 and 5 min enhancement time becomes apparent. Starting at 5 min, the height growth slows down by nearly an order of magnitude, indicating two different mechanisms before and after 5 min.

The last part of this work presents the results of our investigation into the volume of the enzymatically grown particles. As shown before, the particle height was quite heterogeneous. Due to the asymmetrical shape of the generated silver nanoflakes, the height measurement was unsuccessful. The calculation of particle volume rather than planar size is more representative and should therefore provide additional

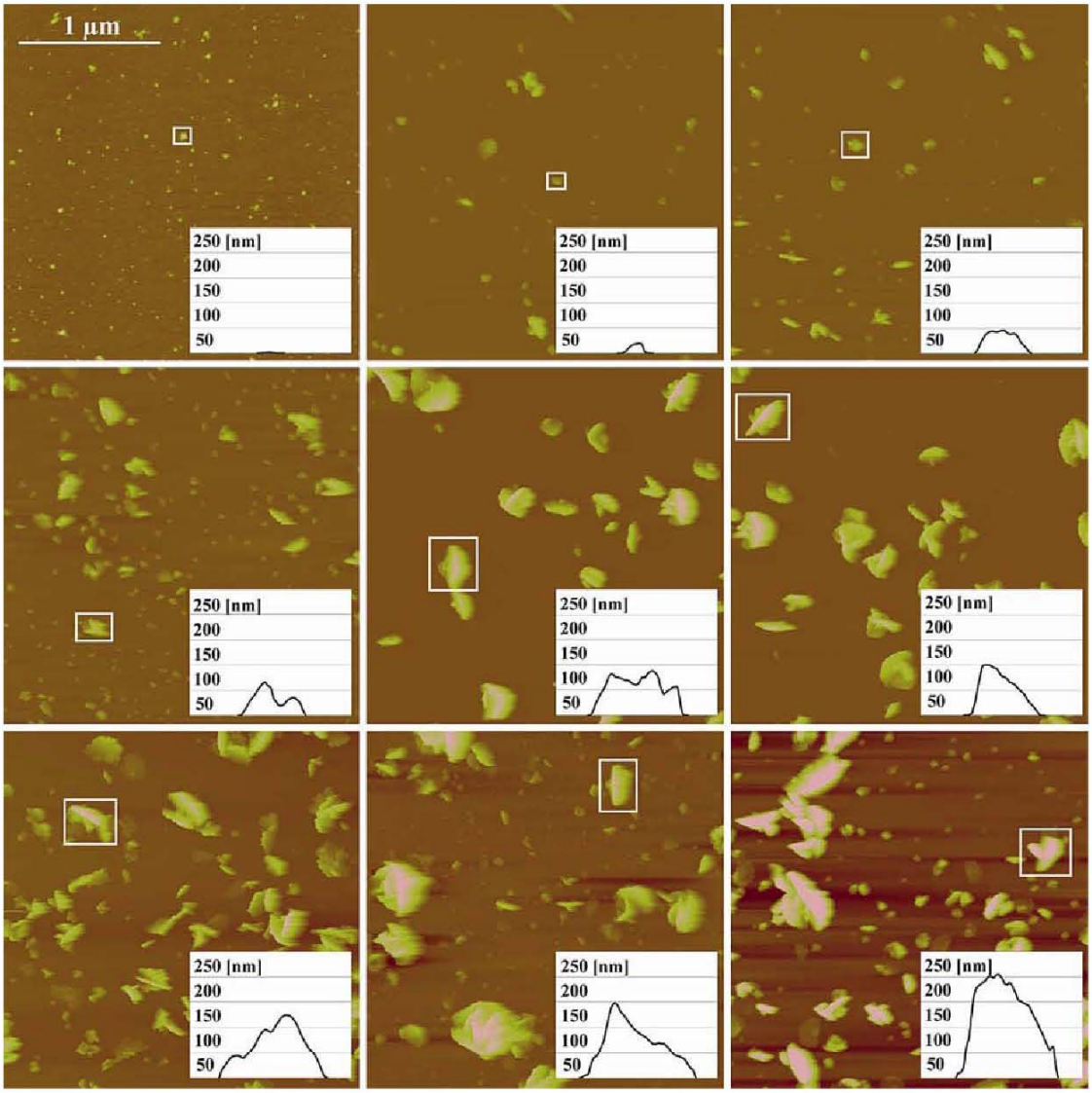

Fig. 3 The AFM images show the stepwise enzymatic silver deposition starting with the untreated enzyme (horseradish peroxidase polymer) (top left) followed by 1, 2, 3, 4, 5, 10, 20, and 30 min enhancement time (bottom right)

information about the particle growth rate. For this reason, the AFM images after every enhancement step were investigated using free software Gwyddion to estimate the particle volume. In order to estimate the median volume, the most frequent grey value of the single images was subtracted to determine the background/sample plane. A manual adjustable threshold allowed the clear demarcation of the single particles. Since every particle consists of many pixels, each of them with a well defined grey value; this information could be used to calculate the volume of the single particles (Fig. 5).

Figure 5 shows a noticeable increase in the particle volume after 1 min enhancement time. In order to verify this observation, further measurements were carried out at 20 and 40 s enhancement time. Consistent with the mean values, we assumed a linear growth behavior in the first minute of silver

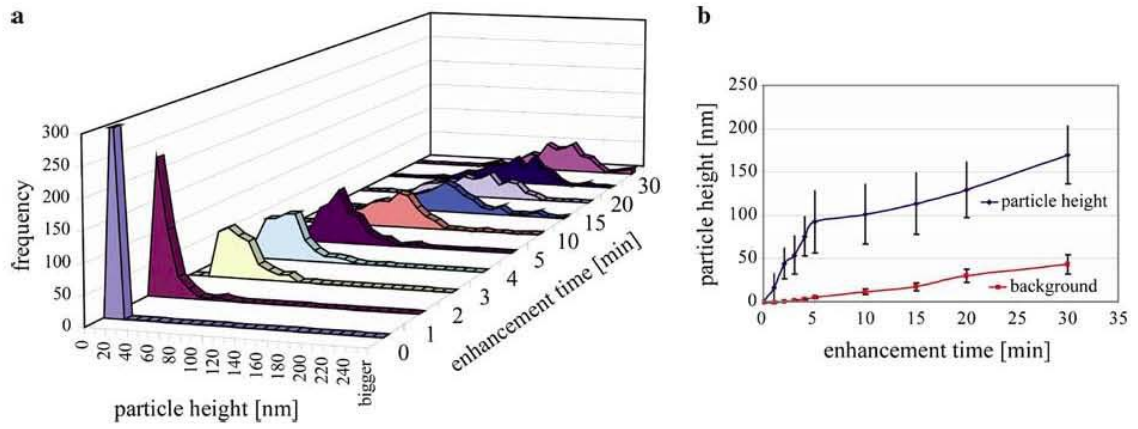

Fig. 4 Particle height distribution (**a**) over enhancement times for the enzyme complex (horseradish peroxidase). The deposition of silver was measured every enhancement step (400 particles) using the maximum height. In the first 5 min, a fast and linear growth of the enzymatic seeds becomes apparent (**b** blue curve) before it slows down considerably. The red curve in (**b**) displays the development of the background (silver enhancement kit without enzyme)

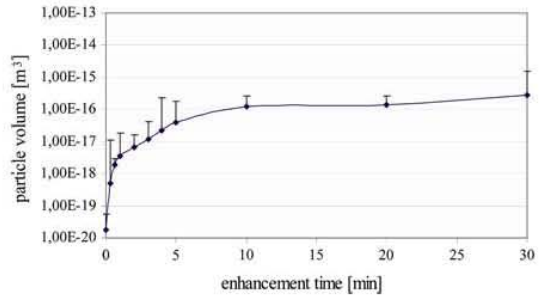

Fig. 5 Increase in particle volume in dependence on enhancement time

deposition. However, the error bars show significant variance within each enhancement step. The rapid growth is equal to the speed of enzymatic reactions, which are usually very fast. The reaction decelerates at longer enhancement times.

Conclusion

The deposition of metal-induced growth by the enzymatic reaction of horseradish peroxidase was studied on the nanoscale at the single particle level using microscopic techniques. Both shapes and dimensions of the individual structures could be observed and characterized. An unusual desert rose-like structure was commonly found with a base plate and perpendicular plate. The irregular growth of the enzyme-induced silver deposition, shown in the height distribution could be caused by the different numbers of enzymes in each macromolecule of the polymer conjugate used for particle generation. The investigations of particle height as well as particle volume clearly visualize a loss of the fast enzymatic reaction after 5 min. This effect can be explained by the inactivation of the enzyme polymer. With longer enhancement times, the enzyme deposits a silver shell around itself, which leads to an inaccessibility of enzyme substrates and perhaps enzyme alteration. Later on, a slower second reaction using the already enzymatically generated silver particles as reaction seeds continues the particle growth. This second reaction is comparable to the conventional autocatalytic silver deposition onto gold nanoparticles. Moreover, the enzyme polymers can coalesce over enhancement time and create much larger, irresolvable structures. Different amounts of enzyme may be responsible for the difference in reactivity. Another possibility for the observed growth kinetics are diffusion-limited processes, but since metal deposition onto nanoparticles (which occurs under similar conditions) is more homogeneous, this effect appears to be less significant. The streptavidin-conjugate of the horseradish peroxidase-polymer was studied due to the importance of streptavidin and HRP in many detection schemes, and particularly in the field of chip-based DNA detection, where it will be compatible with biotinylated target DNA. Further

experiments to elucidate the contributions of the enzyme directly will be conducted using native horseradish peroxidase. Therefore we will investigate the dependence of optical properties in terms of light scattering of the single particle shape, height, and size (e.g., enhancement time).

Acknowledgment Funding of research project "Jenaer Biochip Initiative" (JBCI) within the framework "Unternehmen Region—Inno Profile" from the Federal Ministry of Education and Research, Germany (BMBF) is gratefully acknowledged. This work was supported by the DFG (FR 1348/5-2). We thank Nanoprobes for the kind support with EnzMet enhancement kit, Richard Powell, Vishwas Joshi, Wenqiu Liu, and James Hainfeld for helpful discussions, James Vesenka for the help with AFM measurements, and Daniell Malsch for the discussions about volume measurement as well as Franka Jahn for SEM imaging. Development of the enzyme metallographic reagent was supported by Small Business Innovation Research Grant 5R44 GM064257-03 from the National Institute of General Medical Sciences (NIH), USA.

References

Barrett S (2008) Image SXM v1.85. http://www.liv.ac.uk/~sdb/ImageSXM/. Accessed 9 July 2007

Basnar B, Weizmann Y et al (2006) Synthesis of nanowires using dip-pen nanolithography and biocatalytik inks. Adv Mater 18:713–718. doi:10.1002/adma.200502320

Burmeister J, Bazilyanska V et al (2004) Single nucleotide polymorphism analysis by chip-based hybridization and direct current electrical detection of gold-labeled DNA. Anal Bioanal Chem 379(3):391–398. doi:10.1007/s00216-004-2601-6

Csaki A, Kaplanek P et al (2003) The optical detection of individual DNA-conjugated gold nanoparticle labels after metal enhancement. Nanotechnology 14:1262–1268. doi:10.1088/0957-4484/14/12/006

Csaki A, Garwe F et al (2007) A parallel approach for sub-wavelength molecular surgery using gene-specific positioned metal nanoparticles as laser light antennas. Nano Lett 7(2):247–253. doi:10.1021/nl061966x

Davis J, Vaughan DH, Cardosi MF (1995) Elements of biosensor construction. Enzym Microb Technol 17:1030–1035. doi:10.1016/0141-0229(95)00013-5

Festag G, Steinbrück A et al (2007) Single particle studies of the autocatalytic metal deposition onto surface-bound gold nanoparticles reveal a linear growth. Nanotechnology 17:1–10

Fritzsche W, Taton TA (2003) Metal nanoparticles as labels for heterogeneous, chip-based DNA detection. Nanotechnology 14:R63–R73. doi:10.1088/0957-4484/14/12/R01

Hacker GW, Grimelius L et al (1988) Silver acetate autometallography: an alternative enhancement technique for immunogold-silver staining (IGSS) and silver amplification of gold, silver, mercury and zinc in tissues. J Histotechnol 11:213–221

Hainfeld JF, Eisen RN et al (2002) Enzymatic metallography: a simple new staining method. In: Voekl E, Piston D, Gauvin R et al. (eds) Proceedings of microscopy and microanalysis, vol 8. Cambridge University Press, New York, pp 916CD

Hwang S, Kim E, Kwak J (2005) Electrochemical detection of DNA hybridization using biometallization. Anal Chem 77:579–584. doi:10.1021/ac048778g

Katz E, Willner I (2004) Nanobiotechnology: integrated nanoparticle-biomolecule hybrid systems: synthesis, properties, and applications. Angew Chem Int Ed Engl 43(45):6042–6108. doi:10.1002/anie.200400651

Klapetek P (2007) Gwyddion. http://gwyddion.net/. Accessed 19 Oct 2007

Lang C, Schüler D, Faivre D (2007) Synthesis of magnetite nanoparticles for bio-and nanotechnology: genetic engineering and biomimetics of bacterial magnetosomes. Macromol Biosci 7:144–151. doi:10.1002/mabi.200600235

Liu WT (2006) Nanoparticles and their biological and environmental applications. J Biosci Bioeng 102(1):1–7. doi:10.1263/jbb.102.1

Möller R, Csaki A et al (2001) Electrical classification of the concentration of bioconjugated metal colloids after surface adsorption and silver enhancement. Langmuir 17:5426–5430. doi:10.1021/la0102408

Möller R, Powell RD et al (2005) Enzymatic control of metal deposition as key step for a low-background electrical detection for DNA chips. Nano Lett 5(7):1475–1482. doi:10.1021/nl050824k

Park SJ, Taton TA et al (2002) Array-based electrical detection of DNA with nanoparticle probes. Science 295(5559):1503–1506

Patolsky F, Zayats M, Katz E, Willner I (1999) Precipitation of an insoluble product on enzyme monolayer electrodes for biosensor applications: characterization by Faradaic impedance spectroscopy, cyclic voltammetry and microgravimetric quartz crystal microbalance analyses. Anal Chem 71:3171–3180. doi:10.1021/ac9901541

Patolsky F, Lichtenstein A et al (2001) Detection of single-base DNA mutations by enzyme-amplified electronic transduction. Nat Biotechnol 19(3):253–257. doi:10.1038/85704

Reichert J, Csaki A et al (2000) Chip-based optical detection of DNA hybridization by means of nanobead labeling. Anal Chem 72:6025–6029. doi:10.1021/ac000567y

Storhoff JJ, Lucas AD et al (2004) Homogeneous detection of unamplified genomic DNA sequences based on colorimetric scatter of gold nanoparticle probes. Nat Biotechnol 22(7):883–887. doi:10.1038/nbt977

Sun H, Chattopadhaya S, Wang J, Yao SQ (2006) Recent developments in microarray-based enzyme assay: from functional annotation to substrate/inhibitor fingerprinting. Anal Bioanal Chem 386:416–426. doi:10.1007/s00216-006-0511-5

Urban M, Möller R et al (2003) A paralleled readout system for an electrical DNA-hybridization assay based on a microstructured electrode array. Rev Sci Instrum 74:1077–1081. doi:10.1063/1.1533103

Willner I, Baron R et al (2006) Growing metal nanoparticles by enzymes. Adv Mater 18:1109–1120. doi:10.1002/adma.200501865

Willner I, Basnar B, Willner B (2007) Nanoparticle-enzyme hybrid systems for nanobiotechnology. FEBS J 274:302–309. doi:10.1111/j.1742-4658.2006.05602.x

Yguerabide J, Yguerabide EE (1998) Light-scattering submicroscopic particles as highly fluorescent analogs and their use as tracer labels in clinical and biological applications. Anal Biochem 262(2):157–176. doi:10.1006/abio.1998.2760

Zhang G-J, Möller R et al (2002) Optical detection of DNA constructs based on nanoparticles and silver enhancement. In: Fritzsche (ed) DNA based molecular construction, vol 640. American Institute of Physics, MD, pp 13–21

2.8 A disposable and cost efficient microfluidic device for the rapid chip-based electrical detection of DNA

Thomas Schüler, Robert Kretschmer, Sven Jessing, Matthias Urban, Wolfgang Fritzsche, Robert Möller, and Jürgen Popp

Biosensors Bioelectronics (**2009**), 25 (2009) 15–21

Biosensors and Bioelectronics 25 (2009) 15–21

Contents lists available at ScienceDirect

Biosensors and Bioelectronics

journal homepage: www.elsevier.com/locate/bios

A disposable and cost efficient microfluidic device for the rapid chip-based electrical detection of DNA

Thomas Schüler[a,1], Robert Kretschmer[a,1], Sven Jessing[a], Matthias Urban[b], Wolfgang Fritzsche[b], Robert Möller[a,*], Jürgen Popp[a,b]

[a] Jenaer Biochip Initiative, Friedrich Schiller University, Institute of Physical Chemistry, Helmholtzweg 4, Jena, Germany
[b] Institute of Photonic Technology, Albert-Einstein-Straße 9, Jena, Germany

ARTICLE INFO

Article history:
Received 6 March 2009
Received in revised form 19 May 2009
Accepted 21 May 2009
Available online 18 June 2009

Keywords:
Electrical DNA-chip
Enzyme-induced silver deposition
Automation
Integration
Flow cell

ABSTRACT

Requirements for a point-of-care device are an easy and robust read-out and – above all – a simple handling. We integrated an established robust electrical read-out for DNA-chips into a microfluidic device, thereby creating an automated analysis system that combines the necessary steps for a chip-based analysis. It is based on the electrical detection of biotin-labeled DNA in a gap between two microstructured electrodes on the surface of a DNA-chip. The biotin serves as binding molecule for streptavidin-conjugated horseradish peroxidase. A following enzyme-induced silver deposition bridges the gap by a conductive layer. The miniaturized chip gives the possibility to realize a durable system suitable for point-of-care applications.

To enable an initial automation, all corresponding process steps were executed in a miniaturized silicone flow cell. The required defined temperatures for the hybridization and the washing steps can be adjusted by a heating foil.

This paper characterizes the performance of the flow cell based system in terms of reaction speed and analysis time, sensitivity as well as specificity, and the comparison to a conventional system, without flow cell. These first steps of automation and integration will help to realize a laboratory-independent bioanalytical tool, for the use outside of specialized laboratories for fast analysis of different chemical and biological applications.

1. Introduction

Since its introduction the microarray technology is used in many different fields exploiting the advantages of biochips, such as high throughput screening, high specificity, miniaturization, and so on (Schena et al., 1995). In principle, short single stranded DNA, so-called capture molecules, become immobilized on a planar chip surface like glass, silicon or polymeric materials (Oh et al., 2006). Later the sample is delivered to the microarray surface (Diehl et al., 2001).

In the last years many endeavors have been made to further develop the microarray technology. Different techniques were used to integrate biochips (Dittrich et al., 2006; Morais et al., 2007). Acoustic piezo elements (Toegl et al., 2003), centrifuges (Peytavi et al., 2005), rotators (Pappaert et al., 2003), and electric fields (Edman et al., 1997) are utilized to induce an additional movement of the sample solution on the chip to overcome the diffusion limitation of the capture-target molecule interaction. Furthermore microfluidic applications are a promising complementation of microarray technology, especially for the on-site analysis. Microfluidics is an enabling technology behind a whole new class of miniaturized analysis systems for chemical and biological applications (Haeberle and Zengerle, 2007). All the benefits of microfluidics and miniaturization such as smaller sample requirement, reduced reagent consumption, decreased analysis time, higher levels of throughput, and automation can be realized in such applications (Abgrall and Gué, 2007).

Combining microfluidics and biochips aims to improve binding efficiency, and to maximize the speed of the individual process steps on a biochip (Pappaert et al., 2006). However, the expenses for the analysis of a test rise unnecessarily by the additional instrumentation that usually leads to higher costs and efforts.

The detection of biomolecules on a biochip is nowadays mainly performed using fluorescent dyes (Schena et al., 1998). Disadvantages (like photo bleaching and quenching of the fluorescent dyes) can be overcome by using quantum dots (Han et al., 2001). Nowadays, different working groups could successfully demonstrate the miniaturization of the mostly sophisticated fluorescence equipment (Kang et al., 2007; Basabe-Desmonts et al., 2008; Myers and

* Corresponding author. Tel.: +49 3641 206306.
E-mail address: robert.moeller@ipht-jena.de (R. Möller).
[1] Both authors contributed equally to the paper.

0956-5663/$ – see front matter © 2009 Elsevier B.V. All rights reserved.
doi: 10.1016/j.bios.2009.05.040

Lee, 2008). But, the developed handheld and point-of-care systems are limited in terms of their sensitivity and robustness. Due to the difficulties, the use of biomolecule detection via fluorescence is usually limited to specialized laboratories (Festag et al., 2005).

Here we introduce a disposable and cost efficient microfluidic device for the rapid nanoparticle-based electrical detection of DNA (Möller et al., 2005). We focused on this technology because of its robustness, simplicity and the potential to refine it to a mobile, disposable and cost efficient device for on-site testing.

Therefore, the DNA-chip with electrical detection was integrated into a custom-made flow cell. This work describes for the first time the integration of the enzyme-induced deposition of silver nanoparticles that do not fade or bleach for the specific and sensitive chip-based detection of DNA in a microfluidic system.

Developing point-of-care applications it is important to focus on flexible, inexpensive, and reliable devices with a simple handling. Since photolithographic methods allow microstructuring of nearly any channel geometry and extremely small sizes the use of other structuring technologies like molding seems not suitable anymore in terms of microstructure geometry (Abgrall and Gué, 2007).

Our approach is based on the idea to use alternative techniques that can be used to produce cost efficient and robust fluidic systems that guarantee an easy exchange of all main components of the flow cell. The exchange of the essential parts ensures that no cross-contamination can occur, thereby avoiding false positive signals through cross-contamination. Further the integrating of the DNA-chip into the flow cell reduces the analysis time remarkably and improves the sensitivity of the system.

The results of these investigations represent an initial step for the development of a fully automated system, in order to realize a transportable analysis of biomolecules for the chip-based electrical detection of DNA.

2. Experimental

2.1. Materials

Screen printed DNA-chips were obtained from Heraeus Sensor Technology GmbH, Hanau, Germany. The streptavidin-horseradish-peroxidase-polymer was purchased from Sigma (Streptavidin-Peroxidase Polymer, Ultrasensitive, Sigma-Aldrich, Germany). Silver enhancement kit for enzyme-induced silver deposition was supplied by Nanoprobes (EnzMet kit, Nanoprobes Inc., Yaphank, NY). Microarray printing buffer was obtained from Arraylt (Micro Spotting Solution Plus, TeleChem International, Sunnyvale, CA). Chemicals for phosphate buffer solution (PBS pH 7.4), saline buffered sodium citrate (SSC pH 7), and sodium dodecyl sulphate (SDS) were ordered from Merck (Merck KGaA, Darmstadt, Germany). Tween20, hydroquinone and silver acetate were also ordered from Sigma.

2.2. Microarray printing

The DNA-chips were chemically modified with (3-glycidyloxypropyl)-trimethoxysilane (GOPS) (Wong and Krull, 2005) for the binding of amino-modified single stranded (ss) capture-DNA molecules. First, the chips were cleaned by sonication for 5 min each with acetone, ethanol, and water. After a drying step by nitrogen the chips were modified in a 10 mM GOPS solution in dry toluene for 7 h at 70 °C. Finally they were washed 2 × 5 min with toluene, ethanol, and water each (Möller et al., 2000).

The deposited capture DNA was modified with a C6-Aminolink on the 5′ or 3′ end. These modified molecules were attached to the epoxy (introduced by GOPS) modified surface. The attachment occurs by a secondary amine formation between the epoxysilane monolayer and the 5′ or 3′-amino modification of the DNA (Lamture et al., 1994). The capture-sequences were spotted by a non-contact Nanoplotter from GeSIM (Gesellschaft fuer Silizium-Mikrosysteme mbH, Großerkmannsdorf, Germany). Beside a positive (already biotin-labeled) and a negative control, we immobilized a complementary sequence, a sequence containing 1 mismatch, and a sequence containing 3 mismatches. The concentration of the spotted capture DNA in the microarray printing buffer was 10 μM.

2.3. Hybridization and enzyme-induced silver deposition

A microstructured glass chip with screen printed electrodes and 42 measurement points (electrode gaps) serves as microarray platform (Schüler et al., 2009). The capture molecules are immobilized in the gap between the electrodes. After the specific binding event of biotinylated target molecules, a streptavidin-horseradish-peroxidase-polymer is bound in the electrode gap (Diamandis and Christopoulos, 1991). A following enzyme-induced deposition of silver nanoparticles leads to bridging the electrode gap by a conductive silver layer (Möller et al., 2005; Schüler et al., 2008). Finally, the increase of the conductivity over the electrode gap can be measured by a DC measurement (Urban et al., 2003). Due to the easy DC measurement the required equipment is reduced to a minimum.

Prior work describes the use of the chip-based electrical detection of biomolecules without flow cell (Möller et al., 2008). Following this approach will be denoted as "conventional" system.

Different from the conventional system the best specificity for the hybridization of the used biotin-labeled target-DNA sequences was achieved in 0.5× SSC buffer and 0.1% SDS hybridization buffer at 42 °C. The hybridization was performed in the microfluidic device using a tubing pump with a planetary drive at a flow rate of 600 μl/min in 3 s intervals for 3 min. A following washing step in 0.2× SSC for 1 min (in continuous flow) removed unbound DNA to avoid false positive signals. The streptavidin-horseradish-peroxidase-polymer was diluted 1:1000 in PBS buffer and 0.05% Tween20. This buffer was also used for the washing step, in continuous flow, after a 3 min incubation step. The binding of the enzyme was also carried out at the same pump parameters as for the hybridization. After binding of the streptavidin-enzyme conjugate, the three solutions (A, B, C) of silver enhancement kit (EnzMet) from Nanoprobes (Nanoprobes Inc., Yaphank, NY) were introduced to the chip surface in ratio 1:1:1 (as given by the manufacturer). The reaction was stopped after 3 min to avoid unspecific silver deposition. Before enzyme-induced silver deposition the flow cell was rinsed with deionised water to remove any chloride from the PBS buffer. Fig. 1 shows the principle steps of the detection system.

2.4. Instrumental setup

The flow cell consists of a polycarbonate base containing microfluidic connections and an embedded thermal management to adjust the optimal environment for the biomolecular recognition reactions. To guarantee impermeability of the flow cell a custom-made PDMS (polydimethylsiloxane) component seals the reaction chamber (Sia and Whitesides, 2003). Additionally, the PDMS seal carries meandering structures (Fig. 4d). The DNA-chip serves as cover to close the reaction chamber whereby, in combination with the PDMS seal, the formed microfluidic channel guides all solutions over all measurement points on the chip (Fig. 4e). A specially developed read-out device allows online measurement of the electrical signal.

To move liquid through the flow cell a flexible tube pump IPC-N-4 (Ismatec Laboratoriumstechnik GmbH, Wertheim-Mondfeld, Germany) with a RS232 remote control and flow rates between 0.0004 and 11 ml/min, depending on the used tube diameter, was used. A PC running a custom build Delphi program capable of changing flow rate and switching between clockwise and counter

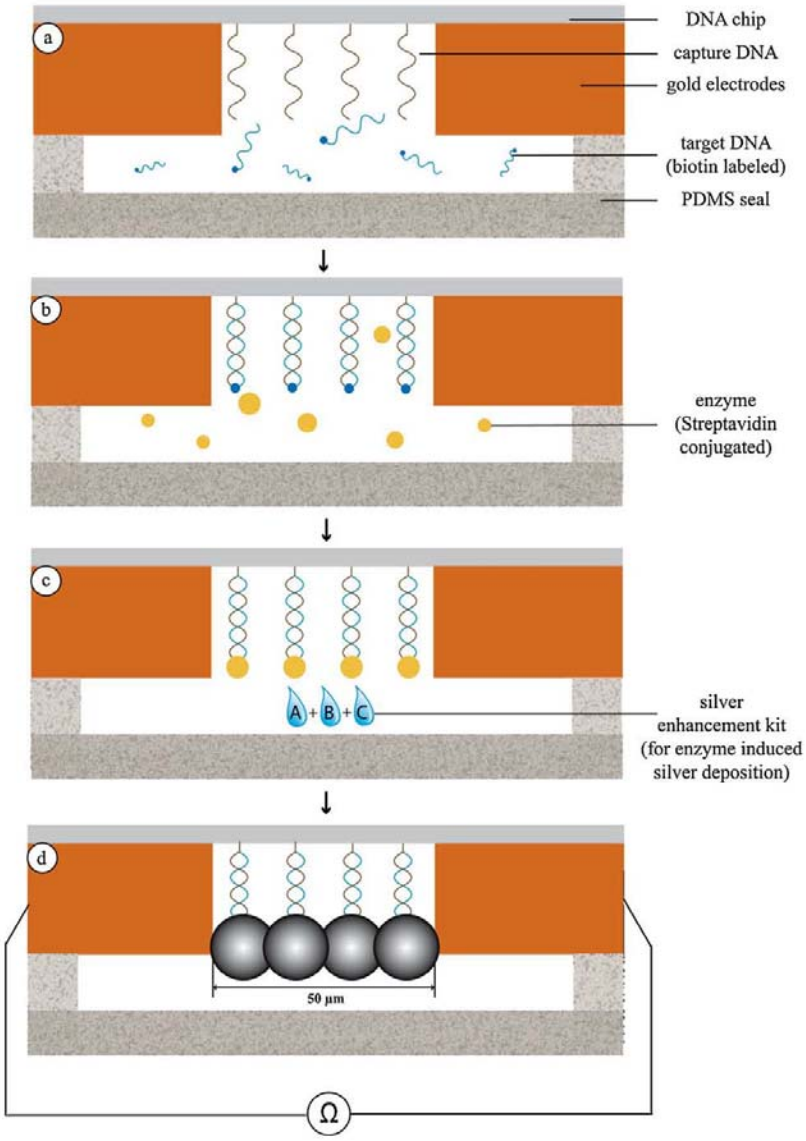

Fig. 1. After immobilization of single stranded capture-DNA sequences (a), the biotin labelled target-DNA hybridizes to its specific partner on the DNA chip (b). In a following step a streptavidin-horseradish peroxidase conjugate is bound to the biotin modification (c). In the end an enzymatic reaction leads to deposition of silver nanoparticles (d). The read-out could be performed by electrical measurement (conductivity of the gap filled by interconnected silver nanoparticles) or by optical transmission measurements (light absorption of the deposited silver). Thereby, the silver nanoparticles can reach diameters of approximately 500 nm and a height between 200–300 nm after standard reaction time.

clockwise rotation was used to control the pump via the RS232 interface. This was necessary to adjust an interval mode (time of the intervals can be adapted by the program). Interval mode means that a defined volume is pumped in the microfluidic chamber and the pumping direction changed every 3 s. All binding steps on the DNA-chip were performed in interval mode, to improve the speed of the reaction by breaking the diffusion limitation. This mode created a constant movement of the fluid over the chip but limited the necessary amount of fluid. The fluid volume for the interval mode was chosen so that during all interval steps the microfluidic channel over the chip was filled with sample solution. Washing steps and enzyme-induced silver deposition were carried out in continuous forward flow to assure a permanent supply with fresh washing buffer. Using a segmented flow the different solutions (DNA, washing buffer, enzyme polymer) can be separated by an air bubble. Temperature control on the chip in the flow cell is performed by a Pt 100 temperature sensor from Telemeter (Telemeter Electronic GmbH, Donauwörth, Germany). A polyimide heating foil (stable up to 200 °C) also purchased from Telemeter with the dimensions of 12.7 mm × 12.7 mm was used as heating element with an accuracy of 0.2 K. The temperature was regulated by a PIC controller and running a custom-made software.

Both, Pt 100 and heating foil are directly placed on the back of the DNA-chip to avoid contaminations with the liquids and a damage

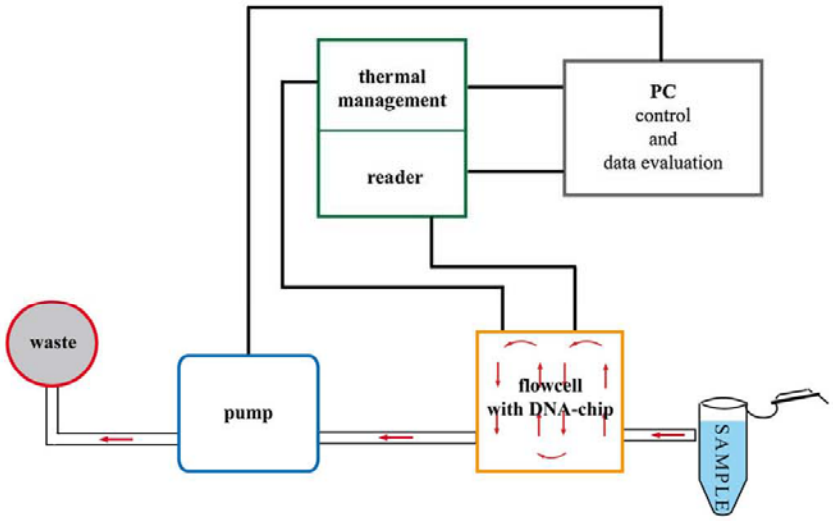

Fig. 2. Scheme of needed components and their necessary connections. Thermal management and the reader are connected to the flow cell to adjust the optimal temperature and to receive the electrical signals for further data evaluation in the PC. The pump is also connected to the PC to control flow rate as well as time and number of revolutions.

of the foil during the heating process by overheating. Fig. 2 shows the necessary instrumental setup with all components.

3. Results and discussion

3.1. Flow cell design and fabrication

The flow cell (Fig. 3) is build up by two principal PC (polycarbonate) components: the cover and the base. Four screws integrated in the base were used to connect the cover with the base. The dimensions of the cell are 70 mm (in height) × 48 mm × 48 mm. For the microfluidic system PTFE (polytetrafluorethylene) tubes were attached to the flow cell. HPLC connectors made of PEEK (polyetheretherketone) were used to fix the tubes and avoid leakages.

Integrated in the polycarbonate cover are the heating foil and a Pt 100 temperature sensor for adjustment of a defined temperature for the biomolecular reactions performed in the flow cell. To guarantee an optimal heat transfer the heating foil is pressed against the backside of the DNA-chip, which is positioned in the base, by screwing the cap to the base. The temperature is regulated and controlled by a Pt 100 placed directly to the heating foil.

A disposable silicone seal made of PDMS (polydimethylsiloxane) (Fig. 4c) exhibits multiple functions, first of all the impermeability of the flow cell. An integrated meandering structure in the PDMS seal generates the microfluidic channel that guides the liquids over the chip surface (Fig. 4d). To form the microfluidic channel the DNA-chip is placed with the biofunctionalized side (modified with GOPS and single stranded capture DNA) directly on the silicone seal (Fig. 4a and b). The PDMS seal has dimensions of 0.8 mm (in height) × 11 mm × 11 mm. The meandering structure for the microfluidic channel has a depth of 0.5 mm, so the resulting volume of the microfluidic channel is 30 μl. After each experiment the low cost PDMS seal can be easily replaced to avoid contaminations in the flow cell.

To realize the electrical read-out of the DNA-chip simultaneously to the enzyme-induced silver deposition, the flow cell contains contact areas for the electrical measurement of the 42 electrode gaps on the DNA-chip. The contact pads are aligned in a 4 × 12 pattern on the four sides of the chamber and made of elastic flat cables as

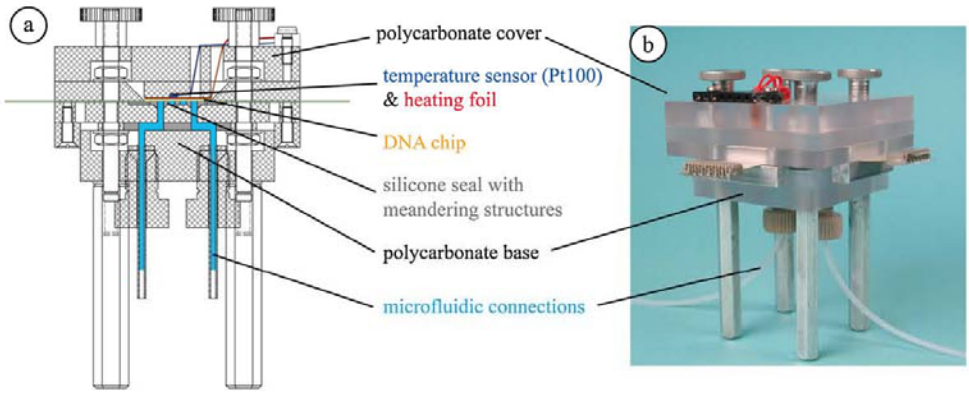

Fig. 3. Flow cell with thermal management, electrical signal detection, and microfluidic setup for the integration of the chip based electrical detection of DNA. Image (a) shows a technical drawing and (b) the realized flow cell. The blue areas in the cross section show the fluidic connections and the channel in the flow cell given by the silicone seal.

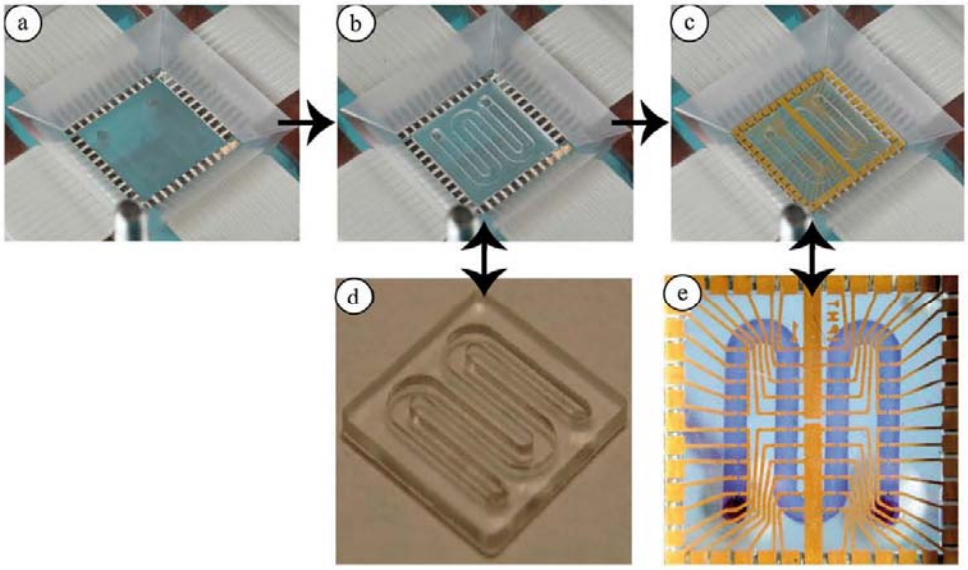

Fig. 4. Close-up view of the inner flow cell with imbedded electrical contacts for the later read-out of the DNA chip (a). The silicone seal (d) with meandering structures is inserted in the flow cell (b). Image (c) displays the DNA chip that forms the reaction chamber. A microfluidic channel will be automatically generated as soon as the chip is placed on the silicone seal and the electrical contacts. By filling the chamber with bromophenol blue the channel that transports all fluidics over each measurement point on the chips becomes visible (e).

used in mobile phone technology. Due to the bendable flat cables, flexible supported on a separate PDMS component, a reliable and reproducible contact to the contact pads of the DNA-chip is assured.

Because of the PC case the working temperature usable for the experiments in the flow cell is limited to 120 °C. All other components are stable also at higher temperatures. However, temperatures above 100 °C are not required for biological reactions, because even for denaturation of DNA the required temperature will be 95 °C. A prefixed heating step up to more than 60 °C could be used to avoid biological contamination of the chamber, for example by DNases or RNases.

3.2. Flow cell parameter characterization

The introduced flow cell allows the defined adaptation of flow rate and temperature to utilize the detection system for various biological applications. The flow rate is the defining factor in this setup, with respect to analysis time, hybridization and washing efficiency, and specificity of each experiment. Different flow rates were tested to find the optimum flow rate for the chip-based electrical detection of DNA. Lower flow rates would lead to low binding efficiencies, so that the signal intensities are reduced. Excessive flow rates also lead to weak signals, because the target molecules cannot sufficiently interact with the capture molecules. Also the specificity of the hybridization reaction could be influenced by the flow rate. Therefore, different flow rates were tested to find the optimal value for the described DNA detection.

In our tests we found the optimal value for the binding of biomolecules on the electrical DNA-chip at 600 μl/min. Also the discrimination between perfect match and mismatch probes shows the best result at this flow rate.

The fluid temperatures were set by the heating foil pressed onto the chip, so there is no direct control of the temperature of the liquid on the DNA-chip. The adaptation of temperatures was tested using an infrared camera, controlling the temperature of the DNA-chip on the biofunctionalized side (printed with capture molecules). Because of the 0.5 mm thin glass substrate it takes only 30 s to heat the chip to a uniform temperature distribution. This temperature offset has to be accounted for planning an experiment.

To investigate the correlation between the measured temperature of the Pt 100 sensor and the actual temperature inside the reaction chamber, a second Pt 100 was temporarily installed under the silicone seal to monitor the heat transfer between heating foil, glass chip, and liquid. Finally, a correction factor was calculated to assure the optimal temperature for reactions in the flow cell.

To determine the correction factor tests were performed in constant continuous flow of 600 μl/min with deionised water. During the experiment the temperature in the flow cell was raised stepwise (in 5 °C steps) from 25 °C up to 70 °C, and cooled back to room temperature. The tests were performed with glass and silicon chips, to show the influence of the material properties. We found a linear fit to the data from this experiment that yielded a correlation of the measured temperature $y = 0.17x - 3.81$ for glass surfaces and $y = 0.12x - 3.03$ for silicon surfaces. This corresponds to a maximum deviation of 8.5 K for glass and 5.3 K for silicon at a set point of 70 °C. The temperature sensor has a precision of ±0.06 K at 0 °C. Tests performed at a temperature at 95 °C confirmed the calculated linear fit. The correction factor can be used to refine the optimal temperature for a hybridization experiment to assure a specific binding event on the DNA-chip.

3.3. Comparison with conventional hybridization assay

An important factor for every bioanalytical tool is the total analysis time. Due to the active movement of the different solutions by the described interval pumping, the binding processes are no longer solely diffusion limited, which should lead to faster reactions and higher binding efficiencies. To investigate the influence of the active hybridization, different hybridization times were tested. The used concentration of biotin modified target-DNA was 500 nM. A weak signal was already detectable for 30 s hybridization time (Fig. 5). The signal intensity increases up to 5 min. With longer hybridization times up to 15 min the signal intensity approaches in saturation. Additionally the necessary incubation time for the

With regard to the specificity the flow cell system achieved the same discrimination between perfect match and mismatch probes compared to the conventional hybridization assay. By a reduction of the salt content of the hybridization buffer and an adjustment of the hybridization temperature the stringency was improved. Through this it was possibly to differentiate between complementary sequence and the complementary sequence containing just one mismatch. Depending on the hybridization time the total analysis time gain for the flow cell based system is 180 min. The flow cell system also achieves the same sensitivity and at a target-DNA concentration of 50 pM (LOD) it is 70% faster compared to the conventional system.

4. Conclusion

We could demonstrate the integration of an easy, robust, and economical technology into a microfluidic system in order to develop an approach to realize an on-site analytical tool. The easy and cost efficient microfluidic setup offers the same sensitivity and specificity without loss of functionality. A volume reduction for all reagents and the controlled flow rate over the electrode gaps further improve the technology. The total time of an experiment could be drastically reduced by the active binding of biomolecules.

This system demonstrates a simple approach suitable for the use as mobile bioanalytical tool that can be easily adjusted to various applications. The disposable components help to avoid cross-contaminations. In addition, different parts and features of the system can be easily adapted to other applications, for instance the design of the chip layout (measurement points and arrangement of the electrode structures) or the structures in the PDMS seal.

In further work we will integrate all components (pump, reader, flow cell) of the system in one device and use a rechargeable battery in order to build a bioanalytical tool suitable for point-of-care applications. A precise investigation of the online detection should clarify the possibility to quantify the signals on the DNA-chip, to give an additional statement beside the qualitative analysis.

We considered a prefixed PCR to use this system for biological applications on the electrical DNA-chip, by afterwards analyzing the whole PCR product on the DNA-chip. For that purpose it is planned to couple the flow cell with a chip-based PCR.

A further challenge is the automation of the complete protocol to simplify the use of the described system even for non-trained personal. Therefore, the installation of valves and the development of special software to connect the DNA-chip reader by a Bluetooth link to a PDA or a common mobile phone (that visualizes the measured data in a color code) will help to achieve an easy to use device.

Acknowledgements

Funding of research project "Jenaer Biochip Initiative" (JBCI) within the framework "Unternehmen Region – Inno Profile" from the Federal Ministry of Education and Research, Germany (BMBF) is gratefully acknowledged. We thank Nanoprobes for discussions and the kind support with EnzMet® enhancement kit.

Appendix A. Supplementary data

Supplementary data associated with this article can be found, in the online version, at doi:10.1016/j.bios.2009.05.040.

References

Abgrall, P., Gué, A.M., 2007. J. Micromech. Microeng. 17, 15–49.
Basabe-Desmonts, L., Benito-López, F., Gardeniers, H.J.G.E., Duwel, R., van den Berg, A., Reinhoudt, D.N., Crego-Calama, M., 2008. Anal. Bioanal. Chem. 390, 307–315.
Benoit, V., Steel, A., Torres, M., Yu, Y.Y., Yang, H., Cooper, J., 2001. Anal. Chem. 73 (11), 2412–2420.
Diamandis, E.P., Christopoulos, T.K., 1991. Clin. Chem. 37 (5), 625–636.
Diehl, F., Grahlmann, S., Beier, M., Hoheisel, J.D., 2001. Nucleic Acids Res. 29 (7), e38.
Dittrich, P.S., Tachikawa, K., Manz, A., 2006. Anal. Chem. 78 (12), 3887–3908.
Edman, C.F., Raymond, D.E., Wu, D.J., Tu, E., Sosnowski, R.G., Butler, W.F., Nerenberg, M., Heller, M.J., 1997. Nucleic Acids Res. 25 (24), 4907–4914.
Erickson, D., Liu, X., Krull, U., Li, D., 2004. Anal. Chem. 76 (24), 7269–7277.
Festag, G., Steinbrück, A., Csaki, A., Fritzsche, W., 2007. Nanotechnology 17, 1–10.
Festag, G., Steinbrück, A., Wolff, A., Csaki, A., Moller, R., Fritzsche, W., 2005. J. Fluoresc. 15 (2), 161–170.
Haeberle, S., Zengerle, R., 2007. Lab Chip 7 (9), 1094–1110.
Han, M., Gao, X., Su, J.Z., Nie, S., 2001. Nat. Biotechnol. 19, 631–635.
Kang, C.C., Chang, C.C., Chang, T.C., Liao, L.J., Lou, P.J., Xie, W., Yeung, E.S., 2007. Analyst 132 (8), 745–749.
Lamture, J.B., Beattie, K.L., Burke, B.E., Eggers, M.D., Ehrlich, D.J., Fowler, R., Hollis, M.A., Kosicki, B.B., Reich, R.K., Smith, S.R., Varma, R.S., Hogan, M.E., 1994. Nucleic Acids Res. 22 (11), 2121–2125.
Möller, R., Csaki, A., Köhler, J.M., Fritzsche, W., 2000. Nucleic Acids Res. 28 (20e91), 1–5.
Möller, R., Powell, R.D., Hainfeld, J.F., Fritzsche, W., 2005. Nano Lett. 5 (7), 1475–1482.
Möller, R., Schüler, T., Günther, S., Carlsohn, M.R., Munder, T., Fritzsche, W., 2008. Appl. Microbiol. Biotechnol. 77 (5), 1181–1188.
Morais, S., Carrascosa, J., Mira, D., Puchades, R., Maquieira, A., 2007. Anal. Chem. 79 (20), 7628–7635.
Myers, F.B., Lee, L.P., 2008. Lab Chip 8 (12), 2015–2031.
Noerholm, M., Bruus, H., Jakobsen, M.H., Telleman, P., Ramsing, N.B., 2004. Lab Chip 4 (1), 28–37.
Oh, S.J., Hong, B.J., Choi, K.Y., Park, J.W., 2006. Omics 10 (3), 327–343.
Pappaert, K., Ottevaere, H., Thienpont, H., Van Hummelen, P., Desmet, G., 2006. Biotechniques 41 (5), 609–616.
Pappaert, K., Vanderhoeven, J., Van Hummelen, P., Dutta, B., Clicq, D., Baron, G.V., Desmet, G., 2003. J. Chromatogr. A 1014 (1–2), 1–9.
Peytavi, R., Raymond, F.R., Gagne, D., Picard, F.J., Jia, G., Zoval, J., Madou, M., Boissinot, K., Boissinot, M., Bissonnette, L., Ouellette, M., Bergeron, M.G., 2005. Clin. Chem. 51 (10), 1836–1844.
Schena, M., Heller, R.A., Theriault, T.P., Konrad, K., Lachenmeier, E., Davis, R.W., 1998. Trends Biotechnol. 16 (7), 301–306.
Schena, M., Shalon, D., Davis, R.W., Brown, P.O., 1995. Science 270 (5235), 467–470.
Schüler, T., Asmus, T., Fritzsche, W., Möller, R., 2009. Biosens. Bioelectron. 24 (7), 2077–2084.
Schüler, T., Steinbrück, A., Festag, G., Möller, R., Fritzsche, W., 2008. J. Nanopart. Res., doi:10.1007/s11051-008-9496-7.
Sia, S.K., Whitesides, G.M., 2003. Electrophoresis 24 (21), 3563–3576.
Toegl, A., Kirchner, R., Gauer, C., Wixforth, A., 2003. J. Biomol. Tech. 14 (3), 197–204.
Urban, M., Möller, R., Fritzsche, W., 2003. Rev. Sci. Instrum. 74, 1077–1081.
Wong, A.K., Krull, U.J., 2005. Anal. Bioanal. Chem. 383 (2), 187–200.

2.9 UV cross-linking of unmodified DNA on glass surfaces

Thomas Schüler, Alla Nykytenko, Andrea Csaki, Robert Möller, Wolfgang Fritzsche, Jürgen Popp

Analytical Bioanalytical Chemistry (**2009**) DOI 10.1007/s00216-009-3045-9

Anal Bioanal Chem
DOI 10.1007/s00216-009-3045-9

ORIGINAL PAPER

UV cross-linking of unmodified DNA on glass surfaces

Thomas Schüler · Alla Nykytenko · Andrea Csaki · Robert Möller · Wolfgang Fritzsche · Jürgen Popp

Received: 10 March 2009 / Revised: 22 June 2009 / Accepted: 7 August 2009

Abstract The performance of DNA microarrays strongly depends on their surface properties. Furthermore, the immobilization method of the capture molecules is of importance for the efficiency of the microarray in terms of sensitivity and specificity. This work describes the immobilization of single-stranded capture oligonucleotides by UV cross-linking on silanated (amino and epoxy) glass surfaces. Thereby we used amino (NH_2) and poly thymine/poly cytosine modifications of the capture sequences as well as unmodified capture molecules. The results were compared to UV cross-linking of the same DNA oligonucleotides on unmodified glass surfaces. Immobilization and hybridization efficiency was demonstrated by fluorescence and enzyme-induced deposition of silver nanoparticles. We found out that single-stranded DNA molecules do not require a special modification to immobilize them by UV cross-linking on epoxy- or amino-modified glass surfaces. However, higher binding rates can be achieved when using amino-modified oligonucleotides on an epoxy surface. The limit of detection for the used settings was 5 pM.

Keywords DNA microarray · Enzyme-induced silver deposition · UV cross-linking · Silanated glass surfaces

Thomas Schüler and Alla Nykytenko contributed equally to this paper.

T. Schüler · R. Möller (✉) · J. Popp
Jenaer Biochip Initiative, Institute of Physical Chemistry,
Friedrich Schiller University,
Helmholtzweg 4,
07743 Jena, Germany
e-mail: robert.moeller@ipht-jena.de

A. Nykytenko · A. Csaki · W. Fritzsche · J. Popp
Institute of Photonic Technology,
Albert-Einstein-Straße 9,
07745 Jena, Germany

Published online: 29 August 2009

Introduction

The quality of microarrays and their efficiency mainly depend on the properties of the microarray surface and the method to immobilize the capture molecules on the surface. Because the microarrays are usually fabricated on a solid support, coating of the surface and immobilization strategy of the biomolecules are major issues for successful microarray fabrication [1, 2]. Basically, two different approaches are commonly used to immobilize biomolecules on microarray surfaces: the on-chip synthesis of the capture molecules by photolithographic masks or micromirror arrays and the immobilization of pre-synthesized oligonucleotides directly to the microarray surface. The latter requires an additional modification of the biomolecules with functional groups (e.g., amino, thiol, and biotin) to improve the binding efficiency on the chip surface.

Glass surfaces are usually modified with a surface monolayer containing active organic functional groups such as thiol [3], amine [4], aldehyde [5], or epoxy [6], which bind the capture molecules either covalently or through electrostatic interactions. The functional groups are introduced to the glass surface via covalent bonds between various functionalized siloxane compounds and surface silanol groups [1]. Thiol, aldehyde, or epoxy groups on the surface are advantageous because they can directly bind with thiol- or amino-modified oligonucleotides via covalent bonds, such as via disulfide (–S–S–) bonds between surface thiols and thiol groups in oligonucleotides [7], carbon–nitrogen bonds between surface aldehydes [8] or epoxides [9], and amino groups in oligonucleotides. Because of this advantage, these types of surfaces are widely used for fabrication of DNA microarrays.

However, immobilization of capture probe DNA molecules on these surfaces is relatively inefficient. Somewhat

enhanced efficiency was achieved on surfaces having two functional groups, amino and epoxy, that were developed by self-assembly of a mixture of amino and epoxy silanes [10]. The DNA microarrays fabricated on glass slides modified with a thin layer of active functional groups as described exhibit advantages of good reproducibility and low background signal using fluorescent detection. Solid substrates modified with thin layers of various functional groups have been widely utilized as substrates for DNA microarrays because they are inexpensive and easy to prepare. Furthermore it is known that the binding efficiency of oligonucleotides can be improved by terminal modification with functional groups compared to unmodified oligonucleotides [11]. Nevertheless these additional modifications usually increase the costs of the microarray fabrication.

An approach that allows the immobilization of modified oligonucleotides even on unmodified glass surfaces is UV cross-linking [12–14]. This well-known method is widely used in different applications for the attachment of DNA or proteins on membranes, solid surfaces, and polymers [15–18]. One approach describes the use of a polyC/polyT modification of DNA for the immobilization on agarose films [19] by UV cross-linking.

However, the exposure by UV light can induce damage to the DNA [20]. Due to the cross-linking between the nucleotides in the capture-DNA strand and the microarray surface, the reactivity as well as the specificity of the hybridization could be hampered. A recent publication described the extension of the polyT/polyC tail approach to unmodified glass surfaces [21].

We are interested in new efficient methods to immobilize DNA capture strands to glass surfaces. Therefore, we tested this proposed technique and extended it to further modifications for DNA and glass surfaces.

Here we demonstrated the potential of UV cross-linking for different modified and even unmodified oligonucleotides for microarray applications. The oligonucleotides were immobilized to modified (epoxy or amino) and different unmodified glass surfaces.

For this purpose, we used a fluorescent dye or horseradish peroxidase (attached via streptavidin to biotinylated DNA) as label to determine the efficiency of the immobilization of the capture molecules as well as the hybridization efficiency. In case of peroxidase, a following enzyme-induced deposition of silver nanoparticles led to dense layer of silver nanoparticles that can be detected by light microscopy [22]. The advantages using an enzymatic reaction to deposit silver nanoparticles compared to other enzyme based methods like chemiluminescence are the highly localized, stable signals that do not fade or bleach. Furthermore this approach allows the combination of the specific and fast enzymatic reaction with the unique properties of metal nanoparticles [23].

This work points out the advantages as well as disadvantages of different surfaces and DNA modifications and their applicability for UV cross-linking in the field of DNA microarrays. It demonstrates a UV cross-linking approach without the need for modified DNA.

Materials and methods

Oligonucleotides

Concentrations of oligonucleotides were measured spectrophotometrically at 260 nm by NanoDrop 1000 (NanoDrop Technologies, Wilmington, DE, USA). Non-, amino-, or polyT/polyC-modified oligonucleotide probes (Table 1) were dissolved in sterile distilled water at 100 µM concentration.

Microarray fabrication

In the experiments, various glass slides were used (26 mm× 76 mm), which were purchased from Menzel, Roth, Marienfeld (MF), and Superfrost (SF). Each substrate was pre-cleaned with acetone, ethanol, and deionized distilled water, each for 10 min in ultrasonic bath.

For enhanced binding of the capture oligonucleotides, the glass surfaces were chemically modified by 3′-aminopropyltrimethoxysilane (APTES) or 3′-glycidoxypropyltrimethoxysilane (GOPS). For that purpose, the substrates were activated after pre-cleaning in 1:1:1 hydrochloric acid, 30% hydrogen peroxide, and deionized water for 15 min. Finally, the slides were dried under a nitrogen flow.

For the modification with APTES, the slides were silanized in 1% APTES with 1 mM acetic acid at room temperature for 10 min. A following washing step in deionized water for 5 min in ultrasonic bath removed unbound silane. Afterward, the slides were tempered for 2 h at 80 °C.

The chemical modification of the pre-cleaned glass slides with GOPS was performed for 7 h at 70 °C in 10 mM GOPS in dry toluene under continual mixing at 250 rpm [24]. Then the slides were washed three times 5 min each with toluene and finally dried and stored under vacuum in a desiccator.

Afterward, the single-stranded capture-DNA with (amino modification and polyT/polyC tail) or without linker was immobilized on the modified as well as unmodified glass surfaces. All capture molecules were diluted in different spotting buffers to a concentration ranging from 25 to 0.5 µM. In the experiments, different spotting solutions were used: ArrayIt (Micro Spotting Solution Plus, TeleChem International, Sunnyvale, USA), potassium phosphate and sodium phosphate buffer 150 mM at pH 8, and 5× phosphate buffered saline (PBS). Each probe was spotted five times on each slide with a Nano-Plotter 2.1 (GeSiM, Großerkmannsdorf, Germany) in 8 nl droplets. For covalent

Table 1 All of the oligonucleotides used in this study and shown in the list below were synthesized by Operon Biotechnologies GmbH

Oligonucleotides	Modif. 5′-end	Sequences	Modif. 3′-end
Capture-DNA			
1	NH_2	TTT TTT CAG CAT GTG CTC CTT GAT TCT ATG	
2	NH_2	TTT TTT CAG CAT **GGG** CTC CTT GAT TCT ATG	
3	NH_2	TTT TTT CAG CAT **TAT** CTC CTT GAT TCT ATG	
4[a]		ttttttttttcccccccccc TTT TTT CAG CAT GGG CTC CTT GAT TCT ATG	
5[a]		ttttcccccc AGA GAG AGA GAG AGA GAG AGA GAG AGA GAG	
6		AGA GAG AGA GAG AGA GAG AGA GAG AGA GAG	
Target-DNA			
I	Fam	CAT AGA ATC AAG GAG CAC ATG CTG	
II	Bio	CAT AGA ATC AAG GAG CAC ATG CTG AAA AAA	
III	Bio	CTC TCT CTC TCT CTC TCT CTC TCT CTC TCT	
Controls			
Negative		ACT GAC TGA CTG ACT GAC TGA CTG GGC GGC GAC CT	
Negative[a]		ttttttttttcccccccccc ACT GAC TGA CTG ACT GAC TGA CTG GGC GGC	
Positive biotin	NH_2	TTT TTT CAG CAT GTG CTC CTT GAT TCT ATG	Bio
Positive biotin[a]		ttttttttttcccccccccc TTT TTT CAG CAT GTG CTC CTT GAT TCT ATG	Bio
Positive fluorescein	NH_2	TTT TTT CAG CAT GTG CTC CTT GAT TCT ATG	Fam
Positive fluorescein[a]		ttttttttttcccccccccc TTT TTT CAG CAT GTG CTC CTT GAT TCT ATG	Fam

The DNA sequences 1–3 were modified by an amino linker and were used to capture the target-DNA sequences I (fluorescence) and II (biotin). The capture sequences 5 and 6 contain only adenine and guanine to show the efficiency of the polyT/polyC modification. These sequences should capture the biotin-labeled target-DNA III. Furthermore, different negative and positive controls were used to check the immobilization without the need for a hybridization step

1 perfect match, *2* complementary sequence containing one mismatch, *3* complementary sequence containing three mismatches

[a] Sequences that were modified with a poly/polyC tail used as linker to the glass surfaces

binding of DNA probes after spotting, the slide surfaces were exposed to 254 nm UV light for different times at 10, 5, 2.5, and 1 min, i.e., 23 mW/cm^2 by using a UV Bender NU-6KL (Bender, Wiesloch, Germany). After immobilization, it is important to remove unbound DNA molecules and salt from the slides by washing with 0.1× saline sodium citrate (SSC)/0.5% sodium dodecyl sulfate (SDS) for 10 min and 20 s in distilled water at room temperature. The slides were dried under nitrogen before hybridization.

Hybridization and enzyme-induced silver deposition

For the tests, DNA, which was labeled on the 5′ end with a fluorescent dye or a biotin modification, was used. The target-DNA was diluted in 5× SSC/0.1% SDS buffer with concentration from 5 μM to 500 fM. The slides are placed in humidity chambers for hybridization for 1 h at 40 °C. It is important to ensure that the slides are adequately covered with hybridization solution. Do not allow slides to dry. After the hybridization, the volume of the washing solution should be at least 20 ml for two slides. Slides that had been hybridized with different target-DNA concentrations were washed separately to avoid cross-contamination. Each slide is washed for 5 min at room temperature with 2× SSC/0.1% SDS buffer then with 2× SSC buffer and 0.2× SSC buffer. Finally, the slides were dried under nitrogen.

The biotin serves as a binding molecule for streptavidin-conjugated horseradish peroxidase (Sigma-Aldrich, Taufkirchen, Germany). An initial dilution of 1:1,000 in 1× PBS/0.5% Tween 20 was incubated for 1 h at room temperature on each slide. The slides were washed six times in 1× PBS/0.5% Tween 20 buffer. Do not allow slides to dry during washing steps to avoid a loss in reactivity of the enzyme. A final, short washing step with deionized water removed any chloride from the solution to guarantee an optimal enzymatic reaction.

The specific binding event of biotinylated target-DNA (followed by the binding of streptavidin-conjugated horseradish peroxidase) was visualized using a specially developed silver enhancement kit (EnzMet®) from Nanoprobes (Nanoprobes Inc., Yaphank, NY, USA). The three solutions (A, B, and C) were applied in small droplets on the chip surface in ratio 1:1:1. After adding the enhancement kit, silver nanoparticles will be immediately formed by the enzymatic activity. The silver spots do not fade or bleach, and a minimal background (unspecific silver deposition) was observed. The reaction was stopped after 5 min by washing the glass surface with distilled deionized water prior to drying under a nitrogen

flow to avoid unspecific silver deposition. The principle of both detection methods for a sensitive and specific analysis of DNA is shown in Fig. 1.

Signal detection and data evaluation

For characterization of the fluorescence-labeled DNA, a fluorescence microscope Axiotech (Carl Zeis, Jena, Germany) equipped with CCD camera Sensicam (PCO computer optics, Kehlheim, Germany) was used. The produced eight-bit grayscale images were analyzed with the image analysis software ImageJ, and the background signal was subtracted from the given data. In the case of the enzyme-induced deposition of silver nanoparticles, a transmissive optical detection of the signal was performed using a flatbed Duoscan T2500 AGFA scanner (Agfa Deutschland, Köln, Germany). Gray values of the individual spots were measured using converted tiff images, and the signal intensities were quantified by ImageJ software from NIH [25]. The average signal values were taken from five spots on each slide. All measurements were background-corrected.

Negative controls

All tests were performed with negative controls using the same concentrations and buffers. This should assure the specificity of UV cross-linking and its applicability in microarray technology. Different negative controls were implemented in all tests. To ensure the specificity, non-complementary sequences containing all used modifications were also immobilized on all slides. Further all tests were also performed without immobilized capture-DNA or without target-DNA. Finally, to control the efficiency of the UV cross-linking, all experiments were repeated without exposure of UV light.

Results

At first, the immobilization of single-stranded fluorescent or biotin-labeled DNA mediated by UV cross-linking was tested and analyzed by fluorescence as well as enzyme-induced silver deposition. These detection methods were used to study two different linker groups to bind the DNA

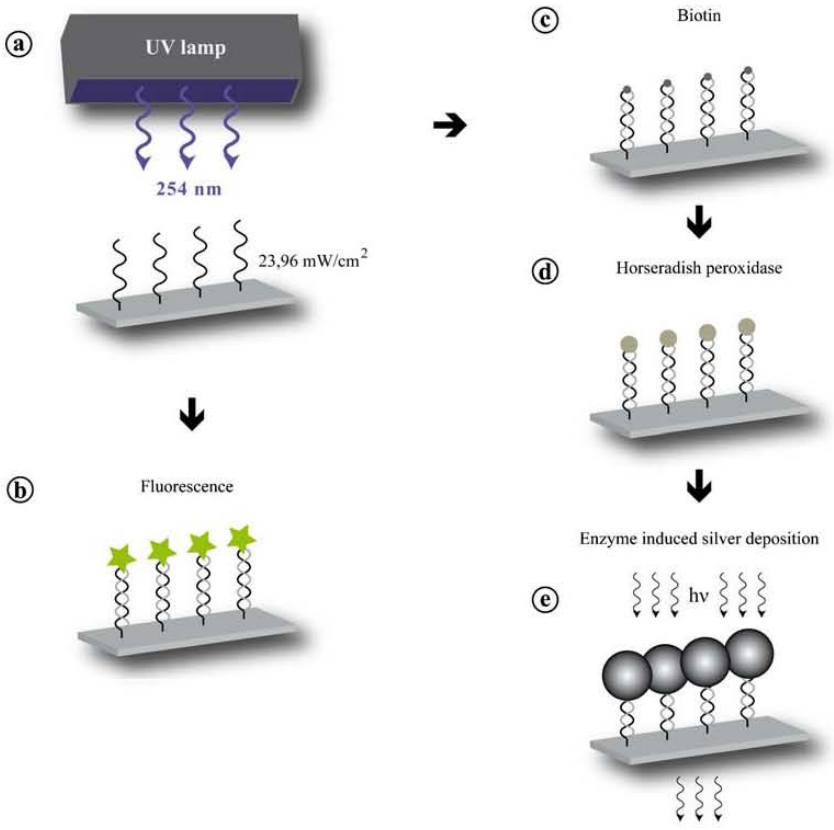

Fig. 1 Scheme of the different used detection methods after UV cross-linking. After spotting, the single-stranded capture-DNA becomes immobilized by UV cross-linking at 254 nm (**a**). This allows a later hybridization of target-DNA labeled by a fluorescent dye (**b**) or a biotin-labeled target-DNA (**c**). The biotin serves as attachment site for streptavidin–horseradish peroxidase– polymers (**d**). A final enzyme-induced silver deposition leads to a metallic layer (**e**); the read-out can be performed by optical transmission measurements (light absorption of the deposited silver)

at the glass surfaces. For that purpose, single-stranded DNA sequences modified either with an amino modification or a polyT/polyC modification were immobilized on different glass surfaces. The concentration of the immobilized single-stranded DNA was 25 µM.

We used commercial glass slides from Marienfeld, Menzel, Roth, and Superfrost. Furthermore we investigated the binding behavior on modified glass surfaces. In this case, the organosilanes GOPS and APTES were used to introduce either an epoxy functionalization or an amino functionalization to the glass surface. The surface modification by organosilanes was only performed on glass slides from Menzel. Due to the surface activation, the surface differences between slides of different suppliers become minimal. The following silanization leads to a homogenous monolayer by internal cross-linking between neighbored silane molecules on the glass surface.

For the DNA immobilization by 10 min UV cross-linking, the most suitable buffer was figured out by using different spotting buffers: Spotting solution from ArrayIt, 5× PBS, potassium phosphate, and sodium phosphate buffer 150 mM at pH 8 (data not shown). The best result was obtained for 5× PBS. Additionally, the glass surfaces treated with GOPS and APTES showed the highest signal intensities (Fig. 2). Also the amino-modified DNA (Fig. 2a) showed higher signal intensities compared to the polyT/polyC modification (Fig. 2b). This effect was determined for fluorescence as well as enzyme-induced silver deposition (Fig. 2c). The controls without exposure of UV light showed low signal intensities that indicate only low binding efficiency of the biomolecules on the glass surfaces. Only amino-modified DNA showed a significant binding without UV exposure, which is an expected effect [6].

Because of these results, all further tests were performed only on GOPS and APTES surfaces. Due to comparable signals between both detection methods, only the enzyme-induced silver deposition was used in the following tests. Exclusively, the capture-DNA was diluted in 5× PBS.

The parameter to be investigated was the exposure time of the UV cross-linking. To find optimal conditions, single-stranded DNA directly labeled with a biotin modification was exposed to UV light for 10, 5, 2.5, and 1 min. The results were controlled by enzyme-induced silver deposition. The immobilized biotin-labeled DNA was modified either with an amino link or a polyT/polyC modification to further investigate the differences in signal intensity depending on the linker group. Again the amino modification showed higher binding efficiencies to both the GOPS and the APTES surface (Fig. 3a, b).

At fluency of 23.96 mW/cm^2, the best results were obtained at 5 min exposure time. The comparison between GOPS and APTES surfaces displayed no significant differences in the signals.

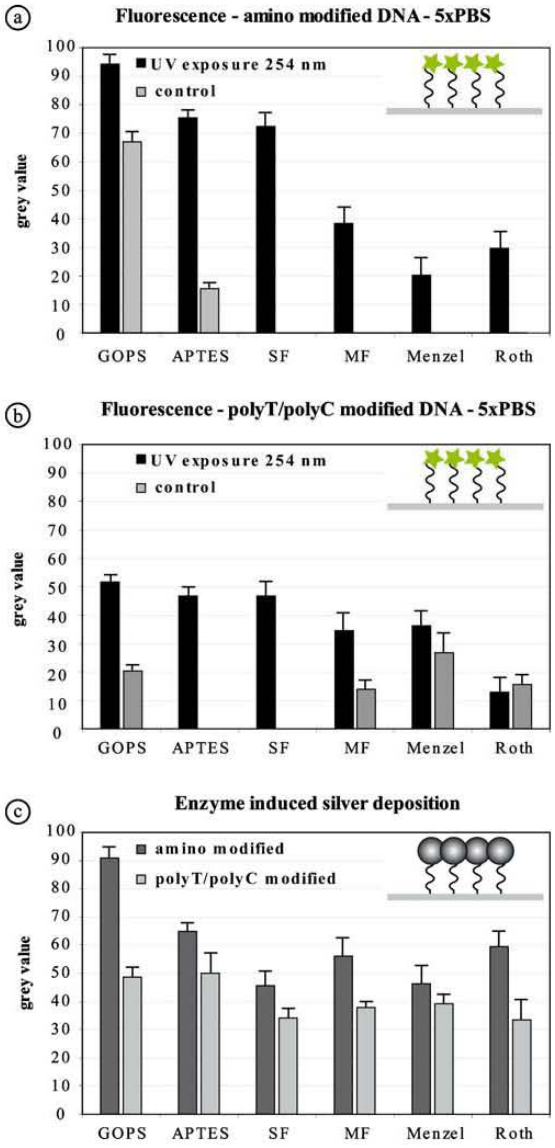

Fig. 2 Investigation of different glass surfaces to find the optimal surface for the immobilization of singe stranded capture-DNA by UV cross-linking (*SF* Superfrost, *MF* Marienfeld, *GOPS* glass modified by (3-glycidyloxypropyl)-trimethoxysilane, *APTES* glass surface modified by aminopropyltriethoxysilane). The DNA was modified at the 5′ end either with an amino link (**a**) or a polyT/polyC tail (**b**). The efficiency of the immobilization was evaluated by fluorescence **a** and **b** or by enzyme-induced silver deposition **c**. Therefore the DNA was labeled on the 3′ end with a fluorescent dye or a biotin modification to bind the streptavidin–peroxidase afterward. The control was not exposed to UV light

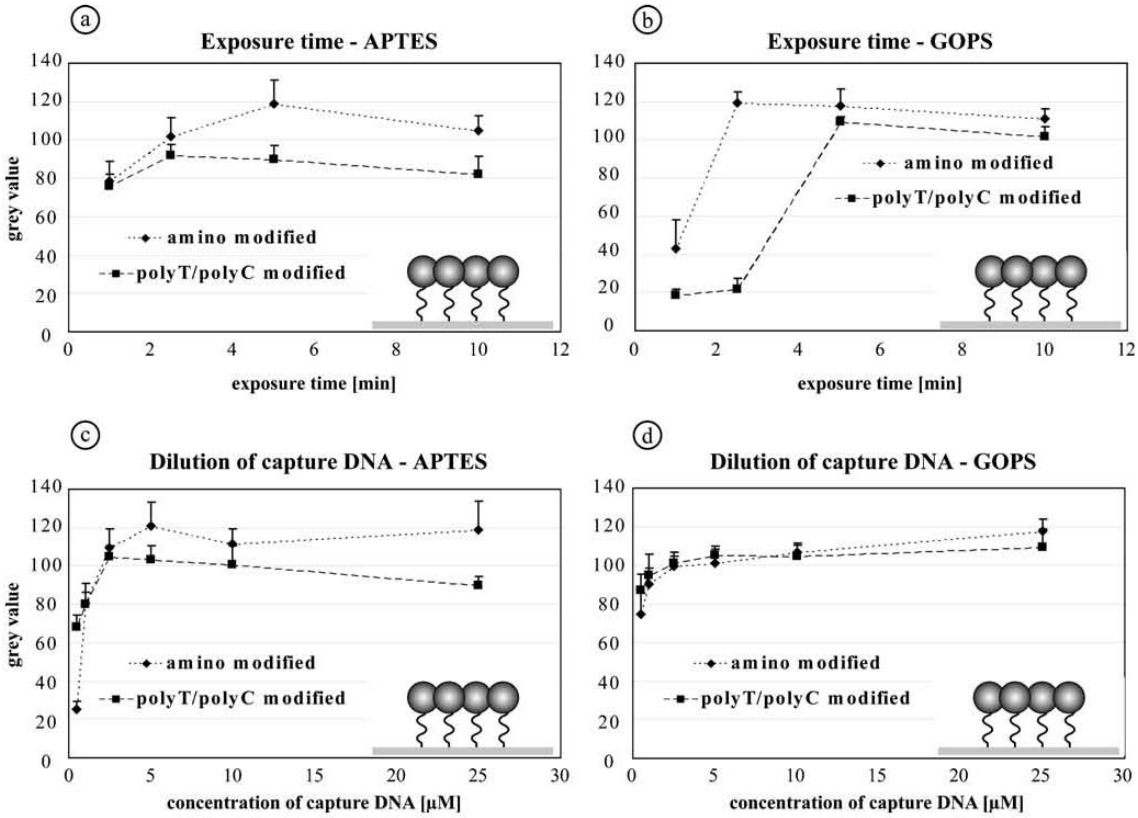

Fig. 3 Finding the best parameters for UV cross-linking, the exposure time and DNA concentration were optimized. The optimal exposure time for the UV cross-linking was found to be at 5 min on APTES (**a**) as well as GOPS (**b**) surfaces. Furthermore, the optimal concentration of single-stranded capture-DNA is 5 µM for both surfaces (**c** and **d**). The results were obtained by enzyme-induced silver deposition

In the next step, we reduced the concentration of the single-stranded DNA, later used as capture molecules for the hybridization, from 25 down to 0.5 µM, to identify the optimal concentration for the UV light-mediated immobilization of DNA. The optimal concentration was found at 5 µM for 5 min exposure time at 23.96 mW/cm^2. Higher concentrations displayed no significant additional increase in signal intensity. With lower concentrations, the signals decrease. However, even the lowest DNA concentration of 0.5 µM still gave detectable signals on GOPS surfaces. Hence, GOPS surfaces were more sensitive for low DNA concentrations (Fig. 3c, d).

Zhuravlev studied in 1987 the concentration of hydroxyl groups on glass surfaces [26]. He measured a concentration of five hydroxyl groups per square nanometer, around 5×10^{12} hydroxyl groups/mm^2. Each further process step leads to a decrease of surface density by one order of magnitude [27]. So, the surface density after silanization and immobilization of the capture sequences is approximately 5×10^{10} DNA molecules/mm^2.

At a capture-DNA concentration of 5 µM, the signal intensity points to a saturation of surface density. We used 8 nl droplets for each spot in our tests; this is equal to about 2×10^{10} DNA molecules. This value is close to the theoretical number of the maximal binding positions on the glass surface. In comparison, DNA concentrations below 5 µM lead to a decrease of signal intensity because of fewer molecules, for instance 4.8×10^9 for 1 µM.

Literature data describe for proteins a surface coverage of 2 ng/mm^2 at a concentration of 30 nM and a maximal coverage of 5 6 ng/mm^2 for a complete monolayer [28]. In case of capture-DNA, a surface coverage was achieved at 10 400 pg/mm^2 [29].

Thereby signals of DNA immobilized by an amino modification were slightly higher compared to the polyT/polyC tail. All results were performed by enzyme-induced silver deposition.

A key parameter in biochip technology is the limit of detection. We hybridized biotinylated target-DNA in different concentrations to UV cross-linked single-stranded

capture-DNA on GOPS and APTES surfaces. The capture-DNA concentration was 5 μM. In previous experiments, amino-modified DNA showed better signals (Fig. 3), so only amino-modified DNA was used in these tests. The limit of detection for GOPS as well as APTES surfaces is 5 pM. This is already described and corresponds to the literature even without UV cross-linking [30]. Gudnadson demonstrated 2008 a limit of detection for fluorescent labeled DNA immobilized by UV cross-linking of 10 nM.

In previous work, we already compared different DNA analysis methods on a polymeric platform in terms of sensitivity and specificity [31]. Thereby, the enzyme-induced silver deposition had a detection limit of 500 fM (optical transmission measurements, light absorption of the deposited silver) compared to MALDI TOF/MS with 500 nM and fluorescence labeling at 500 pM. However, the sensitivity of the enzyme-induced silver deposition can be improved by additional enhancement steps following the initial particle formation [32]. Nevertheless the APTES surface produced signal intensities below those of the GOPS surface (Fig. 4).

Beside test sensitivity, specificity represents an important parameter. A study of the specificity was performed by using different mismatch sequences as capture-DNA (next to a complementary sequence, a complementary sequence containing 1 mismatch and a complementary sequence containing three mismatches).

The higher signal intensities on the GOPS-treated surfaces point to higher binding efficiencies of amino-modified DNA. This effect leads directly to a higher amount of immobilized DNA and possible binding partners for the target-DNA on GOPS surfaces. A better specificity was achieved on APTES surfaces. Due to the higher number of immobilized capture molecules on GOPS surfaces, the hybridization probability increases also for the mismatch probes. Using more stringent conditions, the specificity will be improved even on the GOPS surfaces.

On both surfaces (GOPS and APTES), no signals on the negative control were detectable (non complementary target-DNA). It was possible for both organosilanes to discriminate between the complementary sequences and the complementary sequence containing one or three mismatches at any concentration.

The influence of the terminal modification of the oligonucleotides is of importance when working with UV cross-linking. Here we compared the immobilization efficiency of four different terminal modifications at single-stranded capture-DNA sequences. A sequence with an amino linker, a poly thymine/poly cytosine (polyT/polyC) tail, a sequence without modification containing only adenine and guanine, and the same (only adenine/guanine) sequence were modified by a short polyT/polyC tail.

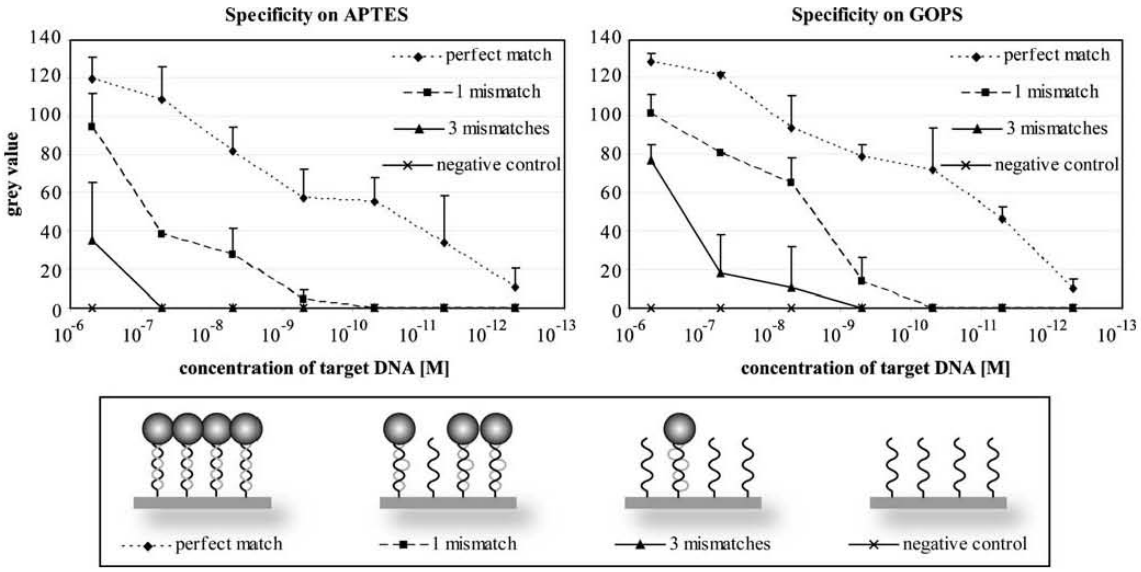

Fig. 4 Testing the limit of detection and the specificity after UV cross-linking. The limit of detection is 5 pM (for hybridization with biotin-labeled DNA and followed by enzyme-induced silver deposition) for GOPS as well as APTES surfaces. This value is comparable to previous work without using UV cross-linking. The specificity of the hybridization is displayed in both diagrams (*APTES* and *GOPS*). A clear discrimination between one mismatch, three mismatches, and negative control is possible. Furthermore, the signals are significantly lower compared to the perfect match

The immobilized capture molecules (5 min at 254 nm in 5× PBS) were hybridized with complementary biotin-labeled target-DNA at a concentration of 500 nM.

After enzyme-induced silver deposition, the results showed that it is not necessary to modify the oligonucleotides by any linker group to immobilize single-stranded DNA on GOPS or APTES surfaces (Fig. 5). However, the amino-modified sequence showed again the best signals on both surfaces. An additional modification by a polyT/polyC tail produced better results compared to the unmodified DNA sequence containing only adenine and guanine that still gave detectable signals. When comparing the results of the experiment, one can conclude that the highest signals can be achieved using the amino modification followed by the polyT/polyC tail and the unmodified sequences.

Discussion

This work demonstrated the potential of UV cross-linking for use in microarray technology. The advantage of the UV light exposure is the time saving for the binding of the capture molecules on the microarray. After a 5 min exposure time (UV light at 254 nm), the spotted microarrays can be directly used for a hybridization experiment. Thereby, we did obtain the same sensitivity and specificity compared to capture molecule immobilization on the microarray surface by overnight incubation.

Surface modifications with an amino (APTES) or an epoxy (GOPS) functionalization are widely used in the field of microarray technology. Thereby, the functionalized surfaces showed higher and more homogeneous signals compared to unmodified surfaces. However, also the unmodified glass surfaces can be used as substrates for microarray applications if they were exposed to UV light after the spotting of the capture molecules.

Furthermore, different modifications of the capture-DNA were investigated in terms of binding behavior and signal intensity. Here we used capture molecules with an amino modification, an additional polyT/polyC tail, and unmodified molecules. It was demonstrated that all capture molecules can bind to the surface by using UV cross-linking. However, the best signals were obtained with amino-modified capture molecules on surfaces functionalized with amino or epoxy groups.

Without UV light exposure, reproducible signals could be only detected on the epoxy-modified surface in combination with the amino-modified capture molecules. This gave the opportunity to compare this conventional system with the additional UV cross-linking. With respect to sensitivity and specificity, we achieved the same results as described in the literature for the interaction of epoxy surfaces with amino-modified oligonucleotides. The limit of detection was determined at 5 pM. Additionally, we were able to differentiate between the complementary sequence and the complementary sequence containing one mismatch.

One essential implication of this work refers to the costs that arise by the surface functionalization and the modification of the capture-DNA. So, the key point is the benefit of modifications in combination with their expenses. For that purpose, we checked the costs for different modifications of DNA. A 30-bp oligonucleotide in a 1 µmol scale with HPLC purification and an additional C6-NH_2 is about one third cheaper compared to the extra polyT/polyC tail at the same scale and purification. The unmodified sequence would be one fifth cheaper as the amino-modified oligonucleotide. The surface modification of a common glass slide more than triples the price for a modified GOPS slide

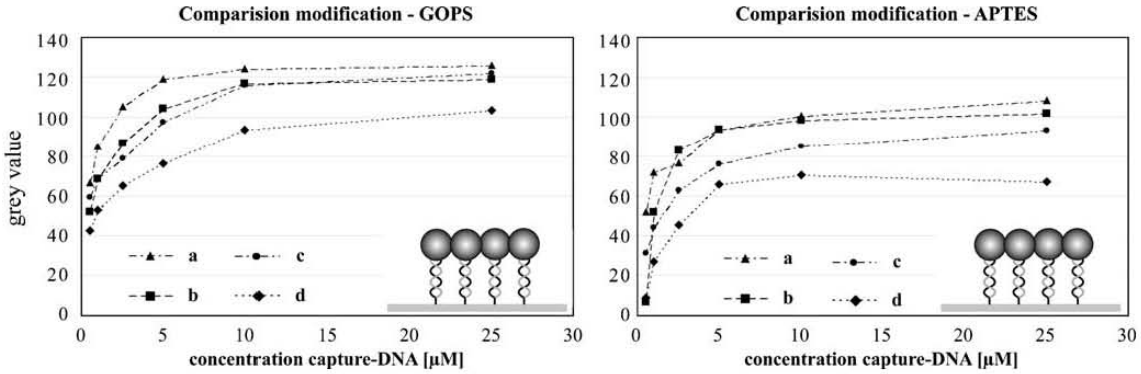

Fig. 5 Influence of the terminal DNA modification. The diagrams demonstrate the potential of UV cross-linking to immobilize different modified and unmodified oligonucleotides on silanated surfaces (*GOPS* and *APTES*). We immobilized single-stranded capture DNA molecules: (*a*) an amino-modified oligonucleotide, (*b*) AG (only adenine and guanine) modified with a polyT/polyC tail, (*c*) a polyT/polyC tail modified sequence, and (*d*) AG (only adenine and guanine) without modification

(including dried toluene, glass slide, and GOPS). Of course, the costs depend on the amount of glass slides; we considered 50 glass slides in both cases.

Single-stranded DNA molecules do not require a special modification to immobilize them by UV cross-linking on epoxy - or amino-modified glass surfaces. However, the amino-modified oligonucleotides show the highest signal on the epoxy surface. The modification by APTES shows comparable signals even for the unmodified DNA sequences. This leads to the conclusion that also unmodified sequences can be immobilized on silanated surfaces by UV cross-linking. Because of this relationship, the optimal use for UV cross-linking is apparently in combination with GOPS surfaces and amino-modified oligonucleotides.

During this work, we did not notice a loss in specificity of the biomolecular reactions after UV cross-linking immobilization due to possible UV damages. Owing to the fact that we could clearly differentiate between perfect match and mismatch probes, the presence of significant damages to the DNA by UV exposure can be neglected. Furthermore, these results were reproducible in all of our experiments.

Further work will be performed to investigate the immobilization of proteins by UV cross-linking. The process of UV cross-linking will also be investigated on different polymer substrates and compared to the results on glass. It is also planned to transfer this protocol to an already developed DNA chip with electrical detection [33].

Acknowledgments Funding of research project "Jenaer Biochip Initiative" (JBCI) within the framework "Unternehmen Region—Inno Profile" from the Federal Ministry of Education and Research, Germany (BMBF) is gratefully acknowledged. This work was supported by the DFG (FR 1348/5-2).We thank Nanoprobes for the kind support with EnzMet® enhancement kit.

References

1. Oh SJ, Hong BJ, Choi KY, Park JW (2006) Omics 10:327–343
2. Bier FF, Kleinjung F (2001) Fresenius' J Anal Chem 371:151–156
3. Rogers YH, Jiang-Baucom P, Huang ZJ, Bogdanov V, Anderson S, Boyce-Jacino MT (1999) Anal Biochem 266:23–30
4. Oh SJ, Cho SJ, Kim CO (2002) Langmuir 18:1764–1769
5. Schena M, Shalon D, Heller R, Chai A, Brown PO, Davis RW (1996) Proc Natl Acad Sci U S A 93:10614–10619
6. Lamture JB, Beattie KL, Burke BE, Eggers MD, Ehrlich DJ, Fowler R, Hollis MA, Kosicki BB, Reich RK, Smith SR, Varma RS, Hogan ME (1994) Nucleic Acids Res 22:2121–2125
7. Chrisey LA, Lee GU, O'Ferrall CE (1996) Nucleic Acids Res 24:3031–3039
8. Zammatteo N, Jeanmart L, Hamels S, Courtois S, Louette P, Hevesi L, Remacle J (2000) Anal Biochem 280:143–150
9. Taylor S, Smith S, Windle B, Guiseppi-Elie A (2003) Nucleic Acids Res 31:e87
10. Chiu SK, Hsu M, Ku WC, Tu CY, Tseng YT, Lau WK, Yan RY, Ma JT, Tzeng CM (2003) Biochem J 374:625–632
11. Schena M (2003) Microarray analysis. Wiley, Hoboken
12. Boa Z, Ma WL, Hu ZY, Rong S, Shi YB, Zheng WL (2002) J Biochem Mol Biol 35:532–535
13. Duroux M, Gurevich L, Neves-Petersen MT, Skovsen E, Duroux L, Petersen BS (2007) Applied Surface Science 254:1126–1130
14. Kabilov MR, Pyshnyi DV, Dymshits GM, Gashnikova NM, Pokrovskii AG, Zarytova VF, Ivanova EM (2002) Mol Biol 36:424–431
15. Kimura N (2006) Biochem Biophys Res Commun 347:477–484
16. Nahar P, Naqvi A, Basirb SF (2004) Anal Biochem 327:162–164
17. Soper SA, Hashimoto M, Situma C, Murphy MC, McCarley RL, Cheng YW, Barany F (2005) Methods 37:103–113
18. Pack PS, Kamisetty KN, Nonogawa M, Devarayapalli CK, Ohtani K, Yamada K, Yoshida Y, Kodaki T, Makino K (2007) Nucleic Acids Res 35:1–10
19. Dufva M, Petersen J, Stoltenborg M, Birgens H, Christensen CB (2006) Anal Biochem 352:188–197
20. Sinha RP, Häder DP (2002) Photochem Photobiol Sci 1:225–236
21. Gudnason H, Dufva M, Duong BD, Wolff A (2008) Biotechniques 45:261–271
22. Fritzsche W, Taton TA (2003) Nanotechnology 14:R63–R73
23. Schüler T, Steinbrück A, Festag G, Möller R, Fritzsche W (2008) J Nanopart Res 11:939–946
24. Möller R, Csaki A, Köhler JM, Fritzsche W (2000) Nucleic Acids Res 28:1–5
25. Barrett S (2008) *Image SXM v1.85*. http://www.liv.ac.uk/~sdb/ImageSXM/.
26. Zhuravlev LT (1987) Langmuir 3:316–318
27. Reichert J (2003) Thesis, Friedrich Schiller Universität Jena
28. Piehler J, Brecht A, Geckeler KE, Gauglitz G (1996) Biosens Bioelectron 11:579–590
29. Piehler J, Brecht A, Gauglitz G, Zerlin M, Maul C, Thiericke R, Grabley S (1997) Anal Biochem 249:94–102
30. Schüler T, Asmus T, Fritzsche W, Möller R (2009) Biosens Bioelectron 24:2077–2084
31. Ibanez AJ, Schüler T, Möller R, Fritzsche W, Saluz HP, Svatos A (2008) Anal Chem 80:5892–5898
32. Festag G, Steinbrück A, Csaki A, Fritzsche W (2007) Nanotechnology 17:1–10
33. Möller R, Powell RD, Hainfeld JF, Fritzsche W (2005) Nano Lett 5:1475–1482

Dokumentation der Autorschaft der Publikationen

2.1 Electrical DNA-chip-based identification of different species of the genus *Kitasatospora*

Appl. Microbiol. Biotechnol. (**2008**) 77:1181–1188

Robert Möller:	Anfertigung des Manuskripts
Thomas Schüler:	Versuchsdurchführung, Auswertung der Messdaten
Sebastian Günther:	Vorarbeiten
Marc René Carlsohn:	Herstellung PCR Produkte verschiedener Spezies von *Kitasatospora*
Thomas Munder:	Diskussion und Korrektur des Manuskripts
Wolfgang Fritzsche:	Diskussion und Korrektur des Manuskripts

2.2 Screen printing as cost-efficient fabrication method for DNA-chips with electrical readout for the detection of viral DNA

Biosensors Bioelectronics (**2009**) 24(7): 2077-84

Thomas Schüler:	Anfertigung des Manuskripts, Versuchsdurchführung, Auswertung der Messdaten
Tim Asmus:	Herstellung der Siebdruckchips, Korrektur des Manuskripts
Wolfgang Fritzsche:	Diskussion und Korrektur des Manuskripts
Robert Möller:	Diskussion und Korrektur des Manuskripts

2.3 Flexible biochips for detection of biomolecules

Langmuir (**2009**) 25(9): 5384-90

Mária Péter:	Anfertigung des Manuskripts
Thomas Schüler:	Anfertigung des Manuskripts, Versuchsdurchführung, Auswertung der Messdaten
Francois Furthner:	Strukturierung der PEN Folien
Peter A. Rensing:	Partner im Projekt vom TNO Eindhoven
Gert T. van Heck:	Partner im Projekt vom TNO Eindhoven
Herman F. M. Schoo:	Partner im Projekt vom TNO Eindhoven
Robert Möller:	Anfertigung und Diskussion des Manuskripts
Wolfgang Fritzsche:	Diskussion und Korrektur des Manuskripts
Albert J. J. M. van Breemen:	Diskussion und Korrektur des Manuskripts
Erwin R. Meinders:	Diskussion und Korrektur des Manuskripts

2.4 DNA detection using a triple readout optical/AFM/MALDI planar microwell plastic chip

Anal. Chem. (**2008**) 80(15): 5892-8

Alfredo J. Ibanez:	Anfertigung des Manuskripts, Versuchsdurchführung, Auswertung der Messdaten
Thomas Schüler:	Anfertigung des Manuskripts, Versuchsdurchführung, Auswertung der Messdaten
Robert Möller:	Anfertigung und Diskussion des Manuskripts
Wolfgang Fritzsche:	Diskussion und Korrektur des Manuskripts
Hans-Peter Saluz:	Diskussion und Korrektur des Manuskripts
Ales Svatos:	Diskussion und Korrektur des Manuskripts

2.5 Chip-based molecular diagnostics using metal nanoparticles

Expert Opinion on Medical Diagnostics (**2008**) 2(7): 813-828

Grit Festag:	Anfertigung des Manuskripts
Thomas Schüler:	Anfertigung des Manuskripts
Andrea Steinbrück:	Anfertigung des Manuskripts
Andrea Csáki:	Diskussion und Korrektur des Manuskripts
Robert Möller:	Anfertigung und Korrektur des Manuskripts
Wolfgang Fritzsche:	Diskussion und Korrektur des Manuskripts

2.6 Growth and percolation of metal nanostructures in electrode gaps leading to conductive paths for electrical DNA analysis

Nanotechnology (**2008**) 19 (125303): 1-9

Grit Festag:	Anfertigung des Manuskripts, Versuchsdurchführung, Auswertung
Thomas Schüler:	Versuchsdurchführung
Robert Möller:	Diskussion und Korrektur des Manuskripts
Andrea Csáki:	Diskussion und Korrektur des Manuskripts
Wolfgang Fritzsche:	Diskussion und Korrektur des Manuskripts

2.7 Enzyme-induced growth of silver nanoparticles studied on single particle level

Journal of Nanoparticle Research (**2008**) 11(4): 939-946

Thomas Schüler:	Anfertigung des Manuskripts, Versuchsdurchführung, Auswertung der Messdaten
Andrea Steinbrück:	TEM-Aufnahmen

Grit Festag:	Ergebniss-Diskussion
Robert Möller:	Diskussion und Korrektur des Manuskripts
Wolfgang Fritzsche:	Diskussion und Korrektur des Manuskripts

2.8 A disposable and cost efficient microfluidic device for the rapid chip-based electrical detection of DNA

Biosensors Bioelectronics (**2009**) 25 (2009) 15–21

Thomas Schüler:	Anfertigung des Manuskripts, Versuchsplanung und -durchführung, Auswertung der Messdaten
Robert Kretschmer:	Konstruktion und Herstellung der Durchflusskammer
Sven Jessing:	Versuchsdurchführung
Matthias Urban:	Entwicklung des Auslesegerätes
Wolfgang Fritzsche:	Diskussion und Korrektur des Manuskripts
Robert Möller:	Diskussion und Korrektur des Manuskripts
Jürgen Popp:	Diskussion und Korrektur des Manuskripts

2.9 UV cross-linking of unmodified DNA on glass surfaces

Analytical Bioanalytical Chemistry (2009) DOI 10.1007/s00216-009-3045-9

Thomas Schüler:	Anfertigung des Manuskripts, Versuchsplanung und -durchführung, Auswertung der Messdaten
Alla Nykytenko:	Versuchsdurchführung, Auswertung der Messdaten
Andrea Csaki:	Diskussion und Korrektur des Manuskripts
Robert Möller:	Diskussion und Korrektur des Manuskripts
Wolfgang Fritzsche:	Diskussion und Korrektur des Manuskripts
Jürgen Popp:	Diskussion und Korrektur des Manuskripts

Konferenzbeiträge

Posterpräsentation

1. *Electrical DNA-Chip with screen printed electrodes*
   Thomas Schüler, Robert Kretschmer, Robert Möller, Wolfgang Fritzsche
   Statusseminar Chiptechnologien **2006**, Frankfurt am Main

2. *DNA-Chips for the electrical detection*
   Thomas Schüler, Robert Möller, Wolfgang Fritzsche
   High End BioChip Engineering **2006**, Eindhoven

3. *DNA-Chips for the electrical detection*
   Thomas Schüler, Robert Möller, Wolfgang Fritzsche
   VAAM (Vereinigung für allgemeine und angewandte Mikrobiologie) **2006**, Jena

4. *Characterization of metal deposition on nanoparticles at single particle level*
   Grit Festag, Thomas Schüler, Andrea Csaki, Robert Möller, Wolfgang Fritzsche
   Particles **2006**, Orlando, Florida

5. *Fabrication of microelectrodes by self-organization of metal enhancement seeds*
   Thomas Schüler, Robert Kretschmer, Robert Möller, Wolfgang Fritzsche
   DNA based nanoscale integration **2006**, Jena

6. *Fabrication of microelectrodes by metal enhancement seeds*
   Thomas Schüler, Robert Kretschmer, Robert Möller, Wolfgang Fritzsche
   Summer School, VW Stiftung, **2006**, Bremen

7. *Potential of enzymatic silver deposition*
Thomas Schüler, Katharina Hering, Uwe Klenz, Robert Möller,
Wolfgang Fritzsche
TNT Trends in Nanotechnology, **2006**, Grenoble, France

8. *Specific metal deposition at the single particle level*
Thomas Schüler, Grit Festtag, Sven Jessing, Daniell Malsch, Robert Möller,
Wolfgang Fritzsche
SPM Workshop, **2006**, Dresden

9. *Immobilization of fluorescence dyes and biomolecules in hydrogel arrays*
Uwe Klenz, Thomas Schüler, Wolfgang Fritzsche, Thomas Henkel
ChemoChip Symposium, **2006**, Weimar

10. *DNA-Chips for the electrical detection*
Thomas Schüler, Robert Möller, Wolfgang Fritzsche, Jürgen Popp
Anakon, **2007**, Jena

11. *DNA Chips for the electrical detection integrated in microfluidic systems*
Thomas Schüler, Robert Möller, Wolfgang Fritzsche, Jürgen Popp
Anakon, **2007**, Jena

12. *Immobilization and detection of oligonucleotides in PEG based hydrogel arrays*
Uwe Klenz, Thomas Schüler, Wolfgang Fritzsche, Thomas Henkel
Symposium on Functional Polymer Based Materials, **2007**, Jena

13. *Characterization of silver nanoparticles deposited by an enzyme*
Thomas Schüler, Robert Möller, Wolfgang Fritzsche, Jürgen Popp
European Conferences on Biomedical Optics - Biophotonik **2007**, München

14. *A novel polymeric platform for chip-based biomolecule analysis*
Thomas Schüler, Alfredo J. Ibáñez, Robert Möller, Wolfgang Fritzsche,
Hans-Peter Saluz, Ales Svatoš
Statusseminar Chiptechnologien, **2008**, Frankfurt am Main

15. *A microfluidic device for the rapid chip based electrical detection of DNA*
Thomas Schüler, Robert Kretschmer, Matthias Urban, Wolfgang Fritzsche, Robert Möller
MMB (Microtechnologies in Medicine and Biology), **2009**, Quebec, Canada

Vorträge

1. *DNA-Chips for the indentification of microorganisms*
Thomas Schüler, Robert Möller, Marc Rene Carlsohn, Thomas Munder, Wolfgang Fritzsche
VAAM (Vereinigung für allgemeine und angewandte Mikrobiologie) **2006**, Jena

2. *AFM-studies of enzymatic silver deposition*
Thomas Schüler, Sven Jessing, Daniell Malsch, Robert Möller, Wolfgang Fritzsche
SPM Workshop, **2006**, Dresden

3. *A diagnostic tool for the detection of Legionella RNA*
Thomas Schüler, Robert Möller, Antje Breitenstein, Wolfgang Fritzsche
DGHM *(*Deutsche Gesellschaft für Hygiene und Mikrobiologie), **2007**, Göttingen

4. *Microarray basierte Bioanalytik*
Thomas Schüler, Robert Möller, Wolfgang Fritzsche
Absolvententreffen, FH Jena, **2007**, Jena

5. *An automated system for the chip-based electrical detection of DNA*
Thomas Schüler, Robert Möller, Wolfgang Fritzsche, Jürgen Popp
Statusseminar Chiptechnologien, **2008**, Frankfurt am Main

6. *A microfluidic device for the rapid chip based electrical detection of DNA*
Thomas Schüler, Robert Kretschmer, Matthias Urban, Wolfgang Fritzsche, Robert Möller
MMB (Microtechnologies in Medicine and Biology), **2009**, Quebec, Canada

Danksagung

An dieser Stelle möchte ich mich bei allen bedanken, die mich bei dieser Arbeit unterstützt haben. Ein besonderer Dank gilt dabei:

Prof. Dr. Jürgen Popp für die Betreuung meiner Arbeit, seine Unterstützung und anhaltendes Interesse;

PD Dr. Wolfgang Fritzsche für sein stetiges Interesse am Fortgang meiner Arbeiten und die vielfältigen Diskussionen meiner Ergebnisse;

Dr. Robert Möller für die hilfreichen Diskussionen, Ratschläge und Freiheiten bei der Durchführung meiner Arbeit;

Dr. Andrea Csaki und Dr. Grit Festag für die vielfältige Hilfe und Klärung von labortechnischen Problemen;

Dr. Alfredo Ibanez für die gute Zusammenarbeit bei der Herstellung und Untersuchung der getesteten Polymere;

Franka Jahn für die Erstellung der vielen REM-Aufnahmen;

Katrin Kandera für die Aktivierung der ganzen Chipsubstrate;

Matthias Urban und Robert Kretschmer für die Realisierung des neuen DNA-Chip-Readers und die Konstruktion der Durchflusskammer als auch bei der Lösung ingenieurtechnischer Probleme;

Sven Jessing, Delf Conrad und Maren Wagenhaus für ihre Unterstützung und die vielen durchgeführten Versuche;

den Mitarbeitern von TNO und dem Holste-Center in Eindhoven für ihre Unterstützung und stetige Mitarbeit bei der Entwicklung der PEN-Folien basierten Biochips;

Prof. Dr. Thomas Munder (FH Jena) und Dr. Marc René Carlsohn für ihre Hilfe bei den Arbeiten zum Nachweis von *Kitasatospora*;

Prof. Dr. Hans-Peter Saluz (HKI Jena) und Dr. Ales Svatos (MPI für chemische Ökologie Jena) für die hilfreichen Diskussionen bei der Untersuchung des PBEMA-Polymers und der Erstellung des Manuskripts;

Dr. Tim Asmus (Heraeus Sensor Technology) für die Bereitstellung der Siebdruckchips;

Dr. James F. Hainfeld und Dr. Richard D. Powell (Nanoprobes) für die Bereitstellung des EnzMet Entwicklungskits zum enzyminduzierten Wachstum von Silber-nanopartikeln;

allen Mitgliedern der Abteilung Nanobiophotonik des IPHT, der Jenaer Biochip Initiative und der Arbeitsgruppe des Institutes für physikalische Chemie der Universität Jena die während der gesamten Dauer meiner Arbeit ein angenehmes und freundliches Arbeitsklima schufen;
und nicht zuletzt meinen Eltern, meiner Familie und meinen Freunden für ihre fortwährende Unterstützung.

Selbstständigkeitserklärung

Ich erkläre hiermit, dass ich die vorliegend Arbeit selbstständig und unter Verwendung der angegebenen Hilfsmittel, persönlichen Mitteilungen und Quellen angefertigt habe.

Jena, den

Thomas Schüler